1987

Diffusivity Characteristics Of Glucose In Alginate Immobilization Matrices

Fahar Jehangir Merchant

300 kg m^{-3}, an exponential increase in D_e values was observed. However, at all concentrations, the ratio D_e/D was found to remain constant at 0.91. The temperature dependence of D_e obeyed the Arrhenius relationship and the activation energy for diffusion of glucose in the Ca-alginate gel was evaluated to be 21.3 $kJ.mol^{-1}$, which is only 2.2 $kJ.mol^{-1}$ higher than the corresponding value in water. The ratio D_e/D gradually increased as the temperature was raised from 20 to 50°C.

Some literature correlations based on the obstruction effects were found to give good estimates of D_e values when low concentrations of alginate were used for gel formation, but failed at higher concentrations of Ca-alginate indicating that hydrodynamic drag effects cannot be neglected. According to the Renkin equation, mean pore diameters in different alginate gels were estimated to vary from 35 to 8 nm, depending on the type and concentration of chelating agent and Na-alginate used for gel preparation. These values were found to be comparable to pore diameters reported in the literature.

Increase in the concentration of either Ca-alginate, chelating agent, or entrapped yeast cells, all caused significant reductions in the values of D_e. For instance, the D_e value of glucose in Ca-alginate gel containing 118 kg dry weight/m^3 of cells (4.67×10^{-10} m^2s^{-1}) decreased by about 30 percent when compared to the D_e value in a cell-free Ca-alginate gel.

DIFFUSIVITY CHARACTERISTICS OF GLUCOSE IN ALGINATE IMMOBILIZATION MATRICES

by

Fahar J. A. Merchant
Department of Chemical and Biochemical Engineering
Faculty of Engineering Science

Submitted in partial fulfilment
of the requirements for the degree of
Doctor of Philosophy

Faculty of Graduate Studies
The University of Western Ontario
London, Ontario
December 1986

ISBN 0-315-36612-5

ABSTRACT

In recent years, alginate gels have emerged as popular matrices for the entrapment of microbial, plant and mammalian cells. As in the case of most entrapment matrices, the presence of an additional diffusional barrier may profoundly influence the overall reaction rate. Although fundamental engineering techniques and formulations for describing combined reaction and mass-transfer rates, can be applied to predict the overall performance of a given entrapped cell bioreactor system, prior knowledge of certain physical parameters such as, effective substrate diffusivities, D_e, and equilibrium partition coefficients, K_p, is required. Therefore the objective of this research was to study the diffusivity characteristics of a universal substrate, glucose, in alginate entrapment matrices.

Conventional techniques of measuring D_e in gel entrapment matrices are not practical due to the poor mechanical stability of such solids. A novel apparatus was therefore designed to measure D_e and K_p of glucose in alginate gels using radiotracer techniques. In this method, a specially prepared, large spherical alginate bead was mounted to a stainless-steel rod and the sphere immersed in a liquid phase of limited volume. By rotating the bead at high angular velocities (corresponding to rotational Reynolds' number of $> 5,000$) the rate of C^{14}-glucose uptake or release was measured using a scintillation spectrometer, under condi-

tions of near ideal mixing (mixing time < 4.0 s) and negligible film mass transfer resistance (film mass transfer coefficient, $k_L > 2.0 \times 10^{-5} m.s^{-1}$; mass transfer Biot number, $N_{Bi} > 200$). A model equation describing unsteady-state mass transfer in a sphere immersed in a liquid phase of limited volume was used to evaluate D_e.

The optimum D_e value was determined by fitting the theoretical predictions to experimental data, using a non-linear regression analysis computer program. Using 2% Ca-alginate beads the D_e and K_p values of glucose at 30°C were found to be 6.73×10^{-10} $m^2.s^{-1}$, ($\pm$ 0.12×10^{-10} $m^2.s^{-1}$), and 0.98 ($\pm$ 0.03), respectively. The former corresponds to a D_e/D ratio of 0.91.

The equilibrium adsorption isotherm for diffusion of glucose into Ca-alginate beads was found to obey a linear relationship. Using several estimation techniques for calculating D_e values, the approximate analytical solution due to Lee (1981b) gave a value that was similar to that obtained using the exact solution. Two correlations were also developed in this study to accurately predict the free-phase diffusivity values of glucose in water. These correlations were subsequently used in all comparisons between D_e and D.

The effect of temperature, glucose concentration and variation in the composition of alginate gels on the D_e and K_p values was examined. When the initial 'cold' glucose concentration in the liquid phase was increased from 3 to

300 kg m^{-3}, an exponential increase in D_e values was observed. However, at all concentrations, the ratio D_e/D was found to remain constant at 0.91. The temperature dependence of D_e obeyed the Arrhenius relationship and the activation energy for diffusion of glucose in the Ca-alginate gel was evaluated to be 21.3 $kJ.mol^{-1}$, which is only 2.2 $kJ.mol^{-1}$ higher than the corresponding value in water. The ratio D_e/D gradually increased as the temperature was raised from 20 to 50°C.

Some literature correlations based on the obstruction effects were found to give good estimates of D_e values when low concentrations of alginate were used for gel formation, but failed at higher concentrations of Ca-alginate indicating that hydrodynamic drag effects cannot be neglected. According to the Renkin equation, mean pore diameters in different alginate gels were estimated to vary from 35 to 8 nm, depending on the type and concentration of chelating agent and Na-alginate used for gel preparation. These values were found to be comparable to pore diameters reported in the literature.

Increase in the concentration of either Ca-alginate, chelating agent, or entrapped yeast cells, all caused significant reductions in the values of D_e. For instance, the D_e value of glucose in Ca-alginate gel containing 118 kg dry weight/m^3 of cells (4.67×10^{-10} m^2s^{-1}) decreased by about 30 percent when compared to the D_e value in a cell-free Ca-alginate gel.

By increasing the concentration of the gelling agent (i.e. either $CaCl_2$ or $BaCl_2$), a significant decrease in D_e values was observed especially with $BaCl_2$. The guluronic acid content of the alginate did not appear to affect the D_e values of glucose at low gel concentrations, but lower D_e values were recorded at higher Ca-alginate concentrations when the guluronic acid content was raised from 40 to 70% . Appropriate correlations are presented to predict D_e values and mean pore diameters as a function of Ca-alginate concentration in the gel.

As in the case of cell-free Ca-alginate beads, the activation energy for diffusion of glucose over a temperature range of 20 to 50°C was 2.0 $kJ.mol^{-1}$ higher than the corresponding value in water (19.1 $kJ.mol^{-1}$). Significant differences were not observed in the D_e values of a non-metabolizable glucose analogue, 3-0-methyl glucose, when live yeast cells were entrapped (106 kg dry weight/m^3 of gel) in the Ca-alginate gel instead of non-viable cells.

The significance of the data reported in this study were assessed in terms of the stability characteristics of the alginate gel matrix and the reported kinetic properties of entrapped cells.

ACKNOWLEDGEMENTS

I wish to express my profound appreciation and thanks to my supervisor, Dr. A. Margaritis, for suggesting this research topic, and for his excellent guidance, encouragement and momentum that he always provided throughout this research.

The invaluable advice and suggestions provided by Dr. A. Vardanis and use of laboratory facilities at the Agriculture Canada Research Centre is gratefully acknowledged.

Gratitude is also extended to the Faculty of Engineering Science for their administrative and financial support. The assistance of Mr. Wayne Vollick for drafting most of the figures is also appreciated. I must also thank Mrs. Eileen Quigg and Miss Carol Quigg for their excellent typing skills.

My gratitude must also be reserved for the Aga Khan Foundation (Canada) for providing me with a Scholarship. This research was supported by an Operating Grant from NSERC awarded to Professor A. Margaritis.

I am especially grateful to my parents for their optimism, trust, and financial assistance throughout my academic career. Most of all, I wish to offer my sincerest gratitude to my wife, Nina, for spending unending hours at the computer terminals processing all the data. Her contribution, encouragement and infinite patience throughout the course of this study was the key factor for the successful completion of this research.

TO MY DEAR WIFE

NINA

FOR HER LOVE

AND

RESOLUTE ENDURANCE

TABLE OF CONTENTS

LIST OF TABLES

DESCRIPTION

LIST OF FIGURES

DESCRIPTION

LIST OF APPENDICES

NOMENCLATURE

A = Arrhenius pre-exponential constant for diffusion of glucose in water ($m^2.s^{-1}$)

A_g = Arrhenius pre-exponential constant for diffusion of glucose in calcium alginate gel ($m^2.s^{-1}$)

A^o = Arrhenius pre-exponential constant for diffusion of glucose at infinite dilution ($m^2.s^{-1}$)

A_s = Surface area of sphere (m^2)

a_s = Surface area to particle volume ratio

b_c = Exponential constant in Equation 5.14 ($m^3.kg^{-1}$)

b_o = Constant in Equation 5.21 ($m^3.kg^{-1}$)

b_T = Temperature dependent exponential constant in Equation 5.18 ($m^3.kg^{-1}$)

b_{TG} = Temperature dependent exponential constant in Equation 5.28 ($m^3.kg^{-1}$)

c = Concentration of Na-alginate in solution on a dry wt. basis (kg D.W./m^3 of solution)

$\acute{c}$ = Concentration of Na-alginate in solution ($kg.m^{-3}$)

c_g = Concentration of alginate in the gel (kg D.W./m^3 of gel)

c_{ts} = Total solids concentration in the gel (kg D.W./m^3 of gel)

c_x = Cell concentration in the gel (kg D.W./m^3 of gel)

C_L = Substrate concentration in the bulk liquid phase ($kg.m^{-3}$)

C_L^* = Substrate concentration in the liquid phase at the solid-liquid interface ($kg.m^{-3}$)

C_L^o = Initial glucose concentration in the liquid phase ($kg.m^{-3}$)

C_L^t = Solute concentration in the liquid phase at time, t ($kg.m^{-3}$)

C_L^∞ = Equilibrium solute concentration in the bulk liquid phase ($kg.m^{-3}$)

C_S = Substrate concentration within the spherical gel matrix ($kg.m^{-3}$)

C_S^* = Substrate concentration on the spherical gel surface ($kg.m^{-3}$)

C_S^o = Initial solute concentration in the sphere ($kg.m^{-3}$)

C_S^t = Solute concentration in the entire gel volume at time, t ($kg.m^{-3}$)

C_S^∞ = Equilibrium solute concentration in the entire gel volume ($kg.m^{-3}$)

$\overline{C_S^t}$ = Average solute concentration in the sphere at time, t ($kg.m^{-3}$)

d_p = Pore diameter in Ca-alginate gel (nm)

d_s = Diameter of spherical bead (m)

d_t = Inside diameter of the diffusion vessel (m)

D = Diffusivity of glucose in water ($m^2.s^{-1}$)

D_e = Effective diffusivity of glucose in Ca-alginate gel ($m^2.s^{-1}$)

$D_{e,o}$ = Effective diffusivity of glucose in calcium alginate gel at infinite dilution ($m^2.s^{-1}$)

D_o = Diffusivity of glucose in water at infinite dilution ($m^2.s^{-1}$)

Da = Damköhler number defined by Equation 3.6

$\overline{Da}$ = Observable Damköhler number defined by Equation 3.15

$\overline{Da}$ = Modified Damköhler number defined by Equation 3.10

ΔE = Difference in activation energy for diffusion of glucose in gel when compared to that in water, $\Delta E = E_{ag} - E_a$ ($kJ.mol^{-1}$)

E_a = Activation energy for diffusion of glucose in water ($kJ.mol^{-1}$)

E_a^o = Activation energy for diffusion of glucose in water at infinite dilution ($kJ.mol^{-1}$)

E_{ag} = Activation energy for diffusion of glucose in calcium alginate gel ($kJ.mol^{-1}$)

E_{AB} = Activation energy for diffusion of solute A through medium B ($kJ.mol^{-1}$)

f_d = Frictional drag factor given by Equation 5.44

ΔG_{AB} = Gibbs free energy for diffusion defined by Equation 5.33 ($kJ.mol^{-1}$)

k^1 = Intrinsic first-order rate constant

k_L = External film mass transfer coefficient ($m.s^{-1}$)

k^n = Intrinsic nth-order rate constant

K_m = Saturation constant ($moles.m^{-3}$)

K_p = Equilibrium partition coefficient

L = Concentration of the fibre in the gel ($cm\ fibre/cm^3$)

m = Constant in Equation 5.12

M_B = Molecular weight of the solvent

M_L^o = Amount of labelled glucose in the liquid phase at time, t = 0 (cpm)

M_L^t = Amount of labelled glucose in the liquid phase at time, t = t (cpm)

$\frac{M_L^t}{M_L^\infty}$ = Ratio of amount of solute in the liquid phase at time, t, to that at equilibrium

M_L^{BG} = Amount of background radioactivity in liquid sample (cpm)

M_S^o = Amount of labelled glucose in the sphere at time, t = 0 (cpm)

M_S^t = Amount of labelled glucose in the sphere at time, t = t (cpm)

M_S^∞ = Amount of labelled glucose in the sphere at equilibrium (cpm)

$\frac{M_S^t}{M_S^o}$ = Ratio of the amount of solute remaining at time t = t to the total amount of solute originally present in the sphere

$\frac{M_S^t}{M_S^\infty}$ = Ratio of the amount of solute in the sphere at time, t, to that at equilibrium

$\overline{MW}$ = Average molecular weight of Na-alginate

n = Number of terms used in series solutions

N = Avogadro's number (6.022×10^{23} mol^{-1})

N_{Bi} = Mass transfer Biot number defined by Equation 3.38

$N_{Re,r}$ = Rotational Reynolds' number defined as ($\omega \rho d_s^2/\mu$)

N_s = Total number of samples withdrawn from liquid phase

N_{sc} = Schmidt number ($\bar{\nu}/D$)

N_{sh} = Sherwood number ($k_L d_S/D$)

q_n = Eigen values defined by Equation 3.62

r = Distance from the centre of the sphere (m)

$\bar{r}$ = r/R, dimensionless radial position

R = Radius of bead (m)

$\bar{R}$ = Universal gas constant (8.3143 $kJ.mol^{-1}$)

r_f = Radius of the fibre in gel (cm)

r_p = Pore radius in the gel (nm)

r_s = Stokes radius of the solute (nm)

S_{AB} = Entropy of activation ($kJ.mol^{-1}.K^{-1}$)

t = Time, t, (min or s)

T = Temperature (^{o}C or K)

t_m = Mixing time (s)

t_s = Sampling time (min)

$\bar{V}$ = Observed rate of reaction per unit volume of the entrapment matrix ($moles.s^{-1}.m^{-3}$)

V_{max} = Saturation reaction rate per unit volume of the entrapment matrix ($moles.s^{-1}.m^{-3}$)

$\bar{V}/V_{max}$ = Dimensionless effective reaction rate

V_L^o = Volume of liquid phase at time, t=0 (μL)

V_L^t = Volume of liquid phase at time t=t (μL)

V_L = Volume of liquid phase in the diffusion vessel (μL)

v_s = Volume of sample withdrawn from liquid phase (μL)

V_S = Spherical bead volume (m^3)

V_A = Molar volume of solute at its normal boiling point (m^3/kg mol)

W_d = Dry weight of the Ca-alginate bead (kg)

W_{ts} = Total dry weight of solids (cells + alginate) in Ca-alginate gel (kg)

W_h = Amount of water in Ca-alginate bead (kg)

W_w = Wet weight of the Ca-alginate bead (kg)

x = Distance measured from the centre of solid (m)

X = Concentration of cells in the gel on a wet weight basis (kg wet wt./litre of gel)

y = Constant in Equation 5.21

z = Dimensionless substrate concentration defined by Equation 3.36

z^* = Dimensionless substrate concentration defined by Equation 3.4

Greek Letters

α = Alpha - factor defined by Equation 3.61.

β = Volume fraction of entrapped yeast cells in Ca-alginate gel

ε = Porosity or void fraction in the gel

η = Effectiveness factor

$\bar{\eta}$ = Overall effectiveness factor

η_E = External effectiveness factor

η_I = Internal effectiveness factor

η_o = Zero-order overall effectiveness factor

$\bar{\eta}_1$ = First-order overall effectiveness factor

Θ = Given by Equation 3.47

κ = Dimensionless saturation constant defined by Equation 3.5

λ = Volume fraction of alginate in the gel matrix

μ = Viscosity of a given solution ($kg.m^{-1}.s^{-1}$)

$[\mu]$ = Intrinsic viscosity of aqueous solution of sodium alginate (100 mL/g)

μ_{alg} = Viscosity of a Na-alginate solution ($kg.m^{-1}.s^{-1}$ or cps)

μ_B = Solvent viscosity ($kg.m^{-1}.s^{-1}$)

μ_{H_2O} = Viscosity of water ($kg.m^{-1}.s^{-1}$ or cps)

μ_r = Relative viscosity of the alginate solution at a given concentration defined by Equation 4.3

μ_{sp} = Specific viscosity of the alginate solution defined by Equation 4.4

ν = Specific volume of the alginate in the gel ($m^3.kg^{-1}$)

$\bar{\nu}$ = Kinematic viscosity ($m^2.s^{-1}$)

ρ = Density of solvent ($kg.m^{-3}$)

ρ_b = Bead density ($kg.m^{-3}$)

ρ_h = Density of water ($kg.m^{-3}$)

σ^* = Dimensionless substrate concentration at the particle surface defined by Equation 3.9

σ_i = Dimensionless internal substrate concentration defined by Equation 3.21

σ_o = Dimensionless bulk substrate concentration defined by Equation 3.8

τ = Dimensionless time defined as $D_e t/R^2$

Φ = Generalized Thiele modulus defined by Equation 3.32

ϕ = Thiele modulus for Michaelis-Menten type of kinetics defined by Equation 3.37

ϕ_m = Modified Thiele modulus defined by Equation 3.24

ϕ_o = Zero-order Thiele modulus defined by Equation 3.45

ϕ_m^1 = Modified first-order Thiele modulus defined by Equation 3.31

ϕ_1 = First-order Thiele modulus defined by Equation 3.43

ψ = Association parameter of solvent in Equation 5.25

ω = Alginate weight fraction in the gel

Ω = Angular velocity of bead ($rad.s^{-1}$)

CHAPTER 1

INTRODUCTION

1.1 Potential of Immobilized Cell Systems

Currently, most of the biotechnological industries employ conventional batch fermentation processes developed at least 40 years ago. These processes are slow, inefficient and are associated with high capital and operating costs. They have been aptly described as "a lot of water containing a dash of catalyst in large expensive fermenters." The continual start-up and shut-down nature of such systems makes them difficult to automate and are therefore very labour intensive (Atkinson et al., 1980).

The use of continuous processes, which are simple to operate with low energy requirements would significantly lower operating costs. Capital costs may be further reduced by the use of mechanically simple and small bioreactors capable of high rates of product formation which can only be achieved if a high concentration of viable cells is retained within the bioreactor. This can be achieved by a process known as "live cell immobilization" which has received considerable attention during the past decade.

1.2 Definition of Immobilized Cell Systems

The definition of immobilized cells proposed by Abbot (1977) has been widely used. Accordingly, any system in which cells are confined within a bioreactor and thereby permitting their economical reuse is defined as an immobilized cell system. The term "economical" has been used to exclude processes in which cells are recovered and reused by employing techniques such as centrifugation and microfiltration which may introduce high capital and operating costs. On the other hand, flocculant cells are categorized as being immobilized since their recovery can be accomplished with relative ease by employing static settling tanks.

1.3 Selection Criteria for Cell Immobilization

In selecting a suitable technique for live cell immobilization, a number of criteria need to be considered.

(i) Primarily, the procedure should be mild enough to ensure retention of cell viability and at the same time able to achieve and maintain a high cell concentration.

(ii) Furthermore, the immobilized cell system must be capable of reactivation, if necessary, and be stable for prolonged periods of time under the operating conditions.

(iii) Finally, the technique should be simple, relatively inexpensive and capable of scale-up.

1.4 Advantages of Immobilized Cell Systems

Thus, a suitable technique may confer all or some of the advantages listed below to a fermentation system. These include:

(i) Possibility of much greater cell concentrations within the bioreactor facilitating faster fermentation rates.

(ii) Operation at high dilution rates without fear of cell washout.

(iii) Reduced risk of microbial contamination due to the combined effects of (i) and (ii).

(iv) Less susceptible to the effects of inhibitory compounds and nutrient depletion.

(v) <u>In situ</u> removal of cells from the product stream eliminates the cost of a cell separation unit normally used as the first step in product recovery, thus reducing energy and capital cost requirements.

(vi) As opposed to free cell continuous stirred tank bioreactor (CSTBR) systems, most immobilized cell bioreactors can be operated in the plug-flow mode. The latter is especially beneficial

when product inhibition occurs in a fermentation process.

1.5 Methods of Cell Immobilization

A wide variety of immobilization techniques have been developed in recent years and these have been classified according to the mode of immobilization as shown below.

(i) Entrapment within gel matrices
(ii) Adsorption onto inert supports
(iii) Attachment to solid supports by covalent bonding
(iv) Mechanical containment within the bioreactor
(v) Microencapsulation within polymeric membranes
(vi) Immobilization without inert supports (cell flocculation)

1.6 Cell Immobilization by Entrapment

The entrapment of live cells in polymeric gels and their subsequent growth within such supports was first demonstrated by Updike et al. (1969). Entrapment has since become a common method for the immobilization of not only yeast and bacterial cells (Linko and Linko, 1984; Margaritis and Merchant, 1984; 1987) but also for subcellular organelles and enzymes (Kierstan and Bucke, 1977), filamentous

fungi (Vaija et al., 1982) algae (Mosbach, 1984), plant cells (Bordelius, 1984), plant protoplasts (Linse and Bordelius, 1984), animal cells (Nilsson et al., 1983) and genetically engineered cells (Mosbach et al., 1983).

In the case of recombinant cells, the problem of plasmid instability which is associated with the insertion of foreign DNA into the host cells, is a major drawback in the application of continuous fermentation systems. This problem can, however, be circumvented to a certain extent, by placing recombinant cells in an environment in which cellular replication in minimized, while cellular activity, such as the production of enzymes and products, is maintained at high levels. Immobilization by entrapment creates an environment in which cells approach their maximum packing density and consequently cellular replication is inhibited by lack of available space (Blanch, 1984). Entrapped cell systems could therefore form the backbone of new biotechnological processes associated with the use of recombinant cells.

1.7 Entrapment of Live Cells in Alginate Gels

The entrapment of live cells within naturally occurring polymeric matrices, such as alginates, has been shown by Margaritis and Merchant (1984; 1987) to be a very promising immobilization technique. The entrapment procedure is attractive primarily because of its simplicity . Gel formation occurs by dropping a mixture of sodium alginate

solution and the cell suspension into a solution containing multivalent cations. The three dimensional gel network formed is biochemically inert and cells can be trapped in the interstitial spaces of the gel. Furthermore, the immobilization reagents are of low cost, making the procedure attractive for large scale applications.

The immobilization of whole cells within the alginate matrix was first demonstrated by Hackel et al. (1975) for the biodegradation of phenol. Since then the immobilization of microbial, plant, mammalian, and recombinant cells has been attempted for a variety of potential applications using alginate as the entrapment matrix (Table 1.1).

All entrapped cell systems are, however, subjected to mass transfer limitations imposed by the additional diffusion barrier created by the support matrix. As shown in Chapter 3, solute partitioning and intraparticle mass transfer resistance contribute substantially to the kinetic properties of entrapped cell systems. To date, little effort has been directed to quantitatively evaluate partitioning and diffusivity characteristics of solutes in entrapment matrices. This is attributed to the lack of suitable techniques of measuring solute diffusivities in polymeric gels containing entrapped cells. The major objective of this research is therefore directed towards developing a novel, universal method of measuring solute diffusivities and partitioning in gels used for cell immobilization. Alginate gels have emerged as popular matrices for cell immobiliza-

Table 1.1. Biotechnological Applications of Alginates: A Decade of Development

Year	Application	Reference
1975	The use of alginate gel as an entrapment matrix for phenol biodegradation was first demonstrated	Hackel et al., (1975)
1977	Immobilization of bacteria, yeast, mitochondria, chloroplasts and enzymes	Kierstan and Bucke, (1977)
1979	Immobilization of plant cells	Bordelius et al., (1979)
1980	Immobilization and microencapsulation of animal cells	Lim and Sun, (1980); Nilsson and Mosbach, (1980)
1981	Continuous production of ethanol using entrapped yeast and bacterial cells	Merchant, (1981); Margaritis et al., (1981)
1982/83	Pilot scale production of ethanol by entrapped yeast cells	Fukushima and Hanai, (1982); Margaritis et al., (1983)
1983	Immobilization of human hybridoma cells for large scale production of monoclonal antibodies (Damon Biotech. Corp. Ltd.)	Klausner, (1983)
1984	Semi-commercial production of ethanol by entrapped yeast cells (Kyowa Hakko Co. Ltd.)	Samejima et al., (1984)
1985	Entrapment of recombinant cells of *E. coli*	Georgiou et al., (1985)

tion and like most other naturally occurring polysaccharides, alginates are available in a wide variety of structural forms. Consequently, structural features that may influence solute diffusivities in alginate gels will be identified in Chapter 2. The theoretical and practical considerations leading to the development of the diffusivity measurement technique will be discussed in Chapter 3 and details of the methods presented in Chapter 4. In subsequent chapters, the results obtained in this research will be presented and their significance assessed in the light of current knowledge and theoretical models available in the literature.

CHAPTER 2

CHARACTERISTICS OF ALGINATE GELS USED FOR CELL IMMOBILIZATION

The development of an entrapped cell system for commercial application involves a series of considerations beginning with the choice of the entrapment matrix and ending with the decision on the operational mode of the selected bioreactor. As shown in Table 2.1, several factors characterize the properties of a given entrapped cell bioreactor system. Therefore when scaling up such a system, one is faced with a large and complex optimization problem (Buchholz, 1982; Weetal and Pitcher, 1986). Additionally, as shown in Figure 2.1, all these factors influence the stability characteristics of the matrix, the kinetic properties of the entrapped cell system and consequently, the overall economics of the final process. Examination of the extensive literature shows that adequate characterization of immobilized cell matrices is an exception rather than a rule, with the result that a large part of published information cannot be critically evaluated in terms of their potential for industrial application.

Although several properties of alginates have been well defined, to date no attempt has been made to review the role of those parameters that contribute to the stability and operational characteristics of alginate entrapped cell

Table 2.1 Characteristics of Entrapped Cell Systems (Adapted from Margaritis and Merchant, 1984; 1987)

A. ENTRAPMENT TECHNIQUE

1. Entrapment in polymeric networks by cross-linking of polyanions (alginate, carboxy-methyl-cellulose, carboxy-guar-gum), and polycations (chitosan) by multivalent cations (Ca^{2+}, Al^{3+}, Ba^{2+}, Fe^{2+}, Zn^{2+}) and multivalent anions [$Fe(Cn)_6^{4-}$, poly-phosphate, alginate], respectively.

2. Entrapment by precipitation caused by changes in pH and temperature or solvent changes (agar, gelatin, carrageenan)

3. Entrapment within covalent polymeric matrices by cross-linking-copolymerization (polyacrylamide) or by polycondensation (epoxide)

B. PHYSIOLOGICAL CHARACTERISTICS

1. Cell viability and function
2. Cell growth rate and yield
3. Cell concentration
4. Cell wall integrity and membrane permeability
5. Metabolic product formation and yield
6. Respiratory requirements
7. Plasmid stability of recombinant cells

C. CHEMICAL PROPERTIES OF SUPPORT

1. Chemical composition and method of synthesis
2. Functional groups, monomer(s), type(s), etc.
3. Possible toxicity of support component(s) to cell function and viability

D. PHYSICAL PROPERTIES OF THE SUPPORT

1. Temperature and pH stability
2. Solubility characteristics in aqueous solutions containing different solutes and ions
3. Geometry and size distribution of the support
4. Density of particle and void fraction
5. Minimum fluidization velocity
6. Mechanical strength and stability of support
7. Abrasion and cell leakage from support

TABLE 2.1 (Contd)

8. Mass transfer characteristics
   (i) Diffusivity of substrates, products and nutrients into and out of the support
   (ii) Oxygen transfer characteristics for aerobic systems
   (iii) Partitioning of solute between the solid and liquid phase

E. BIOREACTOR TYPE

1. Single or multi-stage stirred tank bioreactor
2. Horizontal or vertical packed bed bioreactor
3. Single or multi-stage fluidized bed bioreactor with or without draft tubes
4. Tower bioreactor
5. Aerated loop bioreactor
6. Circulating bed bioreactor

F. CHARACTERISTICS OF THE BIOREACTOR

1. Hydrodynamic characteristics
2. External film mass transfer resistances
3. Heat transfer characteristics

G. BIOREACTOR OPERATING STRATEGY

1. Fermentation conditions
2. Mode of bioreactor operation
   (i) Batch
   (ii) Fed-batch
   (iii) Repeat-batch
   (iv) Continuous

H. STABILITY CHARACTERISTICS OF THE CELL-MATRIX SYSTEM

1. Activity and half-life in continuous operation
2. Operational stability in a given bioreactor system
3. Possible stabilization of the cell/enzymatic system
4. Stability and activity preservation during storage

Figure 2.1: Development of an Industrial Scale Immobilized Cell Bioreactor System

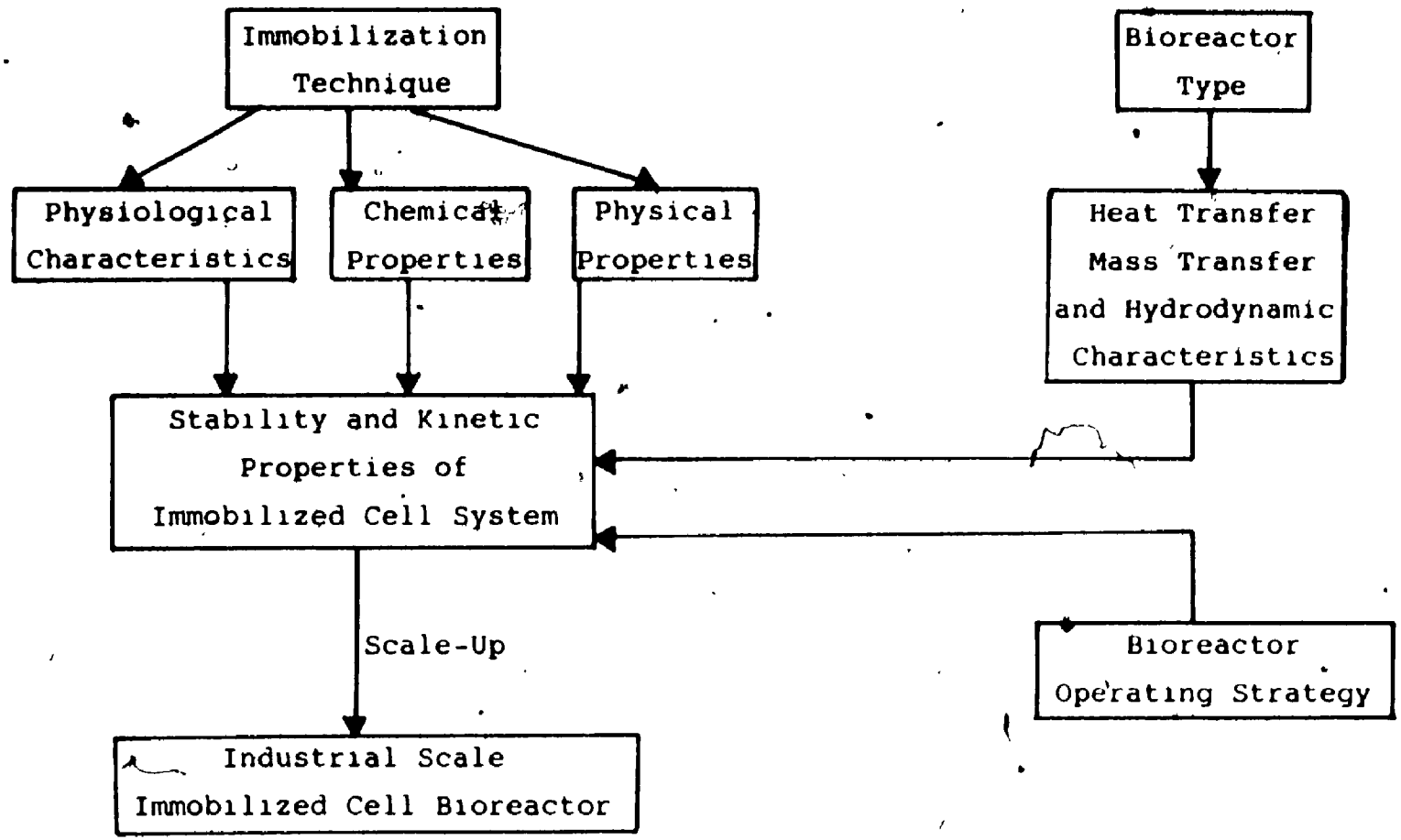
Immobilization Technique
Physiological Characteristics
Chemical Properties
Physical Properties
Bioreactor Type
Heat Transfer Mass Transfer and Hydrodynamic Characteristics
Stability and Kinetic Properties of Immobilized Cell System
Scale-Up
Bioreactor Operating Strategy
Industrial Scale Immobilized Cell Bioreactor

systems. In the following sections, an attempt will therefore be made to address this need. Additionally, the structural and physico-chemical properties of alginate gels will be summarized enabling us to indentify those features that may influence the mass transfer characteristics of solutes within the alginate matrix.

2.1. Sources of Alginates

Alginates are naturally occurring polymers which are extracted from some species of brown seaweeds belonging to the Phaeophyceae class of algae. The most widely used species for the commerical production of alginates belong to the genus Ascophyllum, Laminaria and Macrocystis. Although several species of the bacterium, Azotobacter vinelandii also produce alginates as extracellular mucilages, they are not used as commercial sources for the polysaccharide (Margaritis and Pace, 1985). However, in view of their desirable characteristics, bacterial alginates may in future provide an economic source of the product (Chen et al., 1985.

2.2. The Structure of Alginic Acid and its Polymers

Essentially, alginic acid is a linear polysaccharide composed of two types of uronic acids, namely, D-mannuronic acid and L-guluronic acid (Figure 2.2) linked by β-1,4 and α-1,4 bonds, respectively (Hirst et al, 1964). As shown in

Figure 2.2: Conformation of (a) mannuronic acid (β-D-mannopyranosyluronic acid unit in the C1 conformation) and (b) guluronic acid (α-L-gulopyranosyluronic acid unit in the 1C conformation). Redrawn from Rees (1972a).

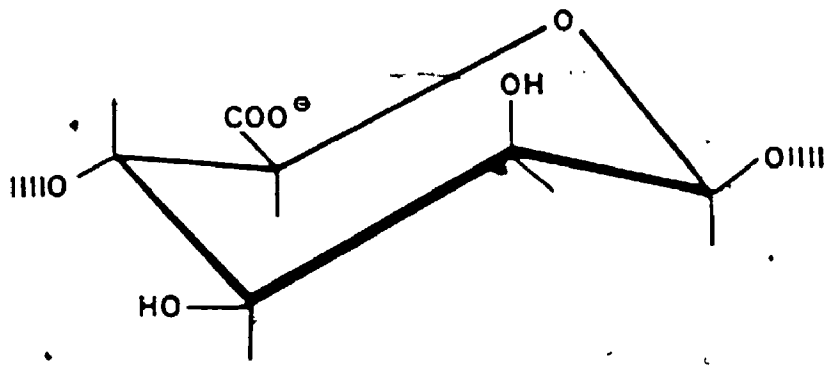

(a)

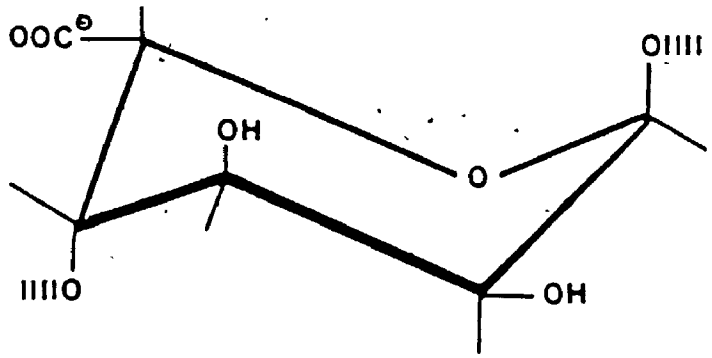

(b)

Figure 2.3, the uronic acid residues are arranged in sequences of three types: contiguous blocks of D-mannuronic acid residues (MM blocks), contiguous blocks of L-guluronic acid residues (GG blocks) and blocks of alternating residues (MG blocks). In the alginate polymer chain, blocks containing one type of the residue (MM or GG blocks) are separated by segments in which the two residues alternate (Haug et al., 1966; 1967a).

The shape of the polymannuronic acid chain is similar to that found in other β-1,4 linked hexosans such as cellulose. Mannuronic acid is in the C1 conformation and consequently di-equatorially linked (Figure 2.4a). Polymannuronic acid is therefore a flat, ribbon-like molecule (Figure 2.4b). On the other hand, polyguluronic acid is a buckled, ribbon-like molecule (Figure 2.4d) in which the guluronic acid is in the 1C conformation and therefore, di-axially linked (Figure 2.4c). As shown in Figure 2.4, the conformation of both polymannuronic and polyguluronic acid is stabilized by a hydrogen bond between adjacent units (Atkins et al., 1971).

Studies have shown that the proportion of polymannuronic acid, polyguluronic acid and alternating segments, in different commercially available alginate samples depends on the species, the season, and region where the seaweed is harvested. (Haug and Larsen, 1962; Haug et al., 1974; Penman and Sanderson, 1972). Commercially available alginates also differ with respect to the degree of polymerization. Thus,

Figure 2.3: Structure of polymer segments contained in alginic acid.

(a) polymannuronic acid (MM-blocks),

(b) polyguluronic acid (MG-blocks), and,

(c) alternating D-mannuronic acid and L-guluronic acid residues (MG-blocks).

Adapted from McDowell (1977).

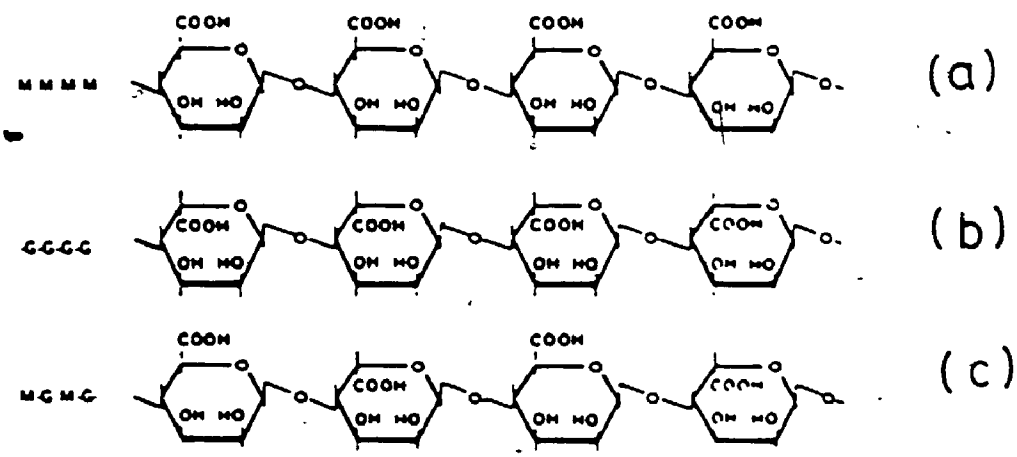
MMMM
GGGG
MGMG
COOH
OH HO
(a)
(b)
(c)

Figure 2.4: (a) Repeating unit of polymannuronic acid in which the 1 → 4 glycosidic linkage is di-equitorial.

(b) Schematic representation of the flat, ribbon-like conformation of polymannuronic acid.

(c) Repeating unit of polyguluronic acid in which the 1 → 4 glycosidic linkage is di-axial.

(d) Schematic representation of the buckled, ribbon-like conformation of polyguluronic acid.

(Adapted from Bryce et al., 1974)

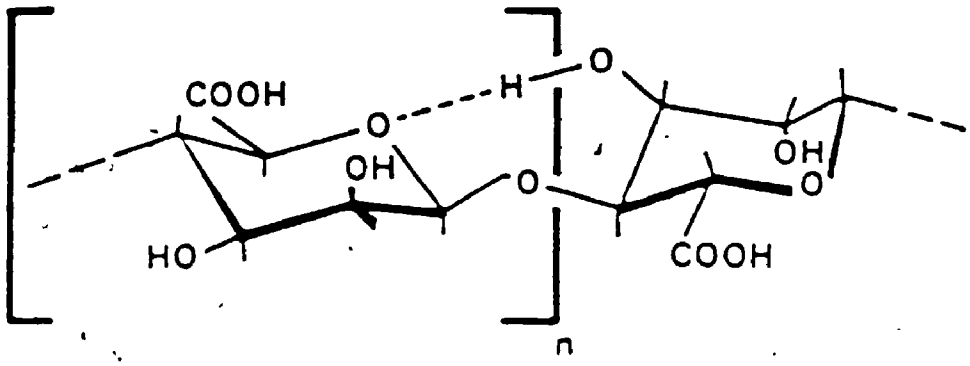

(a)

(b)

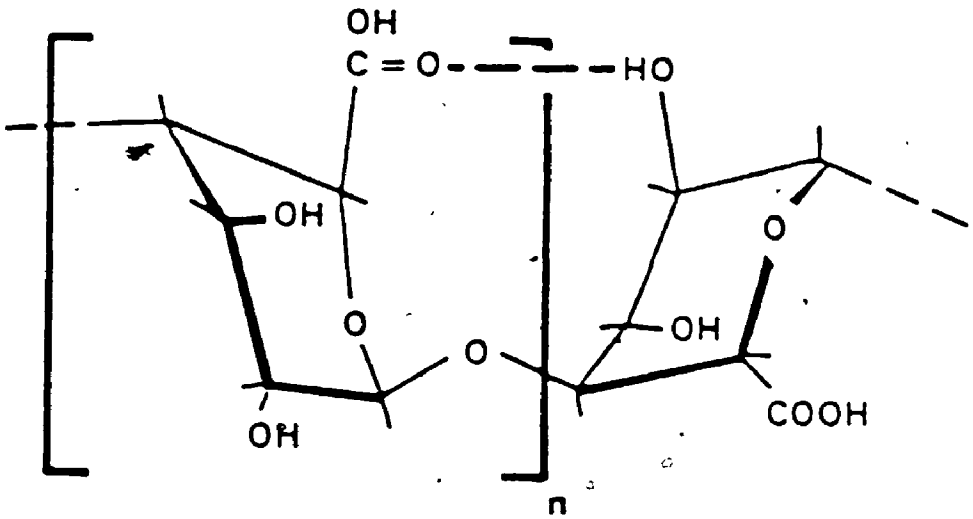

(c)

(d)

alginates having a degree of polymerization ranging from 100 to 4000 corresponding to molecular weights of 20,000 to 800,000 are commonly available (Smidsrod and Haug, 1968a; McDowell, 1977). These differences therefore account for the variability in properties and functionality of alginates isolated from different species of brown algae (Haug et al., 1967b; Smidsrod and Haug, 1968b; Stockton et al., 1980), and as discussed below, also dictate the properties of alginate gels used for cell immobilization.

2.3. Gel Formation and Structure

One of the most important and useful properties of alginates is the ability to form gels by reaction with multivalent cations like Ca^{2+}, Co^{2+}, Zn^{2+}, Mn^{2+}, Ba^{2+}, Sr^{2+}, Fe^{2+}, Al^{3+}, Fe^{3+} etc. The alginate gel formation procedure was orginally developed by Thiele (1954) and since then Ca^{2+} ions have been widely used to induce gelation of soluble alginates such as sodium alginate.

The Ca-alginate gel formation reaction may be considered as the combination of two partial reactions as follows:

$$CaY_2 + 2Na^+ \longrightarrow 2NaY + Ca^{2+} \qquad 2.1$$

$$Ca^{2+} + 2Alg^- \longrightarrow Ca(Alg)_2 \qquad 2.2$$

$$CaY_2 + 2NaAlg \longrightarrow Ca(Alg)_2 + 2NaY \qquad 2.3$$

where Alg^- represents a single uronic acid anion and CaY_2 is a soluble calcium salt (e.g. $CaCl_2$).

Cooperative binding of Ca^{2+} ions by polyguluronic acid has been shown to be primarily responsible for formation of cross-links in Ca-alginate gel (Rees, 1972a). Thus, when increasing quantities of Ca^{2+} are added to a sodium alginate solution, the initial amounts are bound to GG-blocks, and as soon as junction regions are established, further quantities of Ca^{2+} are even more firmly bound to them. Binding to MM-blocks and MG-blocks is unimportant until all the GG-blocks are saturated with Ca^{2+} (Morris et al., 1973).

Based on the above and known coordination geometries of model compounds, Grant et. al, (1973) proposed the "egg-box model" to describe the structure of Ca-alginate matrix. As shown in Figure 2.5 the GG-blocks associate into aggregates with interstices into which the Ca^{2+} ions fit. GG-blocks therefore play a predominant part in gel formation because their combination with each other and with Ca^{2+} is energetically more favourable than for either of the other two blocks (Haug et al., 1967b; Smidsrod and Haug, 1968b). It must be noted that the interaction of Ca^{2+} with MM-blocks plays a secondary role in maintaining the gel structure (Rees, 1972b; Bryce et al., 1974).

2.4. Properties of Alginate Gels

In this section, factors that influence the micro-

Figure 2.5: (a) The proposed structure of calcium alginate gel in which a collection of parallel lines represents a cross-link.

(b) Schematic representation of a cross-link in a Ca-alginate gel formed from blocks of 20 or more contiguous blocks of L-guluronic acid residues. Each residue is shown as a short straight line i.e. ∧ represents two consecutive residues and the overall shape of the block resembles a corrugated ribbon. Such ribbons form aggregates (known as the "egg-box model") with interstices into which Ca^{2+} ions (shown as O) fit. (From Rees, 1972a; 1972b)

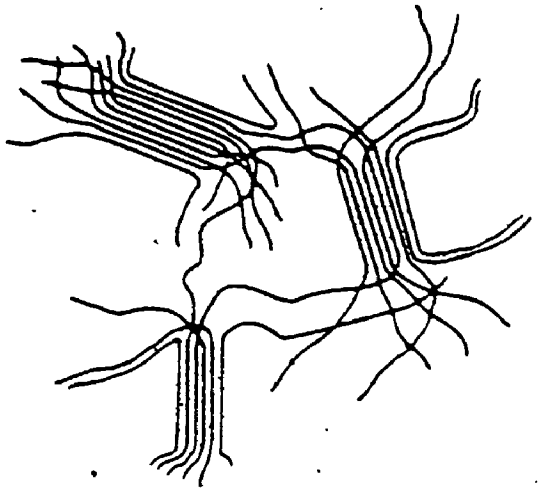

(a)

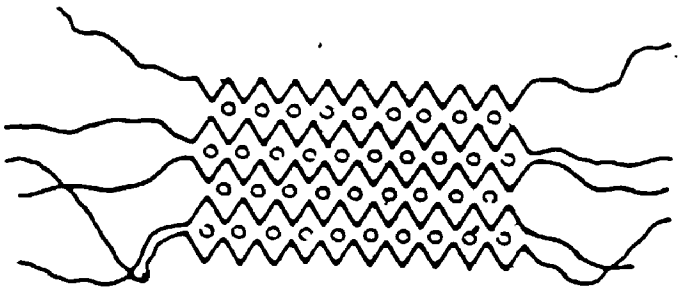

(b)

structure of the alginate gel will be discussed and their influence on the properties of alginate gels assessed.

2.4.1. Ion-Exchange Properties

For reactions of the type,

$$2Na.Alg + MCl_2 \longrightarrow M.Alg_2 + 2\ NaCl \qquad 2.4$$

the affinity of the alginate (Alg^-) for a divalent cation (M^{2+}) in comparison with Na^+, is measured by the selectivity coefficient, K, which is defined by Equation 2.5 as

$$K = \frac{[X_M]\ [C_{Na}]^2}{[X_{Na}]^2\ [C_M]} \qquad 2.5$$

where X represents the mole fraction of the respective cation in the gel phase, and C represents the concentration of the ions in solution (Smidsrod and Haug, 1965).

Several studies (Smidsrod and Haug, 1968b; 1972a; Smidsrod, 1974) have shown that the selectivity coefficient increased as a function of guluronic acid content of the gel and its alginate concentration. Additionally, the affinity of different metal cations for alginates increased in the

following order (Smidsrod and Haug, 1965; Haug and Smidsrod, 1965):

GG blocks : Mg << Ca < Sr < Ba

MM blocks : Mg ~ Ca ~ Sr < Ba

MG blocks : Mg ~ Ca ~ Sr ~ Ba

Higher selectivity coefficients result in stronger binding forces between adjacent chains of the alginate polymer causing a reduction in pore sizes within the alginate matrix (Smidsrod, 1974). Thiele and Hallich (1957) arranged the divalent metals in a "ionotropic series" by measuring the pore diameters in gels formed by allowing divalent metals to diffuse into alginate solutions. The diameter of the pores decreased in the following order:

Ni, Co, Zn > Ca > Sr > Ba > Cd > Cu > Pb

which corresponds to an increase in selectivity coefficients of the divalent cations for the alginates.

2.4.2. Synerisis

The phenomenon of synerisis, exhibited by many gels (especially when the concentration of polysaccharide is low), is the spontaneous release of water with contraction of gel volume (Rees, 1969). Increasing proportions of Ca^{2+}

added to sodium alginate solution causes contraction of the gel volume due to an increasing tendency to exhibit synerisis (Smidsrod and Haug, 1965) indicating that the alginate matrix becomes more and more tightly linked.

According to Rees (1972a), alginates with a high proportion of guluronic acid content would be more prone to synerisis. However, data of Smidsrod and Haug (1972b) seem to contradict this view. Thus, synerisis was found to be minimal at high (>70%) and low (<20%) levels of guluronic acid in the alginate, but synerisis occurred readily with alginates containing intermediate (30% to 50%) amounts of guluronic acid. In terms of cell immobilization, synerisis has important implications in that the concentration of both, alginate and the cells is substantially higher in the gel than in Na-alginate solution, before gelation (Johansen and Flink, 1986a). The actual concentration of cells within the matrix should therefore be determined when comparing mass transfer and kinetic properties of alginate entrapped cell systems.

2.4.3 Chemical Stability of the Alginate Matrix

Ca-alginate gels are generally insoluble in water even at high temperatures used in thermophilic fermentations (Suhaila and Salleh, 1982). However, in the presence of calcium chelating agents such as phosphates, EDTA, citrate etc., the ionic bonds between Ca^{2+} and uronic acid residues

break down which results in swelling of the matrix associated with high rates of cell leakage (Dainty et al., 1986), followed by loss in mechanical stability and, eventually to complete disintegration of the matrix (Cheetham et al., 1979; Vorlop and Klein, 1983). A number of stabilizing agents such as epichlorohydrin (Ferrero et al., 1982), polyethylene amine with and without cross-linking agents (Birnbaum et al., 1981; Veliky and Williams, 1981), and other commerical products such as Dupont's Tyzor TE (Burns et al., 1985) have been used to stabilize the structural integrity of Ca-alginate in the presence of phosphates. However, these stabilization techniques introduce additional expenditure and complexity for large-scale preparation of Ca-alginate based entrapped cell systems and consequently, their use has not been popular.

Based on the above, use of citrate and phosphate buffers in Ca-alginate entrapment matrices is not recommended. A selection of suitable buffers having a minimal effect on the stability of Ca-alginate gels has therefore been suggested (Burns et al., 1985; Vorlop and Klein, 1983). If, however, high concentrations of phosphate (>10mM) are required for maintenance of cell viability, incorporation of trace amounts of $CaCl_2$ in the fermentation media has been found to maintain the structural integrity of the Ca-alginate matrix for prolonged periods of time with minimal rates of cell leakage (Margaritis et al., 1981). Alternatively, superior chelating agents such as Sr^{2+}, Ba^{2+} and

Al^{3+} (Paul and Vignais, 1980; Rochefort et al., 1986) may be used for gel formation instead of Ca^{2+} due to their higher selectivity coefficients (Section 2.4.1), provided the products of the entrapped cell systems are not used in the food or pharmaceutical industry (Vorlop and Klein, 1983).

2.4.4 Mechanical Stability of Alginate Gels

Three different approaches have been generally used to characterize the mechanical stability of alginate gels:

(i) Single particle (sphere or cylinder) compression behaviour

(ii) Compression of spherical alginate beads in packed beds

(iii) Abrasion of spherical alginate beads in stirred tanks

A summary of the major findings of these studies have been listed in Table 2.2. In general, parameters that facilitate stronger binding between adjacent alginate chains seem to enhance the mechanical stability of the gel (Segeren et al., 1974).

2.5 Bioreactor Design Considerations

The most common bioreactor used in preliminary lab-

Table 2.2. Factors Affecting the Mechanical Stability of Alginate Gels

Parameter	Influence on Mechanical Stability of Alginate Gel	Reference
Alginate concentration	Mechanical stability increased with increase in alginate concentration. Rigidity $\alpha[Alg]^2$	Smidrod *et al.*, (1972); Cheetham (1979); Dainty *et al.*, (1986).
$CaCl_2$ concentration	Mechanical stability increases whereas the elasticity decreases with increase in $CaCl_2$ concentration.	Cheetham *et al.*, (1979); Mitchell and Blanshard, (1976).
Guluronic acid content of alginate	Increase in the guluronic acid content (low M/G ratio) leads to an increase in mechanical strength. Gels rich in mannuronic acid are more elastic.	Smidsrod *et al.*, (1972); Imeson *et al.*, (1980).
Degree of polymerization of alginate	Gel formation occurs when DP is at least 65. Up to DP = 400, gel strength increases with increase in DP. When DP > 400, gel strength is independent of DP.	Smidsrod and Haug, (1972b); Smidsrod, (1974) Cheetham *et al.*, (1979).
Type of chelating agent	Mechanical strength improves when gels are prepared with trivalent cations (e.g. Al^{3+} or with divalent cations (e.g. Ba^{2+}, Sr^{2+}) which have higher selectivity coefficients than Ca^{2+}.	Smidsrod and Haug, (1972b); Rochefort *et al.* (1986).
Effect of gelation time	Rigidity of 2.31 ml cylindrical gels (diameter = 1.4 cm; length = 1.5 cm) was found to be independent of time after gelation was complete which occurred in less than 48 hrs.	Smidsrod *et al.*, (1972).

Table 2.2. (cont'd)

Parameter	Influence on Mechanical Stability of Alginate Gel	Reference
Effect of drying	Gel strength increases substantially when Ca-alginate beads are air dried.	Vorlop and Klein (1981); Krouwel *et al.*, (1982); Burns *et al.*, (1985).
Effect of hardening agents	Treatment of Ca-alginate beads with polyethyleneimine, glutaraldehyde, Eudragit etc., improves the mechanical stability of the gel.	Lamberti and Sefton, (1983); Suhaila and Salleh, (1982); Krouwel *et al.*, (1982).
Temperature	Mechanical stability decreases with increase in temperature from 4 to 79°C.	Cheetham *et al.*, (1979); Smidsrod and Haug, (1972)
Entrapped cell concentration	Increase in cell concentration results in weaker gels.	Cheetham, (1979) Krouwel *et al.*, (1982); Klein *et al.*, (1980).
Abrasion in stirred tanks	The abrasion rate of Ca-alginate beads increases with increases in: (a) particle diameter, (b) stirrer speed, (c) volume fraction of gel suspended in liquid phase, and (d) cell concentration.	Klein *et al.*, (1980); Klein and Eng, (1978); van Ginkel *et al.*, (1983).

scale studies has been the vertical packed bed bioreactor (PBBR). The choice of this configuration is obvious, due to the simplicity of construction and desirable kinetic properties (Section 1.4). However, a number of factors tend to limit the use of the vertical PBBR especially when scale-up is considered. These limitations include:

(i) Inability to use feed materials containing particulate matter due to plugging and fouling problems

(ii) In aerobic systems and/or fermentations processes associated with the production of gaseous by-products, difficulty in oxygen supply and/or gas hold-up within the bioreactor, results in reduced bioreactor efficiency (Cho et al., 1982) and poor heat transfer characteristics (Ghose and Bandyopadhyay, 1982).

(iii) Plugging and blockage of the bed due to released cells

(iv) The combined effects of (i), (ii), and (iii) results in extremely high pressure drops which in turn causes deformation of the entrapment matrix (Buchholz and Godelman, 1978; Furusaki et al., 1983).

Some of the above problems may be partially resolved with the use of a sectionalized column (Furui and Yamashita

1985), or a horizontal PBBR (Margaritis and Rowe, 1983). Alternatively, single or multi-stage stirred tank bioreactors (STBR) may be used to alleviate the above problems. However, with the STBR, limitations due to product inhibition in a single stage system, high power requirements, and shear effects near the impeller region causing gel disruption have largely restricted its wider use with entrapped cell systems (Lee et al., 1983).

It appears that the most desirable bioreactor configuration, employing entrapped cell systems, is the fluidized bed bioreactor (FBBR). In this system, immobilized biocatalyst particles are suspended and agitated by the upward flow of fluid through the bed. Thus, based on the operational characteristics of a FBBR, this bioreactor configuration offers unique advantages to entrapped cell systems (Margaritis and Wallace, 1984) which include the following:

(i) Foreign particles in the fluid readily pass through the bed, eliminating plugging problems
(ii) Gases can be readily introduced and removed
(iii) Has low power requirements and operates with relatively low pressure drops
(iv) Reduced shear effects when compared to the STBR
(v) Possesses good heat and mass transfer characteristics

Due to these desirable characteristics, FBBR contain-

ing alginate entrapped yeast cells have been used for pilot-scale (Fukushima and Hanai, 1982; Margaritis et al., 1983) and semi-commercial scale (Samejima et al., 1984) production of ethanol.

From the above discussion and the physico-chemical properties of alginate gels, it is apparent that the long term operational stability of alginate entrapment matrices will depend on many factors, including:

(a) the composition of the alginate matrix,
(b) the fermentation conditions employed,
(c) the concentration of entrapped cells,
(d) media composition,
(e) type of buffers used,
(f) the bioreactor configuration, and
(g) the hydrodynamic characteristics of the bioreactor

At the same time, these factors may also influence the mass transfer characteristics of alginate entrapped cell systems and, consequently, the kinetic properties of the immobilized cell bioreactor (ICBR). To date no effort has been directed to quantitatively evaluate the influence of physico-chemical properties of alginates on their mass transfer characteristics and will therefore form one of the major objectives of this research.

CHAPTER 3

MASS TRANSFER EFFECTS IN ENTRAPPED CELL SYSTEMS

The application of alginates in novel biotechnological processes appears to be very promising indeed. However, this step from the conventional free cell fermentation system to the novel entrapped cell system is a major one. Primarily, the kinetic properties of the entrapped cells alter and consequently, the theoretical treatment of heterogeneous biocatalysis can become complex and difficult (Kasche, 1983; Karel, et al., 1985). As with other immobilized cell systems, the altered kinetic behaviour of entrapped cells may be attributed to either one or both of the following phenomena (Buchholz, 1982).

(i) By virtue of the immobilization technique, changes in the physiological and metabolic properties of the entrapped cells may occur.

(ii) The properties of the local environment, provided by the matrix for the entrapped cells, can be significantly different from that when the same cells are freely suspended in solution.

3.1 Entrapment and the Microenvironment

In the immediate vicinity of the entrapped cells (i.e. the microenvironment), concentration of those species that influence the rate of reaction differ from those in the bulk phase, namely, the macroenvironment. This is attributed to:

(i) Partition effects between the solid phase and the bulk liquid phase.

(ii) Mass transfer resistances.

Consequently, the effect of the above factors on the kinetic properties of entrapped cells can be readily anticipated as shown in Figure 3.1.

3.2 Intrinsic Rate and Kinetic Parameters

The true kinetic behaviour of an entrapped cell system is characterized by its intrinsic kinetic properties which can be observed only if the concentration of the substrate, product, nutrients and other effectors are identical in both, the micro- and macroenvironment. However, the intrinsic kinetic parameters of an entrapped cell system are not necessarily the same as those of a free cell system because the immobilization technique may alter the physiological and metabolic properties of the immobilized cells.

In the following sections, theoretical approaches used

Figure 3.1. Schematic illustration of the different rates and kinetic parameters and their interrelation.

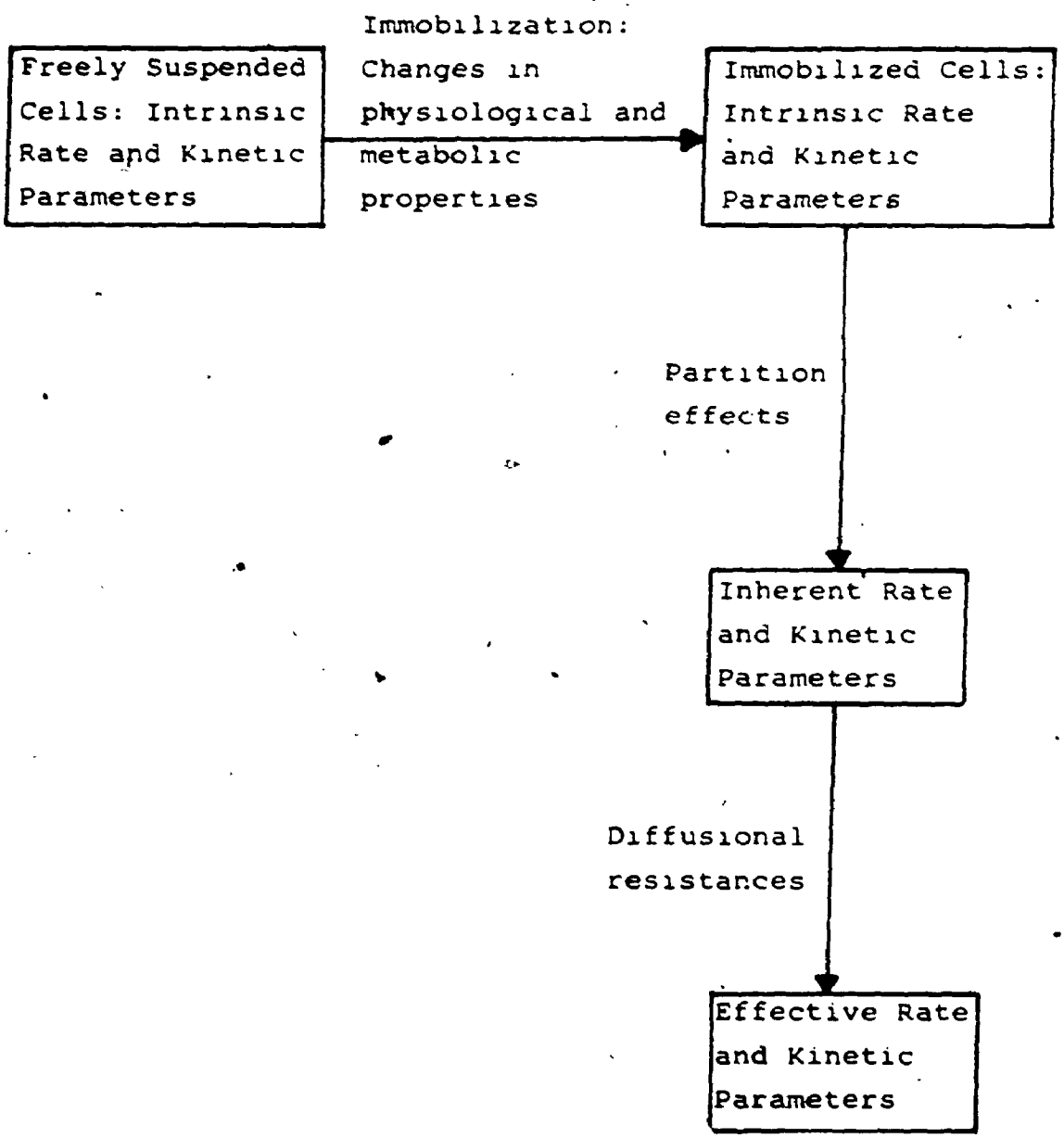
Freely Suspended Cells: Intrinsic Rate and Kinetic Parameters
Immobilization: Changes in physiological and metabolic properties
Immobilized Cells: Intrinsic Rate and Kinetic Parameters
Partition effects
Inherent Rate and Kinetic Parameters
Diffusional resistances
Effective Rate and Kinetic Parameters

to estimate the effective rates of reaction will be discussed for immobilized cell systems exhibiting intrinsic Michaelis-Menten type of kinetic behaviour without substrate and/or product inhibition.

3.3 Partitioning Effects

The inherent rate of reaction is defined as the rate that would be observed in the absence of mass transfer resistances. This modified behaviour can be attributed to the fact that the concentration of charged species, substrates, products, hydrogen and hydroxyl ions, etc. in the domain of entrapped cells may be different from that in the bulk liquid phase owing to either electrostatic, hydrophilic or lipophilic interactions between the support matrix and the soluble species. This phenomenon is called the partition effect and is generally expressed by an equilibrium partition coefficient (or distribution coefficient), K_p.

In the case of solid porous pellets, K_p is defined as the solute concentration in the micropores divided by its concentration in the bulk solution at equilibrium. Gel matrices are, however, regarded as being much more homogeneous than solid porous pellets, and therefore, according to Equation 3.1, K_p is defined in terms of the entire gel volume (Yamane et al., 1981).

$$K_p = C_S^{\infty}/C_L^{\infty} \qquad 3.1$$

where, C_S^∞ and C_L^∞ are the equilibrium solute concentrations in the entire gel volume, and the bulk liquid phase, respectively.

In the absence of physico-chemical interactions between the solute and the gel matrix, K_p is equal to or less than unity depending on the overall decrease in free volume of the gel (Yasuda et al., 1968; Nakanishi et al., 1977). When physico-chemical interactions occur between the gel matrix and the solute, K_p values of greater than unity have been reported (Goldstein et al., 1964; Bunting and Laidler, 1972; Sonomoto et al., 1979). Thus, when $K_p > 1.0$, a higher concentration of substrate is obtained in the microenvironment than that in the bulk liquid phase, which results in faster rates of reaction when compared to an immobilization matrix having $K_p < 1.0$. However, for entrapped cell systems exhibiting substrate and/or product inhibition, a K_p value of less than unity would be more desirable (Kennedy and Cabral, 1983).

In the case of charged solutes, a shift in the optimum pH towards more alkaline or acidic pH values occurs for negatively or positively charged matrices, respectively (Goldstein, 1976; Engasser and Horvath, 1976). In Section 3.4.3 the combined influence of partitioning effects and mass transfer resistances on the effective reaction rates will be discussed in more detail.

3.4 Mass Transfer Effects

The effective rate of reaction and kinetic parameters for entrapped cell systems are observed, in the presence or absence of partitioning effects when diffusional resistances occur during

(i) external mass transfer of the substrate from the bulk liquid phase to the surface of the cell immobilization matrix, and/or

(ii) internal mass transfer of the substrate within the entrapment matrix.

In both, the chemical and biochemical engineering literature, the effectiveness factor, η, (defined by Equation 3.2), has been widely adopted as a numerical measure of the influence of mass transfer resistances (Aris, 1975; Atkinson, 1974). In the absence of partitioning effects,

$$\eta = \text{Effectiveness factor} = \frac{\text{observed reaction rate of immobilized cell system}}{\text{reaction rate which would be observed with no mass transfer resistance (i.e. when } C_L = C_S \text{ [with intraparticle mass transfer] or } C_L = C_S^* \text{ [without internal mass transfer])}} \qquad 3.2$$

where, C_L, C_S and C_S^* are the substrate concentrations in the bulk liquid phase, within the gel matrix, and the gel surface, respectively. Effectiveness factors of less than

unity indicate that the substrate concentration on the gel surface (C_S^*) or within the immobilization matrix (C_S) is lower than that in the surrounding bulk fluid (C_L), in which case the overall reaction rate is limited by diffusional resistances (Bailey and Cho, 1983).

Starting from the equation for diffusion and reaction on the surface and/or within a spherical biocatalyst, mathematical solutions relating the effectiveness factor to various process parameters will be presented, assuming for the moment, that the partition coefficient is unity.

3.4.1 External Mass Transfer

At steady state, the rate of mass transfer of a substrate from the bulk liquid phase to the surface of a non-porous immobilization matrix (i.e. in the absence of intra-particle mass transfer), at which the substrate is consumed by a biochemical reaction, will equal the observed surface reaction rate, $\overline{V}$ (moles of substrate consumed per unit time per unit volume of the matrix) as shown by Equation 3.3. Thus,

$$k_L a_S (C_L - C_S^*) = \overline{V} = \frac{V_{max}\, C_S^*}{K_m + C_S^*} \qquad 3.3$$

where, k_L is the film mass transfer coefficient, a_S is the surface area to particle volume ratio, V_{max} is the satura-

tion rate of reaction per unit volume of the entrapment matrix, and K_m is the saturation constant.

The film mass transfer coefficient, which is a function of physical properties as well as hydrodynamic conditions within the bioreactor can be evaluated from correlations available in the literature. Karabelos et al., (1971) have presented an extensive survey of these correlations applicable to traditional chemical engineering systems. Some of these correlations have been successfully used for predicting k_L at the liquid-solid interface in immobilized cell and enzyme reactors and have been listed in a number of reviews (Moo-Young and Blanch, 1981; 1983; Buchholz, 1979; 1982; Vieth et al., 1976; Pitcher, 1978).

In Equation 3.3, the number of parameters necessary to specify the kinetic properties of the system can be reduced by introducing the following dimensionless variables:

$$z^* = C_S^*/C_L \qquad 3.4$$

$$\kappa = \text{dimensionless saturation constant} = K_m/C_L \qquad 3.5$$

$$Da = \text{Damköhler number} = \frac{V_{max}}{k_L a_S C_L} = \frac{\text{Max. reaction rate}}{\text{Max. mass transfer rate}} \qquad 3.6$$

In terms of these quantities, the substrate mass balance expressed by Equation 3.3 may be rewritten in the form,

$$\frac{\bar{V}}{V_{max}} = \frac{1 - z^*}{Da} = \frac{z^*}{\kappa + z^*} \qquad 3.7$$

where $0 \leq z^* \leq 1.0$, and V/V_{max} is the dimensionless effective reaction rate (Bailey and Ollis, 1977).

The Damköhler number, Da, expressed by Equation 3.6 is defined as the ratio of the maximum reaction rate to the maximum mass transport rate. Thus, if Da << 1.0, the maximum mass transfer rate is much larger than the maximum rate of reaction (i.e. low external film mass transfer resistance) and the system is known to operate in the reaction-limited regime. Conversely, when the film mass transfer resistance is high (Da >> 1.0), then the system operates in the diffusion-limited regime (Carberry, 1976).

The graphical representation of Equation 3.3. can be facilitated by introducing two additional dimensionless quantities (Horvath and Engasser, 1974): the dimensionless substrate concentrations (σ_o or σ^*), and the modified Damköhler number, Dá (also known as the dimensionless external substrate modulus), which are defined by Equations 3.8 to 3.10.

$$\sigma_o = C_L/K_m = 1/\kappa \qquad 3.8$$

$$\sigma^* = C_S^*/K_m \qquad 3.9$$

$$Dá = \frac{V_{max}}{k_L a_S K_m} = Da/\kappa \qquad 3.10$$

The dimensionless effective reaction rate ($\bar{V}/V_{max}$) can now be expressed by Equation 3.11:

$$\frac{\bar{V}}{V_{max}} = \frac{\sigma^*}{1 + \sigma^*} = \frac{\sigma_o - \sigma^*}{D\acute{a}} \qquad 3.11$$

The dependence of $\bar{V}/V_{max}$ on σ_o for different values of Dá is shown in Figure 3.2 which demonstrates the relative importance of external diffusional limitations on the observed rates of reaction.

The effects of external film mass transfer resistance on the biocatalytic activity of an immobilized cell system can be quantitatively expressed by the external effectiveness factor, η_E, which is generally defined by Equation 3.2. For an immobilized cell system exhibiting Michaelis-Menten type of kinetic behaviour, η_E is given by Equation 3.12 (Bailey and Ollis, 1977),

$$\eta_E = \frac{z^*/(\kappa + z^*)}{1/(\kappa + 1)} \qquad 3.12$$

Figure 3.3 shows the dependence of η_E on σ_o and Dá. For Dá (or Da) approaching zero, Equation 3.7 shows that z^* must approach unity, and therefore for the reaction-limited regime

$$\eta_E = 1, \ \bar{V} = \frac{V_{max}\, C_L}{K_m + C_L} \qquad 3.13$$

Figure 3.2. The dimensionless effective reaction rate ($\bar{V}/V_{max}$) plotted against the dimensionless bulk substrate concentration (σ_o) using different values of the modified Damköhler number (Dá), for an immobilized cell system exhibiting intrinsic Michaelis-Menten kinetics at the particle surface coupled in series with external film mass transfer (Adapted from Horvath and Engasser, 1974).

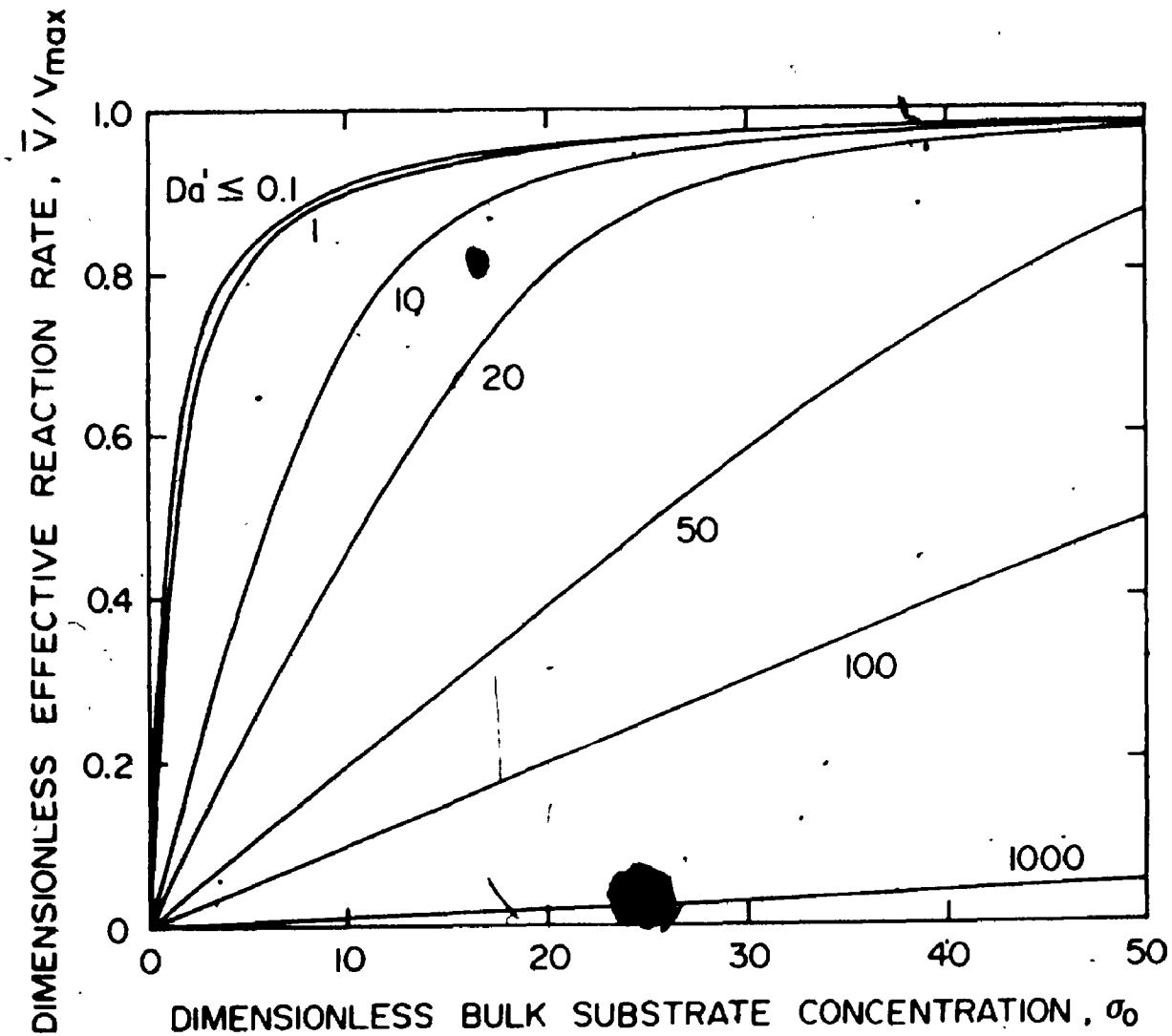
DIMENSIONLESS EFFECTIVE REACTION RATE, $\bar{V}/V_{max}$
1.0
0.8
0.6
0.4
0.2
0
Da' ≤ 0.1
1
10
20
50
100
1000
0
10
20
30
40
50
DIMENSIONLESS BULK SUBSTRATE CONCENTRATION, σ_0

Figure 3.3. Plots of the external effectiveness factor (η_E), as a function of the modified Damköhler number (Dá), with the dimensionless bulk substrate concentration (σ_o) as the variable parameter (Adapted from Horvath and Engasser, 1974).

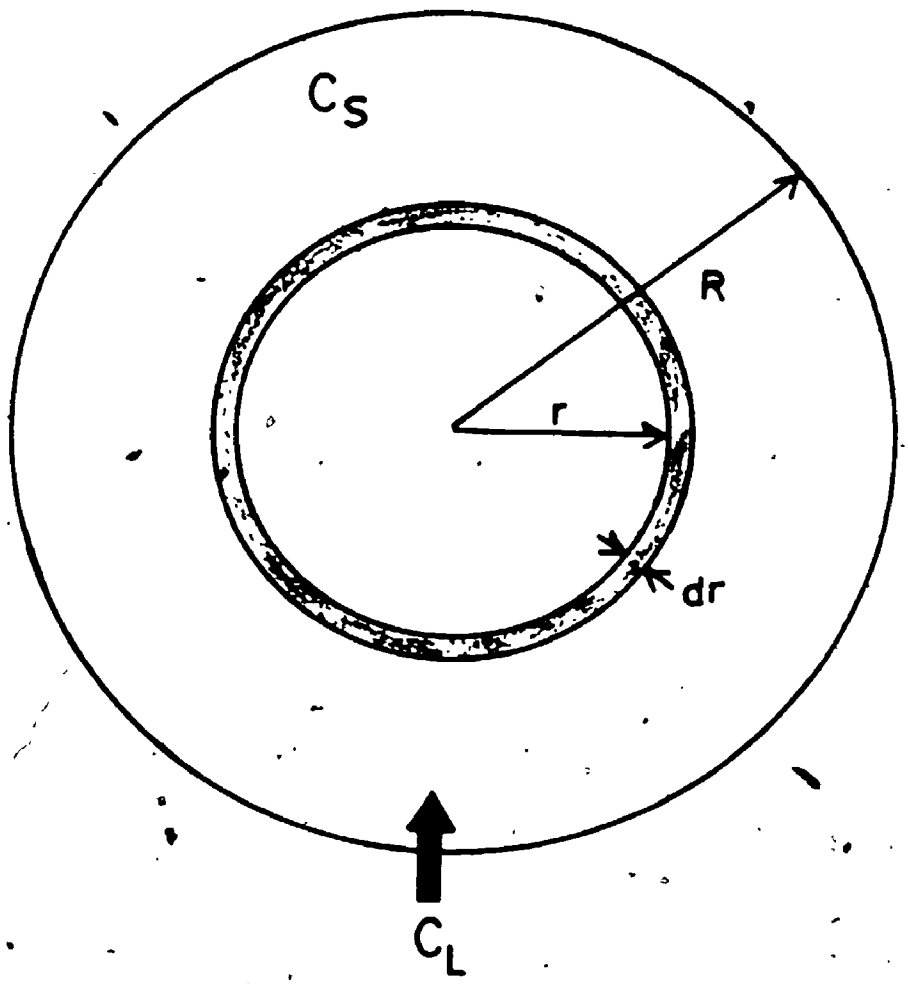
C_S
R
r
dr
C_L

In this case, the effective (or observed) kinetic parameters are the same as the true intrinsic kinetic parameters at the liquid-solid interface. V_{max} and K_m can therefore be experimentally evaluated provided that Da << 1 in order to avoid disguise by significant film mass transfer resistance (Bailey and Ollis, 1977).

The value of η_E decreases with increasing film mass transfer resistance, and as shown in Figure 3.3, the straight lines obtained for high values of Da (or Da), represent the diffusion-limited regime. In this case (i.e. Da → ∞; κ finite), η_E is given by Equation 3.14 (Bailey and Ollis, 1977),

$$\eta_E = \frac{1 + \kappa}{Da}, \quad \bar{V} = k_L a_S C_L \qquad 3.14$$

For immobilized cell systems exhibiting power-law kinetics, charts of η_E versus Da have been presented by Carberry (1976). However, the intrinsic rate constant, k^n, and C_S^* need to be known in order to calculate Da. This problem is avoided by relating η_E to the observable Damköhler number, $\overline{Da}$, (defined by Equation 3.15), which is a dimensionless quantity containing only known parameters:

$$\overline{Da} = \eta_E Da = \frac{\bar{V}}{k_L a_S C_L} \qquad 3.15$$

The external effectiveness factor, η_E, can then be determined from charts of η_E versus $\overline{Da}$ presented by Carberry (1976).

3.4.2 Internal Mass Transfer

When cells are immobilized within an entrapment matrix, besides possible external film mass transfer resistances, the effect of internal mass transfer limitations on the properties of the microenvironment, and consequently the kinetic parameters of immobilized cells, can often be very significant (Klein and Vorlop, 1983; Radovich, 1985; Brink and Tramper, 1986). Unlike external film mass transfer, internal mass transfer proceeds in parallel with the biochemical reaction. Therefore, a substrate concentration-gradient is established within the entrapment matrix in which the concentration of the substrate decreases with increasing distance from the surface of the particle, resulting in a corresponding decrease in the reaction rate.

In order to study the effect of internal diffusional resistance on the overall rate of reaction that takes place in a spherical entrapment matrix, the following assumptions will be made (Karel et al., 1985; Engasser and Horvath, 1973):

(i) There is no concentration dependent interaction between the support and the substrate or product.

(ii) Cells are homogeneously distributed within the matrix as shown by Merchant (1981) and Wada *et al.* (1981).

(iii) The equilibrium partition coefficient (K_p) of the substrate is unity.

(iv) Film mass transfer resistance is negligible.

(v) The reaction is isothermal.

(vi) Reaction takes place according to simple Michaelis-Menten type of kinetics without substrate and/or product inhibition.

(vii) Substrate is transported through the matrix by molecular diffusion only.

(viii) The effective substrate diffusivity, D_e, within the matrix is constant.

Based on the above, for the spherical coordinate system shown in Figure 3.4, a steady-state substrate balance on a spherical shell of thickness dr and radius r, is given by:

(Rate of diffusion into the shell at r = r + dr)
- (Rate of diffusion out of the shell at r = r)
= Rate of reaction in shell 3.16

Equation 3.16 becomes:

Figure 3.4. Spherical coordinate system for steady-state substrate diffusion and reaction in a spherical shell of thickness dr.

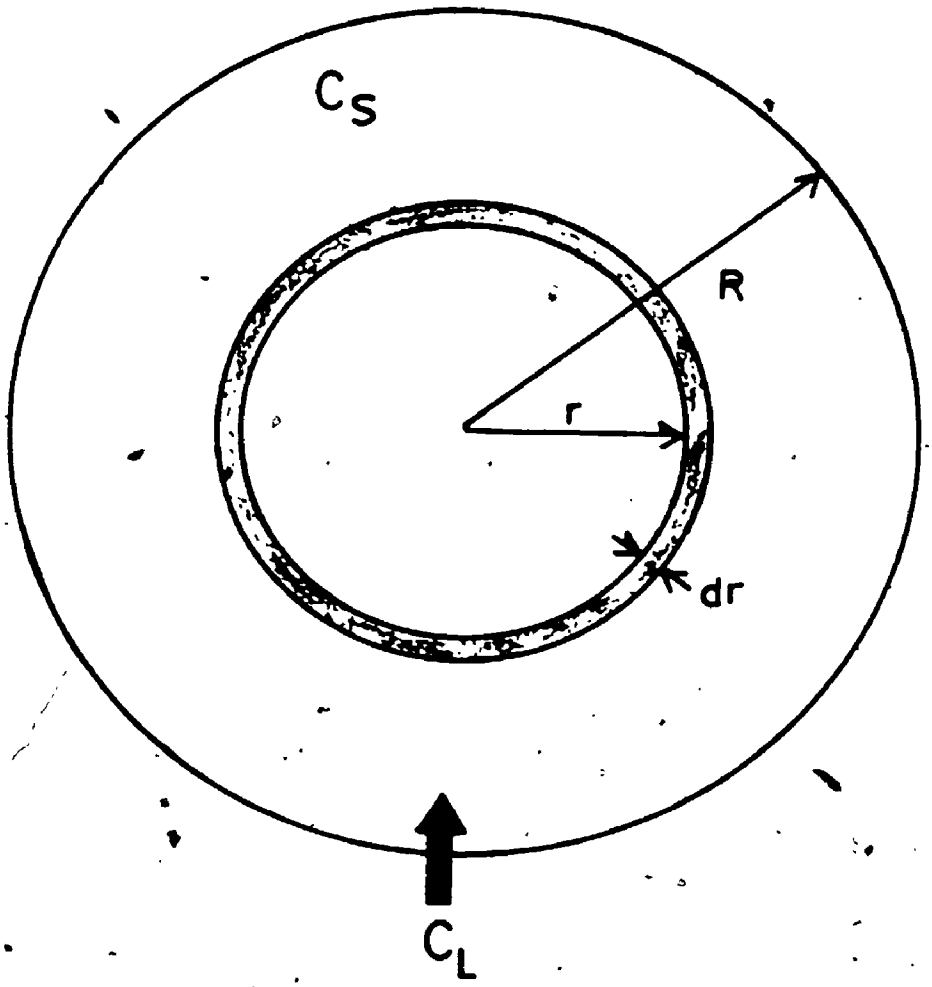
C_S
R
r
dr
C_L

$$4\pi(r + dr)^2 D_e \left[\frac{dC_S}{dr} + \frac{d^2C_S}{dr^2} dr\right] - 4\pi r^2 D_e \frac{dC_S}{dr}$$

$$= 4\pi r^2 dr \left[\frac{V_{max} C_S}{K_m + C_S}\right] \qquad 3.17$$

where $4\pi r^2$ is the inner superficial area of the spherical shell and dC_S/dr is the concentration gradient of the substrate within the sphere at radius r.

Subsequent manipulation of Equation 3.17, yields

$$D_e \left[\frac{d^2C_S}{dr^2} + \frac{2dC_S}{rdr}\right] = \frac{V_{max} C_S}{K_m + C_S} \qquad 3.18$$

with the boundary conditions,

$$C_S = C_L \text{ at } r/R = 1 \qquad 3.19$$

where R is the radius of the sphere, and

$$dC_S/dr = 0 \text{ at } r/R = 0 \qquad 3.20$$

By defining a dimensionless internal substrate concentration

$$\sigma_i = C_S/K_m \qquad 3.21$$

and a dimensionless radial position,

$$\bar{r} = r/R \qquad 3.22$$

Equation 3.18 can be written in a dimensionless form:

$$\frac{d^2\sigma_i}{d(\bar{r})^2} + \frac{2d\sigma_i}{\bar{r}d\bar{r}} = \frac{R^2(V_{max}/K_m D_e)\sigma_i}{1 + \sigma_i} \qquad 3.23$$

From Equation 3.23 it is apparent that the substrate concentration profile within the entrapment matrix depends on the size of the particle, the effective substrate diffusivity in the support, and on the intrinsic kinetic properties of the entrapped biocatalyst. In fact, as first suggested by Thiele (1939), and as shown by Equation 3.24, these three factors can be combined in a single, dimensionless internal substrate modulus for intraparticle diffusion, ϕ_m, which is also known as the modified Thiele modulus (Kennedy and Cabral, 1983; Kuu, 1982; Ryu et al., 1984).

According to Equation 3.24,

$$\phi_m = L \left[\frac{V_{max}}{K_m D_e}\right]^{1/2} \qquad 3.24$$

where L is the characteristic length of the particle. For a sphere, L = R/3 which is the ratio of the sphere volume to the external surface area (Aris, 1957). Thus, the concentration profile of the substrate in the entrapment matrix is

described by the differential equation

$$\frac{d^2\sigma_i}{d(\bar{r})^2} + \frac{2d\sigma_i}{\bar{r}d\bar{r}} = 9\phi_m^2 \frac{\sigma_i}{1 + \sigma_i} \qquad 3.25$$

with the boundary conditions

$$\sigma^* = \sigma_i \Big|_{\bar{r}=1} = \sigma_o \qquad 3.26$$

and

$$\frac{d\sigma_i}{d\bar{r}} = 0 \text{ at } \bar{r} = 0 \qquad 3.27$$

In Equation 3.26 it is implicitly assumed that the film mass transfer resistance is negligible and, consequently, the dimensionless substrate concentration at the particle surface (σ^*) is equal to the dimensionless bulk substrate concentration (σ_o). For convenience, σ_o will therefore be used throughout the remainder of this section instead of σ^*.

Using numerical methods, Engasser and Horvath (1973) solved the above non-linear boundary value problem (Equations 3.25 to 3.27) to obtain the radial substrate concentration profile as a function of ϕ_m and σ_o. Figure 3.5 shows the substrate concentration profile within a sphere for different values of ϕ_m when σ_o is unity. Concentration profiles for other values of σ_o are similar to those shown in Figure 3.5 (Engasser and Horvath, 1973). This figure

Figure 3.5. Substrate concentration profile in a spherical cell immobilization matrix. The dimensionless internal substrate concentration (σ_1) is plotted as a function of the radial position ($\bar{r}$) with the modified Thiele modulus (ϕ_m) as the variable parameter. The dimensionless bulk substrate concentration, σ_o, is unity (Adapted from Engasser and Horvath, 1973).

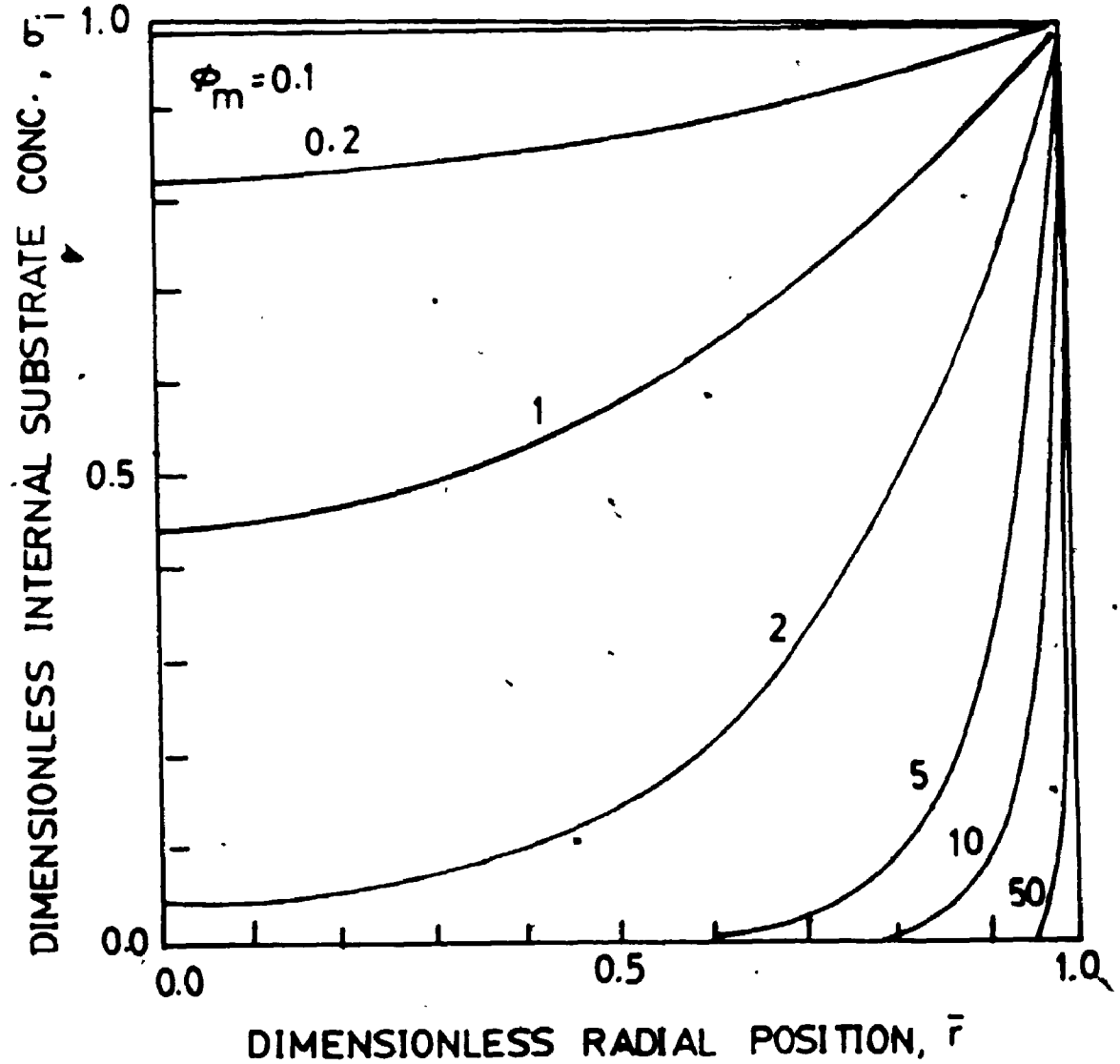
1.0
0.5
0.0
0.0
0.5
1.0
$\phi_m = 0.1$
0.2
1
2
5
10
50
DIMENSIONLESS INTERNAL SUBSTRATE CONC., σ_i
DIMENSIONLESS RADIAL POSITION, $\bar{r}$

demonstrates that at any given value of $\bar{r}$, the effective substrate concentration in the matrix (σ_i) decreases with increasing values of ϕ_m. Additionally, the steepness of the substrate concentration gradient increases with increasing ϕ_m. Thus for large values of ϕ_m (i.e. $\phi_m > 10$), most of the entrapment matrix will be completely devoid of the substrate and therefore only a thin outer shell of the spherical particle will participate in the biocatalytic reaction.

Knowledge of the substrate concentration profile facilitates the determination of the effective rate of reaction, $\bar{V}$, in the entire volume of the entrapment matrix using the following integral equation (Engasser and Horvath, 1973):

$$\bar{V} = 3\, V_{max} \int_{\bar{r}=0}^{\bar{r}=1} \frac{\sigma_i}{1 + \sigma_i} \cdot (\bar{r})^2 \, d\bar{r} \qquad 3.28$$

Numerical integration of Equation 3.28 yields the dimensionless effective rate of reaction ($\bar{V}/V_{max}$) as a function of the dimensionless bulk substrate concentration, σ_o, and ϕ_m. This relationship is plotted in Figure 3.6. For $\phi_m < 1$, the reaction is essentially kinetically controlled; at higher values of ϕ_m, the rate of reaction is slower due to substrate depletion. Comparison of Figures 3.2 and 3.6 shows that the effects of internal diffusional limitations are much more pronounced than those arising from external film mass transfer resistance for comparable values of the

Figure 3.6. The dimensionless effective rate of reaction ($\bar{V}/V_{max}$) in a spherical cell entrapment matrix plotted as a function of the dimensionless bulk substrate concentration, σ_0, with the modified Thiele modulus, ϕ_m as the variable parameter (Adapted from Engasser and Horvath, 1973).

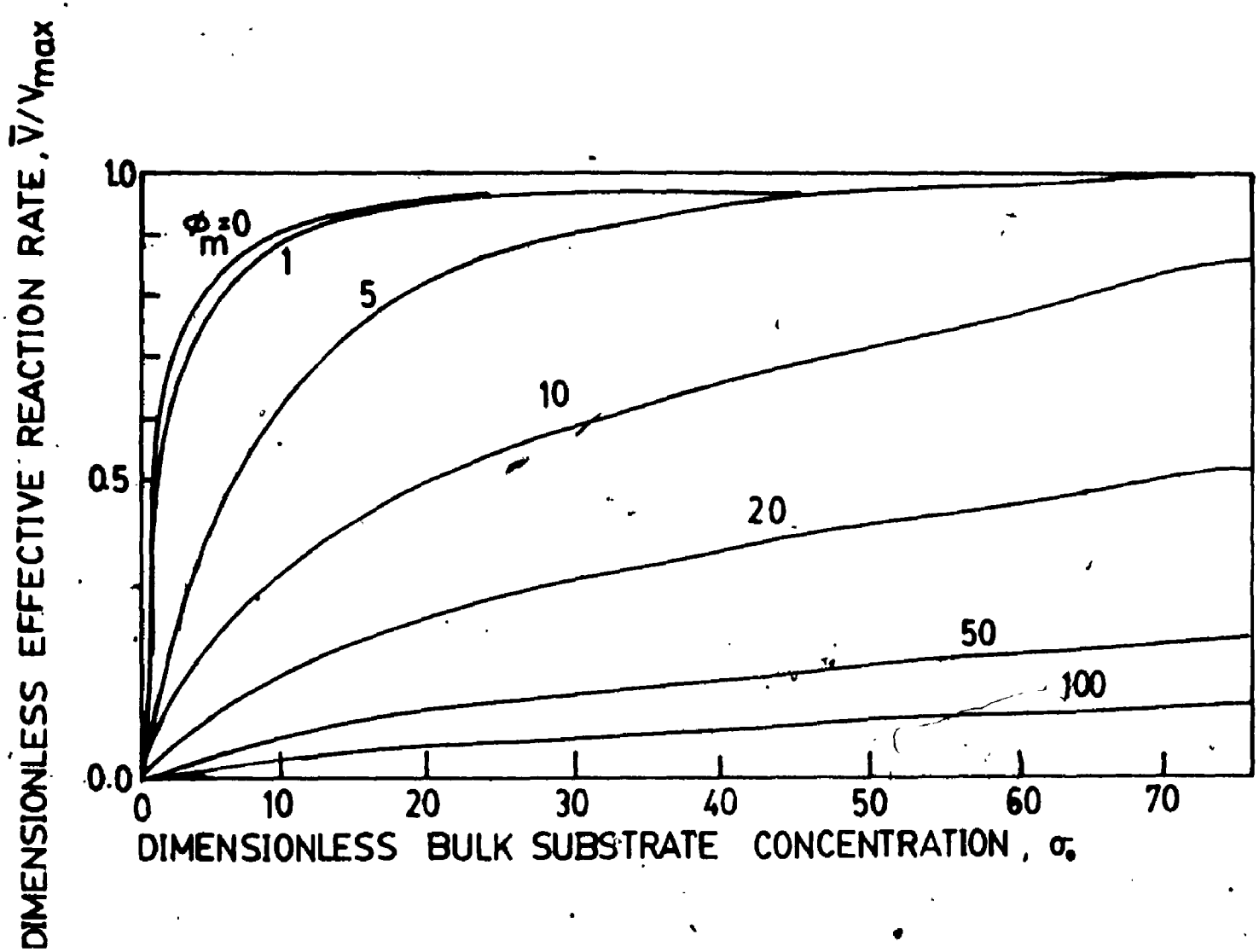
DIMENSIONLESS EFFECTIVE REACTION RATE, $\bar{V}/V_{max}$
1.0
0.5
0.0
$\phi_m = 0$
1
5
10
20
50
100
0
10
20
30
40
50
60
70
DIMENSIONLESS BULK SUBSTRATE CONCENTRATION, σ_0

substrate moduli (Engasser and Horvath, 1976; Goldstein, 1976).

The magnitude of intraparticle mass transfer resistance can be characterized by the internal effectiveness factor, η_I, which is generally defined by Equation 3.2. More specifically, η_I is expressed by the following equation (Lee et al., 1981):

$$\eta_I = \frac{\bar{V}}{V_{max}} \left[\frac{1 + \sigma_o}{\sigma_o} \right] \qquad 3.29$$

As expected from the concentration profiles in Figure 3.6, η_I is a function of ϕ_m and σ_o (Bischoff, 1965; Satterfeld, 1970) and the relationship is illustrated in Figure 3.7.

When ϕ_m is smaller than 0.2, η_I is practically unity for all surface concentrations (Figure 3.7), so that internal mass transfer resistance does not affect the overall rate of reaction. When σ_o approaches zero ($C_L \ll K_m$), η_I converges to the effectiveness factor of the corresponding first-order reaction, η_I^1, which is expressed as follows (Rovito and Kittrell, 1973; Bailey and Ollis, 1977; Bailey and Cho, 1983).

$$\eta_I^1 = \frac{1}{\phi_m^1} \left[\frac{1}{\tanh 3\phi_m^1} - \frac{1}{3\phi_m^1} \right] \qquad 3.30$$

In Equation 3.30, ϕ_m^1 is the modified first-order Thiele

3.4.3 Combined Influence of External and Internal Diffusional Resistances and Partitioning Effects

In practice, the simultaneous effects of external and internal diffusional resistances are likely to have a significant influence on the effective reaction rates in industrial scale immobilized cell and enzyme reactors (Venkatsubramanian et al., 1983). Thus, when the extent of external film mass transfer resistance cannot be neglected, the dimensionless form of the equation for diffusion-reaction at steady state in a sphere is given by Equation 3.33 (Yamane et al., 1981),

$$\frac{d^2z}{d(\bar{r})^2} + \frac{2dz}{\bar{r}d\bar{r}} = \frac{(\kappa + 1)z}{(\kappa + z)} \qquad 3.33$$

subject to the following boundary conditions

$$dz/d\bar{r} = 0 \quad \text{at } \bar{r} = 0 \qquad 3.34$$

$$\left[\frac{dz}{d\bar{r}}\right]_S^* = N_{Bi}\left[1 - \frac{C_L^*}{C_L}\right] \quad \text{at } \bar{r} = 1 \qquad 3.35$$

where $(dz/dr)_S^*$ is the dimensionless substrate concentration gradient at the particle surface, C_L^* is the substrate concentration in the liquid phase at the solid-liquid inter-

Figure 3.7. The internal effectiveness factor, η_I, of a spherical cell entrapment matrix plotted as a function of the modified Thiele modulus, ϕ_m, with the dimensionless bulk substrate concentration, σ_o, as the variable parameter. (Adapted from Engasser and Horvath, 1973).

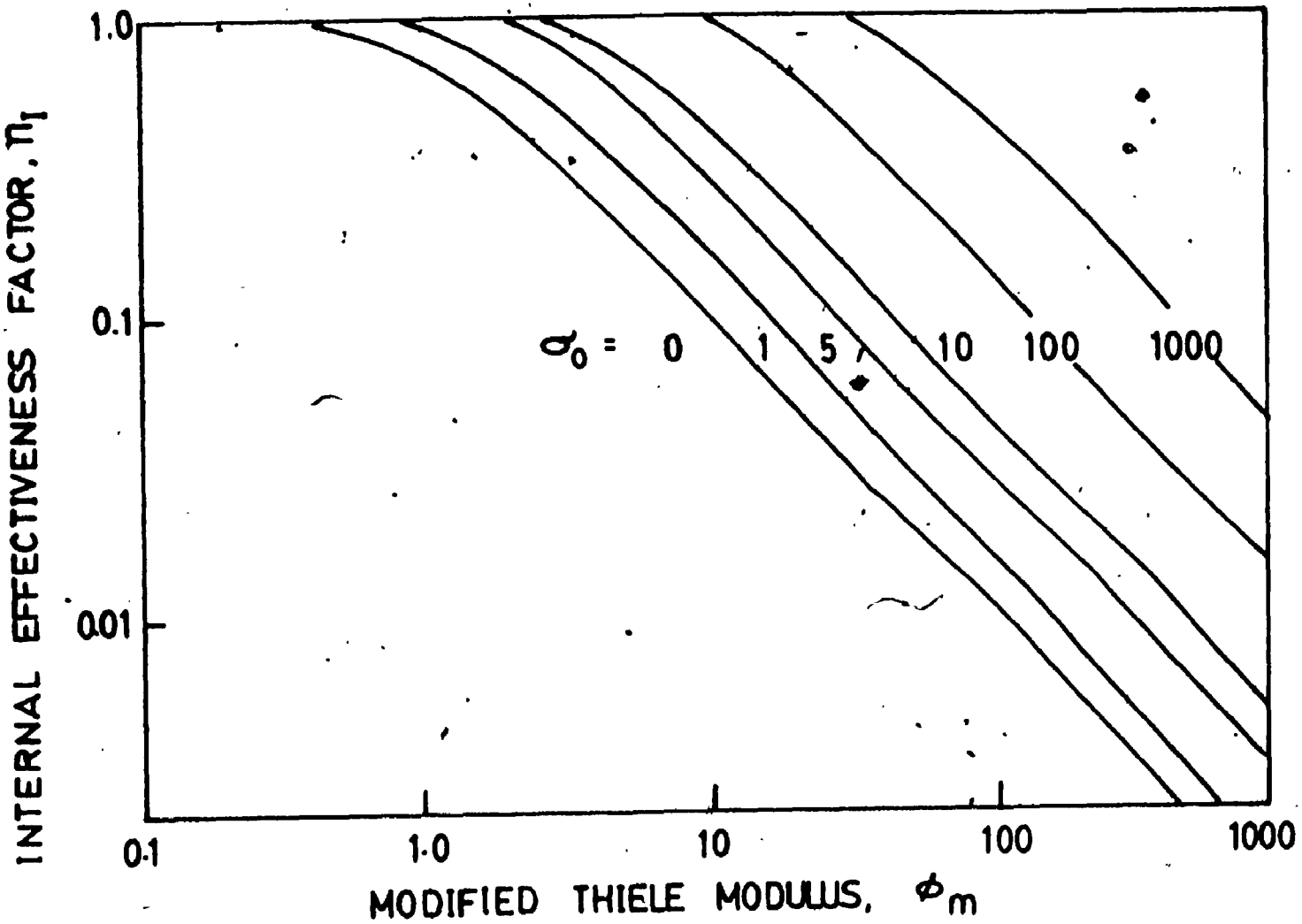
1.0
0.1
0.01
0.1
1.0
10
100
1000
INTERNAL EFFECTIVENESS FACTOR, η_I
MODIFIED THIELE MODULUS, ϕ_m
α_0 = 0 1 5 10 100 1000

modulus which is defined by,

$$\phi_m^1 = \frac{R}{3}\left[\frac{k^1}{D_e}\right]^{1/2} \qquad 3.31$$

where k^1 is the intrinsic first-order rate constant.

A practical problem arises in the use of effectiveness factor correlations of the form given in Equations 3.30 and 3.31, because the intrinsic rate parameters, needed to solve these equations, are frequently unknown. To circumvent this problem, Weisz (1973) developed a powerful relationship between η_I and an observable modulus, Φ, defined by Equation 3.32, which is also known as the generalized Thiele modulus.

$$\Phi = \frac{R^2}{9}\left[\frac{\bar{V}}{D_e C_L}\right] \qquad 3.32$$

The concept of Φ which was conceived independently by Aris (1965a; 1965b) and Bischoff (1965) is especially powerful, since the relationship between η_I and system parameters is expressed in terms of observable quantities. Thus, as shown by Equation 3.32, Φ is independent of the intrinsic kinetic parameters. Plots of η_I versus Φ for $\sigma_o \to 0$ (first-order) and $\sigma_o \to \infty$ (zero-order) are given in Figure 3.8. Thus, at high substrate concentrations ($C_L >> K_m$), η_I can be estimated from the η_I versus Φ plot at $\sigma_o = \infty$, and V_{max} calculated from Equation 3.29 (Lee et al., 1981).

Figure 3.8. The internal effectiveness factor, η_I, of a spherical cell entrapment matrix plotted as a function of the observable modulus, ϕ. (Adapted from Bailey and Ollis, 1977).

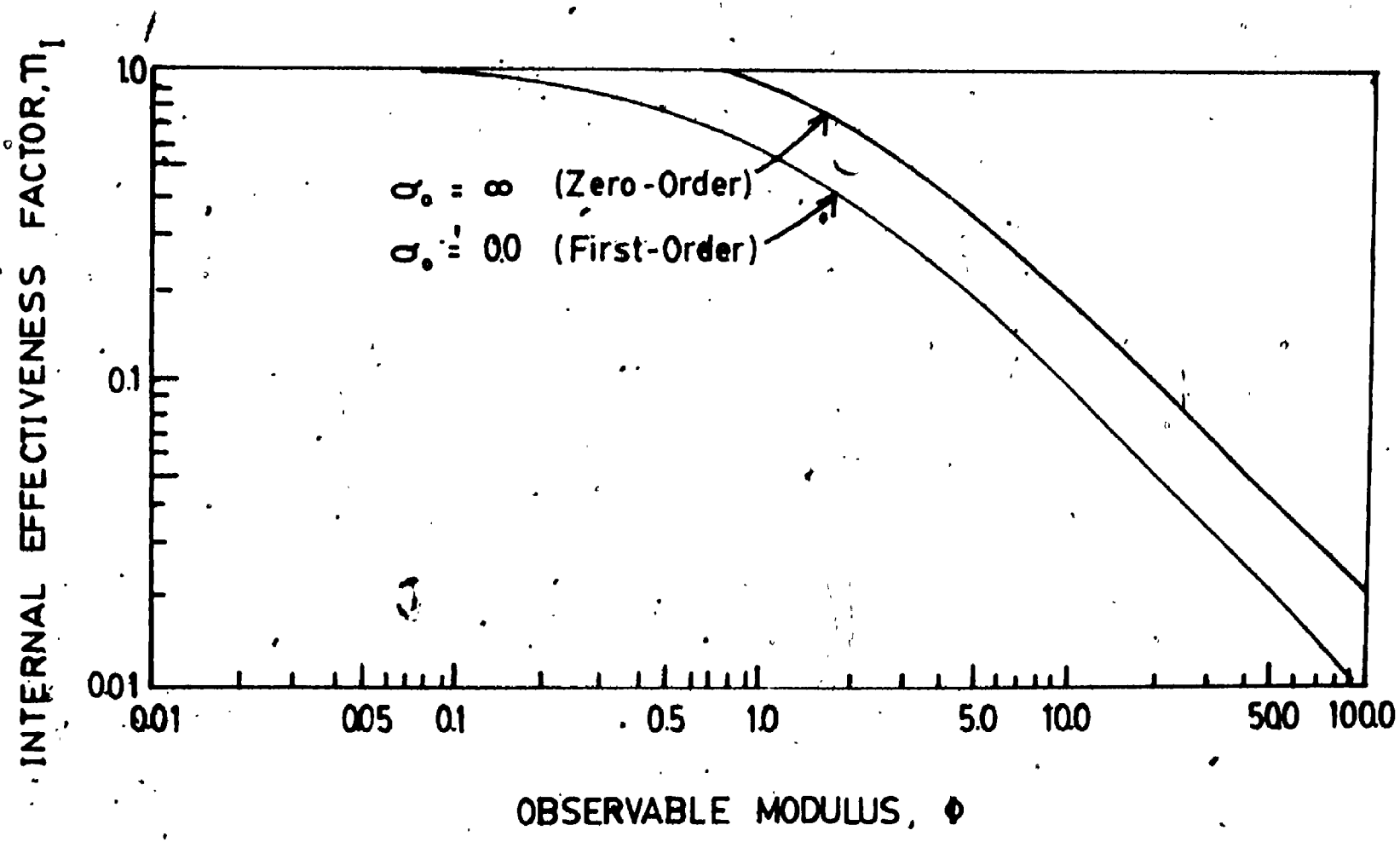
INTERNAL EFFECTIVENESS FACTOR, η_I
1.0
0.1
0.01
$\alpha_0 = \infty$ (Zero-Order)
$\alpha_0 = 0.0$ (First-Order)
0.01
0.05
0.1
0.5
1.0
5.0
10.0
50.0
100.0
OBSERVABLE MODULUS, Φ

3.4.3 Combined Influence of External and Internal Diffusional Resistances and Partitioning Effects

In practice, the simultaneous effects of external and internal diffusional resistances are likely to have a significant influence on the effective reaction rates in industrial scale immobilized cell and enzyme reactors (Venkatsubramanian et al., 1983). Thus, when the extent of external film mass transfer resistance cannot be neglected, the dimensionless form of the equation for diffusion-reaction at steady state in a sphere is given by Equation 3.33 (Yamane et al., 1981),

$$\frac{d^2z}{d(\bar{r})^2} + \frac{2dz}{\bar{r}d\bar{r}} = \frac{(\kappa + 1)z}{(\kappa + z)} \qquad 3.33$$

subject to the following boundary conditions

$$dz/d\bar{r} = 0 \quad \text{at } \bar{r} = 0 \qquad 3.34$$

$$\left[\frac{dz}{d\bar{r}}\right]_S^* = N_{Bi}\left[1 - \frac{C_L^*}{C_L}\right] \quad \text{at } \bar{r} = 1 \qquad 3.35$$

where $(dz/dr)_S^*$ is the dimensionless substrate concentration gradient at the particle surface, C_L^* is the substrate concentration in the liquid phase at the solid-liquid inter-

face, z is the dimensionless substrate concentration given by,

$$z = C_S/C_L \qquad 3.36$$

κ is the dimensionless saturation constant defined earlier by Equation 3.5, ϕ is the Thiele modulus for Michaelis-Menten type of kinetics which is expressed by Equation 3.37,

$$\phi = R \left[\frac{V_{max}}{D_e(K_m + C_L)} \right]^{1/2} \qquad 3.37$$

and N_{Bi} is the mass-transfer Biot number defined by Equation 3.38.

$$N_{Bi} = k_L R/D_e \qquad 3.38$$

Accordingly, N_{Bi} expresses the relative magnitude of external and internal mass transfer resistances. Thus, the higher the value of N_{Bi} the smaller is the effect of external film mass transfer resistance on the overall rate of reaction (Carberry, 1976). In Equation 3.35, the boundary condition, $C_L = C_L^*$ at $\bar{r} = 1$, corresponds to the case when $N_{Bi} = \infty$, i.e. negligible film mass transfer resistance.

In the presence of partitioning effects, a steep concentration change occurs at the solid-liquid interface, and the concentration of the substrate at the gel surface, C_S^*

can be expressed mathematically as:

$$C_S^* = K_p C_L^* \qquad 3.39$$

Assuming rapid equilibration at the solid-liquid interface, the boundary condition given by Equation 3.35 can be rewritten in the form,

$$\left[\frac{dz^*}{d\bar{r}}\right]_S^* = N_{Bi}\left[1 - \frac{z^*}{K_p}\right] \quad \text{at } \bar{r} = 1 \qquad 3.40$$

where, z^* has been defined earlier by Equation 3.4.

Under conditions of combined external and internal mass transfer resistances and partitioning effects, the "overall effectiveness factor" designated by $\bar{\eta}$ can also be defined by Equation 3.2 (Fink et al., 1973; Hamilton et al., 1974).

For the spherical geometry, $\bar{\eta}$ is generally expressed by Equation 3.41 (Yamane et al., 1981).

$$\bar{\eta} = \frac{3}{\phi^2}\left[\frac{dz}{d\bar{r}}\right]_S^* \qquad 3.41$$

where $(dz/dr)_S^*$ is obtained from the solution of Equation 3.33 under the appropriate boundary conditions. Analytical and graphical solutions for determining $\bar{\eta}$ as a function of ϕ, κ, N_{Bi} and K_p have been presented by Yamane et al., (1981) and will be summarized in the remainder of this

section.

For an immobilized spherical biocatalyst exhibiting first-order kinetics, the first-order overall effectiveness factor, $\bar{\eta}_1$ is expressed analytically by Equation 3.42.

$$\frac{1}{\bar{\eta}_1} = \frac{\phi_1^2}{3K_p\ (\phi_1 \coth \phi_1 - 1)} + \frac{\phi_1^2}{3N_{Bi}} \qquad 3.42$$

where ϕ_1 is the first-order Thiele modulus defined by Equation 3.43.

$$\phi_1 = R\ (k_1/D_e)^{1/2} \qquad 3.43$$

In the case of zero-order kinetics ($C_L >> K_m$), the zero-order overall effectiveness factor, $\bar{\eta}_o$, can be expressed as follows:

$$\text{when } \phi_o \geq \left[\frac{6}{1/K_p + 2/N_{Bi}}\right]^{1/2}, \text{ then } \frac{1}{\phi_o^2} = \frac{\bar{\eta}_o}{3N_{Bi}}$$

$$= \frac{1}{6K_p}\left[1 - (1 - \bar{\eta}_o)^{1/3}\right]^2 \left[2(1 - \bar{\eta}_o)^{1/3} + 1\right] \qquad 3.44$$

where, ϕ_o is the zero-order Thiele modulus defined by Equation 3.45

$$\phi_o = R \left[\frac{V_{max}}{C_L D_e} \right]^{1/2} \qquad 3.45$$

However, if $K_p/N_{Bi} < 3/2$ and $K_p/N_{Bi} \neq 1$, then Equation 3.44 may be rewritten in the form,

$$\bar{\eta}_o = 1 - \left[\frac{1/2 + \cos(\Theta/3 + 4\pi/3)}{1 - K_p/N_{Bi}} \right]^3 \qquad 3.46$$

where,

$$\Theta = \cos^{-1} \left(1 - 4 \left[1 - \frac{K_p}{N_{Bi}} \right]^2 \left[\frac{K_p}{N_{Bi}} + \frac{1}{2} - \frac{3K_p}{\phi_o^2} \right] \right) \qquad 3.47$$

Furthermore, for the case when $K_p/N_{Bi} = 1$, Equation 3.44 is simplified and written as

$$\bar{\eta}_o = 1 - \left[1 - \frac{2K_p}{\phi_o^2} \right]^{3/2} \qquad 3.48$$

Additionally, when

$$\phi_o < \left[\frac{6}{1/K_p + 2/N_{Bi}} \right]^{1/2}, \text{ then } \bar{\eta}_o = 1 \qquad 3.49$$

If the intrinsic reaction rate is expressed by Michaelis-Menten type of kinetic behaviour, $\bar{\eta}$ can be obtained by the numerical solution of Equation 3.33. Yamane et

al., (1981) computed $\bar{\eta}$ as a function of ϕ, κ and N_{Bi} when K_p = 0.5 and 3.0 and results for the spherical geometry have been plotted in Figures 3.9 and 3.10, respectively. Thus, as shown in these figures, when K_p exceeds unity, its large value compensates for the decreases in $\bar{\eta}$ due to internal and/or external diffusional limitations, resulting in an overall increase in $\bar{\eta}$. Conversely, when K_p is less than unity, the decrease in $\bar{\eta}$ due to diffusional resistance is compounded by the decrease in $\bar{\eta}$ due to the low value of K_p, leading to a further decrease in $\bar{\eta}$.

Instead of the tedious numerical methods used to compute the overall effectiveness factors for intrinsic Michaelis-Menten type of kinetic behaviour, Yamane, (1981) proposed an approximate algebraic expression for estimating $\bar{\eta}$. Accordingly,

$$\bar{\eta} = \frac{\bar{\eta}_o + 2.6\kappa^{0.8}\bar{\eta}_1}{1 + 2.6\kappa^{0.8}} \qquad 3.50$$

where, $\bar{\eta}_o$ and $\bar{\eta}_1$ are, respectively, the zero-order and first-order overall effectiveness factors expressed by equations presented earlier, except that ϕ_o and ϕ_1 are replaced by ϕ, which is defined by Equation 3.37. The absolute values of the relative errors in $\bar{\eta}$ obtained by using the approximate solution, were less than 3% when compared to the values determined using numerical methods (Yamane, 1981).

Figure 3.9. The overall effectiveness factor for a spherical biocatalyst, $\bar{\eta}$, plotted as a function of the Thiele modulus, ϕ, with the Biot number (N_{Bi}), and dimensionless saturation constant ($\kappa = 1/\sigma_o$), as the variable parameters when $K_p = 0.5$ (From Yamane, 1981).

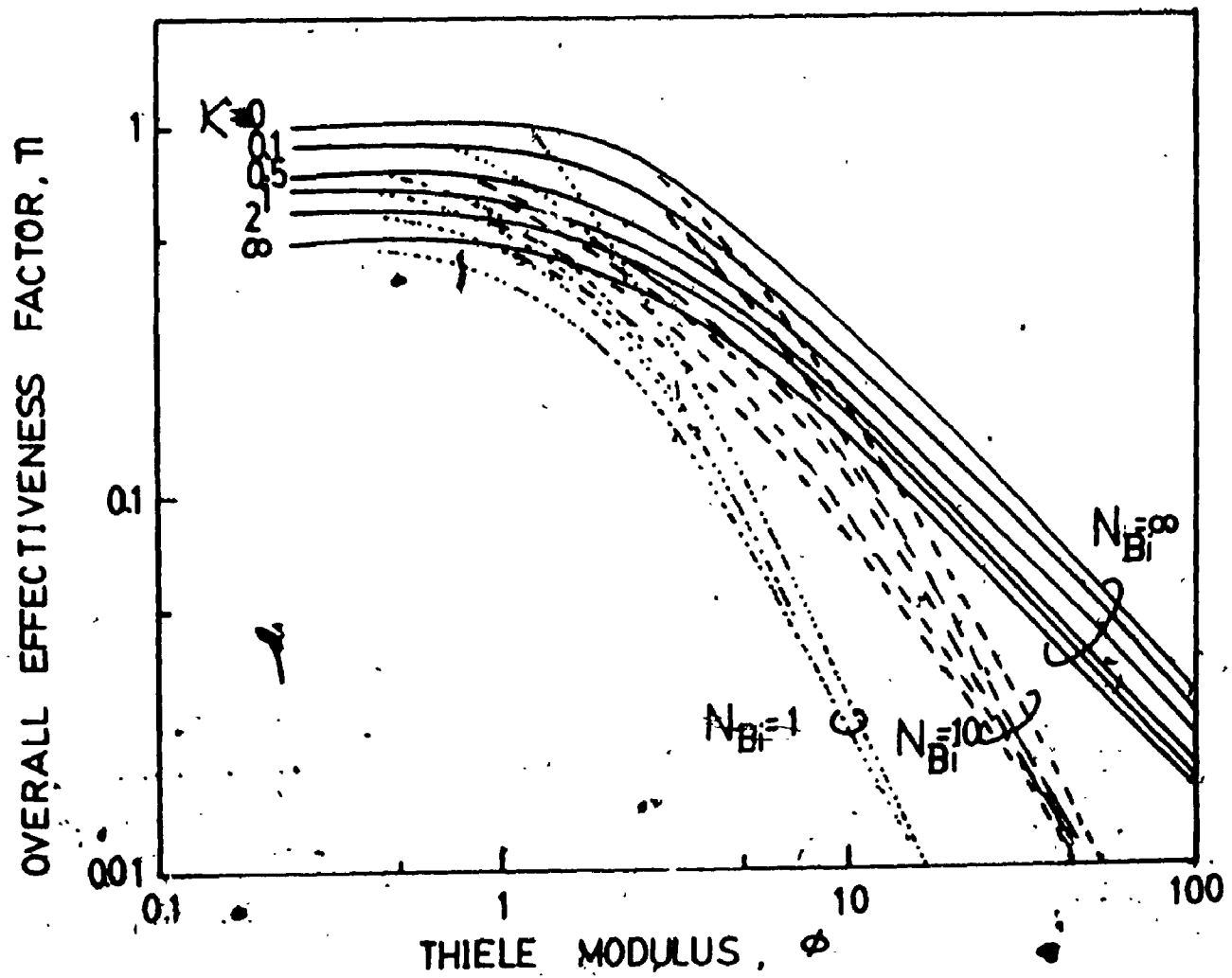
OVERALL EFFECTIVENESS FACTOR, $\bar{\eta}$
THIELE MODULUS, ϕ
1
0.1
0.01
0.1
1
10
100
K=0
0.1
0.5
1
2
8
$N_{Bi}=\infty$
$N_{Bi}=1$
$N_{Bi}=100$

Figure 3.10. The overall effectiveness factor for a spherical biocatalyst, $\bar{\eta}$, plotted as a function of the Thiele modulus, ϕ, with the Biot number (N_{Bi}), and dimensionless saturation constant ($\kappa = 1/\sigma_o$), as the variable parameters when $K_p = 3.0$ (From Yamane, 1981).

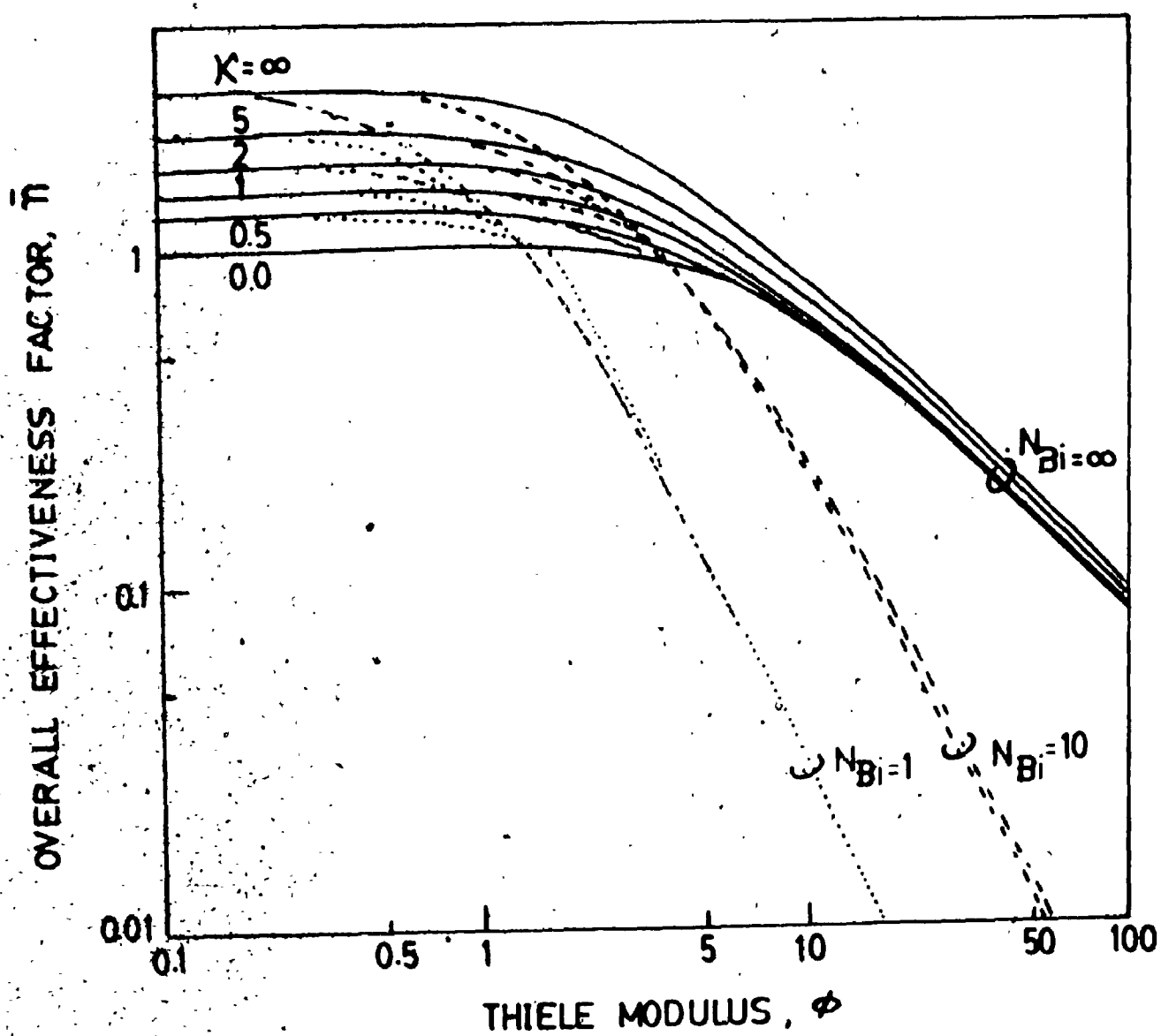
K=∞
5
2
1
0.5
0.0
1
0.1
0.01
0.1
0.5
1
5
10
50
100
OVERALL EFFECTIVENESS FACTOR, η̄
THIELE MODULUS, φ
N_Bi=∞
N_Bi=1
N_Bi=10

3.5 Statement of the Problem

In order to design and scale-up entrapped cell bioreactor systems and make them viable alternatives to conventional fermentation processes, it is imperative that suitable methods exist to determine the effectiveness factors (η) of the immobilized cells (Radovich, 1985; Karel, et al., 1985; Venkatsubramanian et al., 1983). Two general approaches may be used to evaluate η.

(a) As shown in Sections 3.4.1 to 3.4.3, η may be expressed mathematically by a number of well established correlations incorporating the appropriate substrate moduli such as the Damköhler number (Da, Dá) or the Thiele modulus (ϕ, ϕ_m). Depending on the complexity of the reaction rate equation, η can be accurately evaluated using analytical and/or numerical methods, or, alternatively, may be approximated using suitable graphical solutions (i.e. see Figures 3.3 and 3.7). Prior knowledge of the intrinsic rate parameters (V_{max} and K_m) is however required to determine the substrate moduli. A number of experimental methods may be used to determine V_{max} and K_m and these have been reviewed by Engasser and Horvath (1976). Unfortunately, most of these methods are applicable only under a limited set of well defined conditions (Hamilton et al., 1974; Gondo et al., 1975; Engasser and Horvath, 1973; Engasser, 1978), and, in certain cases, may present practical difficulties (Goldstein, 1976;

Lee et al., 1981).

(b) An attractive alternative is therefore to employ correlations in which the intrinsic rate parameters are not required (Karel et al., 1985). As shown in Sections 3.4.1 and 3.4.2 solutions of η_E and η_I expressed in terms of observable moduli such as Da and ϕ respectively, are available and may therefore be preferentially used for determining the appropriate effectiveness factor.

In both of the above cases, quantitative values of the physical parameters (i.e. k_L and $\bar{D}_e$) are also required for the determination of η. The former may be estimated from suitable correlations or determined experimentally. For instance, as mentioned earlier, the film mass transfer coefficient on the surface of an entrapment matrix can be estimated from literature correlations.

The influence of internal mass transfer resistance on the overall rate of reaction can be observed by reducing the particle size until no further increase in the reaction rate occurs (Buchholz, 1982). This final rate is then assumed to be the intrinsic rate of reaction and by applying Equation 3.2, the effectiveness factor can be calculated. Frequently a substantial size reduction of the entrapment matrix may be required which can only be achieved by crushing the gel matrix (Jain and Ghose, 1984). This procedure can have deleterious effects on the size and structure of the pores

within the entrapment matrix and consequently will mask the true intrinsic kinetic parameters (Weetall and Pitcher, 1986). Therefore, reliable estimates of the Thiele moduli, intrinsic rate parameters and consequently, the effectiveness factor can only be made if accurate values of the effective substrate diffusivity (D_e) within immobilization matrices are available.

For inorganic porous chemical catalysts D_e can be related to the diffusivity of the substrate in solution (D) by a well established correlation (Satterfield, 1970) given by Equation 3.51.

$$D_e = D \frac{\varepsilon}{\tau} \qquad 3.51$$

where ε is the porosity, and τ is the tortuosity of the porous support. In the case of gel-entrapment matrices, and τ cannot be directly determined (Pitcher, 1978; Radovich, 1985) and therefore Equation 3.51 is of little use. Additionally, gel-entrapment matrices prepared from biopolymers, such as alginates, are mechanically weak when compared to other solids. Therefore, conventional diffusivity measurement techniques may not be suitable to determine D_e in such immobilization supports and this problem has been frequently cited as a major limitation for predicting the effectiveness factors (Bailey and Ollis, 1977; Pitcher, 1978; Brink and Tramper, 1986; Weetall and Pitcher, 1986).

The need to develop a suitable experimental method of

measuring D_e in biological gels used for cell immobilization is therefore readily apparent. In the following section, the theoretical and practical considerations leading to the development of a novel diffusivity measurement technique will be discussed.

3.6 Measurement of Solute Diffusivities in Alginate Gels: Theoretical and Practical Considerations

Steady-state or unsteady-state mass transfer in solids immersed in dilute solutions may be employed to directly measure effective solute diffusivities (D_e). Under steady-state conditions, Fick's 1st Law provides the basic definition for D_e (which is assumed to be constant)

$$J = -D_e \, (\partial C_S/\partial x) \qquad 3.52$$

where, J is the diffusion induced flux in the x-direction and $\partial C_S/\partial x$ is the solute concentration gradient in that direction. A general form of Fick's 2nd Law which can be used to analyze unsteady-state diffusion in symmetric solids immersed in dilute solutions, is given by Equation 3.53.

$$\frac{\partial C_S}{\partial t} = \frac{1}{x^{n-1}} \cdot \frac{\partial}{\partial x} \left[x^{n-1} D_e \frac{\partial C_S}{\partial x} \right] \qquad 3.53$$

where n is either 1, 2 or 3 for an infinite slab, an infinite cylinder or a sphere, respectively, and x is the dis-

tance measured from the center of the solid (Cranks, 1975).

3.6.1 Steady-State Methods of Diffusivity Measurement

A common method of measuring solute diffusivities in solids and polymeric membranes is by using the diaphragm-diffusion cell in which two well mixed reservoirs are separated by a thin permeable disc or sheet (Cussler, 1984). Using the solution to Fick's first law of diffusion, the D_e value can be easily calculated based on concentration changes that occur in the two half-cells after a time-lag. However, with mechanically weak gels such as alginates, problems associated with gel rupture and/or leakage between the two compartments limits the use of this technique (White, 1960). As shown by Hannoun and Stephanopoulos (1986), this problem is exacerbated when whole cells are entrapped within the alginate gel since the immobilization procedure is associated with a further deterioration in the mechanical stability of the entrapment matrix (see Section 2.4 and Table 2.2).

Alternatively, a cylindrical gel may be used with the capillary method or the diffusion cell. However, for solutes with low D_e values, it may take several days to obtain a steady-state solute concentration profile within the gel and therefore such time-lag techniques can be impractically long (Cussler, 1984; Michaels et al., 1963). Thus, the use of unsteady-state techniques for measuring D_e are generally

preferred (Geankoplis, 1972).

Additionally, for certain types of entrapment matrices, preparation of discs or cylindrical gels of uniform size and shape for use in conventional diffusion cells can be difficult since gelation is frequently associated with contraction of the matrix (Spalding, 1969). For instance, in the case of calcium alginate, which undergoes synerisis during gel formation (see Section 2.4.2), preparation of membranes with uniform thickness can be a problem and consequently, any inconsistency in the membrane thickness introduces serious errors in the measured values of D_e (Hannoun and Stephanopoulos, 1986).

In view of the limitations associated with the use of the diaphragm-diffusion cell, design of a novel unsteady-state technique of measuring D_e which does not have deleterious effects on the integrity of the alginate entrapment matrix even at high cell loadings, would be very desirable. Since spherical alginate gels can be easily prepared and are preferentially used in immobilized cell bioreactors (Margaritis and Merchant, 1984; 1987), equations describing unsteady-state mass transfer in a sphere are presented below.

3.6.2 Unsteady-State Diffusion in a Sphere

In order to develop suitable equations for determining solute diffusivities in spheres using unsteady-state

(i) The solute is uniformly distributed throughout the sphere at time, $t = 0$.

(ii) Diffusion occurs radially outwards, there being no concentration variation with angular position and the physical properties (including D_e) of the sphere are constant.

(iii) The external liquid film mass transfer resistance is negligible.

(iv) As in Equations 3.52 and 3.53 the density of the liquid phase is assumed to be constant.

Equation 3.54 is a mass balance for unsteady-state diffusion of a solute in a sphere using the spherical coordinate system shown in Figure 3.11.

$$\frac{\partial C_S}{\partial t} = D_e \left[\frac{\partial^2 C_S}{\partial r^2} + \frac{2\partial C_S}{r\partial r} \right] \qquad 3.54$$

The final solution of Equation 3.54 depends on the initial and boundary conditions as discussed below for two different cases, namely, when the sphere is immersed in an infinite liquid volume, and when the volume of the liquid is finite.

3.6.2.1 Case 1: Sphere Immersed in an Infinite Liquid Volume

If we consider a single sphere containing the solute,

Figure 3.11. Spherical coordinate system for unsteady-state diffusion of a solute under different initial and boundary conditions.

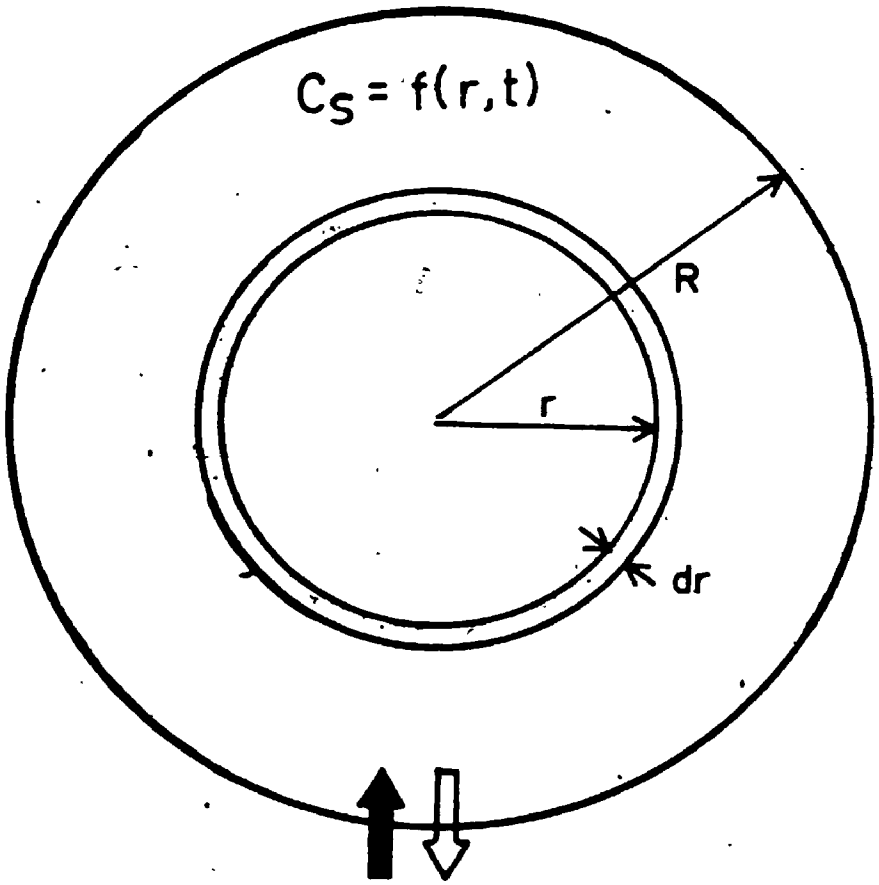

CASE 1 : C_L = CONSTANT

CASE 2 : $C_L = f(t)$

immersed in an infinite liquid phase, then based on the assumptions stated earlier, the initial and boundary conditions are as follows:

$$t = 0, \quad 0 \leq r \leq R, \quad C_S = \text{constant} \qquad \text{I.C. 1}$$

$$t = 0, \quad r > R, \; C_L = 0 \qquad \text{I.C. 2}$$

$$t > 0, \; r = 0, \quad \frac{\partial C_S}{\partial r} = 0 \qquad \text{B.C. 1}$$

$$t > 0, \; r = R, \; C_S = C_L = 0 \qquad \text{B.C. 2}$$

The solution of Equation 3.54 using the above initial and boundary conditions gives the function $C_S(r,t)$. Integration of this function throughout the sphere gives Equation 3.55 (Skelland, 1974).

$$\frac{\overline{C_S^t}}{C_S^0} = \frac{6}{\pi^2} \sum_{n=1}^{\infty} \frac{1}{n^2} \exp\left[- \frac{D_e n^2 \pi^2 t}{R^2} \right] \qquad 3.55$$

where $\overline{C_S^t}$ and C_S^0 are respectively, the average solute concentration in the sphere at time t, and the initial solute concentration in the sphere. The total amount of the solute leaving the sphere is given by Equation 3.56,

$$\frac{M_S^t}{M_S^0} = 1 - \frac{6}{\pi^2} \sum_{n=1}^{\infty} \frac{1}{n^2} \exp\left[- \frac{D_e n^2 \pi^2 t}{R^2} \right] \qquad 3.56$$

where M_S^t/M_S^0 is the ratio of the amount of solute remaining at time, t, (M_S^t), to the total amount of solute originally present in the sphere (M_S^0). Similarly for the case when the sphere is initially free from solute and the solute diffuses into the sphere from an infinite liquid source, the solution to Equation 3.54 is given by Equation 3.57.

$$\frac{M_S^t}{M_S^\infty} = 1 - \frac{6}{\pi^2} \sum_{n=1}^{\infty} \frac{1}{n^2} \exp\left[-\frac{D_e n^2 \pi^2 t}{R^2}\right] \qquad 3.57$$

where M_S^t/M_S^∞ is the ratio of the amount of solute in the sphere at time t, to that at infinite time at equilibrium.

3.6.2.2 Case 2: Sphere Immersed in a Finite Liquid Phase

When a single sphere containing the solute is immersed in a well stirred liquid phase of limited volume initially free of the solute, then the initial and boundary conditions are as follows:

$$t = 0, \quad 0 < r < R, \quad C_S = \text{constant} \qquad \text{I.C. 1}$$

$$t = 0, \quad r > R, \quad C_L = 0 \qquad \text{I.C. 2}$$

$$t > 0, \quad r = 0, \quad \frac{\partial C_S}{\partial r} = 0 \qquad \text{B.C. 1}$$

$$t > 0, \quad r = R, \quad V_L \frac{\partial C_L}{\partial t} = K_p A_S D_e \left.\frac{\partial C_S}{\partial r}\right|_{r=R} \qquad \text{B.C. 2}$$

Assuming a linear equilibrium relationship, a solute partition coefficient of unity and rapid equilibration of the solute between the solid surface and the liquid phase, then the concentration of the solute at the surface of the sphere (C_S at $r = R$) is the same as that in the solution which changes as a function of time i.e. $C_L = f(t)$. However, if K_p is not unity, then C_s (at $r = R$) is given by Equation 3.58 (Cranks, 1975).

$$C_S(R,t) = K_p C_L(t) \qquad 3.58$$

The boundary condition 2 expresses the fact that the rate at which solute leaves the surface of the sphere (area $= A_s$) is equal to that which enters the liquid phase of volume, V_L. According to Cranks (1975), the solution of Equation 3.54 under the above initial and boundary conditions is given by Equation 3.59,

$$\frac{M_L^t}{M_L^\infty} = 1 - \sum_{n=1}^{\infty} \frac{6\alpha\,(1+\alpha)}{9 + 9\alpha + \alpha^2 q_n^2} \cdot \exp\left[-\frac{D_e\, q_n^2\, t}{R^2}\right] \qquad 3.59$$

where M_L^t/M_D^∞ is the ratio of the amount of solute that has entered the liquid phase at time t, (M_L^t), to that which would be transferred into the liquid phase after infinite time (M_L^∞).

Similarly, for diffusion of the solute from a well-stirred liquid phase into a sphere initially free of the

solute, the initial conditions are rewritten in the form,

$$t = 0, \quad 0 < r < R; \quad C_S = 0 \qquad \text{I.C. 3}$$

$$t = 0, \quad r > R, \quad C_L = \text{constant} \qquad \text{I.C. 4}$$

and the solution of Equation 3.54 with B.C.1 and B.C.2 is given by Equation 3.60

$$\frac{M_S^t}{M_S^\infty} = 1 - \sum_{n=1}^{\infty} \frac{6\alpha\ (1+\alpha)}{9 + 9\alpha + \alpha^2 q_n^2} \cdot \exp\left[- \frac{D_e\ q_n^2\ t}{R^2}\right] \qquad 3.60$$

In Equations 3.59 and 3.60, α is defined as the ratio of the volume of liquid phase (V_L), to that of the sphere volume (V_s), divided by the partition coeffficient (K_p), and is expressed by Equation 3.61,

$$\alpha = \frac{3V_L}{4\ \pi\ R^3\ K_p} \qquad 3.61$$

and q_n's are successive, non zero, positive roots of the function

$$\tan q_n = \frac{3\ q_n}{3 + \alpha\ q_n^2} \qquad 3.62$$

The value α is fixed for a given set of experimental

conditions (V_L, V_S and K_p are all constants) and therefore q_n values may be determined for as many terms as desired. Since,

$$\tan q_n - \left[3q_n/(3+\alpha q_n^2)\right] = 0 \qquad 3.63$$

the zeros of Equation 3.62 may be seen as intersections of $f_1(q_n) = \tan q_n$ and $f_2(q_n) = 3q_n/(3 + \alpha q_n)$ as shown in Figure 3.12 in which α is taken to be 4.0.

From the above, two different sets of initial and boundary conditions can be considered in deriving equations for unsteady-state mass transfer in spheres. The first, and simpler condition of Case 1 described by Equations 3.56 and 3.57 involves the assumption of a perfect sink or a constant external solute concentration. Rigorously, this can only allow an approximate evaluation of D_e since there has to be some concentration change in the liquid phase to make the solute uptake, or release, observable. Therefore, a reliable D_e value can only be obtained if the solute content within the solid phase is directly measured as a function of time. Additionally, the validity of the "perfect sink" assumption becomes especially questionable whenever the liquid phase to sphere volume is small, or if the partition coefficient of the solute in the solid phase is high (Lee, 1980).

If the sphere is suspended in a limited volume of solution, as in Case 2, then the change in concentration of the solute in the liquid phase as the solute diffuses into

Figure 3.12. The functions $f_1(q_n) = \tan q_n$ [——] and $f_2(q_n) = 3q_n/(3+\alpha q_n^2)$ [---] are plotted versus q_n (radians) when $\alpha' = 4.0$. The successive, non-zero, positive roots of Equation 3.62 are represented by the intersections of $f_1(q_n)$ and $f_2(q_n)$.

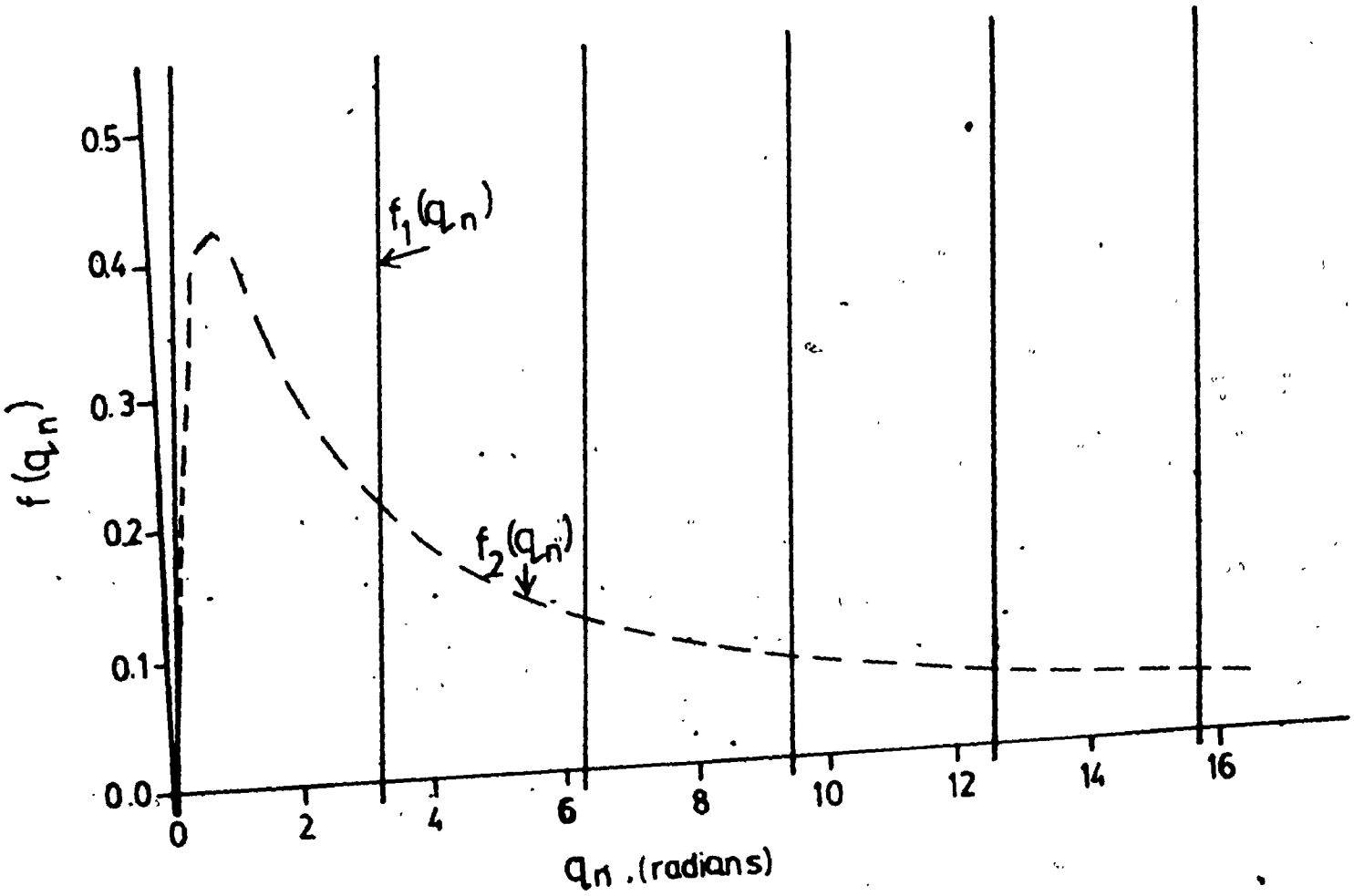
0.5
0.4
0.3
0.2
0.1
0.0
f(q_n)
f_1(q_n)
f_2(q_n)
0
2
4
6
8
10
12
14
16
q_n .(radians)

or effuses out of the sphere, can be easily measured, which is much simpler than directly measuring the amount of solute in the solid phase (Carman and Haul, 1954). Therefore, for a well-stirred solution of limited volume, the concentration of the solute in the liquid phase depends only on time and by using the appropriate Equations (3.59 to 3.62), D_e can be accurately evaluated (Cranks, 1975). This method has a distinct advantage, in that, both, D_e and K_p can be determined from the same diffusion experiment. Numerical and graphical solutions for determining D_e in geometries other than the sphere are available in the literature (Cranks, 1975; Ma and Evans, 1968; Schwartzberg and Chao, 1982).

3.7 Research Objectives

Glucose has been preferentially utilized as a primary carbon- and energy-source for the production of amino acids (glutamic acid, L-isoleucine, D-threonine), antibotics (streptomycin, pencillin), organic acids (citric acid, lactic acid, gluconic acid), organic solvents (acetone, butanol ethanol, propanol), and a miscellany of other products (hydrogen, nucleic acids, vitamins, etc.) using alginate-entrapped cell systems (Linko and Linko, 1984). Thus, a detailed study of the diffusivity characteristics and partitioning of the substrate glucose, in alginate-entrapment matrices is warranted and forms the basis of this research. More specifically, the objectives of this research can be

summarized as follows:

(i) To develop a novel unsteady-state diffusivity measurement technique which fulfills the following criteria:

(a) excellent mixing characteristics,

(b) negligible film mass transfer resistance,

(c) retention of the structural integrity of the alginate entrapment matrix even at high cell loadings,

(d) simplicity of the method, and,

(e) accuracy in determining solute concentration changes in the liquid phase.

(ii) Based on the physico-chemical properties of alginates (Chapter 2), the following factors were examined for their influence on D_e and K_p of glucose:

(a) composition of sodium alginate (M/G ratio),

(b) degree of polymerization of alginate,

(c) concentration of alginates,

(d) type of chelating agent used for gelation, and

(e) concentration of chelating agent.

(iii) To evaluate the effect of entrapped yeast cell concentration and temperature on the diffusivity and partitioning characteristics of glucose.

(iv) Develop suitable correlations for predicting D_e of glucose in alginate entrapment matrices as a function of the parameters listed in (ii) and (iii).

CHAPTER 4

MATERIALS AND METHODS

4.1 Type and Composition of Sodium Alginate

A total of 16 different highly purified commercial grades of sodium alginate were kindly supplied by various manufacturers. The moisture content of Na-alginate was determined by drying approximately 2 gms of the powder to constant weight at 105°C. A laboratory grade of purified Na-alginate (Fisher Chemicals) was also used in these studies. The guluronic acid and moisture content of all the sodium alginate samples are listed in Table 4.1.

4.2 Rheological Properties of Na-Alginate Solutions

The rheological properties of aqueous Na-alginate solutions give important information regarding the size of the linear alginic acid polymer (McDowell, 1977). Aqueous solutions of Na-alginate generally exhibit non-Newtonian, pseudoplastic flow behaviour in which the fluid undergoes shear thinning over a wide range of shear rates (te Bokkel, 1983). However, as shown by McDowell (1966; 1977), dilute Na-alginate solutions ($\leq$ 1 g/100 mL) exhibit Newtonian type of flow behaviour at low shear rates ($<$ 25 s^{-1}) and this phenomenon has been used to develop some useful correlations

Table 4.1: Composition of Different Types of Sodium Alginates Tested (NA = not available)

Sample No.	Trade Name	Manufacturer	Approximate Guluronic Acid Content, (%)	Moisture Content (%)
1	Manucol LB	Alginate Industries Ltd., London, England	42[a]	11.5
2	Manucol DM		42[a]	12.6
3	Manugel HG		44[a]	10.0
4	Manugel GMB		67[a]	12.5
5	Manugel DPB		71[a]	11.0
6	Manugel DJX		NA	11.4
7	Manugel DMB		NA	10.4
8	Manugel GHB		NA	13.5
9	Kelco Gel LV	Kelco, Div. of Merck & Co. Inc., San Diego, CA	40[a]	16.0
10	Kelco Gel HV		40[a]	14.8
11	Keltone		40[a]	17.2
12	Protanal LF 20/60M	Protan A/S, Drammen, Norway	40[b]	14.6
13	Protanal SF 120M		40[b]	14.3
14	Protanal LF 10/40RB		55[b]	15.8
15	Protanal LF 10/60		70[b]	15.2
16	Protanal SF 120		70[b]	12.9
17	Laboratory grade[c]	NA	NA	13.6

(a) Personal communication: Dr. A.P. Imeson, Kelco/AIL International Ltd., London, England (25 January, 1985).

(b) From technical supplements provided by the manufacturers.

(c) Purified sodium alginate powder supplied by Fisher Chemicals Ltd.

to estimate the size of the linear alginate polymer (Donnan and Rose, 1950; Cook and Smith, 1954; Smidsrod and Haug, 1968a).

According to Smidsrod and Haug (1968a), the average molecular weight, $\overline{MW}$, of Na-alginate (determined by light-scattering methods) can be predicted by the correlation,

$$[\mu] = (2.0 \times 10^{-5})\ \overline{MW} \qquad 4.1$$

where $[\mu]$ is the intrinsic viscosity of aqueous Na-alginate solutions (at 20°C) and is defined by Equation 4.2.

$$[\mu] = \lim_{c \to 0} \frac{\mu_r - 1}{c} = \lim_{c \to 0} \frac{\mu_{sp}}{c} \qquad 4.2$$

where c is the concentration of Na-alginate (% w/v, dry weight basis) and μ_r is the relative viscosity of the polymer solution at that concentration. The latter is expressed by Equation 4.3,

$$\mu_r = \mu_{alg}/\mu_{H_2O} \qquad 4.3$$

and μ_{sp} is the specific viscosity of the Na-alginate solution and is defined by Equation 4.4

$$\mu_{sp} = (\mu_{alg} - \mu_{H_2O})/\mu_{H_2O} \qquad 4.4$$

In Equations 4.3 and 4.4, μ_{alg} and μ_{H_2O} are the respective viscosities of the Na-alginate solution (at low shear rates) and water, measured at 20°C.

A difference between the viscosity of aqueous Na-alginate solutions can be caused by different amounts of multivalent cations (e.g. Ca^{2+}) present in the two alginate samples and not only by the variation in their molecular weights (Haug and Smidsrod, 1962). Therefore, in order to eliminate the influence of these cations on the measured values of [μ], and consequently molecular weight estimations, all viscosity measurements (see Section 4.4.2) were carried out using dilute Na-alginate solutions prepared in 0.1M NaCl as suggested by Haug and Smidsrod (1962).

4.2.1 Intrinsic Viscosity of Dilute Na-Alginate Solutions

The influence of polymer concentration on the relative viscosity of dilute Na-alginate solutions was examined by Haug and Smidsrod (1962) using alginates with different values of the intrinsic viscosity (see Figure A.1., Appendix A). Based on their experimental data, a model equation (Equation 4.5) was developed (see Appendix A, Figure A.1, A.2, A.3, and Table A.1) to facilitate estimation of the intrinsic viscosity, [μ], from the measured values of the polymer concentration (c), and the specific viscosity, μ_{sp} of a dilute Na-alginate solution (c < 1.0g D.W./100 mL). Thus, using the least squares method, the experimental data

of Haug and Smidsrod (1962) were found to fit well (Figure A.2, Appendix A) with the model exponential relationship (Equation 4.5) and as shown in Table A.1 (Appendix) the coefficient of determination was > 0.99. Accordingly, the model equation (4.5) is written as,

$$\frac{\mu_{sp}}{c} = [\mu] \exp (bc) \qquad 4.5$$

where b is expressed by the linear relationship (see Figure A.3, Appendix),

$$b = 1.03 + 0.23[\mu] \qquad 4.6$$

and the correlation coefficient was found to be 0.9983. As shown in Table A.1 (Appendix), the estimated values of $[\mu]$ obtained by using Equation 4.5 were similar to the experimental data reported by Haug and Smidsrod (1962). Equation 4.5 can be rewritten as,

$$\frac{\mu_{sp}}{c} = [\mu] \exp(1.03c + 0.23[\mu]c) \qquad 4.7$$

For comparison, the experimental and predicted values of $[\mu]$ are shown in Figure A.3 (Appendix).

4.2.2 Viscosity Measurements

The viscosity of dilute Na-alginate solutions were measured using the Brookfield Synchro-Lectric (Model LVT) viscometer (Brookfield Engineering Laboratories, Stoughton, Mass.). Essentially, this viscometer measures the torque on a rotating cylinder (available in different sizes) which is proportional to the drag offered by the fluid. The drag is detected as a strain on a precalibrated spring which registers as a deflection on the dial. The detailed operational procedures of this viscometer are given elsewhere (van Wazer et al., 1963).

The cylindrical spindle was immersed in Na-alginate solution (400 mL) and rotated at different speeds. The shear stress, τ_w, at the cylindrical wall is given by,

$$\tau_w = \frac{T_w}{R_c} \cdot \frac{1}{2\pi R_c L_c} \qquad 4.8$$

where, L_c and R_c are the respective lengths and radii of the various spindles, T_w is the force acting on the surface of the cylindrical wall which is expressed by Equation 4.9.

$$T_w = k \cdot x \qquad 4.9$$

where k is the torque at full scale deflection (for model LVT, k = 673 dyne. cm), and x is the measured deflection on

the dial.

The shear rate, $\dot{\gamma}$, is defined by Equation 4.10.

$$\dot{\gamma} = \tau_w/\mu \qquad 4.10$$

For different cylindrical spindles rotated at either 6, 12, 30 or 60 rpm, the shear rate was determined by calibrating the meter (Figure A.4, Appendix) using Newtonian fluids of known viscosity.

All viscosity measurements of dilute ($c < 1.0$g/100mL) Na-alginate solutions prepared in aqueous 0.1 M NaCl were determined at room temperature (25°C ± 1°). As shown in Figure A.5 (Appendix), the viscosity of all dilute Na-alginate solutions did not change significantly with the low shear rates (1.43 s^{-1} to 18.6 s^{-1}) used in these measurements. The viscosity at 20°C was determined by applying the appropriate correction factor (tabulated by McDowell, 1977) to the measured values at 25°C.

4.2.3 Estimation of the Average Molecular Weight, $\overline{MW}$, of Na-Alginates

From the known concentration of different alginate solutions and their respective viscosities at 20°C, the intrinsic viscosity [μ] was determined by applying Equation 4.7. Using the correlation (Equation 4.1) of Smidsrod and Haug (1968a), the average molecular weight, ($\overline{MW}$), of all 17

different types of Na-alginates were calculated and the values are listed in Table 4.2.

4.3 Preparation of Large Spherical Alginate Beads

The novel diffusivity measuring apparatus designed for use in this study (described in Section 4.7) can only employ large (> 1 cm in diameter) spherical alginate beads. Conventional methods of preparing alginate gel matrices usually result in spherical beads of up to 0.3 cm in diameter (Tanaka et al., 1984). A special method was therefore developed to prepare larger spherical beads of alginates with or without entrapped yeast cells.

4.3.1 Preparation of Cell-Free Alginate Beads

A 2% (w/v) solution of purified Na-alginate (Fisher Chemicals, Sample #17) was prepared in deionized distilled water and a large drop of this solution was poured into a 4% (w/v) $CaCl_2$ gelling bath containing a top-layer of olive oil. By virtue of surface tension effects, the drop of Na-alginate solution attained the spherical shape in the oil phase. Mild agitation using a magnetic stir bar facilitated the transfer of the Na-alginate spherical drop from the oil phase to the $CaCl_2$ phase where gelation occurred. The resulting Ca-alginate bead was removed from the bath, rinsed with several volumes of distilled water and placed in excess

Table 4.2: Estimated Values of the Average Molecular Weight of Different Types of Na-alginates

Na-alginate Sample #	Na-alginate conc., c, (g.D.W/100mL)	μ_{sp}/c at 20°C, (100mL/g)	Intrinsic viscosity, [μ], (100mL/g)	Approximate Average Molecular Weight, $\overline{MW}$
1	0.885	7.98	2.1	105,000
2	0.874	185	10.0	500,000
3	0.900	175	9.6	480,000
4	0.875	347	12.2	610,000
5	0.890	380	12.3	615,000
6	0.886	82.9	7.4	370,000
7	0.896	122	8.5	425,000
8	0.865	34.0	5.1	255,000
9	0.840	28.5	4.8	240,000
10	0.852	230	11.0	550,000
11	0.828	139	9.6	480,000
12	0.854	104	8.4	420,000
13	0.857	335	12.3	615,000
14	0.843	29.7	4.9	245,000
15	0.848	29.8	4.9	245,000
16	0.871	207	10.4	520,000
17	0.864	435	13.1	655,000

4% $CaCl_2$ solution for at least 48 hours for gelation to be complete. Using this technique, spherical Ca-alginate beads of up to 2 cm in diameter could be easily prepared.

4.3.2 Entrapment of Viable Yeast Cells

Approximately 10 g of dried baker's yeast was suspended in 100 mL of sterile physiological saline solution for about 1 hour. Using the methylene-blue test, yeast cell viability was found to be greater than 90 percent. The yeast cells were centrifuged at 5000 g for 10 minutes, washed and resuspended in distilled water. The procedure was repeated twice to ensure complete removal of sugars and other soluble nutrients present in the dried yeast powder.

To 100 mL of the viable yeast cell suspension, 2.0 g of Na-alginate (sample #17) was added and stirred for approximately 10 minutes to ensure complete dissolution of Na-alginate. Large, spherical Ca-alginate beads containing entrapped viable yeast cells were then prepared as described above (Section 4.3.1).

4.3.3 Entrapment of Non-Viable Yeast Cells

Approximately 2, 4, 6, 8 and 10 g portions of dried baker's yeast were suspended in 100 mL aliquots of 50% v/v ethanol for 10 minutes. Staining with methylene-blue showed that cell death was complete without lysis of the cells.

The non-viable yeast cells were centrifuged and washed three times, and finally entrapped within large spherical beads of Ca-alginate, as described above.

The spherical shape of a typical Ca-alginate bead used in the diffusion apparatus is shown in Figure 4.1 in which a single bead has been photographed from various angles. Furthermore, as shown in Figure 4.2, large spherical alginate beads could also be prepared using different types and concentration of Na-alginates (Figure 4.2a) even when entrapping a high concentration (118 kg D.W. cells/m^3 of gel) of yeast cells within the alginate gel (Figure 4.2b).

4.4 Determination of Bead Volume and Diameter

The bead volume (V_S) was determined by measuring the displaced height (h) of distilled water contained in a tube of known inside diameter (d_t) when the alginate sphere was immersed in it. An expanded scale half-meter cathetometer (The Precision Tool and Instrument Co. Ltd., Surrey, England) accurate to $\pm$ 0.01 mm was used to accurately measure the displacement height enabling the spherical bead volume ($V_S = \pi d_t^2 h/4$) and its diameter ($d_s = (6V_S/\pi)^{1/3}$) to be evaluated. At least five measurements were made with the same bead to minimize the standard error in volume measurement, which was less than $\pm$ 0.5%.

In view of the large size of the alginate beads, it was possible to directly measure the bead diameter using cali-

Figure 4.1: Photograph of a single Ca-alginate bead taken from four different angles showing the spherical shape of the bead.

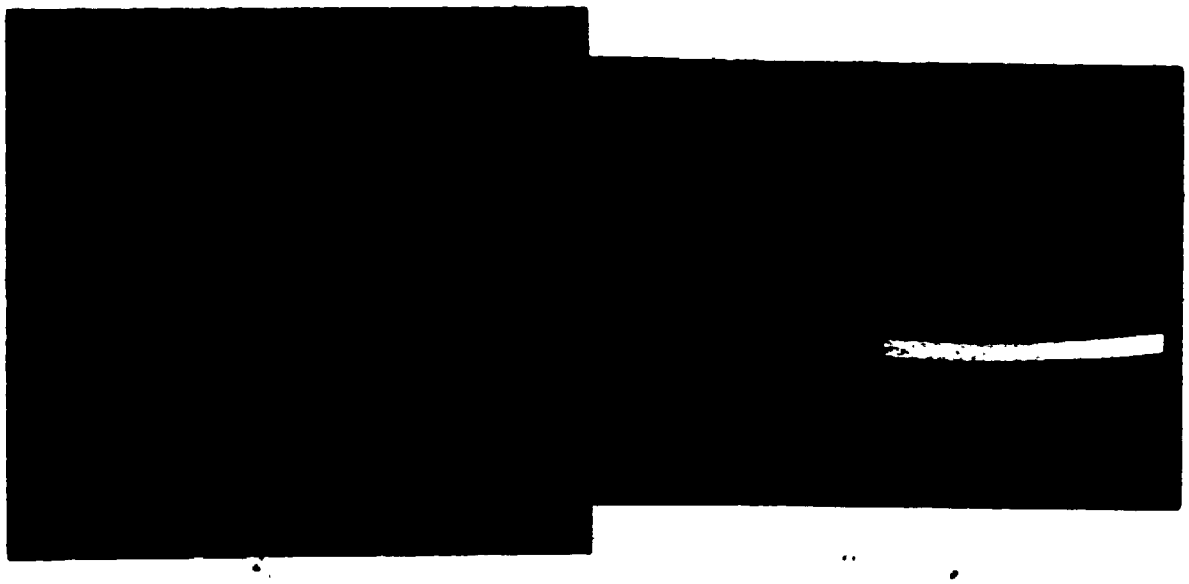

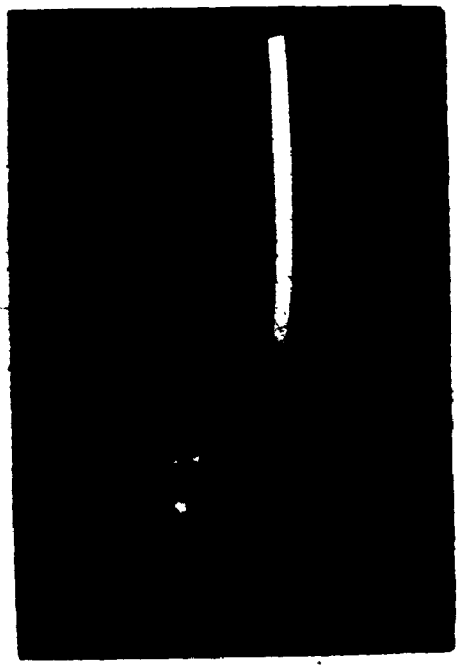

Figure 4.2: (a) Photograph of various cell-free Ca-alginate beads prepared using different types and concentration of Na-alginate.

Figure 4.2: (b) Photograph of Ca-alginate beads prepared from 2% Na-alginate solution, with or without entrapped yeast cells

(A) Cell-free Ca-alginate bead

(B) Ca-alginate bead with entrapped yeast cells (cell concentration = 118 kg D.W./m^3 of gel)

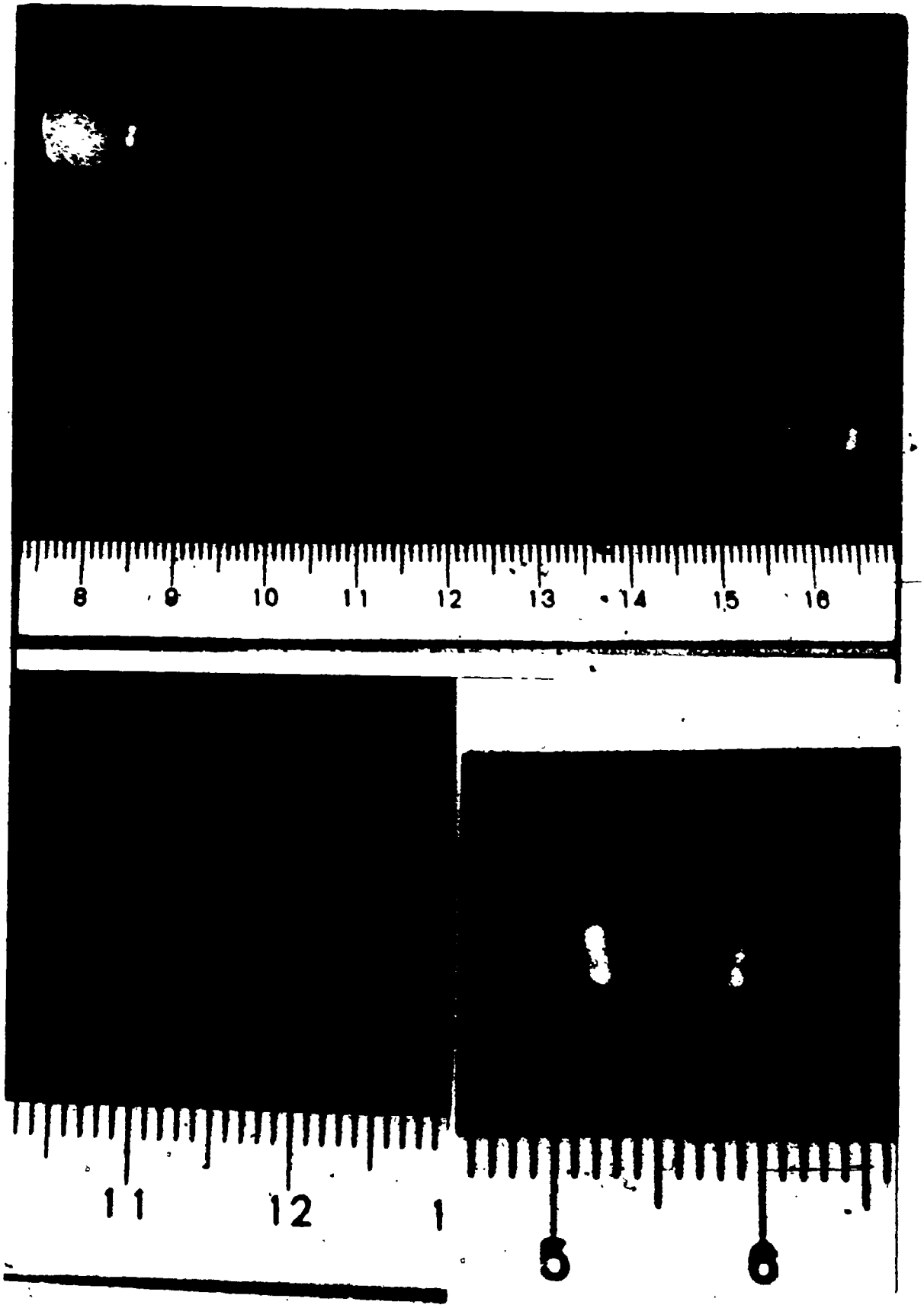
8
9
10
11
12
13
14
15
16
11
12
1

pers or a micrometer. In addition, the diameter was also measured from photographs of a single alginate bead (Figure 4.1). The bead diameter measured by these two direct methods agreed very well with the diameter calculated from the measured volume of the sphere using the displacement technique.

4.5 Determination of Alginate Concentration in the Gel

As discussed in Section 2.4.2, synerisis associated with gel contraction, occurs during the gelation process and consequently, the alginate polymer concentration in the gel will be higher than that in Na-alginate solution. The actual alginate concentration in the gel was therefore determined as described below.

The volume of a spherical alginate bead (V_S) was determined using the displacement technique and the wet weight of that bead measured (W_w). Subsequently, the dry weight (W_d) of the same bead was also determined by drying the gel to constant weight at 105°C. From these three measurements, the bead density ($\rho_b = W_w/V_S$) and alginate concentration in the gel were calculated. The latter was expressed either in terms of the bead volume ($c_g = W_d/V_S$; kg D.W. of alginate/m^3 of gel) or as a fraction of bead wet weight ($\omega = W_d/W_w$, kg dry gel/ kg wet gel).

Knowing the amount of water imbibed in the gel ($W_h = W_w - W_d$) and consequently, its volume ($V_h = W_h/\rho_h$), the

fractional void volume ($\varepsilon = V_h/V_s$) and polymer volume fraction ($\lambda = 1 - \varepsilon$) could be evaluated.

The specific volume, ν, of the alginate polymer in the gel is then given by Equation 4.11 (Rabek, 1980).

$$\nu = \frac{\lambda}{\omega} \cdot \frac{1}{\rho_b} \qquad 4.11$$

4.6 Determination of Yeast Cell Concentration in the Gel

As above, the entrapped yeast cell concentration in the Ca-alginate gel (prepared from sample #17 for all cell immobilization studies) will be higher than that in the Na-alginate/yeast cell suspension. Using a bead of known volume (V_s), the wet weight (W_w) and dry weight (W_d) of the alginate gel containing yeast cells was determined as above. In this case, the dry weight of the bead (W_d) corresponds to the total amount of solids (W_{ts}) in the gel (cells + alginate). The amount of water in the gel ($W_h = W_w - W_{ts}$), its volume ($V_h = W_h/\rho_h$) and the fractional void volume ($\varepsilon = V_h/V_s$), were calculated as before and the solids concentration in the gel ($C_{ts} = W_{ts}/V_s$) also determined.

In order to determine the concentration of the cells in the bead the following procedure was followed. A bead of predetermined volume and wet weight was sliced into small pieces and mixed with approximately 10 mL of 100 mg/mL pentasodium tripolyphosphate solution. After approximately 2 hours complete dissolution of the gel was achieved. The

resulting mixture was then filtered under vacuum through a tarred 0.22 μm filter paper which was subsequently washed with several aliquots of distilled water. The filter paper was re-dried to constant weight and the amount of cells (W_x) in the bead, determined. When the same procedure was applied using a cell-free Ca-alginate bead, there wasn't any noticeable increase in the dry weight of the filter-paper indicating that the alginate polymer was not retained or adsorbed by the filter-paper.

Knowing the cell concentration ($c_x = W_x/V_S$) and the total solids concentration, c_{ts}, the concentration of alginate ($c_g = c_{ts} - c_x$) could also be determined. Using Equation 4.11, the alginate volume fraction (λ) in the cell-entrapped Ca-alginate bead was calculated since values of the alginate weight fraction ($\omega = c_g V_S/W_b$), bead density (ρ_b), and specific volume, ν, of alginate (determined as described in Section 4.5) were all known. The volume fraction of entrapped yeast cells, β, is then given by

$$\beta = 1 - \varepsilon - \lambda \qquad 4.12$$

4.7 Description of the Diffusivity Measurement Apparatus

The apparatus used to measure the diffusivity of glucose in spherical alginate beads is shown in Figure 4.3. The alginate bead was held in place by two adjustable stainless steel fine wire loops which were mounted to a rod (Fig-

ure 4.3b) connected to a variable speed motor. The spherical alginate bead could then be immersed and rotated in a glass tube containing the liquid phase and the temperature maintained at the desired value (± 0.02°C) using a thermostatically controlled refrigerated water bath. The diffusion vessel was covered with a teflon cap equipped with inner and outer O-ring seals as shown in Figure 4.4. Samples of the liquid phase could be withdrawn (using a 10 μL Drummond micropipette) through a single sampling port in the teflon cap, which remained tightly plugged by a piece of stainless steel wire when not in use. Even after 6 hours, the temperature in the liquid phase was not more than 0.15°C higher than the temperature of the water bath.

4.8 Measurement of Glucose Concentration

At least five different methods may be used to measure glucose concentration changes in the liquid phase as a function of time. The sensitivity of some of the methods, based on the lowest detectable concentration of glucose, are listed in Table 4.3.

It is evident that the radiotracer method (described in Section 4.9) is the most sensitive and consequently requires only 3 μL of the sample to accurately measure its radioactivity. The relatively lower sensitivity of the other methods requires much larger sample volumes to be withdrawn from the liquid phase. Due to the small size of the

Figure 4.3: (a) Photograph showing the various components of the diffusivity measurement apparatus when unassembled.

Figure 4.3: (b) Photograph of a fully assembled novel, diffusivity measurement apparatus used in this study.

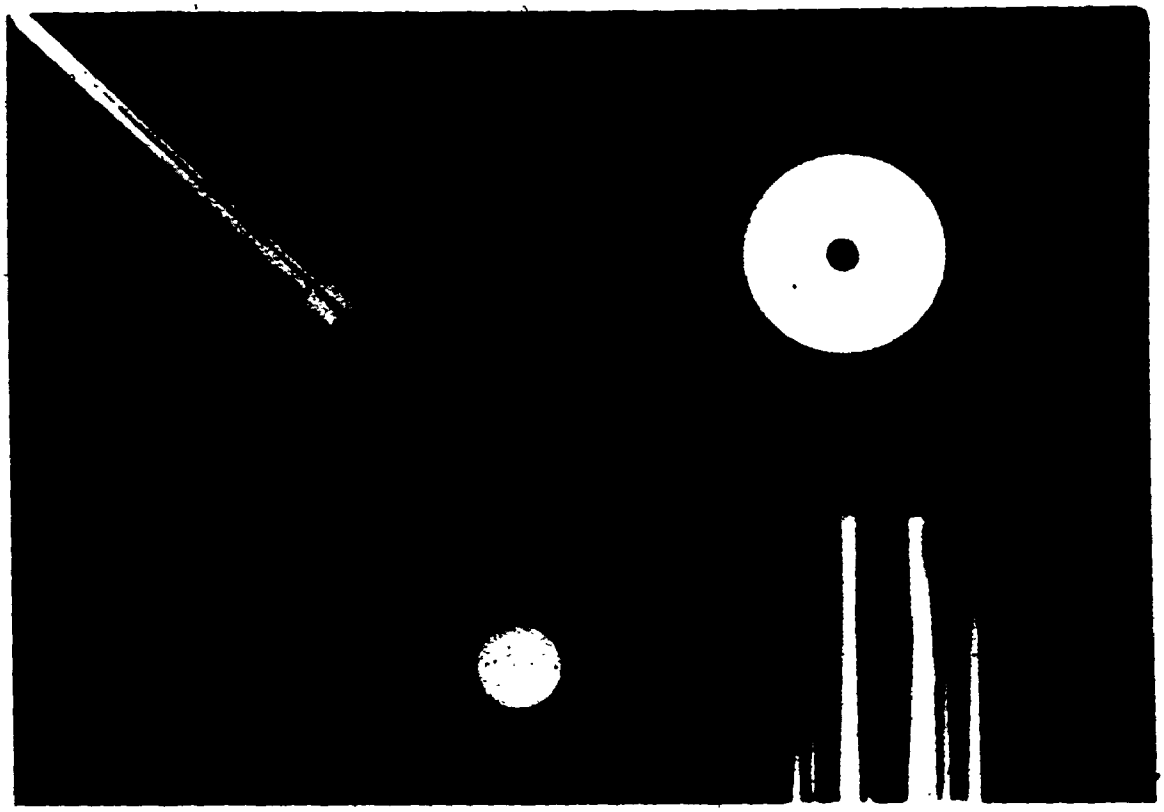

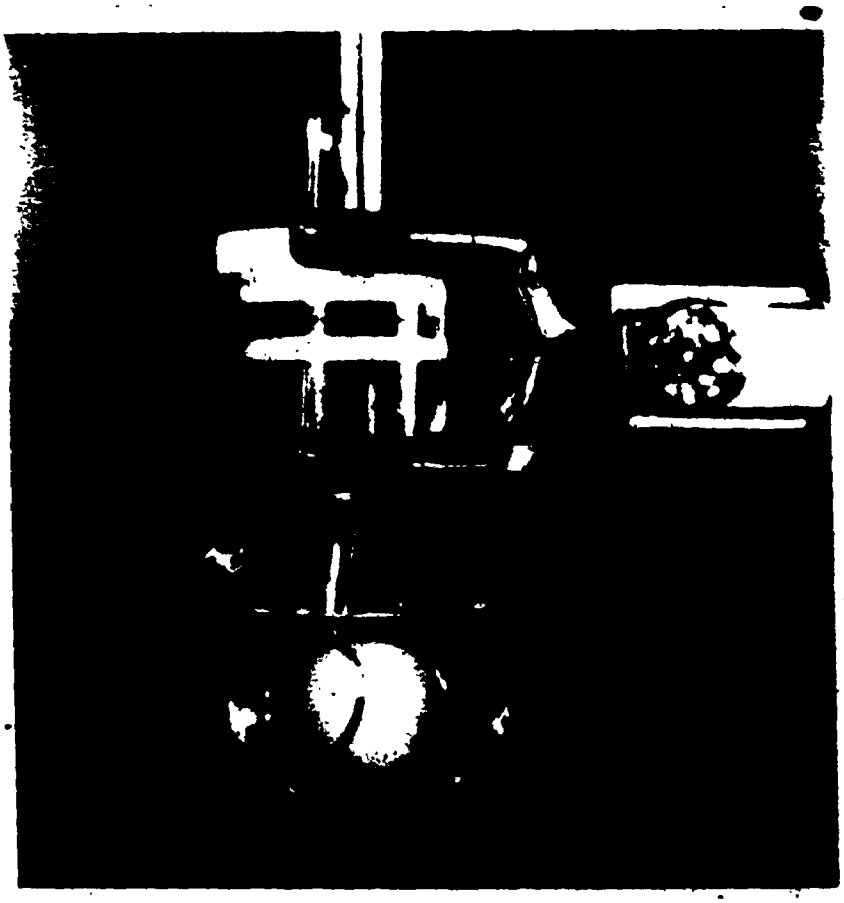

Figure 4.4: Schematic diagram and dimensions of the novel apparatus used to measure solute diffusivity in a spherical alginate sphere.

1. Rotating stainless steel rod (diameter = 0.48 cm; length = 25 cm);
2. Teflon cover with inner and outer O-rings;
3. Cylindrical glass tube (inside diameter = 2.26 cm; height = 4.83 cm);
4. Stainless steel holding wires (wire thickness = 0.5 mm);
5. Liquid phase (volume, V_L = 4.0 mL);
6. Rotating spherical alginate bead;
7. Constant temperature water bath.

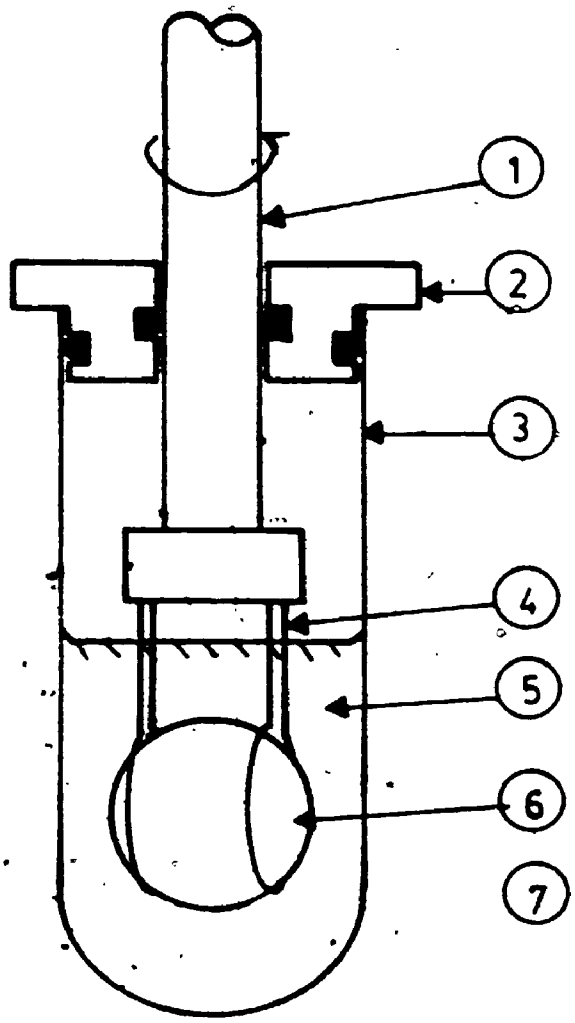
1
2
3
4
5
6
7

Table 4.3: Sensitivity of Different Glucose Measurement Techniques

Method	Sensitivity: Lowest detectable conc. of glucose (mg/mL)	Reference
Glucose analyzer	0.5	Yellowsprings Scientific Instruments, Ohio
Dinitro-salicylic acid method	0.1	Miller, 1959
Somogyi-Nelson method	0.01	Somogyi, 1952
Glucose oxidase method	0.02	Bergmeyer and Bernt, 1963
Glucostat method	0.0025	Worthington Biochemicals Inc. U. S. A.
Radiotracer method using C^{14}-glucose (see Section 4.9 for details)	0.00014	This work

diffusion apparatus and low liquid phase volume, use of non-radioactive glucose measurement techniques are therefore not practical. Furthermore, the high sensitivity of the radiotracer method allows up to 30 to 40, 3 μL samples to be withdrawn during the course of the experiment without causing significant changes (± 1.0 to 1.5%) in the liquid phase volume.

4.9 Diffusion of C^{14}-Glucose into Spherical Alginate Bead

The labelled solute used in these studies was D-^{14}C (U) -glucose obtained from New England Nuclear Corporation. The ^{14}C radionuclide exhibits β-type of decay and is very stable with a half-life of 5730 years. The radioactive glucose solution in ethanol/water (9:1 ratio, volume basis) had a specific activity of 329 mCi/mMol. Ten μL of this solution was placed in the glass diffusion tube and the ethanol evaporated by a stream of nitrogen gas. Unless otherwise stated, 4 mL of a 20 $kg.m^{-3}$ aqueous 'cold' glucose solution was added to the tube and the contents equilibrated at the temperature of the diffusion experiment (usually 30°C except when stu~~dying~~ the influence of temperature on D_e).

A single alginate bead, prepared as described in Section 4.3, was rinsed and equilibrated in distilled water at the temperature of the experiment, for at least 2 hours before initiating diffusion. After equilibration, the bead (which was already mounted to the shaft) was removed from

distilled water and all the excess liquid film withdrawn from the bead surface by suction using a 10 μL micro-pipette.

At time t = 0 min, the bead was immersed into the radiotracer solution and rotated at approximately 550 rpm. Three μL samples of the tracer solution were periodically withdrawn and dispensed into a 20 mL counting vial to which 10 mL of the scintillation fluid (composition : 4 g Omni-fluor, 1000 mL toluene, and 800 mL ethyleneglycol mono-methylether) was added.

The concentration of labelled solute in the liquid phase (C_L^t) was measured by counting for 5 minutes using a scintillation spectrometer (LKB Wallac, Model 1217 Rackbeta) and the total amount of the tracer remaining in the liquid phase (M_L^t) calculated. By a simple mass balance, the amount of solute entering the bead as a function of time (M_S^t) could be also calculated. The diffusion process was allowed to proceed until no further change in the liquid phase solute concentration occurred (i.e., $C_L^t = C_L^\infty$) as measured by the scintillation spectrometer. The fractional uptake of the solute (M_S^t/M_S^∞) was calculated and plotted as a function of time.

4.10 Effusion of C^{14}-Glucose out of Spherical Alginate Bead

At the end of the diffusion process, the equilibrated

alginate bead was removed from the tracer solution, and all the excess liquid film withdrawn from the bead surface. The bead was then immersed in 4.0 mL of distilled water maintained at the desired temperature and the sphere rotated at approximately 550 rpm. Three μL samples of the liquid phase were periodically withdrawn and the tracer concentration (C_L^t) determined as before, except that the samples were counted for 20 minutes. The total amount of the tracer entering the liquid phase (M_L^t) was calculated and the experiment terminated when C_L^t remained constant (i.e. $C_L^t = C_L^\infty$). The fractional release of the solute (M_L^t/M_L^∞) was computed and plotted as a function of time. The initial amount of the solute in the bead (M_S^o) during the effusion process was assumed to be equal to that in the bead at the end of the diffusion process (M_S^∞). Thus, the amount of tracer remaining in the bead at any given time (M_S^t) could be easily calculated by a simple mass balance.

4.11 Determination of Equilibrium Partition Coefficient

The equilibrium partition coefficient, K_p, of glucose in spherical alginate beads was determined knowing the equilibrium tracer concentration in, both, the sphere (C_S^∞) and the liquid phase (C_L^∞), since K_p is defined by Equation 3.1.

4.12 Analysis of Experimental Data

Figure 4.5 is the flowchart for the computer program (DIFPREP) used to calculate the fractional solute uptake (M_S^t/M_S^∞) and release (M_L^t/M_L^∞) rates during diffusion and effusion, respectively, from measured experimental values and known constants. Detailed calculation steps used in the computer program and the definitions of the various terms listed in the flowchart, are given in Appendix B.1. A typical computer output for DIFPREP based on actual experimental data is given in Appendix B.2.

4.13 Determination of the Effective Solute Diffusivity

The optimum D_e values were determined by fitting the theoretical predictions from Equations 3.60 and 3.59 to the experimental solute uptake and release rates, respectively, by varying the value of D_e using a non-linear regression analysis program. This computer program (DIFFIT) used a subroutine package called ESOP (Engineering Systems Optimization Package) to optimize the experimental data (stored in the input program created by DIFPREP) to the supplied model (Dickinson, 1982).

This optimization procedure cycles orthagonal line searches along preferred directions, which were selected from a table of best cases. The computer program DIFFIT also performed a sensitivity analysis providing us with information on the change of the objective function in the region of the minimum as a function of the decision vari-

Figure 4.5: Flowchart for the computer program (DIFPREP) used to calculate the fractional solute uptake or release rates from the user entered experimental measurements and constants. The DIFPREP program also prepares the input files for the DIFFIT optimization package (see Figure 4.6).

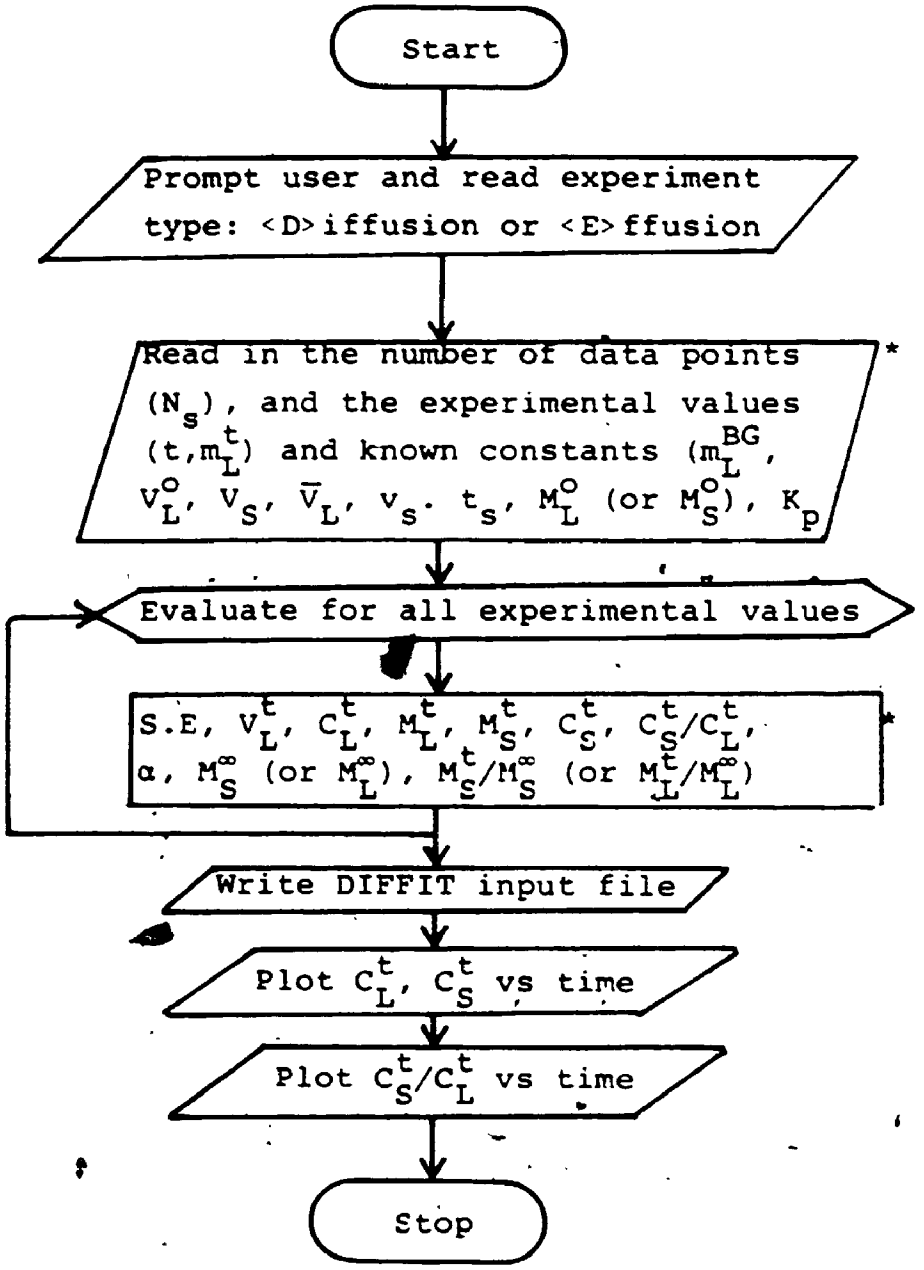

* Note: Detailed calculation steps and definition of all terms are given in Appendix B.1.

ables.

The q_n values in Equation 3.59 and 3.60 defined by Equation 3.62 were determined using Newton's method. The first 25 terms of the series were evaluated, and found to be adequate, when fitting the theoretical predictions to the experimental data. A flowchart of the program DIFFIT is shown in Figure 4.6.

The experimental data were also compared to the theoretical values by determining the percentage deviation according to Equation 4.13.

$$\text{Deviation} = \left[\frac{\sum_{n=1}^{N} \left(\frac{(M^t/M^\infty)_{exp} - (M^t/M^\infty)_{pred}}{(M^t/M^\infty)_{pred}} \right)^2}{N - 1} \right]^{1/2} \times 100 \qquad 4.13$$

where N is the number of experimental points, and the subscripts 'exp' and 'pred' refer to experimental and predicted values of solute mass ratios, respectively. A typical computer output for calculating D_e using DIFFIT is given in Appendix B.3 based on the experimental data given in Appendix B.2 (DIFPREP).

4.14 Determination of Solute Concentration Profile Within a Spherical Alginate Bead

For diffusion of solute into a spherical bead, the

Figure 4.6: Flowchart for the computer program DIFFIT which uses the input program created by DIFPREP (see Figure 4.5) to fit the experimental data to the diffusion model (Equations 3.59 and 3.60). Using the ESOP optimization package written by Dickinson (1982), the optimum effective solute diffusivity, D_e is calculated.

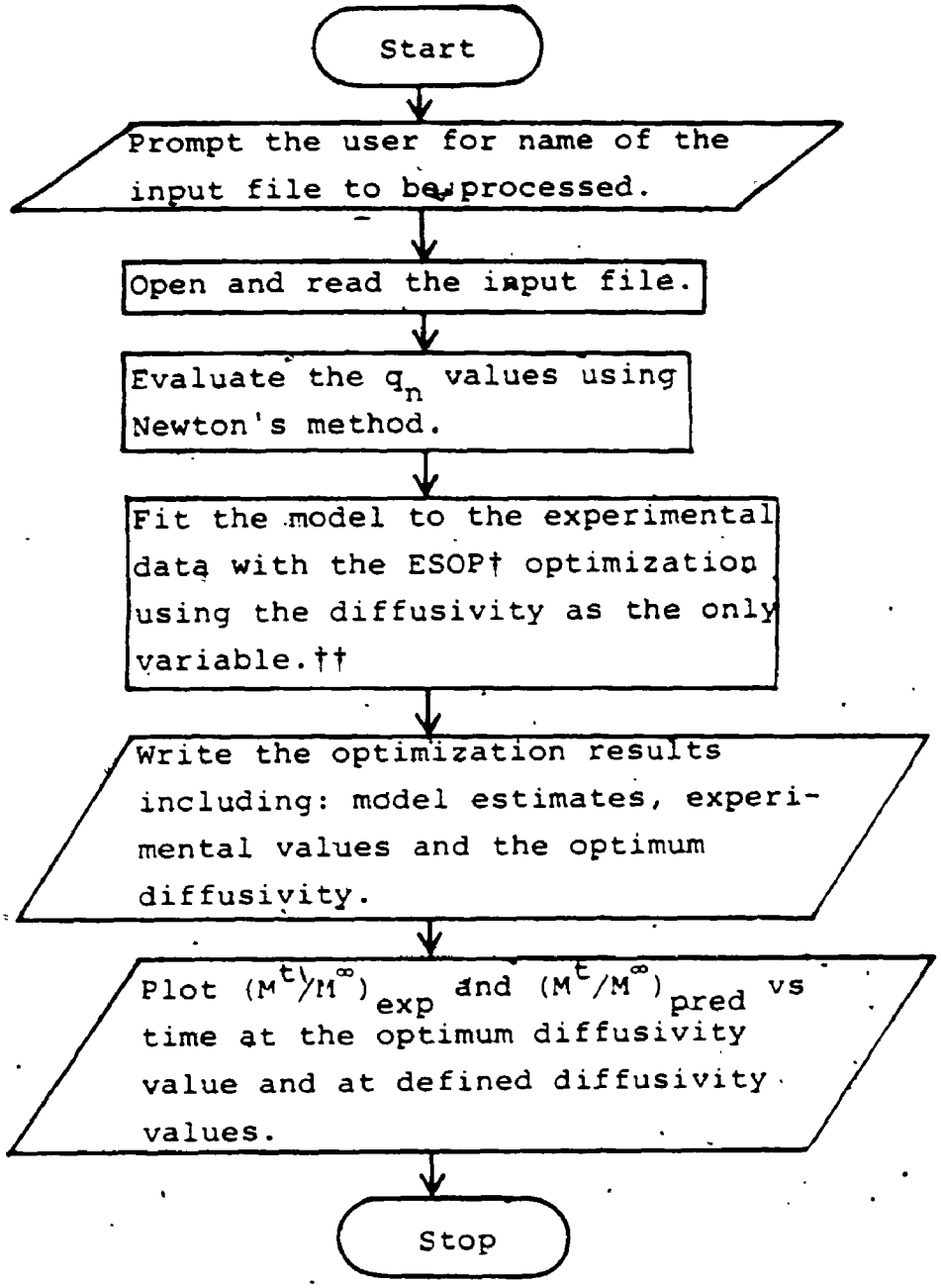

† ESOP: Users Instructions, Engineering Systems Optimization Package, System Analysis, Control and Design Activity - Report No. SACDA 80-21, 1982.

†† Optimization Criterion:

$$\text{Minimize} : [(M^t/M^\infty)_{exp} - (M^t/M^\infty)_{pred}]^2$$

solute concentration at the radial distance, r, from the centre of the sphere at time, t, can be expressed by the following equation given by Cranks (1975):

$$(C_S^t)_{r/R} = C_S^\infty \left[1 + \sum_{n=1}^{25} \frac{6(1+\alpha)\exp\ (-D_e q_n^2\ t/R^2)}{9+9\alpha+q_n^2\alpha^2} \cdot \frac{R}{r} \cdot \frac{\sin(q_n r/R)}{\sin\ q_n} \right] \qquad 4.14$$

where, r/R is the fraction of the radial distance from the center of the bead, $(C_S^t)_{r/R}$ is the solute concentration in the bead after time t, and at the radial distance r/R, C_S^∞ is the equilibrium solute concentration in the sphere after infinite time, and D_e is the optimum effective solute diffusivity obtained in DIFFIT.

At the bead surface (i.e. r/R = 1.0) the solute concentration $[(C_S^t)_{r=R}]$ is given by Equation 4.15

$$(C_S^t)_{r=R} = C_S^\infty \left[1 + \sum_{n=1}^{25} \frac{6(1+\alpha)\exp\ (-D_e q_n^2\ t/R^2)}{9+9\alpha+q_n^2\alpha^2} \right] \qquad 4.15$$

For effusion of a solute from an equilibrated bead (i.e. uniform initial solute concentration within the bead = C_S^o), the solute concentration, $(C_S^t)_{r/R}$, at a radial distance, r/R, at time t, is expressed by Equation 4.16.

$$(C_S^t)_{r/R} = C_S^o - \left((C_S^o - C_S^\infty) \left[1 + \sum_{n=1}^{25} \frac{6(1+\alpha)\exp(-D_e q_n^2 t/\beta^2)}{9+9\alpha+q_n^2\alpha^2} \cdot \frac{R}{r} \cdot \frac{\sin(q_n r/R)}{\sin q_n} \right] \right) \qquad 4.16$$

Using Equation 4.14 (or Equation 4.16), the concentration profile of glucose through a spherical Ca-alginate bead was determined using the computer program called PROFILE. This program plots the solute concentration at 21 fixed values of r/R (i.e. r/R = 0.01, and 0.05 to 1.00 at intervals of 0.05) at various user defined times. The flowchart of PROFILE and a typical computer output are given in Figure 4.7 and Appendix B.4, respectively.

All the computer programs used in this study were compiled by Mr. J.B. Wallace (Personal Communications, 25 April, 1985; 12 April, 1986; 21 July, 1986).

Figure 4.7: Flowchart of the computer program PROFILE which plots the solute concentration profile in the spherical bead at various user defined times.

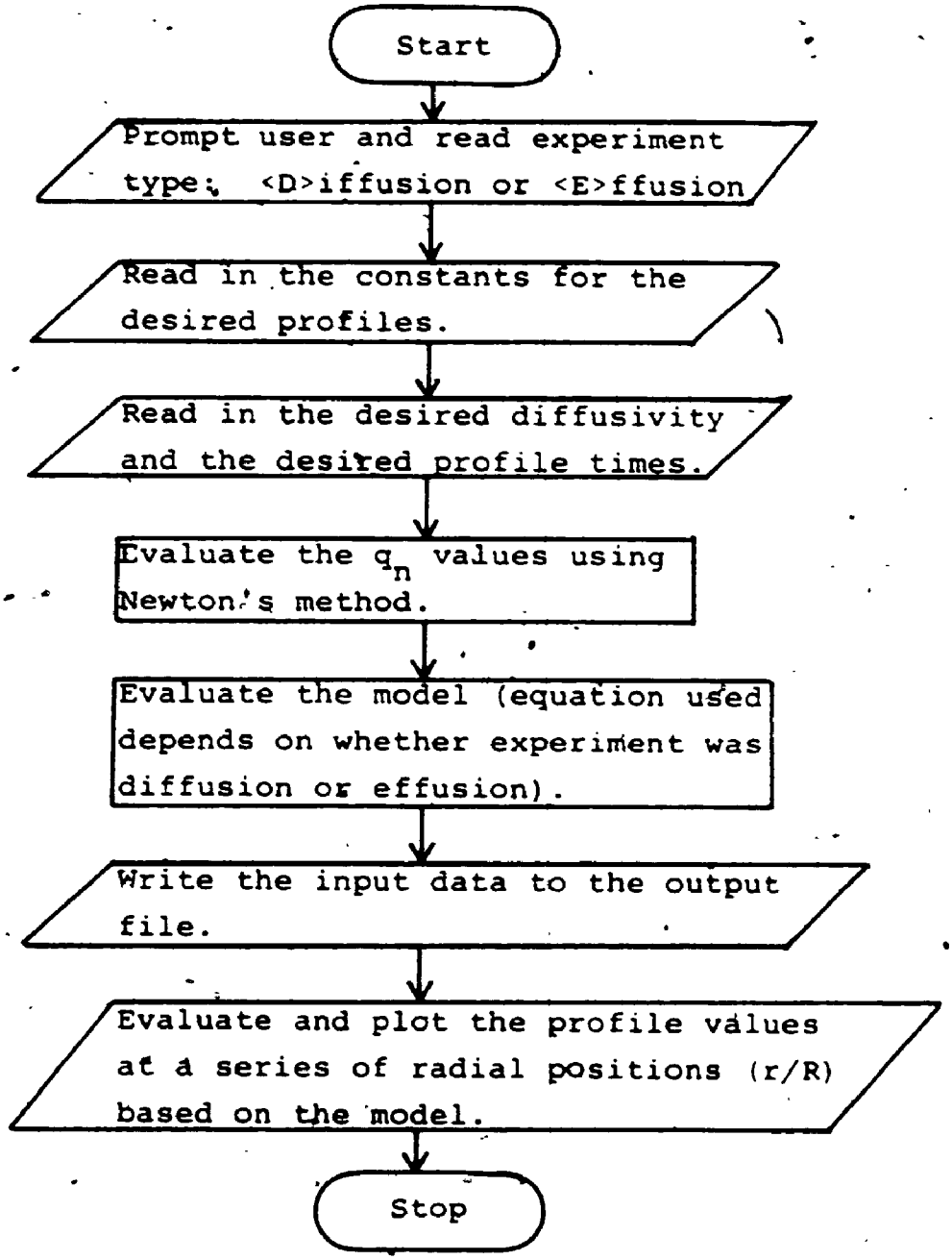
Start
Prompt user and read experiment type: <D>iffusion or <E>ffusion
Read in the constants for the desired profiles.
Read in the desired diffusivity and the desired profile times.
Evaluate the q_n values using Newton's method.
Evaluate the model (equation used depends on whether experiment was diffusion or effusion).
Write the input data to the output file.
Evaluate and plot the profile values at a series of radial positions (r/R) based on the model.
Stop

CHAPTER 5

EXPERIMENTAL RESULTS AND DISCUSSIONS

5.1 Fundamental Studies Using the Novel Diffusivity Measurement Apparatus

In the novel diffusivity measurement apparatus described in Section 4.7 a single Ca-alginate spherical bead was immersed and rotated in a liquid phase of limited volume. Based on the fractional solute uptake or release rates, the effective diffusivity of glucose was calculated using either Equation 3.60 or Equation 3.59, respectively, as discussed in Sections 4.9 to 4.13.

In studies reported below, all Ca-alginate beads were prepared from 2% aqueous solutions of purified sodium alginate (Fisher Chemicals, Sample #17) using 4% $CaCl_2$ solution as the gelling agent. Unless otherwise stated, the initial concentration of 'cold' glucose in the liquid phase was 20 $kg.m^{-3}$ and all D_e and K_p measurements were carried out at 30^oC.

5.1.1 Effect of Bead Rotational Speed on Solute Uptake and Release Rates

A large Ca-alginate bead of diameter (d_s) 1.239 cm prepared as described earlier (Section 4.3.1) was immersed in a 2% (w/v) aqueous solution of D-glucose containing C^{14}-D-glu-

cose as the tracer, and rotated at 117 rpm. In Figure 5.1 the experimental values of the fractional solute uptake (M_s^t/M_s^∞) are plotted as a function of time. Using Equation 3.60 the predicted curve of M_s^t/M_s^∞, at the optimum D_e value, corresponding to the best computer fit of the experimental data is also shown.

After 360 minutes, the equilibrated Ca-alginate bead was removed from the labelled glucose solution and immersed in distilled water to allow the effusion of the solute from the bead to occur. At a rotation speed of 117 rpm, the experimental values of the fractional solute release (M_L^t/M_L^∞) plotted versus time are shown in Figure 5.2. Using Equation 3.59 the predicted M_L^t/M_L^∞ curve corresponding to the optimum D_e value is also plotted. For comparison, the theoretical solute uptake rates at defined D_e values ranging from 1.0×10^{-11} $m^2.s^{-1}$ to 5.0×10^{-9} $m^2.s^{-1}$ are plotted in Figure 5.3.

The uptake of the solute diffusing into the Ca-alginate bead at rotational speeds of 235, 348, 467, and 542 rpm and its subsequent effusion at 467 rpm were also examined. Based on these experimental data, the optimum D_e values, the equilibrium partition coefficients (K_p), and the percentage deviation of experimental points from the predicted curves (calculated using Equation 4.13) are summarized in Table 5.1.

As shown in Figure 5.2 a better fit of the experimental data to the predicted curves is accomplished when determining D_e using the effusion technique. This is expected in

Figure 5.1: Fractional glucose uptake rate at a bead rotational speed of 117 rpm. (●) Experimental points, (——) predicted curve correspondong to the best computer fit of experimental data at the optimum D_e value of $6.22 \times 10^{-10}\ m^2.s^{-1}$ with $K_p = 0.98$.

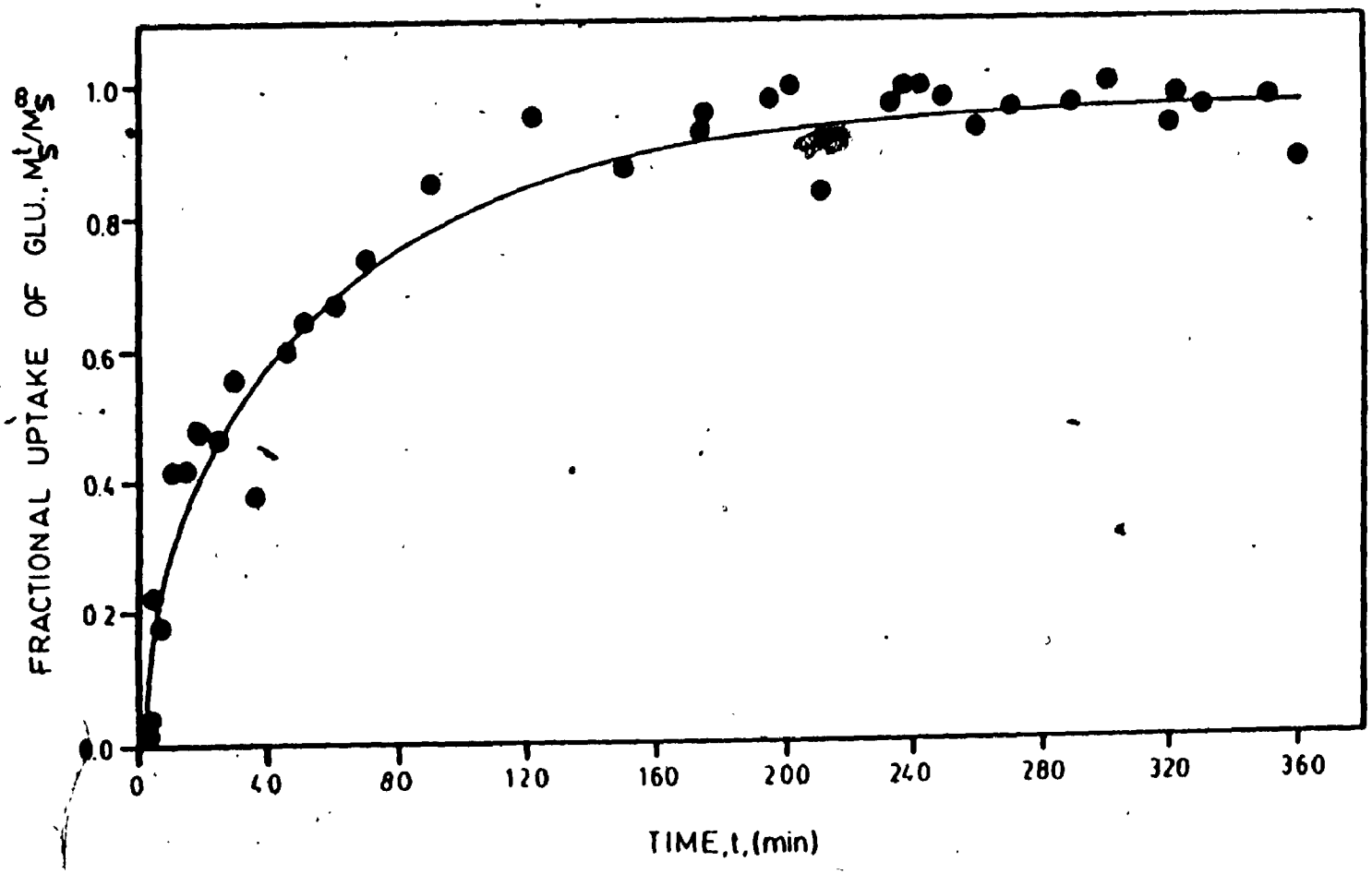
FRACTIONAL UPTAKE OF GLU., M_S^t/M_S^∞
1.0
0.8
0.6
0.4
0.2
0.0
0
40
80
120
160
200
240
280
320
360
TIME, t, (min)

Figure 5.2: Fractional glucose release rate at a bead rotational speed of 117 rpm. (●) Experimental points; (——) predicted curve corresponding to the best computer fit of experimental data at the optimum D_e value of 6.50×10^{-10} $m^2.s^{-1}$ with $K_p = 0.97$.

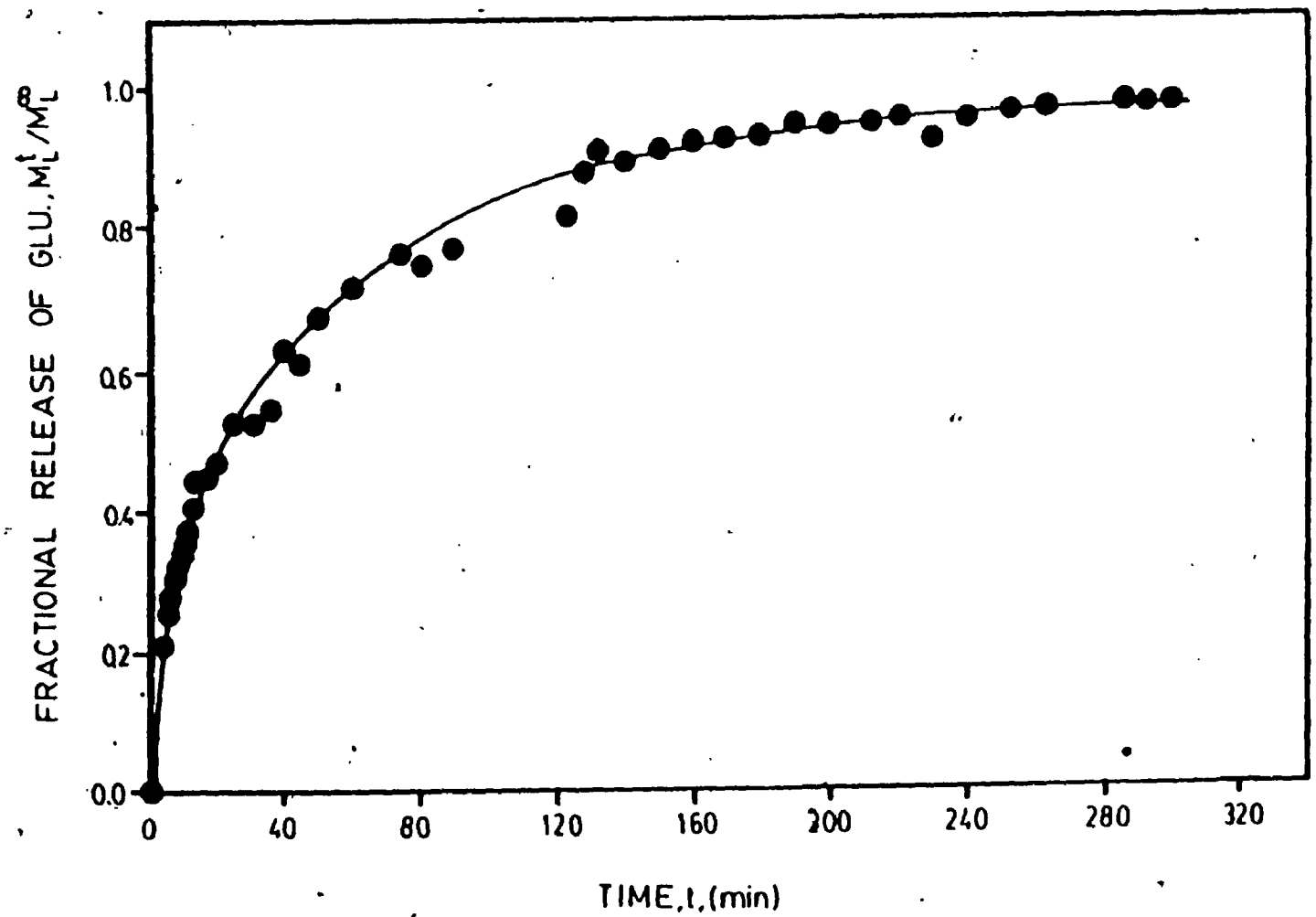
FRACTIONAL RELEASE OF GLU., M_L^t/M_L^∞
1.0
0.8
0.6
0.4
0.2
0.0
0
40
80
120
160
200
240
280
320
TIME, t, (min)

Figure 5.3: Theoretical curves for fractional glucose uptake rate at defined D_e values.

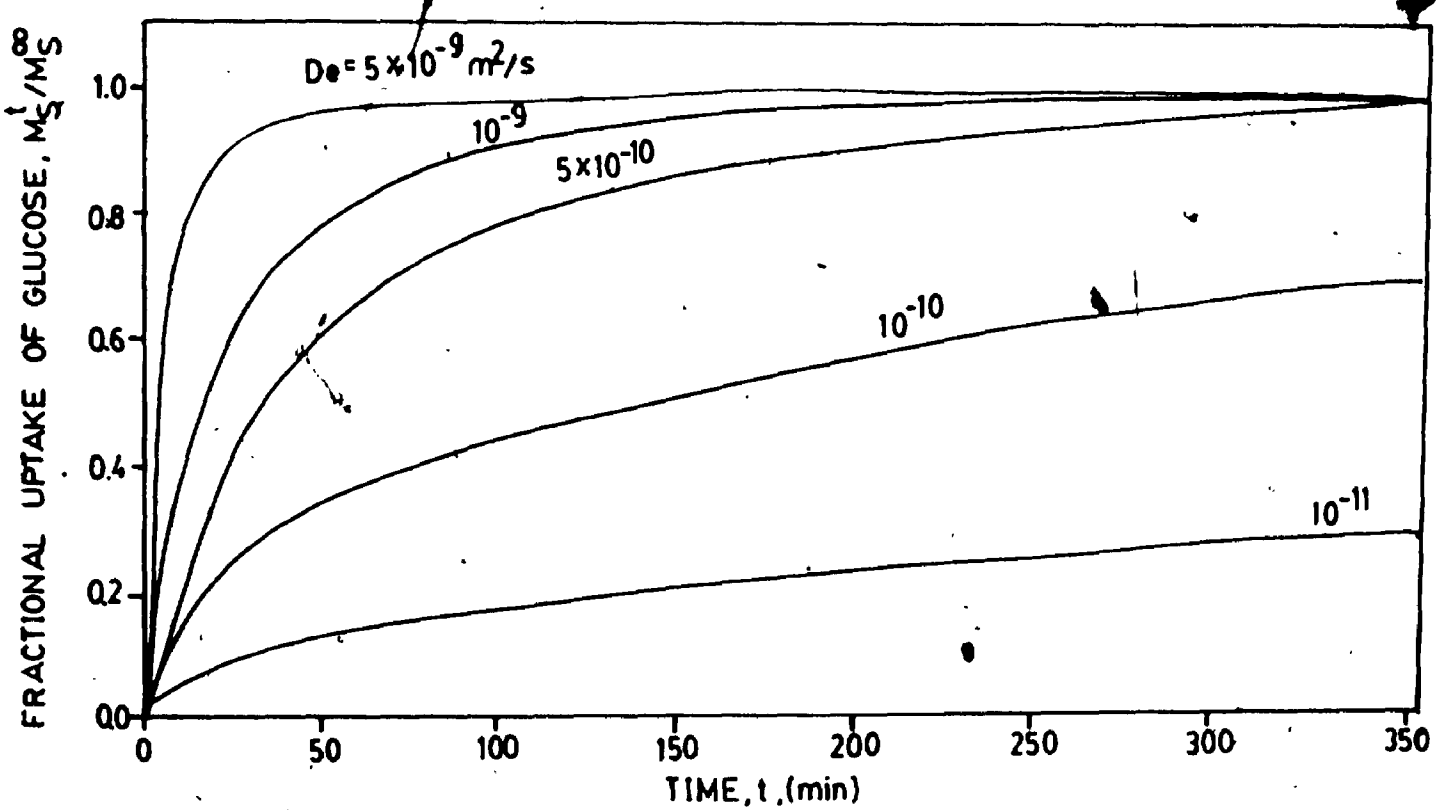
FRACTIONAL UPTAKE OF GLUCOSE, M_S^t/M_S^∞
1.0
0.8
0.6
0.4
0.2
0.0
0
50
100
150
200
250
300
350
TIME, t, (min)
$D_e = 5\times10^{-9}\ m^2/s$
10^{-9}
5×10^{-10}
10^{-10}
10^{-11}

Table 5.1: Effective diffusivity and equilibrium partition coefficients of glucose in 2% Ca-alginate gel determined at different bead rotational speeds.

Bead rotational speed, (r.p.m.)	Bead diameter, $d_s \times 10^2$, (m)	Angular velocity of bead, Ω_1 (rad. s^{-1})	Effective diffusivity, $D_e \times 10^{10}$, ($m^2.s^{-1}$)	Equilibrium partition coefficient, K_p	Percentage** deviation from theoretical (%)
117	1.239	12.25	6.22	0.98	2.34
117*	1.239	12.25	6.50	0.97	0.14
235	1.179	24.61	6.70	1.02	2.16
348	1.249	36.44	6.61	1.00	2.20
467	1.210	48.90	6.79	0.98	1.30
467*	1.210	48.90	6.86	0.93	0.04
542	1.190	56.76	6.66	1.00	2.23

* Effusion of solute from Ca-alginate bead.

** % deviation of experimental data ($[M^t/M^\infty]_{exp}$) from predicted values ($[M^t/M^\infty]_{pred}$) as defined by Equation 4.13

view of the higher overall solute concentration change in the liquid phase. However, the D_e values determined by both, the effusion and diffusion techniques agree very well within 2%.

5.1.1.1 Mixing Characteristics

In using Equations 3.59 and 3.60 it was assumed that the liquid phase was well mixed and the film mass transfer resistance was negligible. The degree of mixing in the liquid phase at different angular velocities of the bead was determined by the simple dye-injection technique. Using Ca-alginate beads of three different diameters (encompassing the size range used in the above experiments), the time taken for 10 μL of methylene blue dye to be homogeneously distributed in 4 mL of distilled water as observed visually was estimated at different bead rotational speeds. At angular velocities exceeding 40 radians/second (corresponding to bead rotational speeds of 467 and 542 rpm), mixing was almost instantaneous whereas at the lowest rotational speed of approximately 117 rpm ($\simeq$ 12 rad.s^{-1}), the mixing time was about 25 seconds. As shown in Figure 5.4, when the rotational Reynolds' number ($N_{Re,r}$) exceeds 5,000, the mixing characteristics of the diffusion apparatus are excellent (t_m < 4.0 s). Consequently, at such high bead rotational speeds the solute will be homongeneously distributed in the liquid phase. In all subsequent studies, the bead rotational speed

Figure 5.4: Mixing characteristics of the diffusion apparatus at different bead rotational Reynolds' number. Bead diameter, d_s = 1.152 cm (●); 1.256 cm (▲); 1.387 cm (■).

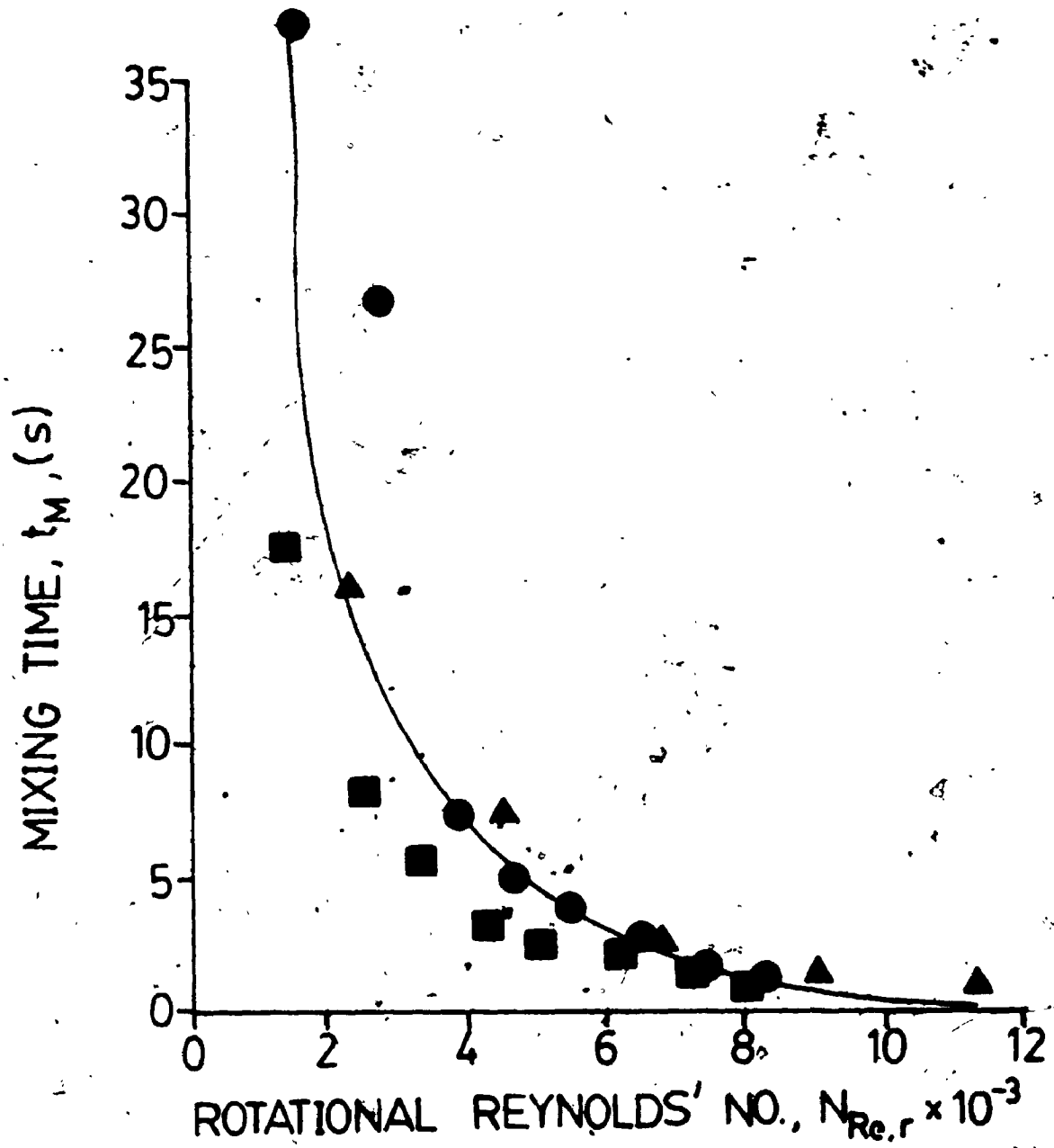
35
30
25
20
15
10
5
0
MIXING TIME, t_M, (s)
0
2
4
6
8
10
12
ROTATIONAL REYNOLDS' NO., $N_{Re,r} \times 10^{-3}$

was set at values such that $N_{Re,r} > 5,000$.

5.1.1.2 Estimation of the External Film Mass Transfer Coefficient, k_L

In measuring effective solute diffusivities in solids, it is important to ensure that the external mass transfer resistance is negligible. The film mass transfer coefficient, k_L, on the surface of the rotating Ca-alginate sphere was calculated by the empirical correlation of Noordsij and Rotte (1967) which is given by Equation 5.1

$$N_{Sh} = 10 + 0.43\,(N_{Re,r})^{1/2}\,(N_{Sc})^{1/3}$$

$$\text{when, } 800 < N_{Re,r} < 27,000$$

$$\text{and } 500 < N_{Sc} < 2,000 \qquad 5.1$$

where, N_{Sh} is the Sherwood number and N_{Sc} is the Schmidt number.

For the diffusion and effusion techniques the physical properties of 2% (w/v) glucose solution and distilled water (listed in Table 5.2) were respectively used to estimate k_L at different bead rotational speeds. Thus, as shown in Table 5.3 and Figure 5.5, by increasing the bead rotational speed from 117 rpm to 542 rpm, the film mass transfer coefficient increases by at least two fold. According to

Table 5.2: Physical Parameters Used to Evaluate the External Film Mass Transfer Coefficient, k_L

Physical parameters	Values	
Composition of liquid phase	Pure water	20 $kg.m^{-3}$ aqueous solution of glucose
Temperature, T (^{o}C)	30	30
Viscosity, $\mu \times 10^3$ ($kg.m^{-1}.s^{-1}$)	0.8007[a]	0.8268[b]
Density, ρ ($kg.m^{-3}$)	995.7[a]	1003.3[c]
Kinematic viscosity, $\bar{\nu} \times 10^7$ ($m^2.s^{-1}$)	8.042	8.241
Diffusivity of glucose in water, $D \times 10^{10}$ ($m^2.s^{-1}$)	7.50[d]	7.18[d]
Schmidt number, N_{Sc} (dimensionless)	1072	1148

[a]from, Geankoplis (1983); [b]from, Thomas (1965); [c]from Bates et al. (1929); [d]from Dadenkova et al. (1973).

Table 5.3: Calculated External Film Mass Transfer Coefficient and Biot Numbers at Different Rotational Reynolds' Numbers

Experimental conditions	Rotational Reynolds' number, $N_{Re,r}$	Sherwood number, N_{Sh}	Film mass transfer coefficient, $k_L \times 10^5$ ($m.s^{-1}$)	Biot number, N_{Bi}
Diffusion, 117 r.p.m.	2282	225.1	1.305	130.0
Effusion, 117 r.p.m.	2338	222.8	1.349	128.6
Diffusion, 235 r.p.m.	4151	300.1	1.828	160.8
Diffusion, 348 r.p.m.	6898	384.0	2.208	208.6
Diffusion, 467 r.p.m.	8688	429.7	2.550	227.2
Effusion, 467 r.p.m.	8903	425.2	2.636	232.5
Diffusion, 542 r.p.m.	9753	454.7	2.744	245.2

Figure 5.5: The effect of bead rotational Reynolds' number on the external film mass transfer coefficient, the mass transfer Biot number, and effective diffusivity of glucose in Ca-alginate gel.

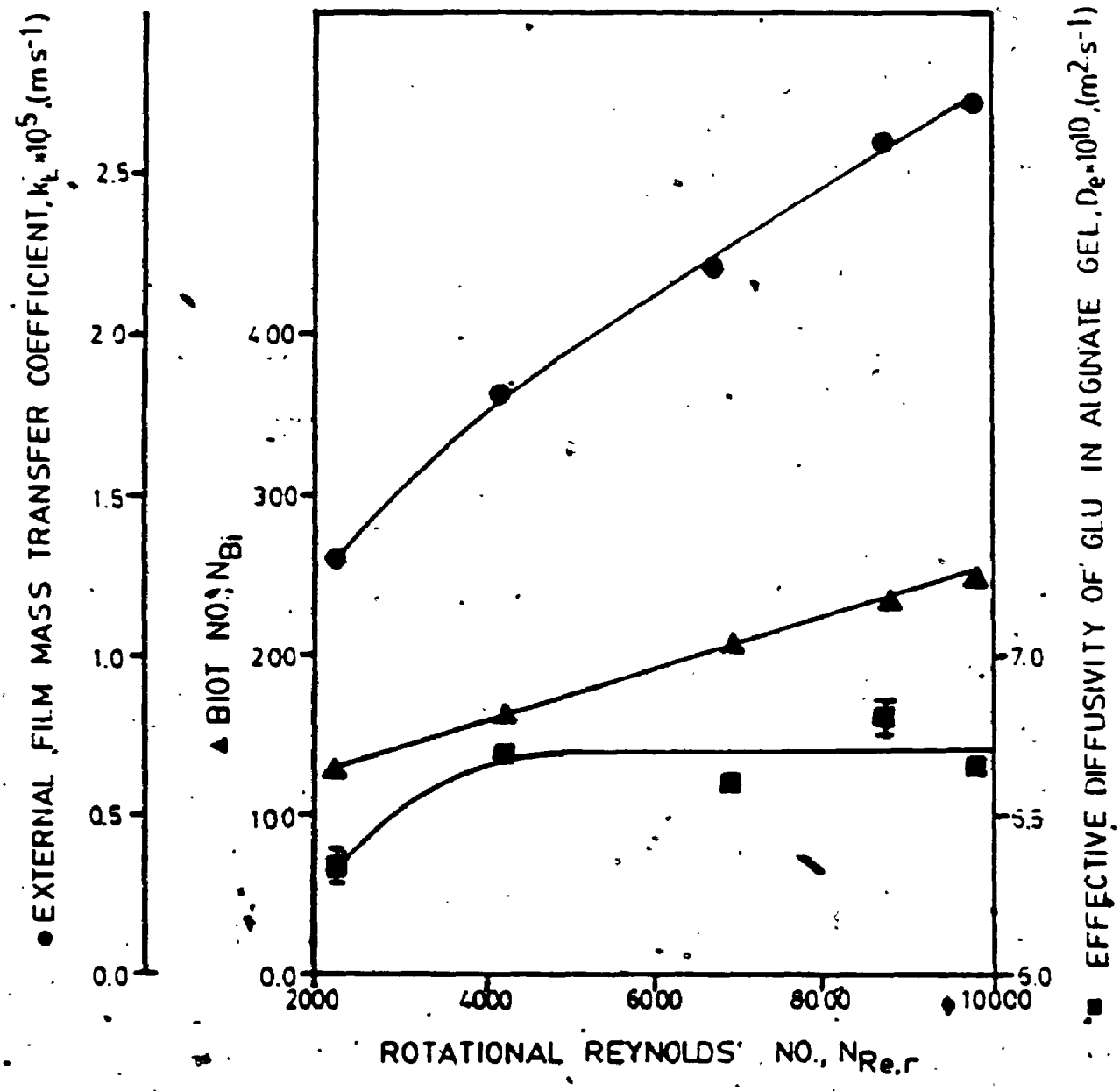
● EXTERNAL FILM MASS TRANSFER COEFFICIENT, $k_L \times 10^5$, $(m\,s^{-1})$
▲ BIOT NO., N_{Bi}
■ EFFECTIVE DIFFUSIVITY OF GLU IN ALGINATE GEL, $D_e \times 10^{10}$, $(m^2 \cdot s^{-1})$
ROTATIONAL REYNOLDS' NO., $N_{Re,r}$
0.0
0.5
1.0
1.5
2.0
2.5
100
200
300
400
5.0
5.5
7.0
2000
4000
6000
8000
10000

Sirotti and Emery (1983), the k_L value of glucose on the surface of controlled pore ceramic beads ($d_s \simeq 150$ μm) packed in a column was estimated, using the McCune-Wilhelm model (1949), to be $3.6 \times 10^{-5} m.s^{-1}$. Ryu et al. (1984) employed the empirical correlation of Williamson et al. (1963) and estimated the k_L value of glucose on the surface of Ca-alginate beads, packed in a column, to be 2.5×10^{-5} $m.s^{-1}$ at the highest superficial velocity of the bulk fluid. These k_L values are of the same order of magnitude as those obtained at high rotational Reynolds' numbers even though the particle size employed in this study was approximately 80 times larger than that used by Sirotti and Emery (1983).

In order to examine the significance of the lower k_L values, at low rotational speeds, on the overall rate of mass transfer, the Biot number, N_{Bi}, defined by Equation 3.38, was calculated at different bead rotational speeds and the respective values are listed in Table 5.3. Even at the lowest bead rotational speed, N_{Bi} exceeds 100 indicating that the film mass transfer resistance does not affect the overall mass transfer rate appreciably (Bailey and Ollis, 1986). For instance, according to Schwartzberg and Chao (1982), when N_{Bi} exceeds 200, the effect of film mass transfer resistance on the overall solute uptake rate and/or release rate, is less than one percent.

As shown in Figure 5.5 and Table 5.1 the D_e value measured at the lowest bead rotational speed is not significantly lower than that measured at high bead rotational

speeds. Therefore, using the novel diffusivity measurement apparatus, conditions of near ideal mixing (τt_m < 4s at $N_{Re,r}$ > 5,000) and negligible film mass transfer resistance (N_{Bi} > 200) could be achieved. Accordingly, the effective diffusivity of glucose in 2% Ca-alginate gel at 30°C was found to be 6.73×10^{-10} $m^2.s^{-1}$ ($\pm$ 0.12×10^{-10} $m^2.s^{-1}$).

5.1.2 Concentration Profile of Glucose in Ca-Alginate Sphere

The radial concentration profile of glucose within a Ca-alginate sphere was determined as a function of time by solving Equation 4.14 (for diffusion when $D_e = 6.79 \times 10^{-10}$ $m^2.s^{-1}$) and Equation 4.16 (for effusion when $D'_e = 6.86 \times 10^{-10}$ $m^2.s^{-1}$) using the computer program called PROFILE (see Section 4.14). The respective glucose concentration profiles for a typical diffusion and effusion experiment are shown in Figures 5.6 and 5.7. Thus, the solute appears to be uniformly distributed within the Ca-alginate bead after 5 to 6 hours indicating that equilibrium is achieved during this time period.

5.1.3 Equilibrium Partition Coefficient, K_p, of Glucose in Ca-Alginate Gel

Figures 5.8 and 5.9 show the typical solute concentration changes that occur in the liquid phase (C_L^t) and the

Figure 5.6: Glucose concentration profile in Ca-alginate sphere at different times during the diffusion process when $D_e = 6.79 \times 10^{-10} m^2.s^{-1}$.

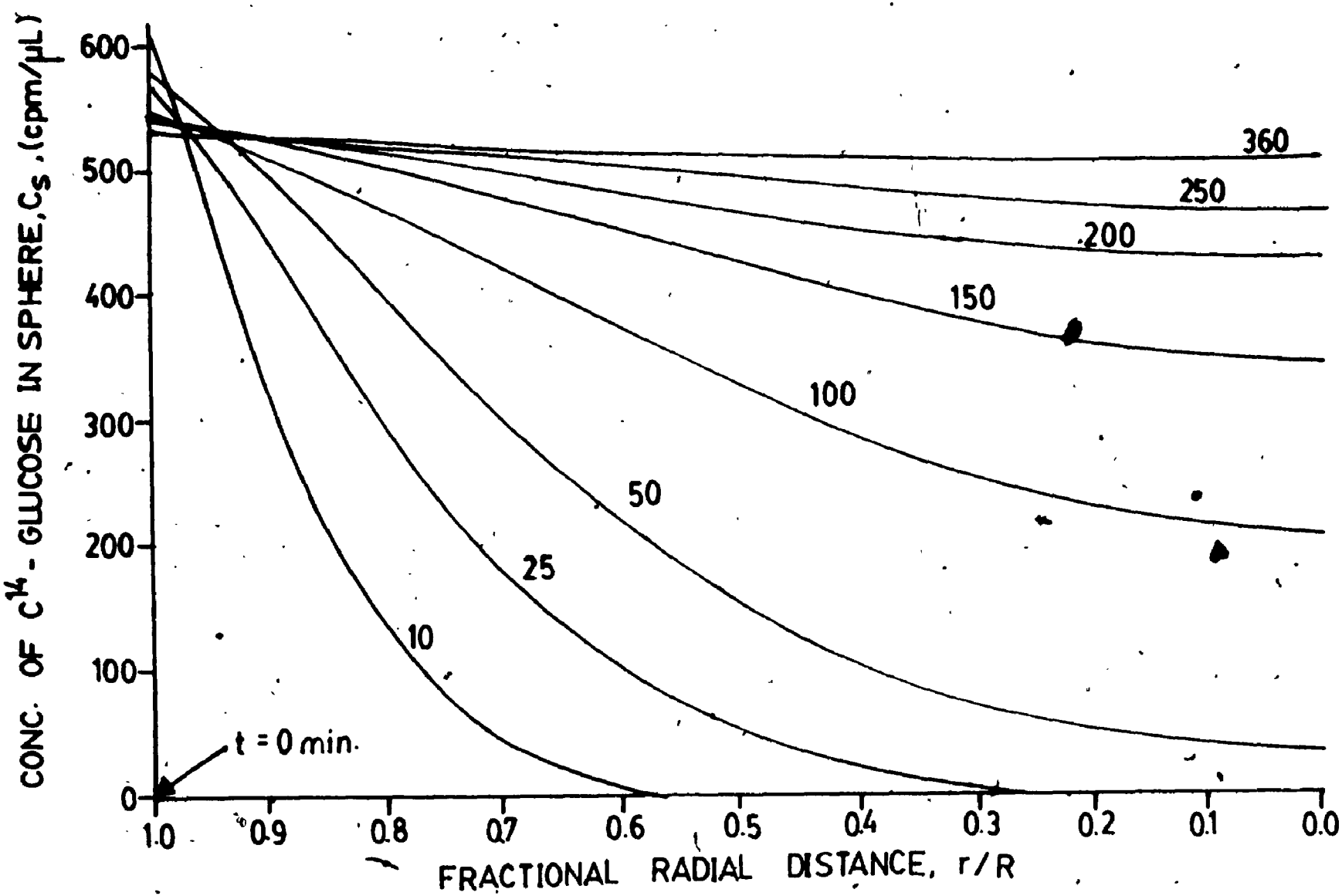
CONC. OF C^{14} - GLUCOSE IN SPHERE, C_s, (cpm/μL)
600
500
400
300
200
100
0
1.0
0.9
0.8
0.7
0.6
0.5
0.4
0.3
0.2
0.1
0.0
FRACTIONAL RADIAL DISTANCE, r/R
360
250
200
150
100
50
25
10
t = 0 min.

Figure 6.7: Glucose concentration profile in Ca-alginate sphere at different times during the effusion process when $D_e = 6.86 \times 10^{-10}\ m^2 \cdot s^{-1}$.

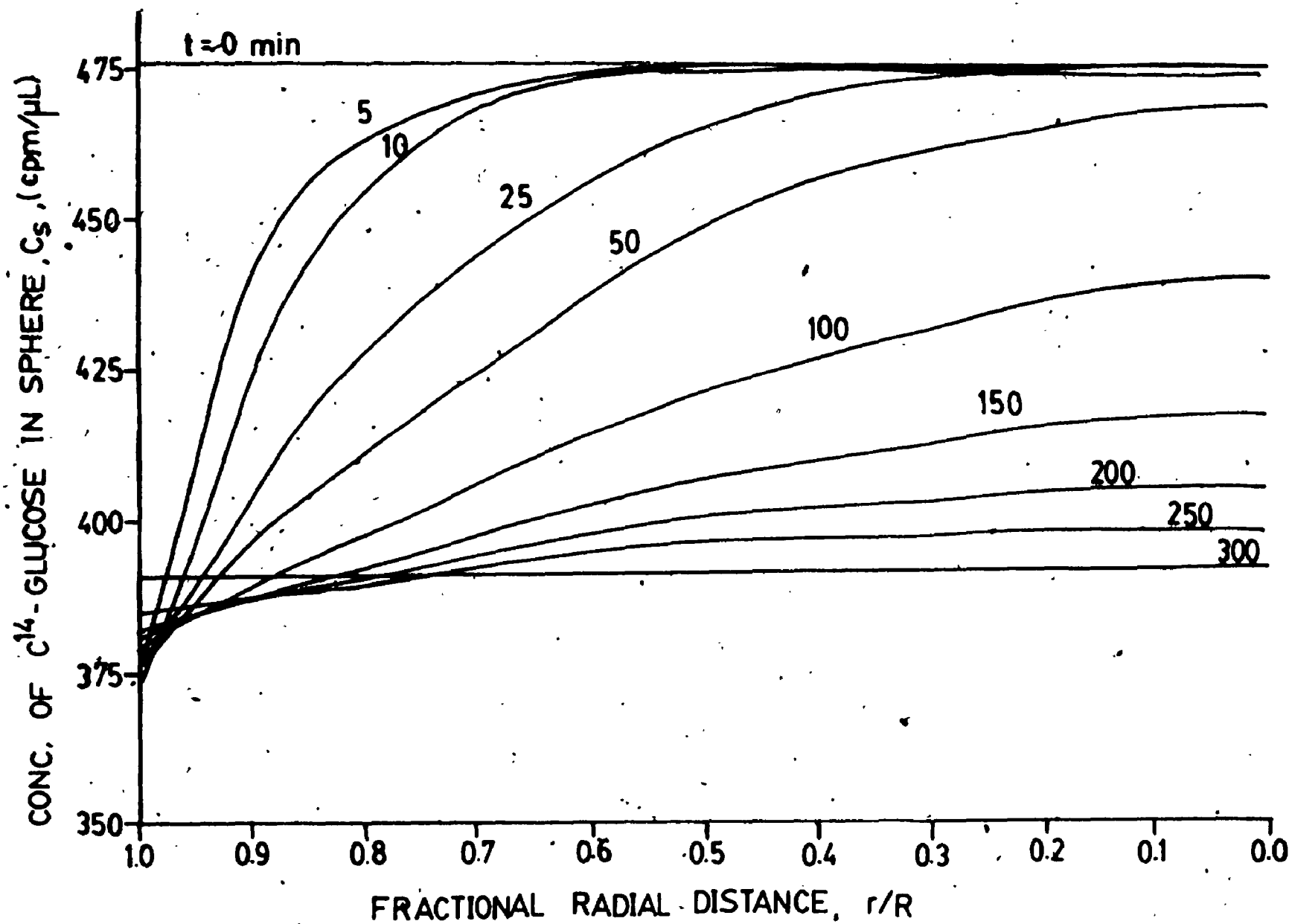
t = 0 min
5
10
25
50
100
150
200
250
300
475
450
425
400
375
350
1.0
0.9
0.8
0.7
0.6
0.5
0.4
0.3
0.2
0.1
0.0
CONC. OF C^{14}-GLUCOSE IN SPHERE, C_s, (cpm/μL)
FRACTIONAL RADIAL DISTANCE, r/R

Figure 5.8: Changes in the concentration of C^{14}-glucose in the liquid phase and Ca-alginate sphere plotted as a function of time during diffusion of glucose into the bead when $D_e = 6.79 \times 10^{-10}$ $m^2.s^{-1}$.

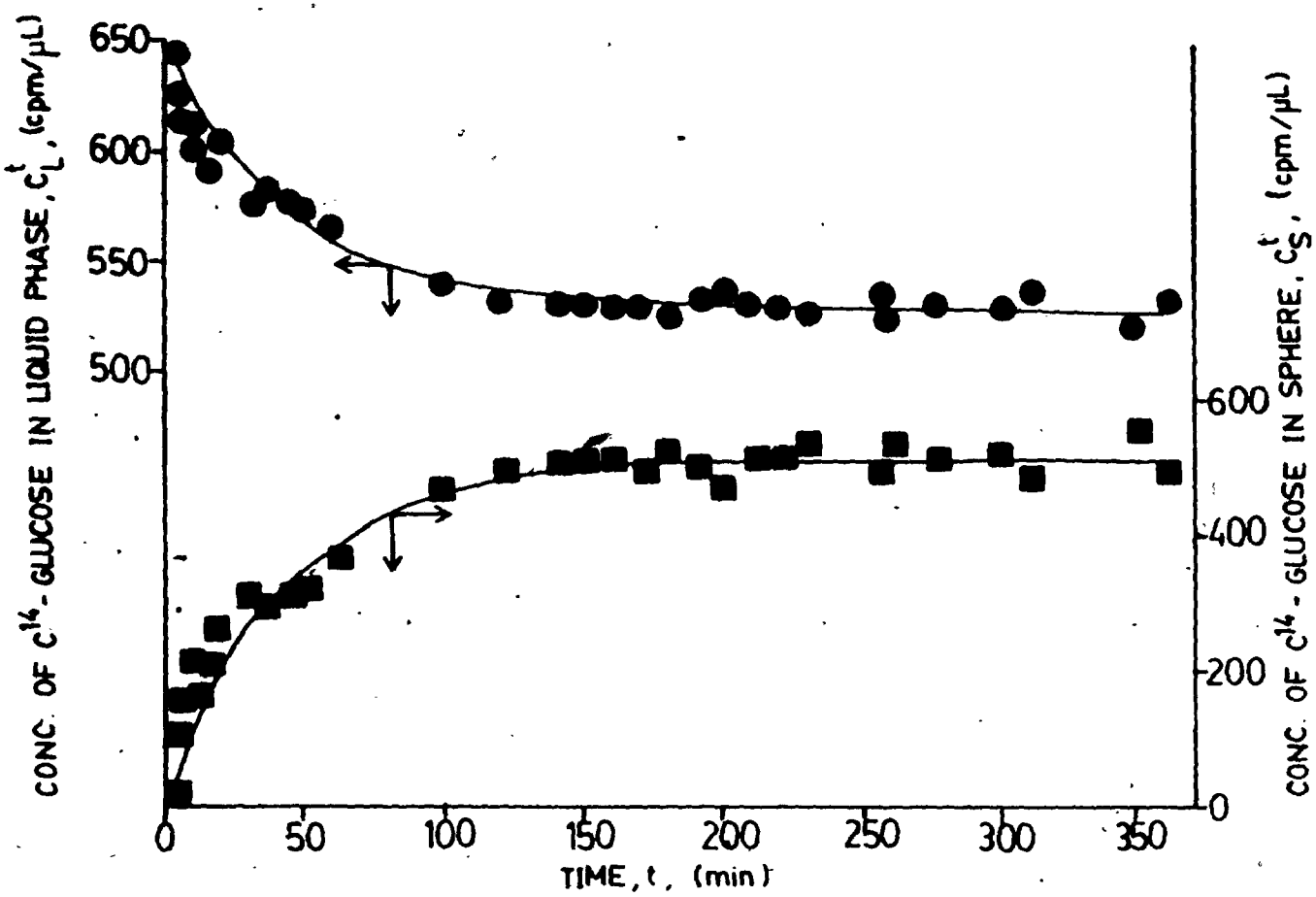
CONC. OF C14- GLUCOSE IN LIQUID PHASE, C_L^t, (cpm/μL)
650
600
550
500
CONC. OF C14- GLUCOSE IN SPHERE, C_S^t, (cpm/μL)
600
400
200
0
0
50
100
150
200
250
300
350
TIME, t, (min)

Figure 5.9: Changes in the concentration of C^{14}-glucose in the liquid phase and Ca-alginate sphere plotted as a function of time during effusion of glucose out of the bead when $D_e = 6.86 \times 10^{-10}\ m^2.s^{-1}$.

3

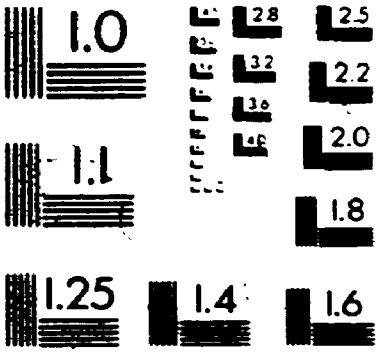

CONC. OF C14-GLUCOSE IN LIQUID PHASE, CL, (cpm/μL)
CONC OF C14-GLUCOSE IN Ca-ALGINATE SPHERE, Cs, (cpm/μL)
TIME, t, (min)
0
25
50
75
100
0
100
200
300
400
0
50
100
150
200
250
300

number of terms, n, used in Equation 3.59. Thus, when n exceeds 10, there is no further change in the value of D_e. However, with the use of only the first term of the series solution, the estimated D_e value (5.86×10^{-10} $m^2.s^{-1}$) is almost 15% lower than the actual value, whereas, by introducing the second term in the series, the error is reduced to less than 5%.

5.1.7.2 Graphical Method

The series solution given by Equation 3.59 can be rewritten in terms of the solute concentration changes that occur in the liquid phase during the effusion process. Accordingly,

$$y = \frac{C_L^t - C_L^\infty}{C_L^o - C_L^\infty} = \sum_{n=1}^{N} A_n \exp(-q_n^2 \tau) \qquad 5.6$$

where A_n is given by Equation 5.7

$$A_n = \frac{6\alpha.(\alpha + 1)}{9 + 9\alpha + \alpha^2 q_n^2} \qquad 5.7$$

When the dimensionless time, τ, is large, then the terms corresponding to $n \geq 2$ in Equation 5.6 can be neglected. Under this condition, Equation 5.6 can be converted into the following linear form

Figure 5.18: The Arrhenius plot for diffusion of glucose in cell-free Ca-alginate gel.

concentrations (Hu et al., 1985). In order to determine the type of adsorption isotherm of glucose in Ca-alginate matrix, the diffusion apparatus was employed in which spherical beads were equilibrated in C^{14}-glucose solutions initially containing 3 to 300 kg. m^{-3} of 'cold' glucose. Equilibrium was reached after 5 to 6 hours when the radioactivities of several consecutive 3 μL samples of the liquid solution were found to be the same.

Knowing the initial (C_L^o) and equilibrium (C_L^∞) concentration of the solute in the liquid phase, the equilibrium glucose concentration in the Ca-alginate sphere (C_S^∞) was determined by a simple mass balance. The results are summarized in Table C.1 (Appendix C) and plotted in Figures 5.10 and 5.11, showing that the adsorption isotherm of glucose in Ca-alginate matrix can be expressed by a linear equilibrium relationship given by Equation 5.2. Thus,

$$q^\infty = K\, C_L^\infty \qquad 5.2$$

where K is a constant and q^∞ is the equilibrium solute concentration in the solid phase which can be defined in terms of the sphere volume ($q^\infty = C_S^\infty$), wet weight of the alginate gel ($q^\infty = [C_S^\infty]_w$), or dry weight of the alginate gel ($q^\infty = [C_S^\infty]_d$).

Following linear regression analysis of the data in Table C.1, Equation 5.2 was rewritten in terms of C_S^∞, $[C_S^\infty]_d$ or $[C_S]_w$. Thus, for the adsorption of glucose in 2% Ca-

Figure 5.10: Equilibrium adsorption isotherm of glucose in Ca-alginate matrix when C_S^{∞} is expressed in terms of the bead volume; (●) represents the experimental data and (—) is the best fit linear relationship given by Equation 5.3.

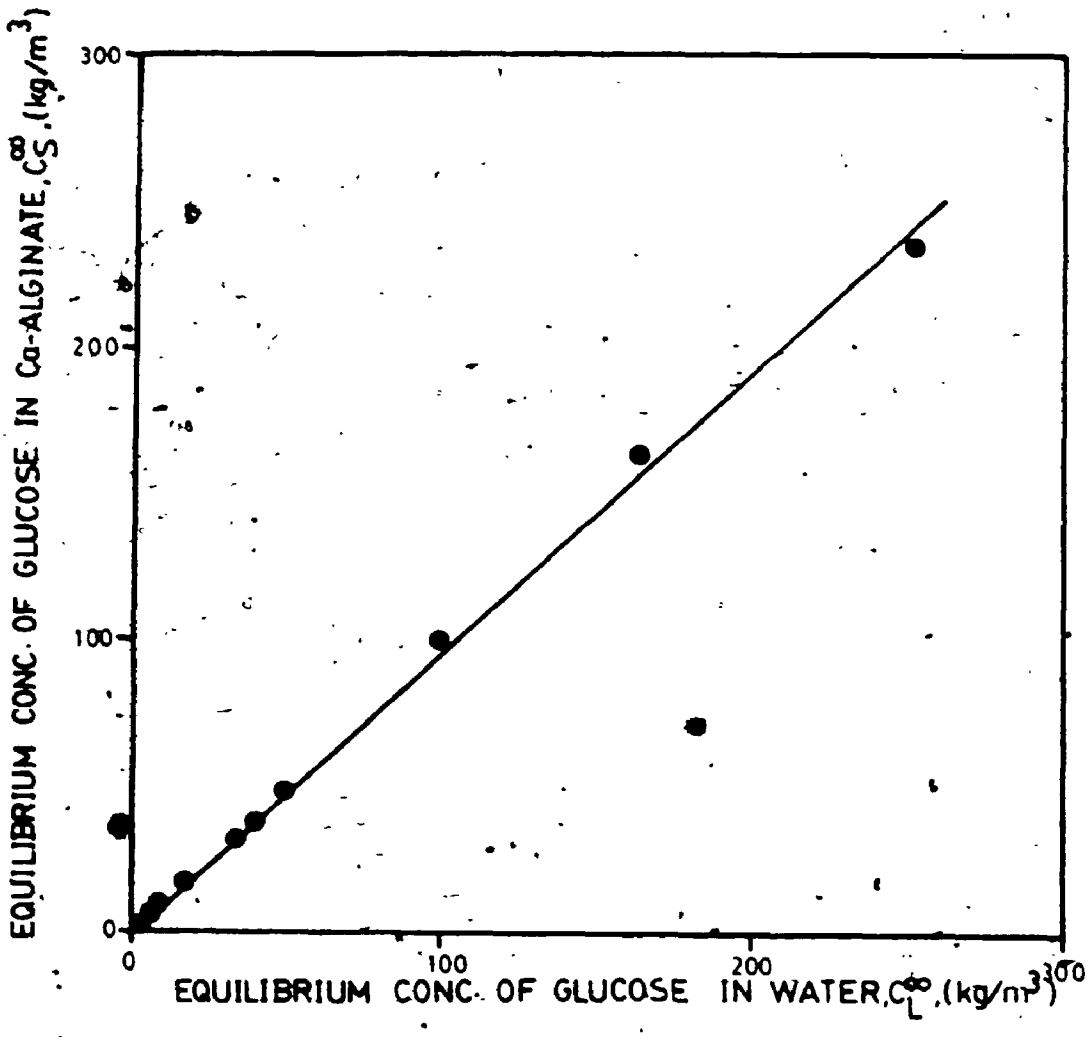
EQUILIBRIUM CONC. OF GLUCOSE IN Ca-ALGINATE, C_S^{∞}, (kg/m^3)
300
200
100
0
0
100
200
300
EQUILIBRIUM CONC. OF GLUCOSE IN WATER, C_L^{∞}, (kg/m^3)

Figure 5.11: Equilibrium adsorption isotherm of glucose in Ca-alginate matrix when C_S^{∞} is expressed in terms of wet weight (●) or dry weight (▲) of bead; (——) and (---) respectively represent the best fit linear relationships given by Equation 5.4 and 5.5.

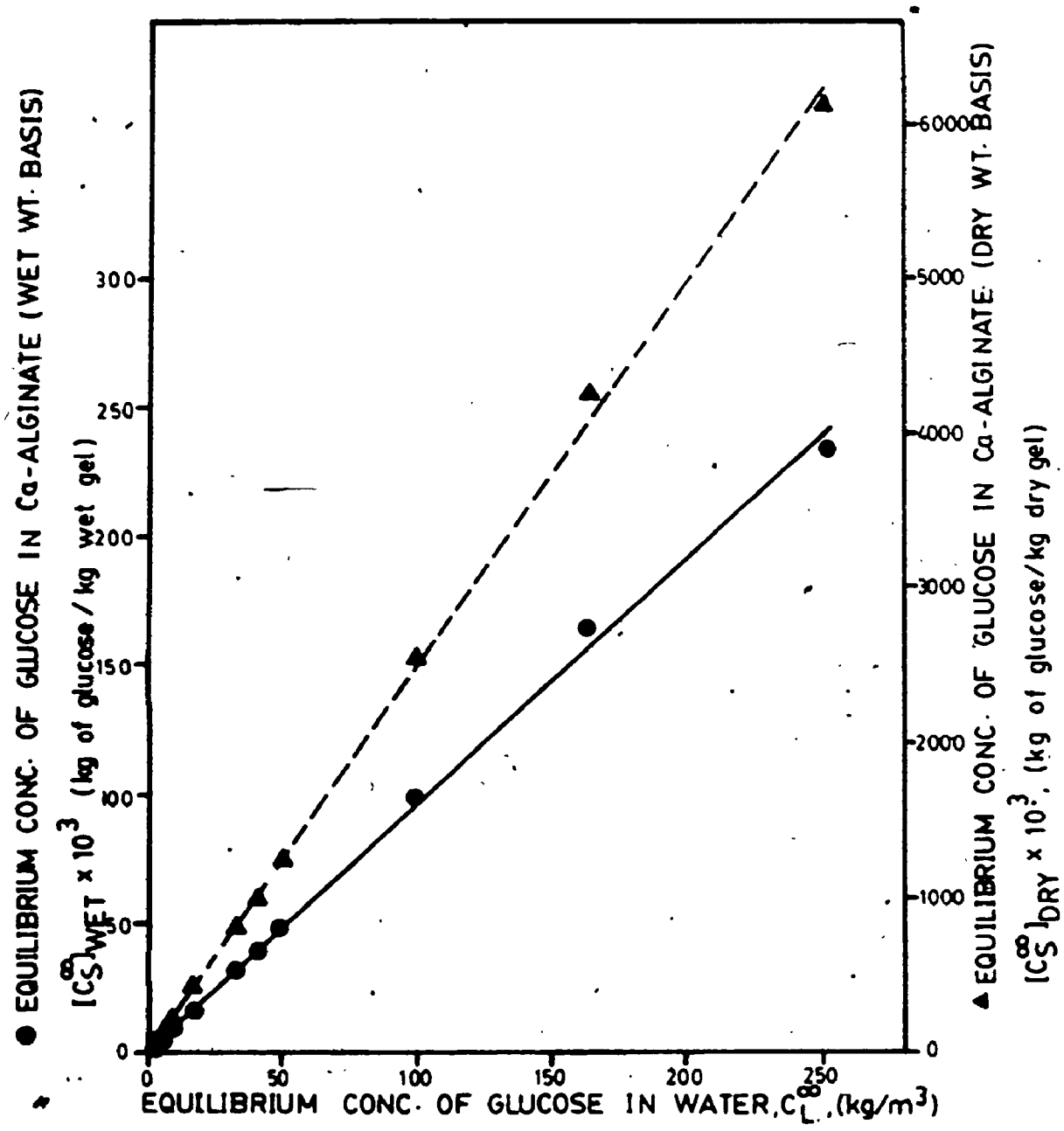
● EQUILIBRIUM CONC. OF GLUCOSE IN Ca-ALGINATE (WET WT. BASIS)
$[C_S^{\infty}]_{WET} \times 10^3$ (kg of glucose / kg wet gel)
▲ EQUILIBRIUM CONC. OF GLUCOSE IN Ca-ALGINATE (DRY WT. BASIS)
$[C_S^{\infty}]_{DRY} \times 10^3$, (kg of glucose/kg dry gel)
EQUILIBRIUM CONC. OF GLUCOSE IN WATER, C_L^{∞}, (kg/m^3)
0
50
100
150
200
250
300
1000
2000
3000
4000
5000
6000

alginate gel at 30°C, the linear adsorption isotherm can be expressed by either Equation 5.3, 5.4, or 5.5

$$C_s^\infty = 0.9514 C_L^\infty \qquad 5.3$$

$$[C_s^\infty]_w = 9.486 \times 10^{-4} \frac{m^3 \text{ liquid phase}}{\text{kg wet gel}} C_L^\infty \qquad 5.4$$

$$[C_s^\infty]_d = 2.479 \times 10^{-2} \frac{m^3 \text{ liquid phase}}{\text{kg dry gel}} C_L^\infty \qquad 5.5$$

The best-fit linear relationship given by Equation 5.3 is plotted in Figure 5.10 whereas Equations 5.4 and 5.5 are plotted in Figure 5.11. The correlation coefficient for the above linear equations was 0.9992. Thus, with glucose as the solute, Equations 3.59 and 3.60 can therefore be used to determine D_e values of glucose in Ca-alginate gel even at high initial concentrations of the solute (C_L^o = 300 kg.m^{-3}).

Hu et al. (1985) and Satterfield et al. (1973) examined the adsorption characteristics of some sugars in porous inorganic supports. Hu et al. (1985) found that the equilibrium data of glucose, fructose and sucrose in untreated porous alumina beads (C_L^∞ < 250 kg.m^{-3}) correlated well with the Langmuir adsorption isotherm. On the other hand, Satterfield et al. (1973) observed that the adsorption isotherm of glucose in porous silica-alumina beads (C_L^∞ < 100 kg.m^{-3}), was linear and the constant K in Equation 5.3 was experimentally determined to be 1.00, which is comparable to

the value of 0.9514 obtained in this study. Thus, glucose is not preferentially adsorbed by the Ca-alginate matrix. To date, the equilibrium adsorption isotherms of glucose and other carbohydrates in gel-entrapment matrices have not been reported in the literature.

5.1.6 Comparison of Effective Diffusivity and Partition Coefficients of Glucose in Immobilization Matrices

The diffusivity characteristics of glucose in polymeric gels, membranes and other porous solids have been frequently reported (Table 5.4). However, most of these studies have been carried out using highly cross-linked and mechanically stable gels enabling conventional diffusivity measurement techniques to be employed.

To date only Tanaka et al. (1984) and Hannoun and Stephanopoulos (1986) have reported D_e values of glucose in Ca-alginate gels, whereas Sellen and colleagues (Mackie et al., 1977; Sellen, 1980) have measured the diffusivity of compact macromolecules (dextrans and globular proteins) in dilute Ca-alginate (0.5% w/v) gels using light scattering techniques. Several qualitative studies on the mass transfer characteristics of biological solutes in alginate gels have also been performed (Kierstan and Bucke, 1977; Kierstan 1981; Kierstan et al., 1982; Cheetham et al., 1979; Leung et al., 1983; Burns et al., 1985; Hubble and Newman, 1985).

Hannoun and Stephanopoulos used a modified version of

Table 5.4: Comparison of Reported Diffusivity and Partition Coefficients of Glucose in Different Types of Immobilization Matrices (NA = not available; ND = not determined)

Type and Composition of Matrix	Initial Glucose conc. ($kg.m^{-3}$)	Temp., (^{o}C)	Effective Diffusivity, $D_e x10^{10}$, ($m^2.s^{-1}$)	$(D_e/D)^{\dagger}$	Partition Coef., K_p	Reference
Porous alumina beads	2.72	25	2.33	0.35*	ND	Hu et al., (1985)
Porous silica-alumina beads	50	25	1.01	0.15	1.00	Satterfield et al., (1973)
Controlled-pore ceramic beads	NA	26	3.00	0.44	ND	Sirotti and Emery, (1983)
Crosslinked methacrylate	0.9	NA	1.95	NA	0.863	Kirstein et al., (1985)
Crosslinked collagen	NA	25	1.40	0.21	ND	Selegny et al., (1971)
5% collagen gel	NA	4	0.67	0.19	1.00	Shaw and Schy, (1981)
2.5% hyaluronate matrix	5.0	37	7.70	0.87*	ND	Norton et al., (1982)
5.0% gelatin gel	30	5	2.55	0.70*	ND	Friedman, (1930a)

Table 5.4: (Continued)

Type and Composition of Matirx	Initial Glucose conc. ($kg.m^{-3}$)	Temp., (^oC)	Effective Diffusivity, $D_e x10^{10}$ ($m^2.s^{-1}$)	$(D_e/D)^\dagger$	Partition Coef., K_p	Reference
0.79% agar gel	30	5	3.27	0.90*	ND	Friedman, (1930b)
1.5% agar gel	18	20	5.9	0.98	ND	Schantz and Lauffer, (1962)
3% agar gel	30	30	3.45	0.50	0.943	Kuu, (1982)
19.7% photocross-linkable resin	180	25	4.22	0.62	0.54	Nakanishi et al., (1977)
19.7% dextran gel	180	25	3.26	0.48	0.76	Nakanishi et al., (1977)
19.7% polyacryl-amide gel	180	25	2.99	0.44	0.89	Nakanishi et al., (1977)
7.125% poly-acrylamide gel	5.0	30	5.10	0.68*	ND	Furusaki et al., (1983)
6.8% polyacryl-amide gel	3.0	25	1.68	0.25	ND	Brown and Chitumbo, (1975b)
5.4% hydroxyethyl cellulose gel	3.0	25	2.62	0.34	ND	Brown and Chitumbo, (1975b)
17% cellulose (C5) gel	3.0	25	2.05	0.30	ND	Brown and Chitumbo, (1975b)

Table 5.4: (Continued)

Type and Composition of Matrix	Initial Glucose conc. ($kg.m^{-3}$)	Temp., (^{o}C)	Effective Diffusivity, $D_e x10^{10}$ ($m^2.s^{-1}$)	$(D_e/D)^{\dagger}$	Partition Coef., K_p	Reference
17% cellulose gel	3.0	25	1.55	0.23	0.55	Brown and Chitumbo, (1975a)
4% kappa-carrageenan gel	NA	30	ND	ND	0.86	Wada et al., (1981)
3% kappa-carrageenan gel	6.5	30	4.80	0.64*	ND	Nguyen and Luong, (1986)
2% Ca-alginate gel	5.0	30	6.83	0.91*	ND	Tanaka et al., (1984)
2% Ca-alginate gel	10	22-26	6.10	0.96*	ND	Hannoun and Stephanopoulos (1986)
2% Ca-alginate gel	20	30	6.73	0.94*	0.98	This work

† D_e/D is the ratio of the diffusivity of glucose in the support matrix (D_e) to the corresponding value in water (D).

* Free phase diffusivity of glucose, D, was calculated using the correlation developed in Section 5.2 (Equation 5.17).

the conventional diffusion cell and found that the diffusivity of glucose in 2% Ca-alginate gel (measured at 22°-26°C) was approximately 96% of that in water. The authors cited the following problems associated with their D_e measurement technique:

(a) Gel rupture in the presence of entrapped cells

(b) Difficulty in preparing Ca-alginate membranes of uniform thickness

(c) Possible influence of external film mass transfer resistance when measuring D_e of glucose in Ca-alginate membranes

In an earlier study, Tanaka et al. (1984) used an unsteady-state technique to measure solute diffusivities in Ca-alginate beads. In their method, approximately 500 Ca-alginate beads were suspended in a baffled vessel containing a limited volume of the liquid phase and the contents agitated at 625 rpm using a magnetic stir bar. By measuring the solute uptake and release rates, the D_e values were calculated using alternate forms of Equations 3.59 and 3.60. The diffusivity of glucose in Ca-alginate gel at 30°C was found to be 6.83×10^{-10} $m^2.s^{-1}$ ($D_e/D = 0.91$). Thus the D_e values of glucose reported above are similar to the diffusivity values obtained in the present study ($D_e/D = 0.94$).

In calculating solute diffusivity in alginate beads, Tanaka et al. (1984) defined the alpha-factor as the ratio

of the liquid volume to that of the total bead volume ($\alpha = V_L/V_s$). However, according to the exact mathematical solutions given by Cranks (1975), the alpha-factor should incorporate the solute partition coefficient (i.e. $\alpha = V_L/V_s K_p$). Thus, in measuring solute diffusivities, Tanaka et al. (1984) tacitly assumed the partition coefficient of glucose and other high molecular weight solutes to be unity. Although this assumption may be acceptable for low molecular weight solutes such as glucose (K_p = 0.98 in Ca-alginate gel; see Section 5.1.3), it may not be justified for larger solutes. For instance, Cheetham et al. (1979) determined the K_p value of sucrose in Ca-alginate beads to be 0.84, whereas Kirstein et al. (1985) observed a tendency towards lower partition coefficients in cross-linked methacrylate with increase in molecular weights (from K_p = 0.9 for glycerol to K_p = 0.5 for sucrose). Additionally, as shown in Table 5.5, the partition coefficient of glucose in several immobilization matrices has been found to be less than 1.0. Incorrect assumptions of K_p values can, in turn, lead to errors in the calculation of effective diffusivities of solutes in gels (Friedman and Kraemer, 1930; White and Dorion, 1961; Nixon et al., 1967; Kirstein et al., 1985; Furui and Yamashita, 1985) and failure of the mathematical solutions of the diffusion equation (Marignan and Crouzat-Reynes, 1956; Muhr and Blanshard, 1982). Thus, as attempted in the present study, it is important to devise an experimental procedure in which both K_p and D_e values can be determined.

Table 5.4 shows that the effective diffusivities of glucose in highly cross-linked gels (e.g. collagen, polyacrylamide, dextran and cellulose gels) and porous solids (alumina, silica and ceramic beads) are substantially lower ($0.15 < D_e/D < 0.5$) than the corresponding values ($0.5 < D_e/D < 1.0$) in polysaccharide gels (alginate, hyaluronate, carrageenan, agar) having a high water content (> 95%).

5.1.7 Determination of Diffusivity Values Using Approximation Techniques

The novel diffusivity measurement technique developed in this study gives accurate D_e values (± 2%) and uses an apparatus which is of simple design and easy to operate. However, unlike steady-state techniques, the complexity of the mathematical solutions (Equations 3.59 and 3.60) used to calculate D_e is the major disadvantage of this and other unsteady-state methods. Thus, in Equations 3.59 and 3.60, the experimentally measurable quantity (fractional uptake or release of solute, M^t/M^∞) is expressed as an infinite series of the unknown variable, namely, the effective diffusivity, D_e.

Determination of D_e values can therefore, only be achieved by employing a curve fitting routine or a laborious master plot (Cranks, 1975). The former requires a suitable curve-fitting, optimization computer program such as the one used in this study. The latter requires construction of a

master plot of fractional solute uptake or release (M^t/M^∞) versus the dimensionless time, τ (defined as $\tau = D_e t/R^2$) using the exact solutions. The values of τ are then read off from the plot at corresponding experimental M^t/M^∞ values A subsequent plot of τ versus time, t, gives a straight line and the D_e value evaluated from the slope (slope = D_e/R^2).

Alternatively, approximate solutions of Equations 3.59 and 3.60 are available in the literature (Carman and Haul, 1954; Schwartzberg and Chao, 1982; Lee, 1980a; 1980b) which may facilitate routine use of the novel diffusivity measurement technique, without making it mathematically cumbersome.

In the following sections, the reliability of these approximate solutions was assessed based on the experimental data given in Appendix B.2, for effusion of glucose from a spherical Ca-alginate bead. The estimated D_e value was then compared to that obtained from the exact solution (Equation 3.59) using the computer program DIFFIT when n = 25 (see Appendix B.3). The experimental fractional release rate of glucose and the best-fit theoretical curve (obtained by using DIFFIT and 25 terms) corresponding to an optimum diffusivity value of 6.85×10^{-10} $m^2.s^{-1}$ is shown in Figure 5.12.

5.1.7.1 Estimation of D_e Using the First Term in the Model Equation

Figure 5.13 shows the calculated optimum diffusivity of glucose in Ca-alginate gel plotted as a function of the

Figure 5.12: Determination of the effective diffusivity of glucose using the exact mathematical solution. [(●) experimental points; (——), predicted curve corresponding to the best computer fit of experimental data at the optimum D_e value of 6.85×10^{-10} $m^2.s^{-1}$ using 25 terms in the series].

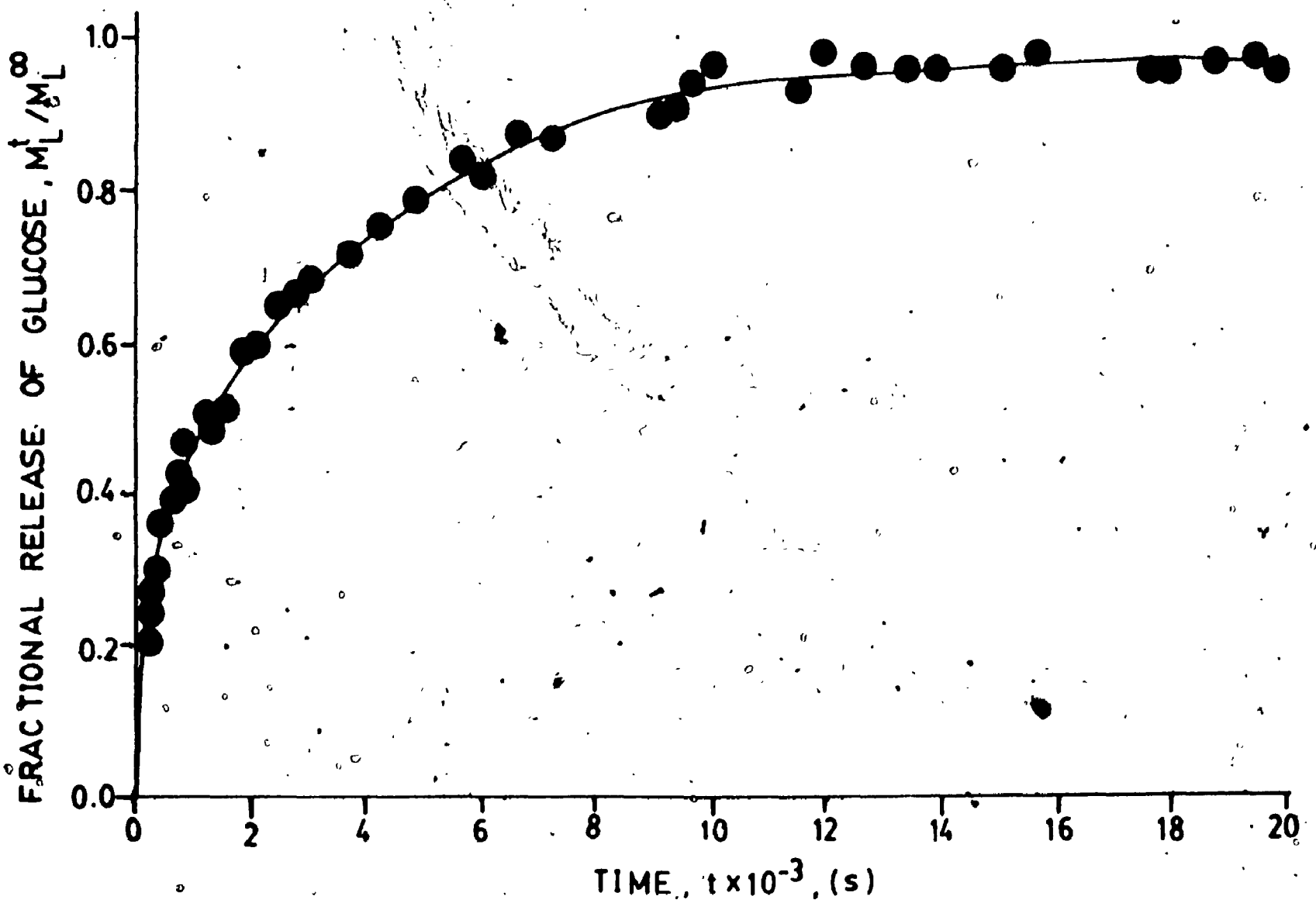
FRACTIONAL RELEASE OF GLUCOSE, M_L^t/M_L^∞
1.0
0.8
0.6
0.4
0.2
0.0
0
2
4
6
8
10
12
14
16
18
20
TIME, $t \times 10^{-3}$, (s)

Figure 5.13: Number of terms required in the series solution for determining the optimum effective diffusivity of glucose in a spherical Ca-alginate bead.

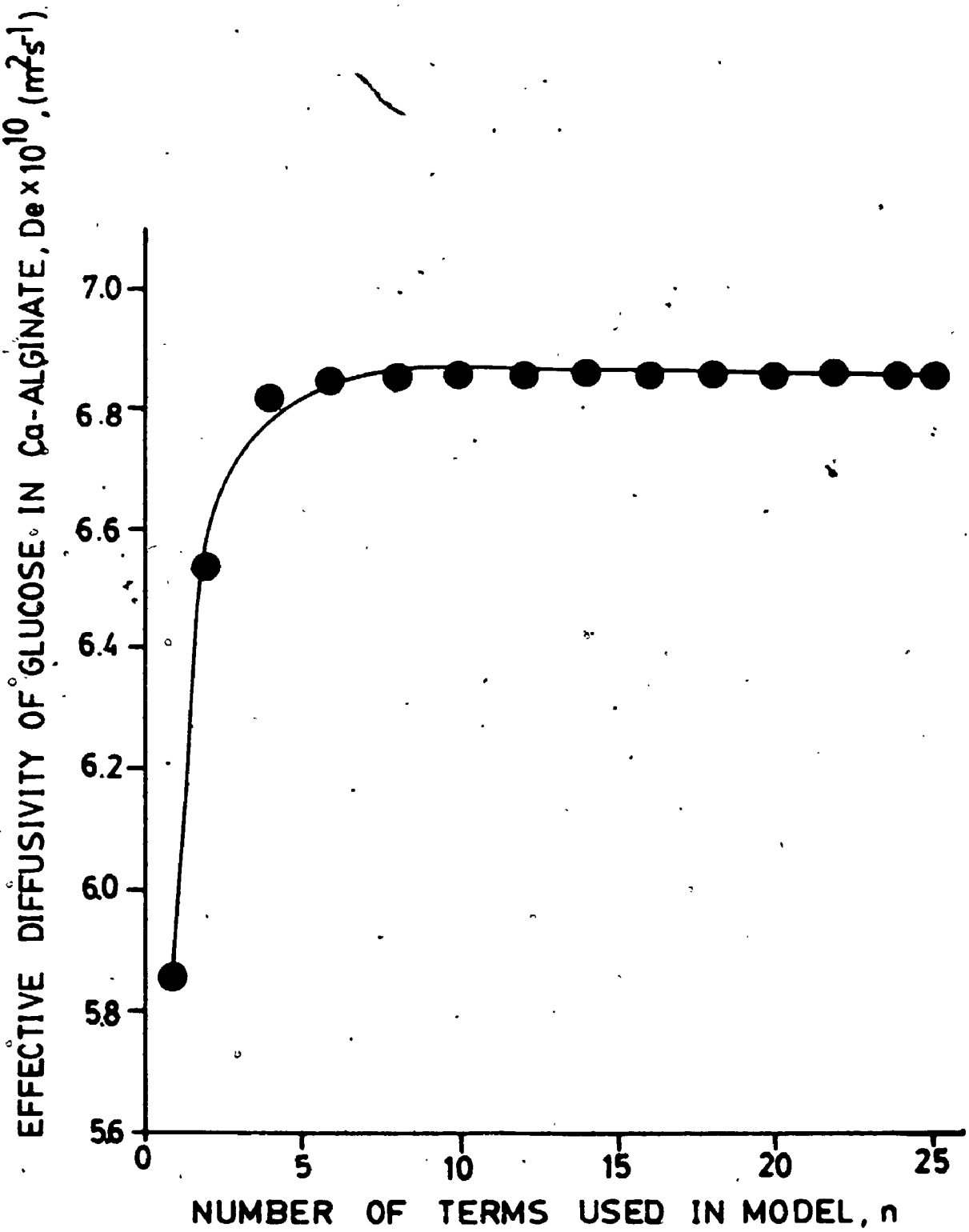
EFFECTIVE DIFFUSIVITY OF GLUCOSE IN Ca-ALGINATE, De × 10^10, (m²s⁻¹)
7.0
6.8
6.6
6.4
6.2
6.0
5.8
5.6
0
5
10
15
20
25
NUMBER OF TERMS USED IN MODEL, n

number of terms, n, used in Equation 3.59. Thus, when n exceeds 10, there is no further change in the value of D_e. However, with the use of only the first term of the series solution, the estimated D_e value (5.86×10^{-10} $m^2.s^{-1}$) is almost 15% lower than the actual value, whereas, by introducing the second term in the series, the error is reduced to less than 5%.

5.1.7.2 Graphical Method

The series solution given by Equation 3.59 can be rewritten in terms of the solute concentration changes that occur in the liquid phase during the effusion process. Accordingly,

$$Y = \frac{C_L^t - C_L^\infty}{C_L^o - C_L^\infty} = \sum_{n=1}^{N} A_n \exp(-q_n^2 \tau) \qquad 5.6$$

where A_n is given by Equation 5.7

$$A_n = \frac{6\alpha.(\alpha + 1)}{9 + 9\alpha + \alpha^2 q_n^2} \qquad 5.7$$

When the dimensionless time, τ, is large, then the terms corresponding to $n > 2$ in Equation 5.6 can be neglected. Under this condition, Equation 5.6 can be converted into the following linear form

$$\ln Y = \ln \left[\frac{C_L^t - C_L^\infty}{C_L^o - C_L^\infty}\right] = \ln A_1 - \frac{q_1^2 D_e t}{R^2} \qquad 5.8$$

Thus, if $\ln Y$ is plotted as a function of time, t, the slope will equal $-q_1^2 D_e/R^2$.

From the experimental data given in Appendix B.2,

$C_L^o = 0$ cpm/μL ; $C_L^\infty = 91.2$ cpm/μL

$R = 6.052 \times 10^{-3}$ m ; $\alpha = 4.5638$

$q_1 = 3.326$; $A_1 = 0.5432$

Thus, as shown in Figure 5.14, by drawing a straight line from the intercept ($\ln A_1$) to fit the majority of the experimental points at $t \geq 2000$ s, the D_e value was calculated to be 7.20×10^{-10} $m^2.s^{-1}$. The graphical method therefore overestimated the D_e value by 5.1% which is a good approximation of the corresponding value determined by using the exact solution. It must be noted that at time t = 2000 s up to 60% of the fractional release of glucose has already occurred (see Figure 5.12). Therefore, the graphical method utilizes the remaining 40% of the effusion process where most of the data fluctuations take place.

Schwartzberg and Chao (1982) have shown that for a sphere, and when $\alpha = 4.0$, the percentage error in the measured D_e value using the graphical method can be reduced to

Figure 5.14: Application of the graphical method for determining D_e

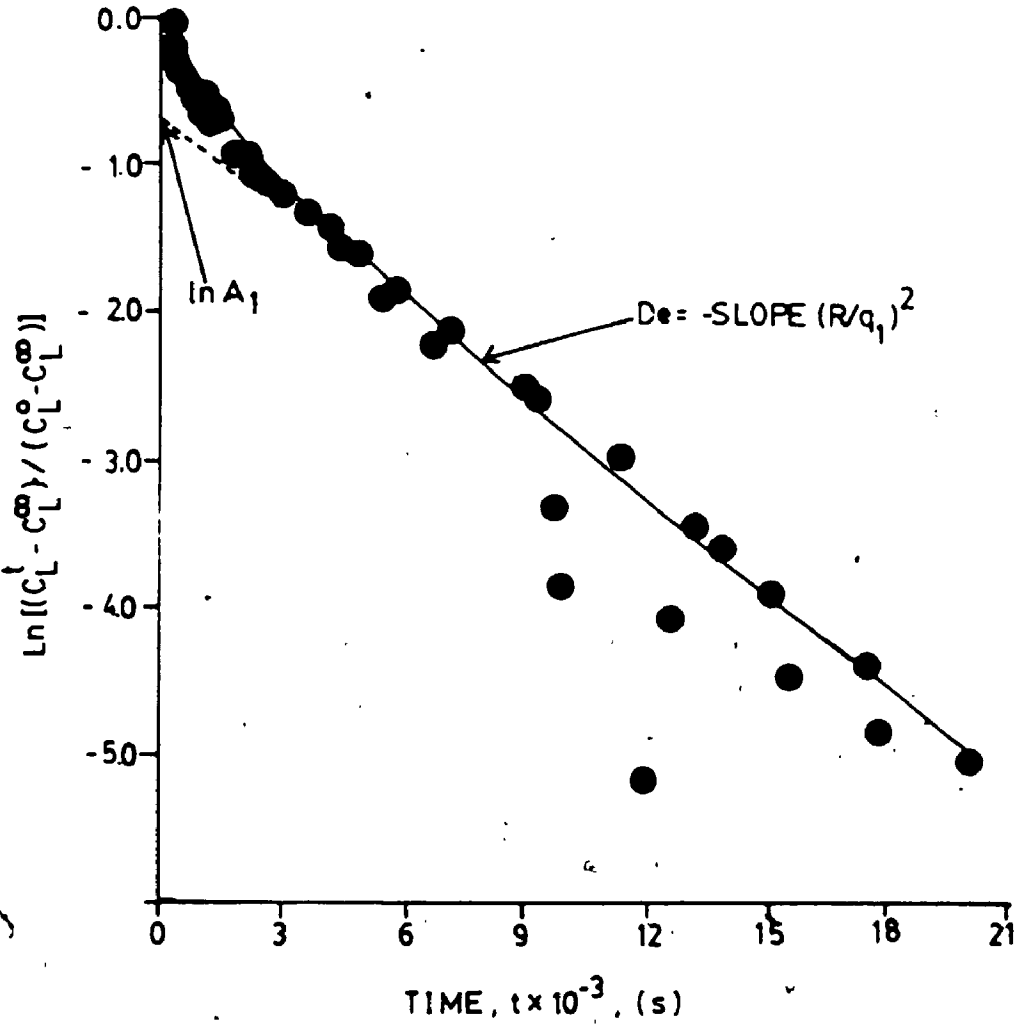
0.0
- 1.0
- 2.0
- 3.0
- 4.0
-5.0
0
3
6
9
12
15
18
21
ln A1
De= -SLOPE (R/q1)2
Ln[(CLt - CL∞)/(CLo - CL∞)]
TIME, t x 10-3, (s)

less than 1% if $\tau > 0.117$ and $Y < 0.146$. The τ and Y values based on the experimental data shown in Figure 5.14 were calculated to be 0.039 and 0.398, respectively, at time, t = 2000 s. Thus, a high level of accuracy cannot be expected using the graphical method since the exact solutions for the spherical geometry do not converge rapidly (Carman and Haul, 1954).

5.1.7.3 Approximate Analytical Solution

Lee (1980b) used a refined integral method to derive approximate analytical solutions for a wide variety of initial and boundary conditions encountered in the diffusional release of a solute from a polymeric matrix. Based on the initial and boundary conditions for a sphere immersed in a finite volume of liquid (Section 3.6.2.2), the analytical solution according to Lee (1980b) is given by Equation 5.9 in which the fractional solute release, M_L^t/M_L^∞, is related to effusion time, t.

$$\tau = -\frac{\delta}{3} - \left[\frac{\alpha+2}{3}\right] \ln\left[\frac{4\alpha + 4 - (\delta-2)^2}{4\alpha}\right]$$

$$+ \frac{2}{3}\left[1+\alpha\right]^{0.5} \ln\left[\frac{[2(1+\alpha)^{0.5} + (\delta-2)][(1+\alpha)^{0.5}+1]}{[2(1+\alpha)^{0.5} - (\delta-2)][(1+\alpha)^{0.5}-1]}\right] \quad 5.9$$

where,

$$\delta = 2 - 2\left[(1+\alpha) - \frac{\alpha(1+\alpha)}{(1+\alpha) - (M_L^t/M_L^\infty)}\right]^{0.5} \qquad 5.10$$

Using Equations 5.9 and 5.10, and the experimental data shown in Figure 5.12, values of τ were calculated and plotted as a function of time (Figure 5.15). Based on the experimental data for the first 165 minutes, and using linear regression analysis (correlation coefficient = 0.9873), the effective diffusivity of glucose was calculated (D_e = slope x R^2) to be 6.70×10^{-10} $m^2.s^{-1}$. This value is only 2.2% lower than that obtained using the exact solution. Thus, unlike the graphical method, Lee's analytical solution utilizes the data obtained during the time period when up to 90% of the solute release occurs. Furthermore, approximate solutions for calculating D_e during diffusion of a solute into a spherical bead and effusion from matrices of other geometrical shapes are also available (Lee 1980a; 1980b).

5.1.7.4 Comparison of Different D_e Approximation Techniques

A comparison of the different approximation techniques used in this study to calculate the effective diffusivity of glucose in Ca-alginate spherical beads is shown in Table 5.5. Lee's analytical technique is by far the most accurate and as reliable as the exact solution method. Thus, it may be possible to routinely employ the novel diffusivity measurement technique without using the complicated mathematical

Figure 5.15: Estimation of diffusivity of glucose in Ca-alginate sphere using Lee's analytical solution.

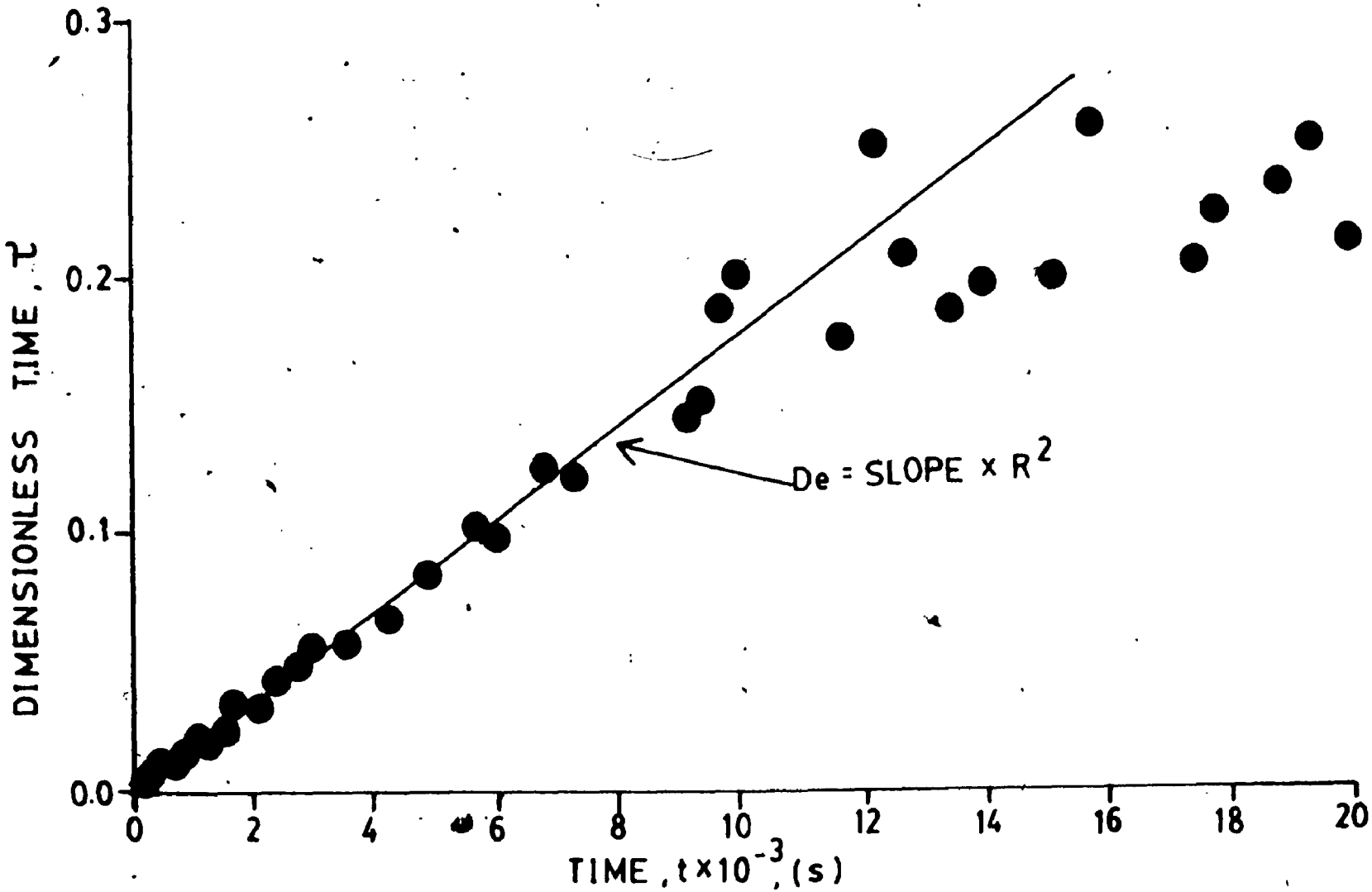
0.3
0.2
0.1
0.0
DIMENSIONLESS TIME, τ
0
2
4
6
8
10
12
14
16
18
20
TIME, t×10^-3, (s)
De = SLOPE × R^2

Table 5.5: Comparison of Different Estimation Techniques Used to Calculate D_e

Method	Effective Diffusivity of Glucose, $D_e \times 10^{10}$, $(m^2.s^{-1})$	% Difference When Compared to Exact Solution
Exact solution (Equation 3.59, n=25 terms)	6.85	-
1st term of series solution	5.86	-14.5
First 2 terms of series solution	6.54	-4.5
Graphical Method	7.20	+5.1
Lee's Analytical Solution	6.70	-2.2

solutions and at the same time, retain the accuracy and simplicity of the method developed in the present study.

It must, however, be noted that, both, the graphical method and Lee's analytical solution amplify the data fluctuations that occur during the last 10 to 20 percent of the effusion process, even though there is little evidence of significant fluctuations in the actual experimental data as plotted in Figures 5.9 and 5.12. Such amplified data fluctuations have also been observed by Lee when analyzing the experimental solute uptake rate during diffusion of NaCl in ion-exchange resin particles (Lee 1980a).

Caution must therefore be exercised when fitting the approximate solutions to the experimental data obtained during the final phase of the diffusion or effusion process. As shown in Figures 5.1, 5.2 and 5.12, the exact solutions (Equations 3.59 and 3.60, when n = 25) fit very well to the experimental data during the entire period of the diffusion and effusion process. Equations 3.59 and 3.60 were therefore used for the remainder of this study to calculate D_e values with n = 25 terms.

5.1.8 Other Potential Applications of the Novel Diffusivity Measurement Technique

Under conditions of near ideal mixing and negligible film mass transfer resistance, the novel diffusion apparatus designed for use in this study may be successfully ap-

plied for measuring, both, K_p and D_e of glucose and other radio-labelled solutes in a variety of different immobilization matrices irrespective of their geometry or mechanical stability. Additionally, the simplicity of the apparatus requiring small volumes of the liquid and solid phases enables one to economically utilize radiotracer techniques, which in turn facilitates the ease and accuracy of rapidly measuring solute concentration changes in the liquid phase.

By modifying the design of the apparatus, measurement of solute diffusion in non-spherical matrices, such as a cylinder, square rod, cube, disc, or a solid of any arbitrary shape, may be possible. Thus, for a non-spherical solid immersed in a liquid phase of limited volume the appropriate mathematical solutions for calculating D_e values are available in the literature (Cranks, 1975; Ma and Evans, 1968; Desai and Schwartzberg, 1980; Schwartzberg and Chao, 1982; Bressan et al., 1981). Additionally, for rotating cylinders and discs, correlations are available for estimating the magnitude of the external film mass transfer coefficient (Sherwood et al, 1975).

For a system exhibiting non-linear Freundlich or Langmuir isotherms, with or without significant film mass transfer resistance, modified versions of Equations 3.59 and 3.60 (Komiyama and Smith, 1974; Huang and Li, 1973) and other numerical (Hashimoto et al., 1975; Komiyama and Smith, 1974; Furusawa and Smith, 1973) and parametric methods (Suzuki and Kawazoe, 1974; Mathews and Weber, 1976;

Neretnieks, 1976; Leyva-Ramos and Geankoplis, 1985) are available in the literature.

5.2 Diffusion Coefficients of Glucose in Water: Correlation Studies

An adequate understanding of the diffusion phenomenon in alginate immobilization matrices can be facilitated by comparing the effective solid phase diffusivity (D_e) with the diffusion coefficient of glucose in water (D). Amongst the variety of factors that are known to influence the free-phase diffusivity of any given solute, temperature and solute concentration are the most important contributing parameters (Cussler, 1984).

The semi-empirical correlation developed by Wilke and Chang (1955) has been widely used to predict the free-phase diffusivities of glucose. However, the reliability of their correlation is limited to infinitely dilute solutions and at temperatures of 5° to $40^{o}C$ (Geankoplis, 1983).

Experimentally measured values of D are available in the literature (Friedman and Carpenter, 1939; Longsworth, 1952; 1953; 1954; Gladden and Dole, 1953; Dadenkova et al., 1973). However, with the exception of the results presented by Dadenkova et al. (1973), most of these studies examined a rather narrow range of temperatures and/or glucose concentrations when measuring the diffusion coefficients of glucose in water. Thus, using the data presented by Dadenkova

et al. (1973), which are compiled in Table D.1 (Appendix), suitable correlations were developed, as described below, to facilitate accurate prediction of the diffusion coefficients of glucose in water over a wide temperature (25 to 70°C) and glucose concentration range (0 to 500 kg. m^{-3}).

5.2.1 Effect of Temperature; Correlation I With Concentration Dependent Constants

The influence of temperature on free-phase diffusivities of a solute at a certain concentration can be expressed by the Arrhenius relationship given by Equation 5.11. Accordingly,

$$D = A \exp(-E_a/\bar{R}t) \qquad 5.11$$

where $\bar{R}$ is the universal gas constant, T is the absolute temperature, and A and E_a are, respectively, the Arrhenius pre-exponential constant and the activation energy for diffusion at a given solute concentration. The diffusivity data listed in Table D.1 (Appendix) were plotted as a function of the inverse of absolute temperature at different concentrations of glucose as shown in Figure D.1 (Appendix).

The E_a and A values were determined by non-linear regression analysis of the data using the least-squares method and the coefficient of determination, r^2, was found to be greater than 0.9985 at all glucose concentrations

(Table D.2, Appendix).

As shown in Figure D.2, the activation energy for diffusion of glucose in water, increases linearly as a function of glucose concentration, C_L, and the relationship can be expressed by Equation 5.12

$$E_a = E_a^o + mC_L \qquad 5.12$$

where m is a constant (10.28×10^{-3} kJ. mol^{-1}/kg. m^{-3}) and E_a^o is the activation energy for diffusion of glucose at infinite dilution (E_a^o = 18.89 kJ.mol^{-1}). The constants, m and E_a^o were determined by using linear regression analysis (Table D.2, Appendix). Equation 5.12 can therefore be rewritten in the form,

$$E_a = 18.89 + [10.28 \times 10^{-3} C_L] \qquad 5.13$$

for which the correlation coefficient was found to be 0.9868.

As shown in Figure D.3 (Appendix), A is exponentially related to glucose concentration and can be expressed by Equation 5.14

$$A = A^o \exp(b_c C_L) \qquad 5.14$$

where b_c is a constant and A^o is the Arrhenius pre-exponential constant at infinite dilution. Following non-linear regression analysis (Table D.2, Appendix) Equation

5.14 can be rewritten in the form,

$$A = 1.36 \times 10^{-6} \exp(2.48 \times 10^{-3} C_L) \qquad 5.15$$

and the coefficient of determination was found to be 0.9506.

Substitution of Equations 5.12 and 5.14 into the Arrhenius Equation 5.11, leads to the general form of correlation I which is expressed by Equation 5.16

$$D = A^{o} \exp\left[\frac{(\bar{R}Tb_c - m)C_L - E_a^{o}}{\bar{R}T}\right] \qquad 5.16$$

Introducing the constants given in Equations 5.13 and 5.15, Equation 5.16 can be rewritten as follows

$$D = 1.36 \times 10^{-6} \exp\left[\frac{(0.00248\bar{R}T - 0.01028)C_L - 18.89}{\bar{R}T}\right] \qquad 5.17$$

5.2.2 Effect of Glucose Concentration; Correlation II With Temperature Dependent Constants

Alternatively, the diffusivity of glucose in water may be expressed in terms of an exponential function of glucose concentration (Figure D.4, Appendix) which is given by Equation 5.18.

$$D = D_o \exp(-b_T C_L) \qquad 5.18$$

where b_T is the temperature dependent exponential constant and D_o is the diffusivity of glucose at infinite dilution at a fixed temperature (Table D.3, Appendix). D_o can be determined from the Arrhenius relationship (Figure D.5, Appendix) given by Equation 5.19

$$D_o = A^o \exp(-E_a^o/\bar{R}T) \qquad 5.19$$

By substituting the appropriate constants (A^o and E_a^o) determined by using non-linear regression analysis (Table D.3, Appendix), Equation 5.19 can be rewritten as

$$D_o = 1.36 \times 10^{-6} \exp(-18.89/\bar{R}T) \qquad 5.20$$

The exponential constant, b_T, in Equation 5.18 is related to the absolute temperature (see Figure D.6, and Table D.3, Appendix) by the following linear equation

$$b_T = b_o - yT \qquad 5.21$$

where y is the slope (1.22×10^{-5} $m^3.kg^{-1}.K^{-1}$) and b_o (5.29×10^{-3} $m^3.kg^{-1}$) is the intercept at T = 0 K. The best fit linear relationship was found to be

$$b_T = \left[5.29 \times 10^{-3}\right] - \left[1.22 \times 10^{-5} T\right] \qquad 5.22$$

for which the correlation coefficient was 0.9885.

Thus, Equation 5.18 can be rewritten in the form,

$$D = A^{o} \exp (yTC_L - b_oC_L - E_a^{o}/\bar{R}T) \qquad 5.23$$

or, by introducing the appropriate constants,

$$D = 1.36 \times 10^{-6} \exp [C_L(1.22 \times 10^{-5}T - 5.29 \times 10^{-3}) - (18.89/\bar{R}T)] \qquad 5.24$$

5.2.3 Application of Correlations I and II.

The correlations given by Equations 5.17 and 5.24 were subsequently used to calculate D as a function of glucose concentration and temperature and the predicted D values plotted in Figure 5.16. Both correlations gave almost identical D values and their plots are not distinguishable in Figure 5.16. The diffusion coefficients of glucose in water reported in the literature are also plotted in Figure 5.16 showing that the two correlations developed in this study can accurately predict the free-phase diffusivities over the entire glucose concentration (20 - 500 $kg.m^{-3}$) and temperature (25 - 75°C) range tested.

5.2.4 Diffusion Coefficients of Glucose at Infinite Dilution

For small solutes (M.W. $\leq$ 1000) such as glucose, the Wilke and Chang (1955) correlation, given by Equation 5.25

Figure 5.16: Comparison of experimental (symbols) and predicted (——) diffusivity values of glucose in water as a function of concentration and temperature (Dadenkova et al., 1973 [●, 25°C; ■, 30°C; ⬢, 40°C; ▲, 50°C; □, 60°C; ▼, 70°C]; Gladden and Dole, 1953 [△, 25°C; ▽, 35°C]; Friedman and Carpenter, 1989 [⬡, 25°C]; Longsworth, 1953 [◇, 25°C]).

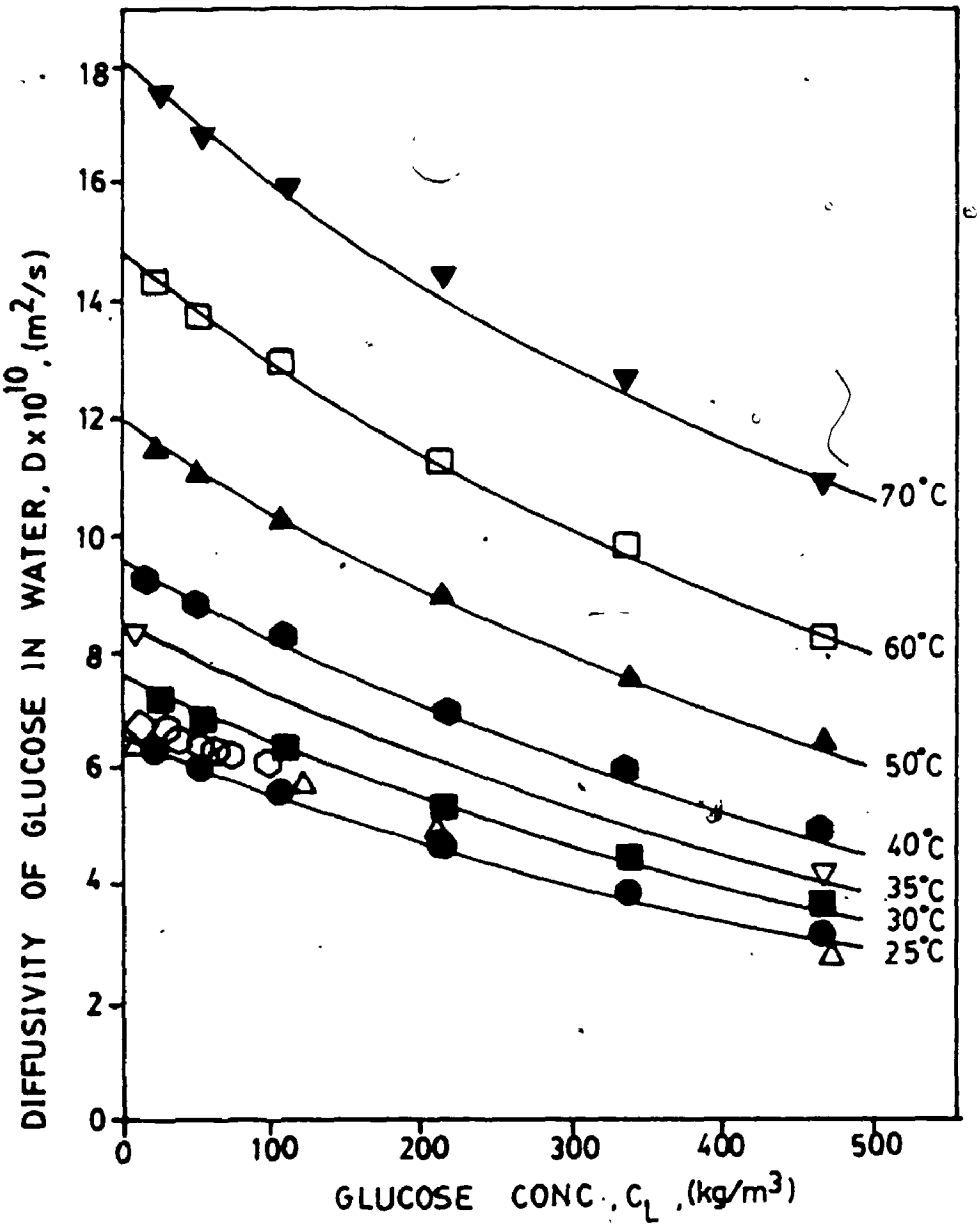
DIFFUSIVITY OF GLUCOSE IN WATER, D x 10^10, (m^2/s)
GLUCOSE CONC., C_L, (kg/m^3)
0
2
4
6
8
10
12
14
16
18
0
100
200
300
400
500
70°C
60°C
50°C
40°C
35°C
30°C
25°C

has been preferentially used to estimate free-phase diffusivities at infinite dilution (D_o). Accordingly, at an absolute temperature, T

$$D_o = 1.173 \times 10^{-16} (\Psi M_B)^{1/2} \frac{T}{\mu_B V_A^{0.6}} \qquad 5.25$$

where, M_B is the molecular weight of the solvent, Ψ is the association parameter of the solvent, μ_B is the solvent viscosity and V_A is the molar volume of the solute at its normal boiling temperature. Using the LeBas atomic volumes of carbon (14.8×10^{-3} m^3/kg mol), hydrogen (3.7×10^{-3} m^3/kg mol) and oxygen (7.4×10^{-3} m^3/kg mol), the molar volume, V_A, of glucose was calculated to be 0.1776 m^3/kg mol (Sherwood et al., 1975). Wilke and Chang (1955) recommended that Ψ be chosen as 2.6 if the solvent is water.

The Wilke and Chang correlation, and Equations 5.17 and 5.24 were employed to predict the diffusion coefficients of glucose in water at infinite dilution (D_o) over a temperature range of 20°C to 50°C. The predicted D_o values are plotted as shown in Figure 5.17. The 'experimental' values of D_o obtained by extrapolating literature data to $C_L = 0$ kg.m^{-3} are also shown in Figure 5.17. It is apparent that the correlations developed in this study are more accurate than the Wilke and Chang correlation. One must, however, note that Equation 5.17 and 5.24 can only estimate D_o values

Figure 5.17: Predicting diffusivity values of glucose in water at infinite dilution as a function of temperature. (——), Wilke and Chang correlation; (---) Equations 5.17 and 5.24; (●), Dadenkova et al., 1973; (▲), Longsworth, 1954; (■), Gladden and Dole, 1953; (⬢), Friedman and Carpenter, 1939.

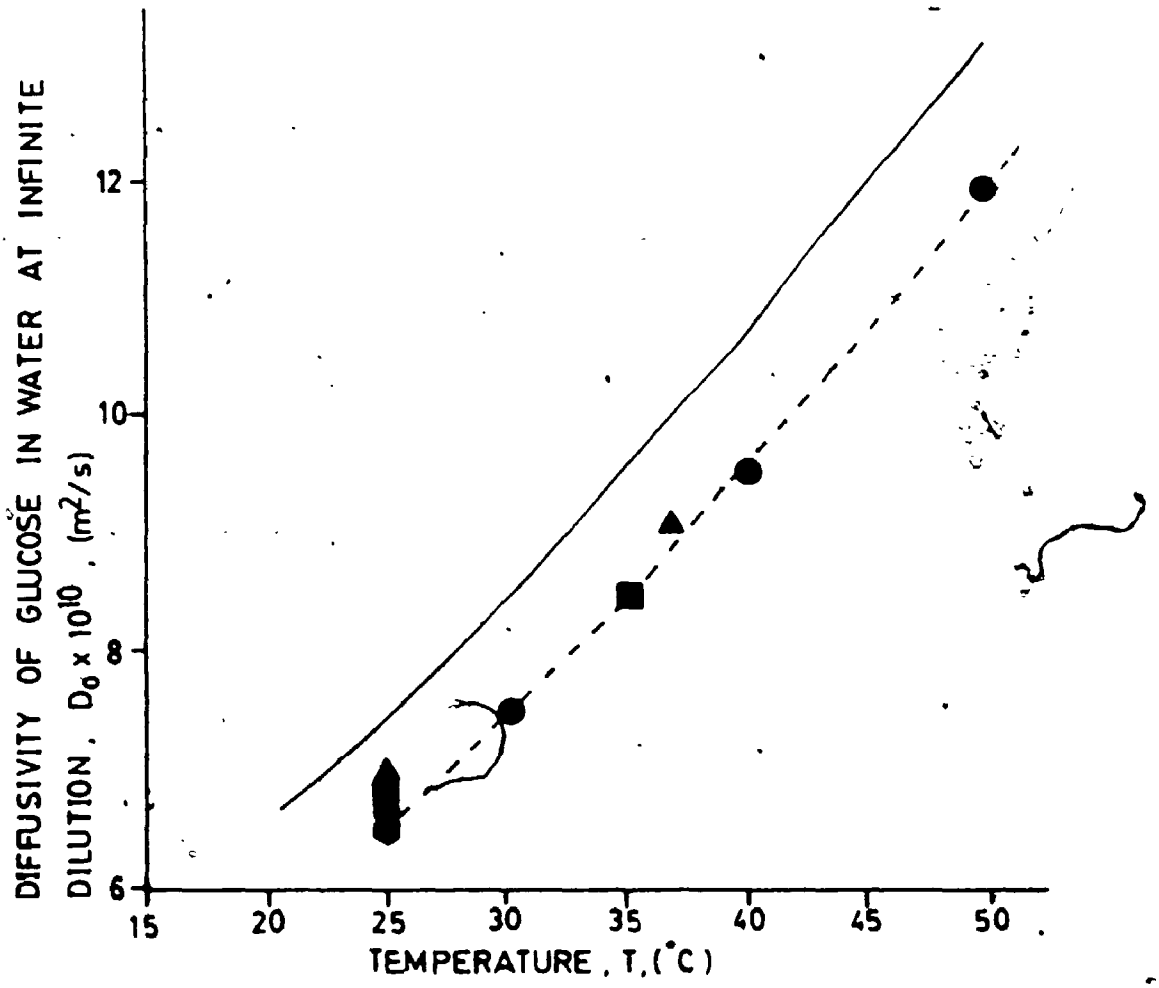
DIFFUSIVITY OF GLUCOSE IN WATER AT INFINITE DILUTION, $D_0 \times 10^{10}$, (m^2/s)
12
10
8
6
15
20
25
30
35
40
45
50
TEMPERATURE, T, (°C)

of glucose (and possibly other hexoses) in water, whereas the Wilke and Chang correlation has universal utility, and as such can predict D_o for solutes with molecular weights of up to 1,000 diffusing in a wide variety of solvents in addition to water.

Due to the accuracy of the correlations developed above (Equations 5.17 and 5.24), they will be used in the remainder of these studies in order to compare the effective diffusivities of glucose in alginate immobilization matrices with the corresponding free-phase diffusivities (D_e/D). As shown later, Equations 5.17 and 5.24 will be employed to develop and also apply literature correlations for estimating D_e values of glucose in alginate immobilization matrices. Additionally, Equations 5.17 and 5.24 may have wider applications for predicting the mass transfer characteristics of hexoses in fermentation media.

5.3 Factors Influencing the Effective Diffusivity of Glucose in Cell-Free Alginate Gels

The effect of temperature, glucose concentration and the composition of alginate gels on the D_e and K_p values of glucose in cell-free alginate matrices were systematically studied as described in this section. All diffusivity measurements were made using the novel diffusion apparatus which was operated under conditions of near ideal mixing and

negligible film mass transfer resistance as discussed in Section 5.1.

5.3.1 The Effect of Temperature

To date, in all the qualitative and quantitative studies of solute diffusion in Ca-alginate gels, no attempt has been made to examine the dependence of D_e on temperature despite the attention it deserves.

The influence of temperature (20°C to 50°C) on the effective diffusivity of glucose in Ca-alginate beads was therefore studied with the initial 'cold' glucose concentration in the liquid phase (C_L^o) of 20 kg. m^{-3}. Ca-alginate beads were prepared using a 2% Na-alginate solution (Sample #17, Fisher Chemicals) and 4% $CaCl_2$ as the chelating agent. The volume fraction of alginate (λ) in the spherical gel matrix was found to be 0.031 which corresponds to a void fraction ($\varepsilon = 1 - \lambda$) of 0.969.

The effect of temperature on the experimental K_p and D_e values of glucose in Ca-alginate beads and the corresponding diffusivity values of glucose in water (calculated using Equation 5.17) are listed in Table 5.6. Thus, as shown in Table 5.6, the partition coefficient remains unchanged (0.99 $\pm$ 0.01) whereas the effective diffusivity increases over the entire temperature range studied.

In general, the increase in solute mobility with temperature is somewhat greater in gel matrices than in aqueous

Table 5.6: Effect of Temperature on Partition Coefficient and Diffusivity of Glucose in Cell-Free Ca-Alginate Gel

Temperature, T, (^{o}C)	$T^{-1} \times 10^4$ (K^{-1})	Partition Coefficient, K_p	Effective Diffusivity, $D_e \times 10^{10}$, ($m^2.s^{-1}$)	Diffusivity in Water*, $D \times 10^{10}$ ($m^2.s^{-1}$)	D_e/D
20	34.13	0.99	4.74	5.63	0.84
25	33.56	1.00	5.76	6.42	0.90
30	33.00	0.98	6.73	7.30	0.92
35	32.47	0.99	7.47	8.25	0.91
40	31.95	0.99	8.32	9.30	0.90
45	31.45	1.00	9.99	10.4	0.96
50	30.96	0.98	10.9	11.7	0.94
Non-Linear Regression Analysis to Calculate Activation Energy Using the Arrhenius Equation			Intercept = A_g $=3.15 \times 10^{-6}$ $m^2.s^{-1}$ slope = -2,570K r^2 = 0.9925 E_{ag} = 21.37 $kJ.mol^{-1}$	Intercept = A $=1.44 \times 10^{-6}$ $m^2.s^{-1}$ slope = -2,298K r^2 = 1.0000 E_a = 19.11 $kJ.mol^{-1}$	

* Calculated using Equation 5.17 when C_L = 20 $kg.m^{-3}$

solutions (Soldano, 1953). The D_e/D values listed in Table 5.6 appear to increase with temperature. It is, therefore, quite likely that at higher temperatures, (> 50°C), the D_e/D ratio may approach unity. This phenomenon has been frequently observed (Soldano, 1953; Helfferich, 1962) and it is believed that the retarding interactions between the solute and the gel matrix become weaker, and the matrix becomes more flexible, with increase in temperature.

5.3.1.1 Activation Energy for Diffusion of Glucose in Cell-Free Ca-Alginate Matrix

The temperature dependence of D_e for diffusion of glucose in Ca-alginate gel follows the typical Arrhenius relationship as shown in Figure 5.18. Following non-linear regression analysis (Table 5.6) the activation energy for diffusion of glucose in Ca-alginate gel, E_{ag}, was determined to be 21.4 $kJ.mol^{-1}$ which is about 2.3 $kJ.mol^{-1}$ higher than the corresponding value ~~in water~~ (E_a = 19.1 $kJ.mol^{-1}$). However, the Arrhenius pre-exponential constant (which includes parameters such as the jump distance and a packing factor) for diffusion of glucose in Ca-alginate gel ($A_g = 3.15 \times 10^{-6}\ m^2.s^{-1}$), was at least twice as high as that for diffusion of glucose in water ($A = 1.44 \times 10^{-6}\ m^2.s^{-1}$). The D_e values of glucose in Ca-alginate beads suspended in dilute solutions (≈ 20 $kg.m^{-3}$) can be estimated using the Arrhenius relationship given by Equation 5.26.

Figure 5.18: The Arrhenius plot for diffusion of glucose in cell-free Ca-alginate gel.

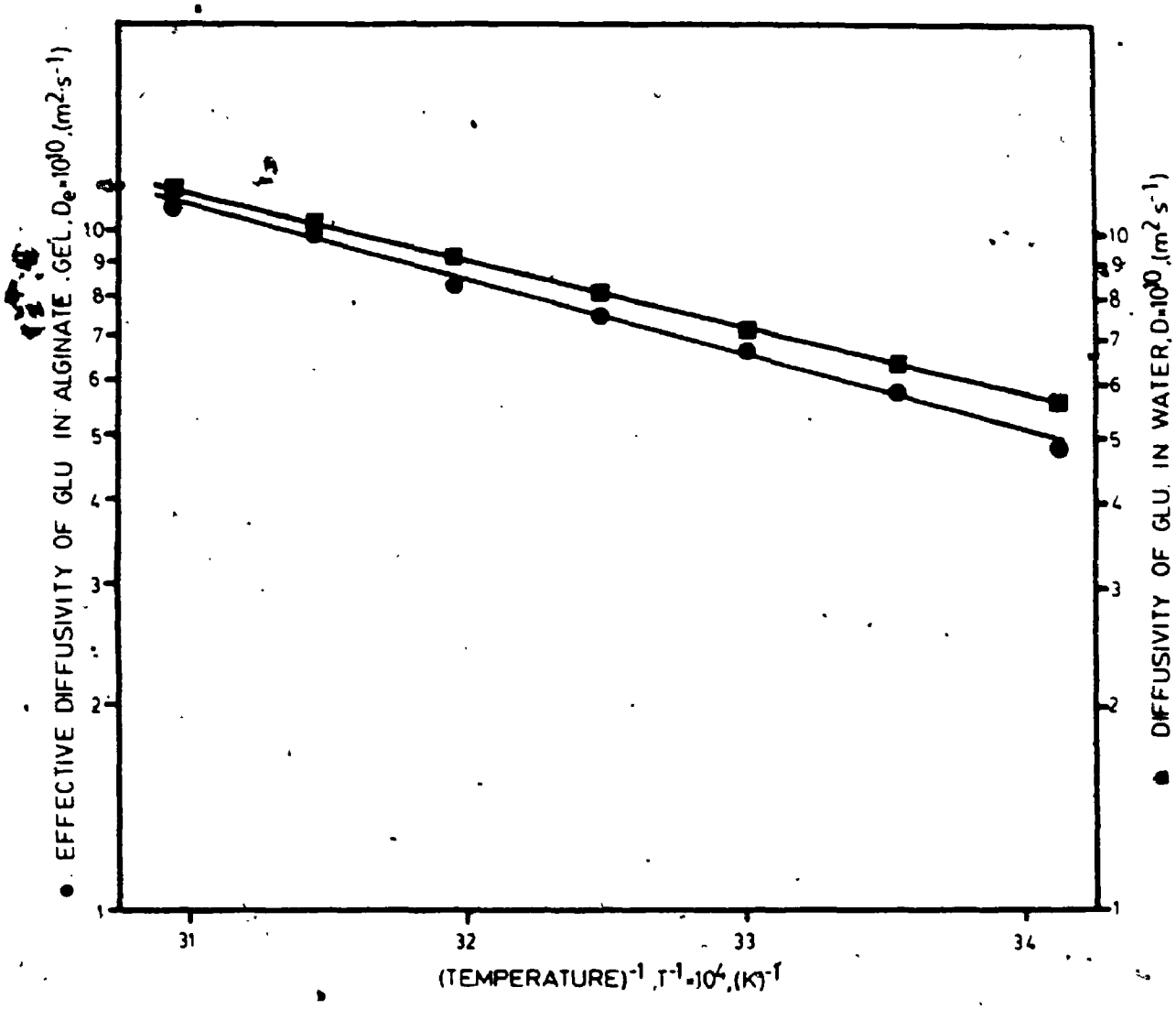
● EFFECTIVE DIFFUSIVITY OF GLU IN ALGINATE GEL, $D_e \cdot 10^{10}$, $(m^2 \cdot s^{-1})$
■ DIFFUSIVITY OF GLU IN WATER, $D \cdot 10^{10}$, $(m^2 s^{-1})$
(TEMPERATURE)$^{-1}$, $T^{-1} \cdot 10^4$, $(K)^{-1}$
31
32
33
34
1
2
3
4
5
6
7
8
9
10

Thus, for the temperature range of 20 to 50°C,

$$D_e = 3.15 \times 10^{-6} \exp(-21.4/\bar{R}T) \qquad 5.26$$

for which the coefficient of determination, r^2, was 0.9925.

The reported values of E_{ag} for diffusion of glucose in different types of gels and membranes are listed in Table 5.7. The E_{ag} value obtained in this study is moderately higher than the activation energy for diffusion of glucose in water ($\Delta E = E_{ag} - E_a = 2.3$ kJ.mol^{-1}). Similarly, Brown et al. (1976) found that ΔE for diffusion of glucose in hydroxyethyl cellulose gel ($\lambda = 0.037$) was 4.0 kJ.mol^{-1} in the temperature range of 25 to 35°C. In other studies, ΔE values have been found to be insignificant during diffusion of various solutes in dextran gels, $\lambda = 0.17$ (Horowitz and Fenichel, 1964); diffusion of glycerol and PEG 600 in polyacrylamide gel, $\lambda = 0.16$ (Brown and Johnsen, 1981a; 1981b); and diffusion of a number of chlorides in agar gels, $\lambda = 0.003$ (Stiles, 1923).

Similarity in E_a and E_{ag} values indicates that the resistance to diffusion in the gel matrix is dictated by solute-solvent interactions, whereas the polymer simply imposes a more tortuous diffusion path (Muhr and Blanshard, 1982).

Nguyen and Luong (1986) recently reported that the D_e values of glucose is 3% κ-carrageenan gel remained unchanged when the temperature was increased from 10 to 25°C. This

Table 5.7: Reported Activation Energy Values for Diffusion of Glucose in Different Types of Gels and Membranes (ND = not determined).

Type and Composition of Gel or Membrane	Volume Fraction of Polymer, λ	Glucose Concentration, C_L ($kg.m^{-3}$)	Temperature Range Studied (^oC)	Activation Energy E_{ag}, ($kJ.mol^{-1}$)	Reference
Cuprophane	0.48	9.0	25-45	26.1	Spriggs and Gainer, 1973
17% w/w Cellulose	ND	3.0	10-35	32.2	Brown and Chitumbo, 1975a
17% w/w Cellulose (C5) gel	ND	3.0	10-25 25-35	9.6 32.2	Brown and Chitumbo, 1975b
17% w/w/ Cellulose (C80) gel	ND	3.0	10-25 25-35	9.6 32.6	Brown and Chitumbo, 1975b
5.4% w/w hydroxymethyl cellulose	0.037	3.0	10-25 25-35	18.0 23.0	Brown and Chitumbo, 1975b; Brown et al., 1976
6.8% polyacrylamide	ND	3.0	10-25 25-35	2.1 38.9	Brown and Chitumbo, 1975b
Ca-alginate gel prepared from 2% w/v Na-alginate solution	0.031	20.0	20-50	21.4	This work

was followed by a linear increase in diffusivity values when the temperature was raised from 25 to 34°C.

Brown and Chitumbo (1975b) have reported sharp discontinuities in the Arrhenius plots for diffusion of glucose in polyacrylamide and cellulose gels. The E_{ag} values below 25° were considerably lower than that for free-diffusion, while above 25°C, E_{ag} exceeded E_a by an equivalent amount. These exceptional results were interpreted as being caused by a sharp increase in the mobility of polymer chains at 25°C. This phenomenon is analogous to the sharp increase in activation energies found for diffusion of gases and solvents through polymers at their glass transition temperature. Thus, at this transition temperature, more energy is required to form 'pores' in between the mobile polymer chains for the diffusing molecules, rather than for diffusive jumps taking place between existing 'pores' (Manson and Chiu, 1973). Although there is some evidence for a second order transition temperature of 25°C for cellulosic polymers (Brown et al., 1976) there is no indication that a similar phenomenon occurs during solute diffusion in polyacrylamide and κ-carrageenan gels at 25°C.

In this work, no discontinuity in E_{ag} values was observed for diffusion of glucose in Ca-alginate gel over a temperature range of 20 to 50°C.

5.3.2 Effect of Glucose Concentration

In applying Equation 3.60 it was assumed that the D_e value remains constant. Although this assumption is valid for dilute solutions, the D_e value changes during diffusivity measurement when the alginate bead is immersed in concentrated solutions. It is therefore important to emphasize that the D_e values obtained in this study at high initial concentrations of glucose (> 20 $kg.m^{-3}$) are only average values which in turn depend on the solute concentration change that occurs in the liquid and gel phase. All D_e values were determined at 30°C.

Figure 5.19 shows that the equilibrium partition coefficient of glucose in Ca-alginate gel remains unchanged when the initial glucose concentration in the liquid phase is increased from 3.0 to 300 $kg.m^{-3}$. This phenomenon is generally expected for systems exhibiting a linear adsorption isotherm (Satterfield et al., 1973).

At low initial concentrations of glucose ($C_L \leq 20$ $kg.m^{-3}$), there is virtually no change in the D_e values as shown in Figure 5.20. This has also been found to be the case for diffusion of glucose in agar (Schantz and Lauffer, 1962) and cellulose gels (Brown and Chitumbo, 1975a).

However, over the entire glucose concentration range of 3.0 to 300 $kg.m^{-3}$ an exponential decrease in D_e values resulted as shown in Figure 5.21. Using non-linear regression analysis of the data listed in Table 5.8, the best-fit exponential relationship could be expressed by the following equations

Figure 5.19: Effect of glucose concentration on the equilibrium partition coefficient in cell-free Ca-alginate beads.

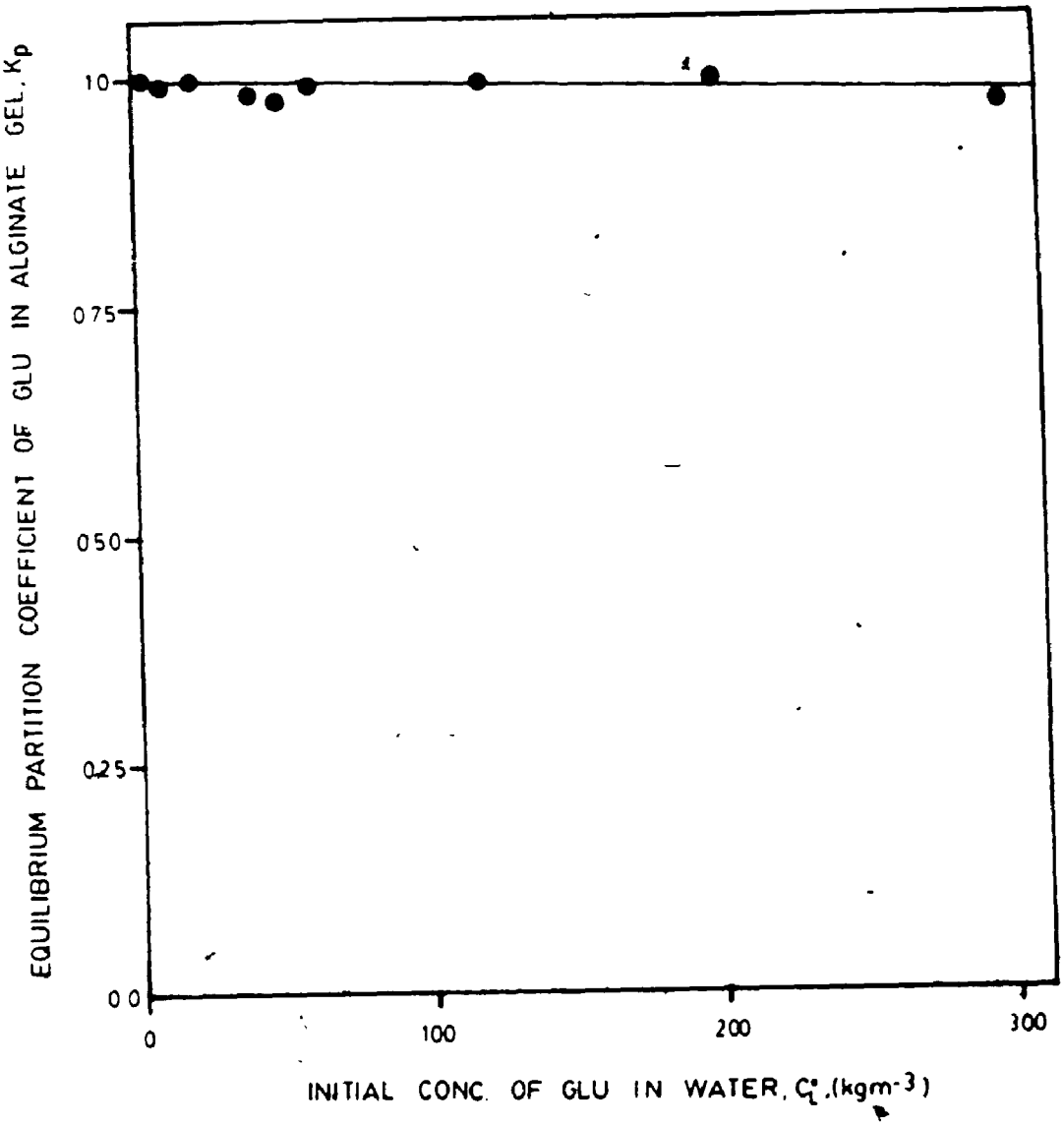
EQUILIBRIUM PARTITION COEFFICIENT OF GLU IN ALGINATE GEL, K_p
1.0
0.75
0.50
0.25
0.0
0
100
200
300
INITIAL CONC. OF GLU IN WATER, C_L^*, (kgm^{-3})

Figure 5.20: Effective diffusivity of glucose in Ca-alginate beads at low solute concentrations ($C_L^o \leq 20$ kg. m^{-3}).

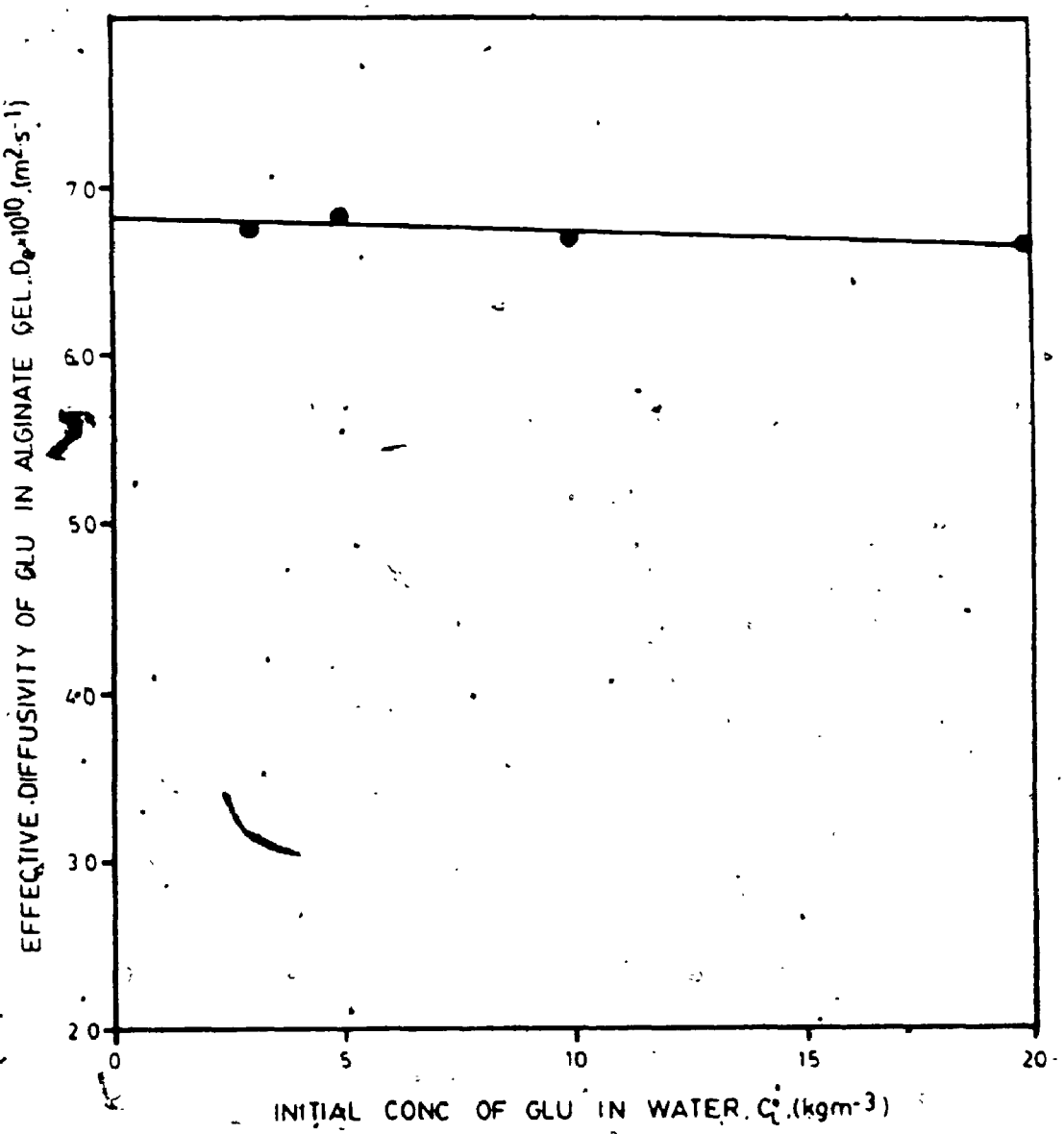
EFFECTIVE DIFFUSIVITY OF GLU IN ALGINATE GEL, $D_e \times 10^{10}$ ($m^2 s^{-1}$)
7.0
6.0
5.0
4.0
3.0
2.0
0
5
10
15
20
INITIAL CONC OF GLU IN WATER, C_L^* (kgm^{-3})

Figure 5.21: Effect of high glucose concentration on the effective diffusivity in cell-free Ca-alginate beads at 30°C.

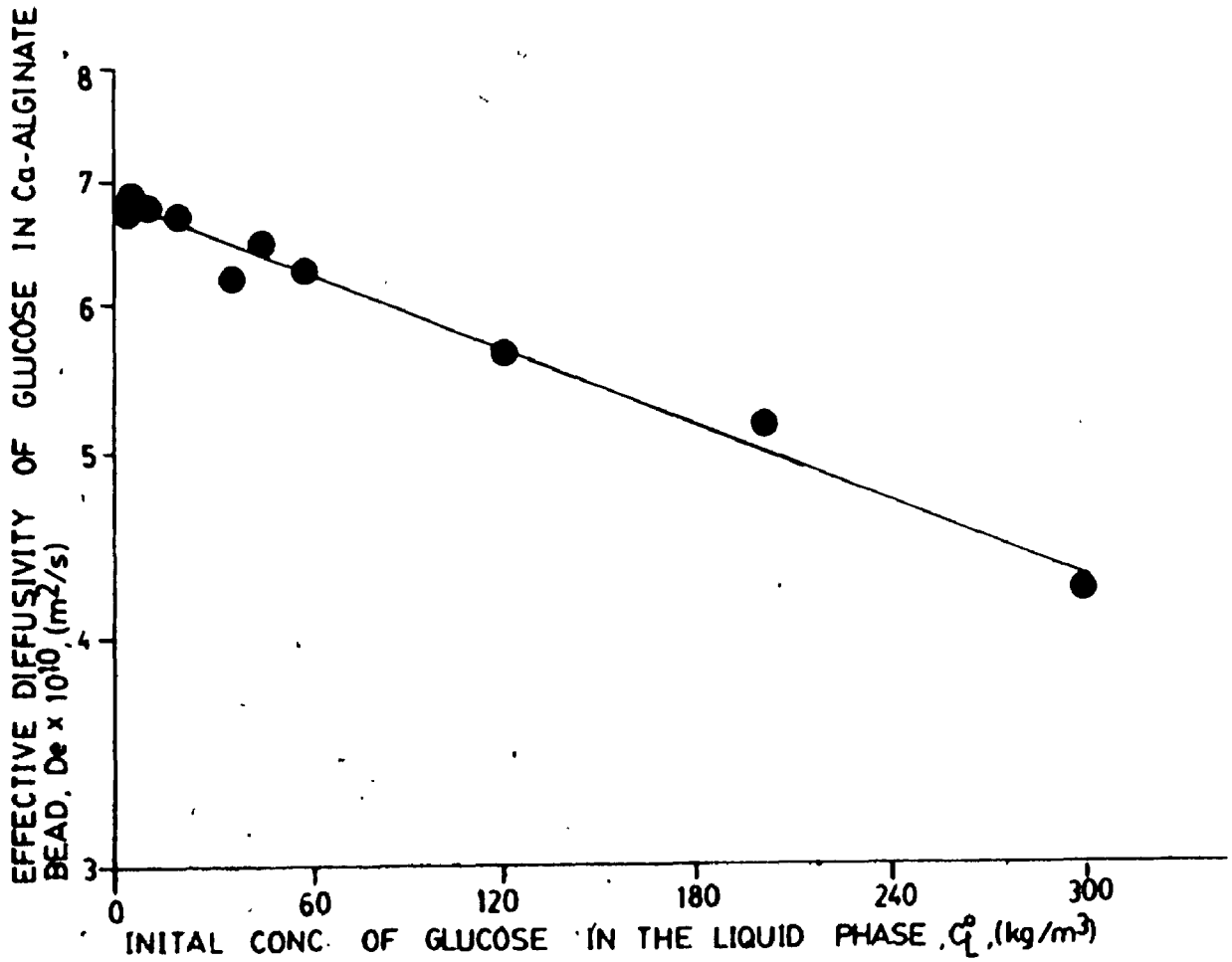
EFFECTIVE DIFFUSIVITY OF GLUCOSE IN Ca-ALGINATE BEAD, De x 10^10, (m^2/s)
8
7
6
5
4
3
0
60
120
180
240
300
INITAL CONC. OF GLUCOSE IN THE LIQUID PHASE, C_L^o, (kg/m^3)

Table 5.8: Effect of Glucose Concentration on the Effective Diffusivity, D_e, of Glucose in Ca-Alginate Gel at 30°C

Initial Conc. of Glucose in Liquid Phase, C_L^o, $(kg.m^{-3})$	Effective Diffusivity of Glucose, $D_e x10^{10}$, $(m^2.s^{-1})$	Diffusivity of Glucose in Water*, $Dx10^{10}$, $(m^2.s^{-1})$	D_e/D	Equilibrium Partition Coefficient K_p
3.0	6.74	7.49	0.900	0.998
5.0	6.83	7.47	0.914	0.997
10	6.70	7.42	0.903	0.980
20	6.66	7.30	0.912	1.00
40	6.17	7.07	0.873	0.969
50	6.47	6.96	0.929	0.954
60	6.20	6.85	0.905	0.986
120	5.63	6.22	0.905	0.996
200	5.12	5.48	0.934	1.00
300	4.16	4.67	0.891	0.933
Non-Linear Regression Analysis:	Intercept = $D_{e,o}$ = 6.83×10^{-10} $m^2.s^{-1}$ Exponential constant = b_{TG} = $1.59x10^{-3}$ $m^3.kg^{-1}$ r^2 = 0.9843	Intercept = D_o = $7.48x10^{-10}$ $m^2.s^{-1}$ Exponential constant = b_T = $1.59x10^{-3}$ $m^3.kg^{-1}$ r^2 = 1.000		

* Calculated using Equation 5.17 (or 5.24).

$$D_e = 6.83 \times 10^{-10} \exp(-1.59 \times 10^{-3} C_L^o) \qquad 5.27$$

or, generally,

$$D_e = D_{e,o} \exp(-b_{TG} C_L^o) \qquad 5.28$$

where, $D_{e,o}$ is the effective diffusivity of glucose in Ca-alginate gel at infinite dilution and b_{TG} is the temperature dependent exponential constant. The coefficient of determination for the above relationship was found to be 0.9843. Incidentally, Equation 5.28 is analogous to Equation 5.18 which relates the free-phase diffusivity of glucose as a function of its concentration.

It is interesting to note that the exponential constant, b_{TG}, in Equation 5.27 is of the same magnitude as the corresponding value b_T (calculated using Equation 5.22), for diffusion of glucose in water at 303 K. Additionally, the fractional decrease in the effective diffusivity of glucose D_e/D, was found to remain constant (see Table 5.8) over the entire glucose concentration range studied (i.e. D_e/D = 0.907 $\pm$ 0.018). Furthermore, the ratio $D_{e,o}/D_o$, at infinite dilution was calculated to be 0.913, whereas the D_e/D values at temperatures of 25 to 40°C (see Table 5.6) were found to be 0.908 ($\pm$ 0.010).

Based on the above observations, the following general correlation may be used to predict the effective diffusivity of glucose in cell-free Ca-Alginate beads. Thus,

$$D_e = 0.91D \qquad 5.29$$

only when C_L^o = 0 to 300 $kg.m^{-3}$ and T = 25°C (298 K) to 40°C (313K). Substitution of Equations 5.17 or 5.24 into Equation 5.29 leads to the following working correlations for predicting D_e. Accordingly,

$$D_e = 1.24 \times 10^{-6} \exp\left[\frac{(0.00248\bar{R}T - 0.01028)C_L - 18.89}{\bar{R}T}\right] \qquad 5.30$$

or,

$$D_e = 1.24 \times 10^{-6} \exp\left[C_L(1.22\times10^{-5}T - 5.29\times10^{-3}) - (18.89/\bar{R}T)\right] \qquad 5.31$$

Substantial decreases in D_e values with increase in solute concentration has also been reported by other workers. For instance, Nguyen and Luong (1986) observed that the decrease in D_e of glucose in 3% κ-carrageenan gel, at 30°C, correlated well with the following equation. Thus,

$$D_e = D_{e,o}(C_L^o)^{-0.106} \qquad 5.32$$

where $D_{e,o}$ was found to be 5.80×10^{-10} $m^2.s^{-1}$.

Similarly, decrease in D_e values of glucose and sucrose in cellulosic membranes has been reported by Spriggs and

Gainer (1973), whereas Furui and Yamashita (1985) observed a significant reduction in D_e values for organic acids and amino acids diffusing in κ-carrageenan and polyacrylamide gels with increase in solute concentration.

Hannoun and Stephanopoulos (1986) have, however, shown that the D_e values in Ca-alginate do not decrease appreciably even at glucose concentrations of 100 $kg.m^{-3}$. Similarly, Tanaka et al. (1984) did not observe any change in the diffusivity values in 2% Ca-alginate beads when the initial concentration of glucose was increased from 5.0 to 300 $kg.m^{-3}$. Contrary to expectations, these results imply that the D_e value of glucose at high concentrations exceed the corresponding values for diffusion of glucose in water. As shown in Section 5.2.2 and literature data (Gladden and Dole, 1953; Dadenkova et al., 1973; Friedman and Carpenter, 1939), the latter decreases exponentially with glucose concentration. Thus, according to the data of Tanaka et al. (1984), when C_L^o = 300 $kg.m^{-3}$, the ratio D_e/D corresponds to a value of 1.50. Enhanced diffusion rates, (D_e/D = 2.0) have also been reported for diffusion of glucose in hyaluronic acid matrix (Hadler, 1980), whereas more recent studies by Norton et al. (1982) have cast doubt on the reliability of these data.

In general values of $D_e/D > 1.0$ can only be explained if significant changes occur in the properties of water imbibed in the matrix (Metzner, 1965). For aqueous gels, Derbyshire and Duff (1974) have shown that the properties of

bulk water in the gel are similar to that of pure water.

5.3.3 Applications of Literature Correlations

Several correlations have been proposed to predict the effective diffusivity of a solute in polymeric gels and membranes. Four different theoretical approaches have been used to derive the final predictive equations. Accordingly, these correlations are based on:

(i) Absolute rate theory

(ii) Obstruction effects

(iii) Fibre matrix model

(iv) Pore diffusion model

The validity of the various correlations, for predicting D_e values of glucose in Ca-alginate gels, was therefore tested by calculating the percentage deviation defined by Equation 5.31

$$\% \text{ Deviation} = \left[\frac{\sum_{n=1}^{N} \left[\frac{[D_e]_{pred} - [D_e]_{exp}}{[D_e]_{exp}} \right]^2}{N - 1} \right]^{1/2} \times 100 \qquad 5.31$$

where N is the number of data pairs used. The experimental D_e values ($[D_e]$exp) listed in Tables 5.6 (effect of temperature) and 5.8 (effect of glucose concentration) were used for comparison with the corresponding predicted values ($[D_e]$pred). Free phase diffusivities of glucose were calculated using the correlations developed in Section 5.2.1 (Equation 5.17) or Section 5.2.2 (Equation 5.24), both of which give identical values of D.

5.3.3.1 Eyring's Absolute Rate Theory

The absolute rate theory provides a general approach for the description of many non-equilibrium processes such as diffusion. In this theory, it is assumed that the diffusion process takes place in a series of activated steps or jumps. Thus, a solute molecule will proceed in the general direction of lower chemical potential and comes to rest at a number of equilibrium positions. In order to make a diffusive jump, a molecule must obtain significant energy to overcome attractive forces holding it to its neighbouring molecules, and also a vacant site must be available into which it can jump. Furthermore, it is assumed that there is equilibrium between a molecule in its resting position and that same molecule in its activated state. The rate of diffusion is then controlled by the breakdown of this activated state (Glasstone et al., 1941).

Based on the above, the diffusivity of a solute A

through a medium B (D_{AB}) is given by the following equation

$$D_{AB} = D^{*}_{AB} \exp(-\frac{\Delta G_{AB}}{\bar{R}T}) \qquad 5.32$$

where D^{*}_{AB} is a group containing the jump distance and a packing factor and ΔG_{AB} is the Gibbs energy of diffusion which is defined by Equation 5.33

$$\Delta G_{AB} = E_{AB} + \Delta PV - \Delta TS_{AB} \qquad 5.33$$

where E_{AB} is the activation energy for diffusion of species A through species B, S_{AB} is the entropy of activation, and $\Delta PV = 0$ since the volume change during the diffusion process in a constant pressure solid-liquid system is negligible. The quantities E_{AB} and S_{AB} are closely related. Thus, the activation energy, E_{AB}, is the energy required to open a hole for the diffusing molecule to enter plus the energy required for the molecule to make that move. Likewise, the entropy of activation, S_{AB}, is the entropy change associated with hole formation and molecule diffusion.

Following systematic theoretical and experimental studies, Spriggs and Gainer (1973) developed the following correlation (Equation 5.34) for predicting effective diffusivities of low molecular weight solutes (glucose, sucrose, urea) in homogeneous swollen cellulosic membranes.

$$D_e = D.\exp\left[-0.3\left(\frac{[1-(1-\lambda)^{0.5}]}{(1-\lambda)^{0.5}}\right)\frac{E_a}{RT}\right] \qquad 5.34$$

where, 0.3 is a constant relating the entropy of activation to the energy of activation.

Knowing the diffusion coefficient (D) and activation energy (E_a) for diffusion of glucose in water (calculated using Equations 5.17 and 5.13, respectively) and taking the volume fraction of alginate in the gel (λ) to be 0.031, the effective diffusivity was calculated (using Equation 5.34) as a function of temperature and concentration. The predicted D_e values are shown as curve A in Figures 5.22 and 5.23, respectively. The corresponding experimental D_e values are also plotted in Figures 5.22 and 5.23 indicating that Equation 5.34 gives a reasonably good estimate of D_e. Furthermore, the percentage deviation of the predicted values from the experimental data was determined to be 7.37%.

5.3.3.2 Obstruction Effects

Correlations based on the obstruction phenomenon arise by virtue of the increased path length in the gel when compared to an equivalent thickness of pure solvent. In porous media, this mean increase in path length is referred to as tortuosity. In these correlations it is generally assumed

Figure 5.22: Experimental and predicted values of D_e plotted as a function of temperature [(●), experimental values; (—) predicted values; curve A, Equations 5.34 or 5.36; curve B, Equations 5.37 or 5.38; curve C, Equations 5.35, 5.39 or 5.42; curve D, best-fit model equation developed in this study, and given by Equations 5.30 or 5.31]

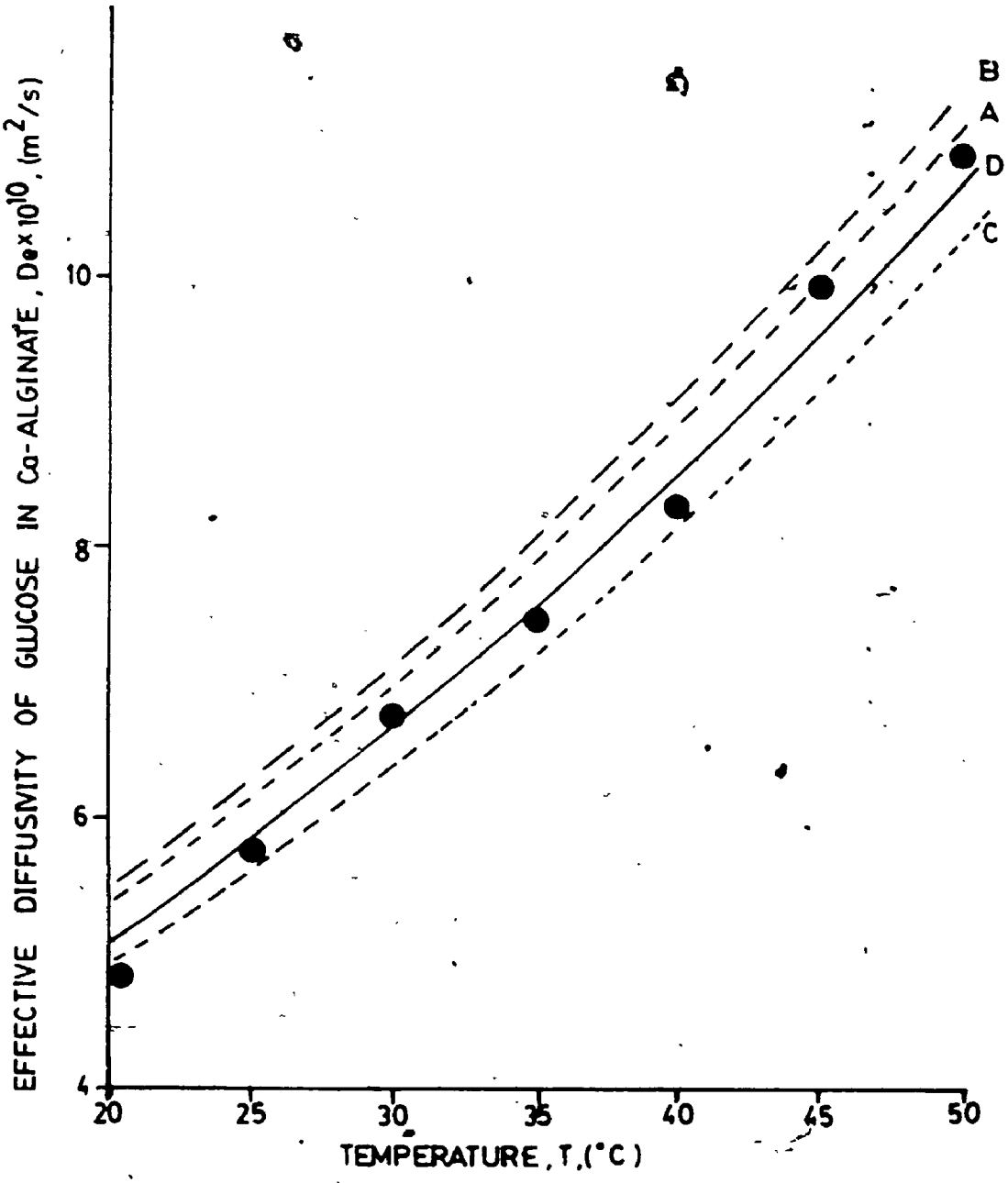
EFFECTIVE DIFFUSIVITY OF GLUCOSE IN Ca-ALGINATE, De×10^10, (m^2/s)
TEMPERATURE, T, (°C)
4
6
8
10
20
25
30
35
40
45
50
A
B
C
D

Figure 5.23: Experimental and predicted values of D_e plotted as a function of glucose concentration [(●), experimental values; (——) predicted values; curve A, Equations 5.34 or 5.36; curve B, Equations 5.37 or 5.38; curve C, Equations 5.35, 5.39 or 5.42; curve D, best-fit model equation developed in this study and given by Equations 5.30 or 5.31].

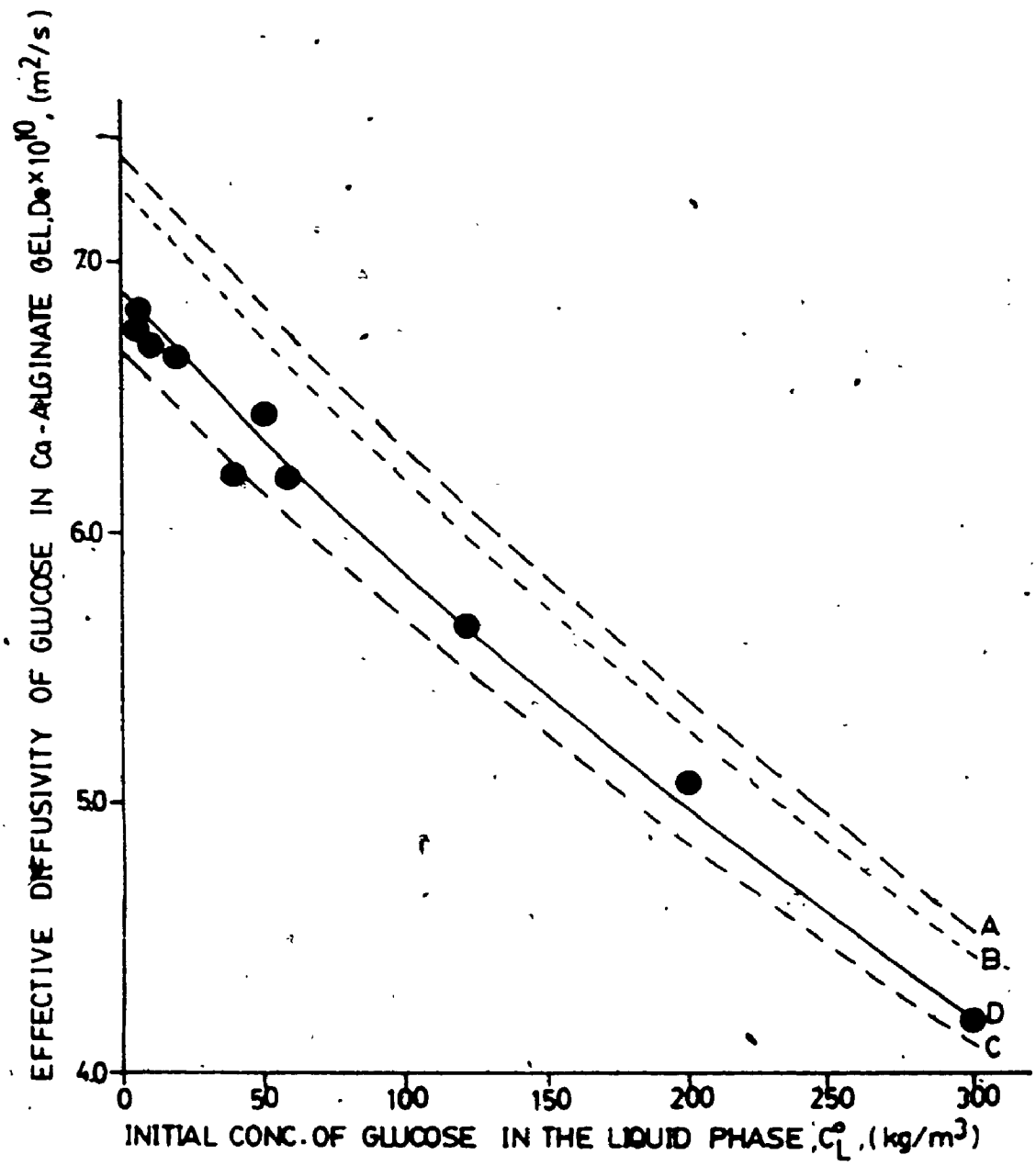
EFFECTIVE DIFFUSIVITY OF GLUCOSE IN Ca-ALGINATE GEL, $D_e \times 10^{10}$, (m^2/s)
7.0
6.0
5.0
4.0
0
50
100
150
200
250
300
INITIAL CONC. OF GLUCOSE IN THE LIQUID PHASE, C_L^o, (kg/m^3)
A
B
C
D

that there are no specific interactions between the polymer and a given solute. Furthermore, the ratio D_e/D is defined by a simple function of the polymer volume fraction, λ (or the void volume, $\varepsilon = 1 - \lambda$). Hence this ratio should be the same for all mobile species in all gels of equal void volume. Some correlations based on the above will be employed to estimate the effective diffusivity of glucose in Ca-alginate gel.

The most widely used equation is that by Mackie and Meares (1955). Accordingly,

$$D_e = D\left[\frac{1 - \lambda}{1 + \lambda}\right]^2 \qquad 5.35$$

The predicted D_e values are plotted as curve C in Figures 5.22 and 5.23. The correlation gives a better estimate of D_e than that due to the absolute rate theory (Equation 5.34) with a percentage deviation of less than 4%. Equation 5.35 has also been shown to give reliable estimates of D_e for glucose and other oligosaccharides diffusing in cellulosic gels and membranes (Brown and Johnsen, 1981b). However, for diffusion in polyacrylamide (Brown and Johnsen, 1981a) and hydroxyethylcellulose gels (Brown et al., 1976) the correlation of Mackie and Meares, (1955) substantially overestimates D_e. Thus, the 'obstruction effect' may be only partly responsible for reducing the diffusion rates in such gels.

Other correlations are based on Fricke's equation which

was originally suggested in 1924 (Muhr and Blanshard, 1982). Thus,

$$D_e = D \left[\frac{1 - \lambda}{1 + \lambda/2} \right] \qquad 5.36$$

or

$$D_e = \frac{D}{1 + \lambda/2} \qquad 5.37$$

Equations 5.36 and 5.37 are represented by curves A and B, respectively in Figures 5.22 and 5.23. Equation 5.36 gives a better estimate of D_e (% deviation = 7.2%) than the alternate solution (Equation 5.37; % deviation = 10.5%).

Lauffer (1961) proposed the following equation for predicting D_e

$$D_e = \frac{D}{[1 + (\alpha - 1)\lambda]} \qquad 5.38$$

where α = 5/3 for randomly oriented polymer fibres. As in the case of Equation 5.37 this correlation (curve B) is not as reliable as that proposed by Mackie and Meares (1955). However, Schantz and Lauffer (1962) successfully predicted D_e of proteins and other solutes in 1.5% agar gels.

More recently, Klein and Schara (1981) proposed that

the effective diffusivity of small solutes (such as glucose and oxygen) in immobilization supports, may be estimated using Equation 5.39

$$D_e = D.\exp(-a\lambda) \qquad 5.39$$

where a = 4 for small molecules (Klein and Manecke, 1982). This correlation (plotted as Curve C) also gave a good estimate of D_e for glucose diffusing in Ca-alginate gel, and has been found to be applicable for glucose, oxygen and other larger solutes (provided the parameter 'a' is increased appropriately) diffusing in chitosan (Klein and Manecke, 1982) and polyacrylamide (Klein and Schara, 1981) gels. Unlike other 'obstruction models' Equation 5.39 takes into account the size of the diffusing species by incorporating a coefficient 'a' in the correlation.

5.3.3.3 Fibre Matrix Model

The most common fibre matrix model is that suggested by Ogston (1958). In this theoretical model, the gel is treated as a three-dimensional network of rigid fibres, randomly distributed and infinitely long. The partition coefficient of a solute is assumed to be determined by the space available to the molecules in the gel-network. According to the Ogston theory, the ratio D_e/D is predicted by

$$D_e/D = \exp[-\pi^{1/2} L^{1/2}(r_f + r_s)] \qquad 5.40$$

where L is the concentration of the fibre in the gel expressed as cm fibre/cm^3, r_f is the radius of the fibre and r_s is the Stokes radius of the solute.

If the glucose molecule is considered to be spherical the partition coefficient can be calculated from an equation given by Ogston (1958) and modified by Laurent (1967). Thus,

$$K_p = \exp[-\pi L (r_f + r_s)^2] \qquad 5.41$$

Since the values L and r_f are not available for alginate gels, Equations 5.40 and 5.41 have little practical use, in their original form. However, by combining these two equations (Sellen, 1980), it can be shown that

$$K_p = \exp[-(\ln D_e/D)^2] \qquad 5.42$$

This relationship is plotted in Figure 5.24.

Based on the data presented in Tables 5.6 and 5.8, the average partition coefficient of glucose in Ca-alginate gel was calculated to be 0.985 ($\pm$ 0.018). Using non-linear regression analysis and the least-squares method this K_p value corresponds to a D_e/D ratio of 0.886 which is very similar to the experimentally determined value of 0.91 (see Equation

Figure 5.24: Ratio of D_e/D plotted as a function of K_p based on Ogston's Theory (Equation 5.42).

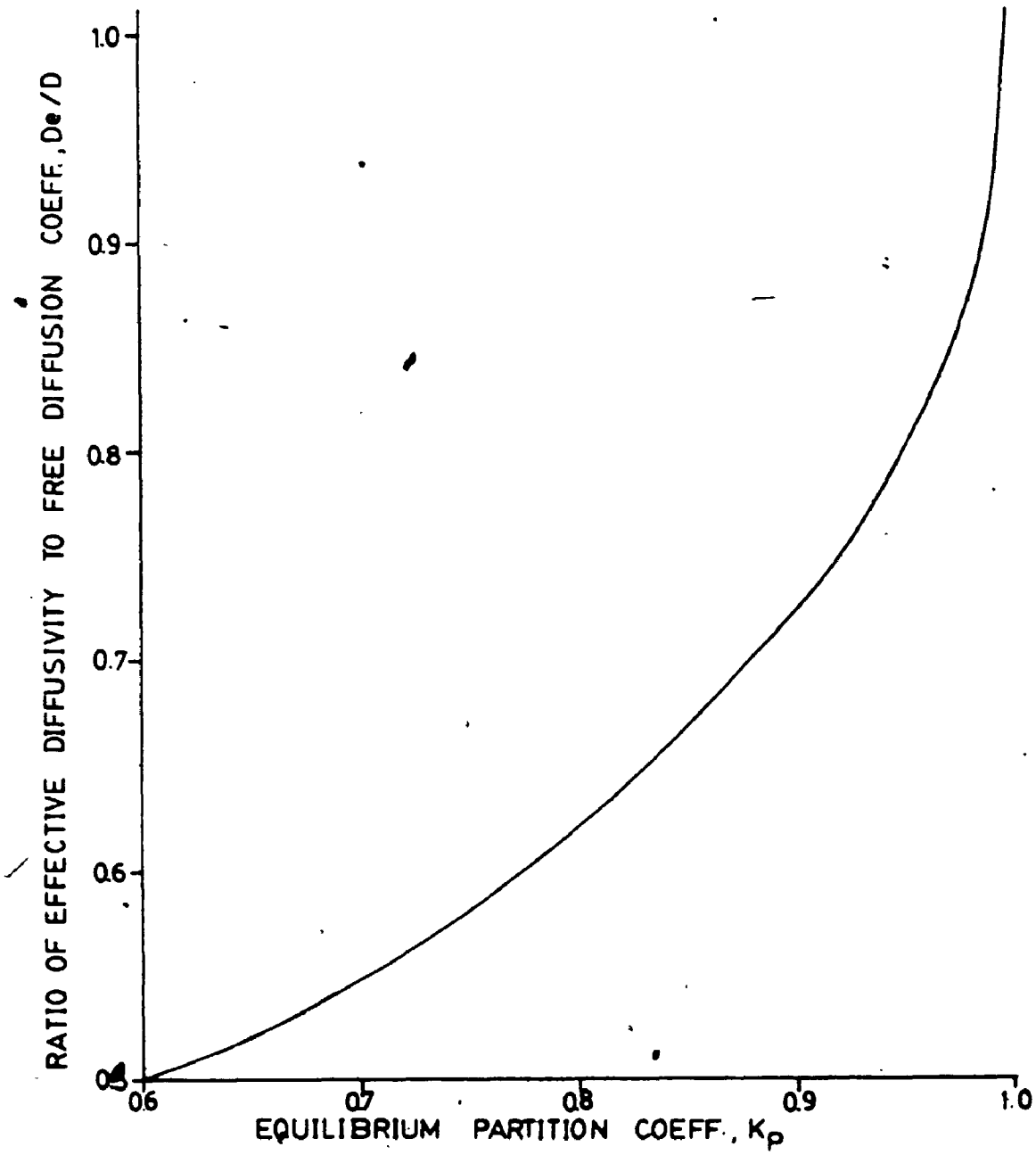
RATIO OF EFFECTIVE DIFFUSIVITY TO FREE DIFFUSION COEFF., De/D
1.0
0.9
0.8
0.7
0.6
0.5
0.6
0.7
0.8
0.9
1.0
EQUILIBRIUM PARTITION COEFF., Kp

5.29). The best-fit model equation based on actual experimental data (Equation 5.30 or Equation 5.31) is plotted as curve D in Figures 5.22 and 5.23, whereas that due to the Ogston theory (Equation 5.42, when $D_e/D = 0.886$) is represented by curve C indicating that the latter can reliably estimate D_e of glucose in Ca-alginate gel (% deviation < 3.0%).

The Ogston expression for D_e/D also compares favourably with the data of White and Dorion (1961) for diffusion of sucrose in polyacrylamide gels at low λ ($\lambda < 0.05$) but progressively overestimates D_e/D for larger values of λ. Also, even at low λ, Equation 5.42 overestimates D_e/D for diffusion of glucose in hydroxyethylcellulose gel (Brown et al., 1976).

As in the case of the 'obstruction effect', the fibre-matrix model also assumes that the pore-wall does not retard the mobility of the solute molecules within the gel. This simplification may be responsible for the occasional failure of these two models in accurately predicting D_e.

5.3.3.4 Pore Diffusion Model

The concept of the pore diffusion model is based on two different phenomena. The first, originally described by Ferry (1936) establishes the condition that for entrance into a pore, a solute molecule must pass through the opening without striking the edge. The centre of the molecule must,

therefore, pass through a circle of radius ($r_p - r_s$) within the mouth of the pore, in which r_p is the pore radius and r_s is that of a solute molecule. This exclusion effect is shown schematically in Figure 5.25. At equilibrium, a concentration distribution will develop between the pore and the bulk solution and this is given by the following equation

$$K_p = 1 - \left[\frac{r_s}{r_p}\right]^2 \qquad 5.43$$

The second factor corrects for the increase in hydrodynamic drag as the solute molecule traverses a pore, analogous to the increase in drag on a sphere falling in a capillary tube of comparable diameter (Lane, 1950). The drag effect results in decrease in the diffusivity of a solute by the factor, f_d:

$$f_d = 1 - 2.104\left[\frac{r_s}{r_p}\right] + 2.09\left[\frac{r_s}{r_p}\right]^3 - 0.95\left[\frac{r_s}{r_p}\right]^5 \qquad 5.44$$

The total restriction to diffusion, due to the combined effects of the exclusion effect (Equation 5.43) and hydrodynamic drag within the pores (Equation 5.44) is given by Equation 5.45 (Renkin, 1954)

Figure 5.25: Cylindrical model of a pore showing the 'exclusion effect' according to Ferry (1936). Adapted from Beck and Schultz, 1972.

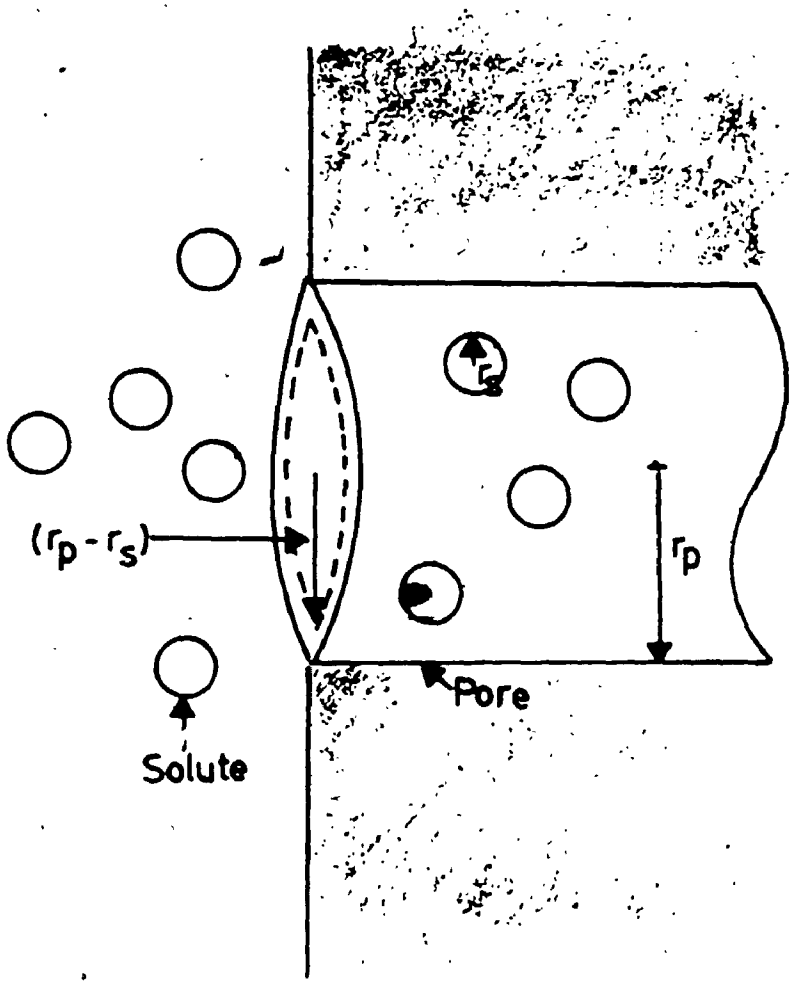
r_s
$(r_p - r_s)$
r_p
Pore
Solute

$$\frac{D_e}{D} = \left(1 - \left[\frac{r_s}{r_p}\right]^2\right)\left(1 - 2.104\left[\frac{r_s}{r_p}\right] + 2.09\left[\frac{r_s}{r_p}\right]^3 - 0.95\left[\frac{r_s}{r_p}\right]^5\right) \qquad 5.45$$

The validity of this equation has been verified experimentally by Beck and Schultz (1972) who measured the diffusivities of molecular solutes through thin, etched mica-membranes containing straight pores of well defined geometry and narrow pore size distribution with diameters ranging from 9 to 60 nm. Their data correlated extremely well especially in the range $0 < r_s/r_p < 0.2$.

For r_s/r_p ranging from 0 to 0.15, the corresponding values of D_e/D are plotted in Figure 5.26. Thus, from known pore size of the gel matrix, the effective diffusivity of a given solute may be predicted from Figure 5.26. Conversely, the pore size may be estimated from diffusivity data.

Based on the studies reported earlier (Section 5.3.2), the ratio D_e/D for glucose diffusing in Ca-alginate gel was found to be 0.91. This corresponds to an estimated r_s/r_p value of 0.021. Using the Stokes-Einstein equation (Geankoplis, 1983) the molecular radius of a glucose molecule was calculated to be 0.36 nm. Thus,

$$r_s = \frac{\bar{R}T}{6\pi\mu D_o N} \qquad 5.46$$

where μ is the viscosity of water, D_o is the diffusion coefficient of glucose in an infinitely dilute aqueous solu-

Figure 5.26: Ratio of effective diffusivity to free phase diffusivity (D_e/D) of a solute molecule with radius r_s diffusing through pores of radius, r_p' (Calculated using Equation 5.45).

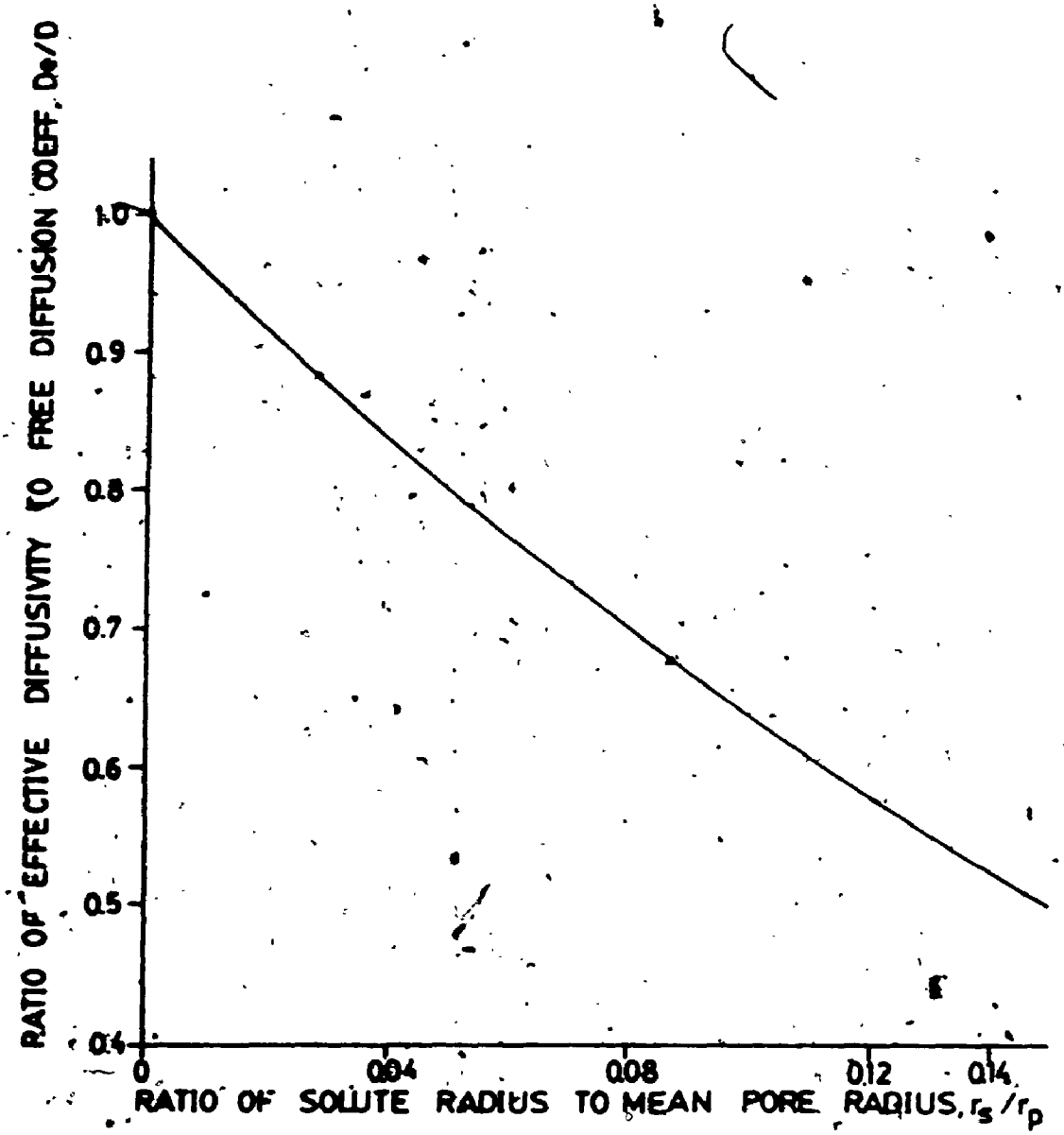
RATIO OF EFFECTIVE DIFFUSIVITY TO FREE DIFFUSION COEFF. D*/D
1.0
0.9
0.8
0.7
0.6
0.5
0.4
0
0.04
0.08
0.12
0.14
RATIO OF SOLUTE RADIUS TO MEAN PORE RADIUS, r_s/r_p

tion, and N is the Avogadro's number (6.022×10^{23} mol^{-1}). Consequently, the mean pore diameter in Ca-alginate gel was estimated to be 34 nm.

Using size exclusion chromatography and Ca-alginate gels prepared from concentrated Na-alginate solutions (up to 7% w/w), Klein et al., (1983) determined the pore diameters be approximately 6 to 17 nm. Mackie et al. (1977) estimated the pore sizes in dilute Ca-alginate gels (0.5% w/v) to be at least 100 nm. Thus, the value of 34 nm determined in this study appears to be a reliable estimate for the pore diameter, d_p, in Ca-alginate gel prepared from a 2% (w/v), Na-alginate solution.

In subsequent sections, the validity of various correlations presented above will be compared with experimental data for diffusion of glucose in a wide variety of alginate gels with or without entrapped yeast cells.

5.3.4 Effect of Chelating Agent Type and Concentration

As discussed in Chapter 2, the type and concentration of chelating agents has a profound influence on the properties of alginate gels. Since, $CaCl_2$ and $BaCl_2$ have been frequently used for preparing alginate immobilization matrices, the diffusivity characteristics of glucose in Ca- and Ba-alginate gels was examined with respect to the concentration of the gelling agents.

Na-alginate, supplied by Fisher Chemicals (sample #17),

was used in this study and large Ca- and Ba-alginate spherical beads prepared as before (Section 5.3.1) except that gelation was carried out by using 5, 20, 40, or 80 kg. m^{-3} solutions of either $CaCl_2$ or $BaCl_2$. All D_e values were determined at 30°C with the initial 'cold' glucose concentration of 20 kg. m^{-3}.

Figure 5.27 shows that with $CaCl_2$ as the gelling agent, the D_e values do not decrease as the concentration of $CaCl_2$ is raised from 5 to 40 kg. m^{-3}. However, a significant (12%) drop in the effective diffusivity of glucose is observed at the highest concentration of $CaCl_2$ (80 kg. m^{-3}). Other studies have also reported insignificant changes in D_e values of glucose (Tanaka et al., 1984), and release rates of NAD and haemoglobin (Kierstan et al., 1982) from Ca-alginate gel when the concentration of $CaCl_2$ was increased from 50 mM (5.5 kg. m^{-3}) to 500 mM (55 kg. m^{-3}).

With $BaCl_2$ as the gelling agent, a linear decrease in D_e values was observed (Figure 5.27) over the entire concentration range (5 to 80 kg. m^{-3}). Additionally, at all concentrations, the effective diffusivity of glucose in Ba-alginate gels, was significantly lower than that in Ca-alginate gels. Kierstan et al. (1982) also observed slower release rates of NAD and haemoglobin when $BaCl_2$ was used as the gelling agent instead of $CaCl_2$. These differences in D_e values of glucose may be attributed to the higher affinity of Ba^{2+} ions for the alginate polymer (Section 2.4.1).

From known D_e/D values (listed in Table C.2, Appendix)

Figure 5.27: Effect of chelating agent concentration on effective diffusivity of glucose (●, $CaCl_2$; ○, $BaCl_2$) and pore size (■, $CaCl_2$; □, $BaCl_2$) in calcium and barium alginate gels.

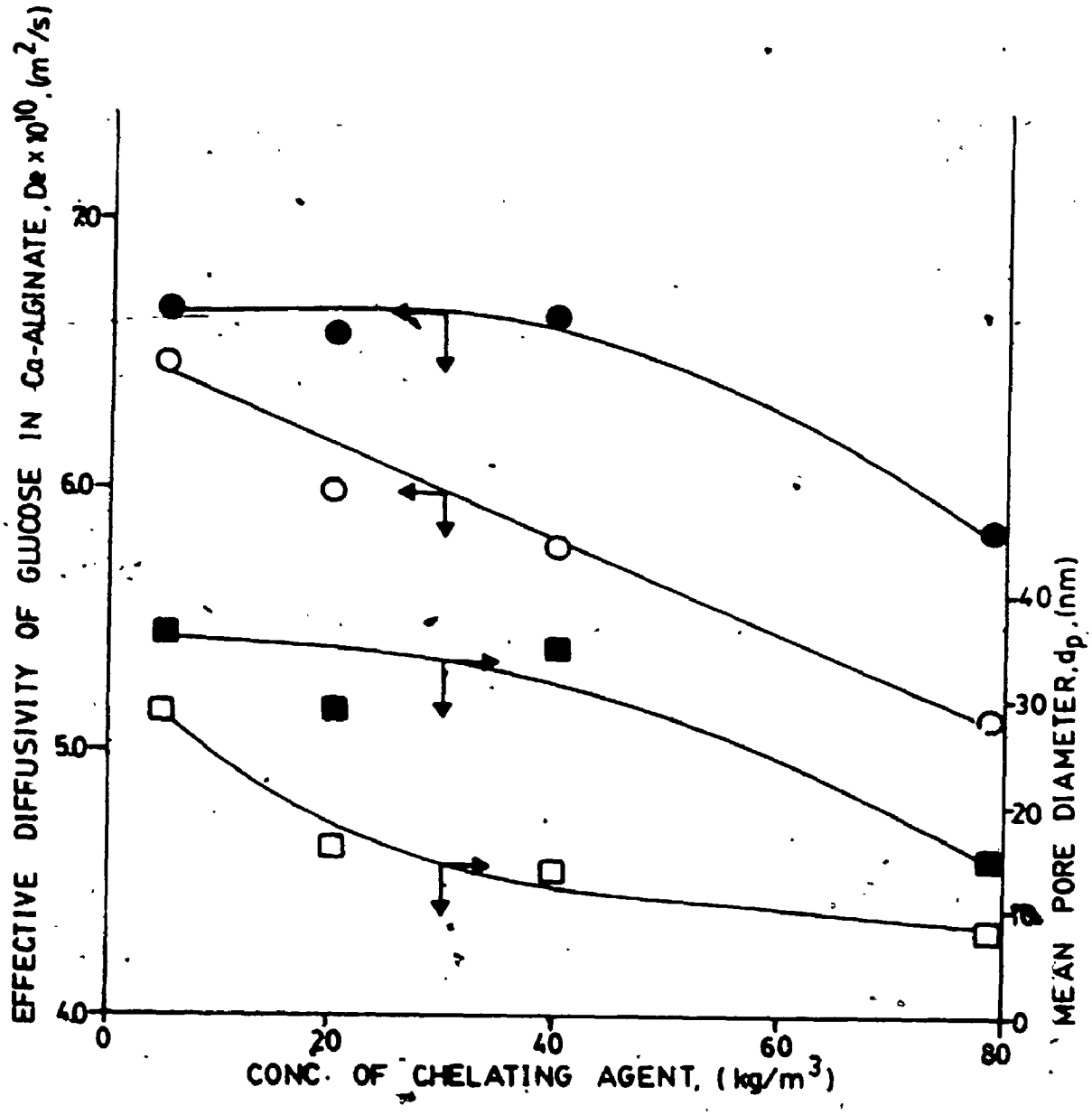
EFFECTIVE DIFFUSIVITY OF GLUCOSE IN Ca-ALGINATE, De x 10^10, (m^2/s)
70
60
50
40
MEAN PORE DIAMETER, dp, (nm)
40
30
20
10
0
0
20
40
60
80
CONC. OF CHELATING AGENT, (kg/m^3)

the mean pore diameter in Ca- and Ba-alginate gels was estimated using the Renkin equation (see Figure 5.26 and Equation 5.45) and plotted as a function of the chelating agent concentration as shown in Figure 5.27. Thus, as the concentration of $CaCl_2$ and $BaCl_2$ is increased, stronger binding forces between adjacent chains of the alginate polymer result (Smidsrod, 1974), causing a reduction in pore sizes (Thiele and Hallich, 1957) within the alginate matrix.

Furthermore, as the alginate matrix becomes more tightly cross-linked, contraction of the gel volume due to synerisis also occurs (Section 2.4.2), and consequently, the final concentration of alginate within the gel increases. As shown in Figure 5.28, for a fixed concentration of Na-alginate in solution ($\simeq$ 17kg DW/m^3 of solution) the concentration of alginate is higher in Ba-alginate gel, and increases as the concentration of $CaCl_2$ and $BaCl_2$ is increased. Figure 5.29 shows that the decrease in D_e values and pore diameters, can be attributed to the relative increase in the concentration of alginate in the gel matrix, which in turn depends on the type and concentration of the gelling agent.

Thus, in order to minimize intraparticle diffusional resistances in alginate matrices use of dilute $CaCl_2$ ($\leq$ 40 kg. m^{-3}) and BaCl ($\leq$ 5 kg. m^{-3}) solutions for cell immobilization would be desirable. Furthermore, with dilute solutions of $CaCl_2$ and $BaCl_2$, the toxic effects of these chelating agents on immobilized viable cells can be mini-

Figure 5.28: Effect of chelating agent type (● $CaCl_2$; ○ $BaCl_2$) and concentration on the final alginate concentration in the gel.

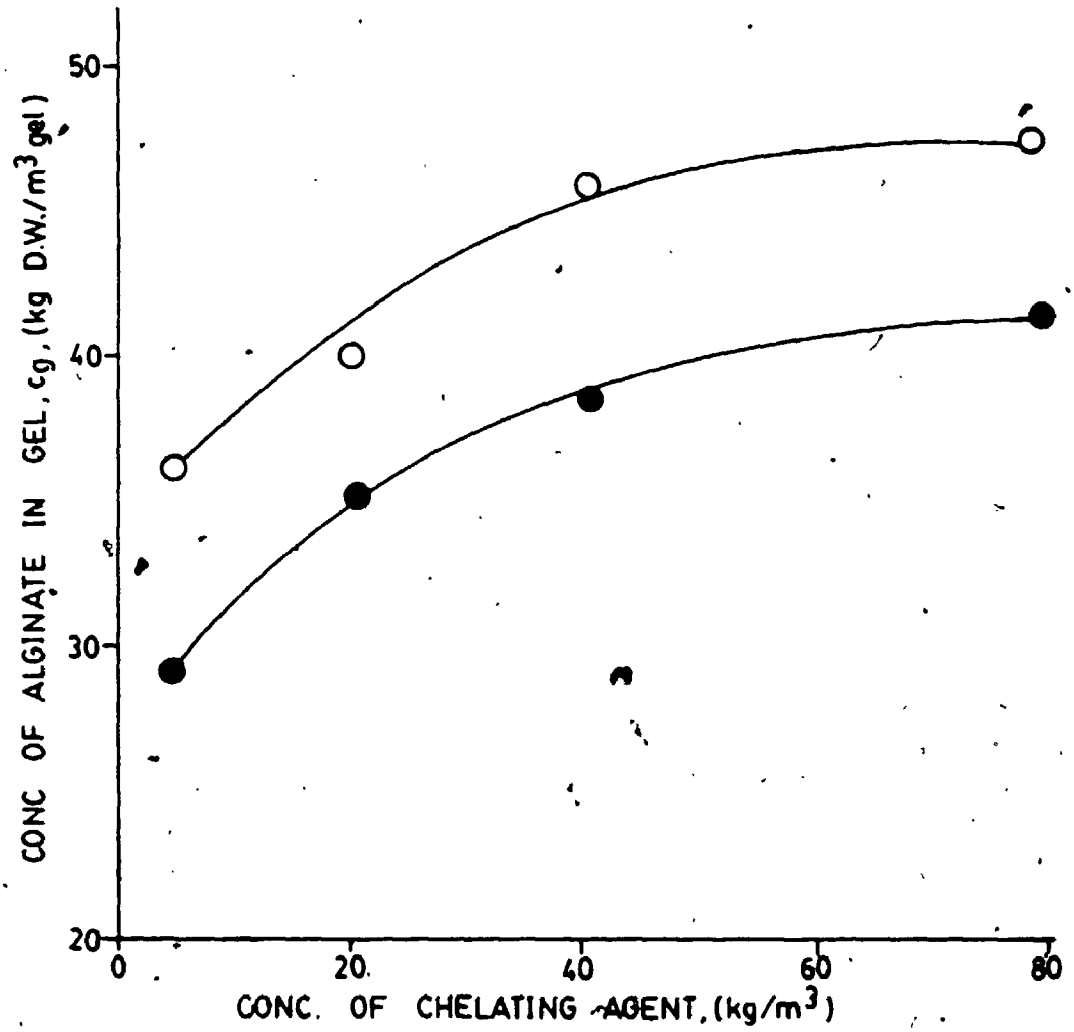
CONC OF ALGINATE IN GEL, cg, (kg D.W./m3 gel)
50
40
30
20
0
20
40
60
80
CONC. OF CHELATING AGENT, (kg/m3)

Figure 5.29: Effective diffusivity of glucose (●, ○) and mean pore diameter (■, □), in Ca-alginate (●, ■) and Ba-alginate (○, □) gels, plotted as a function of alginate concentration in the gel.

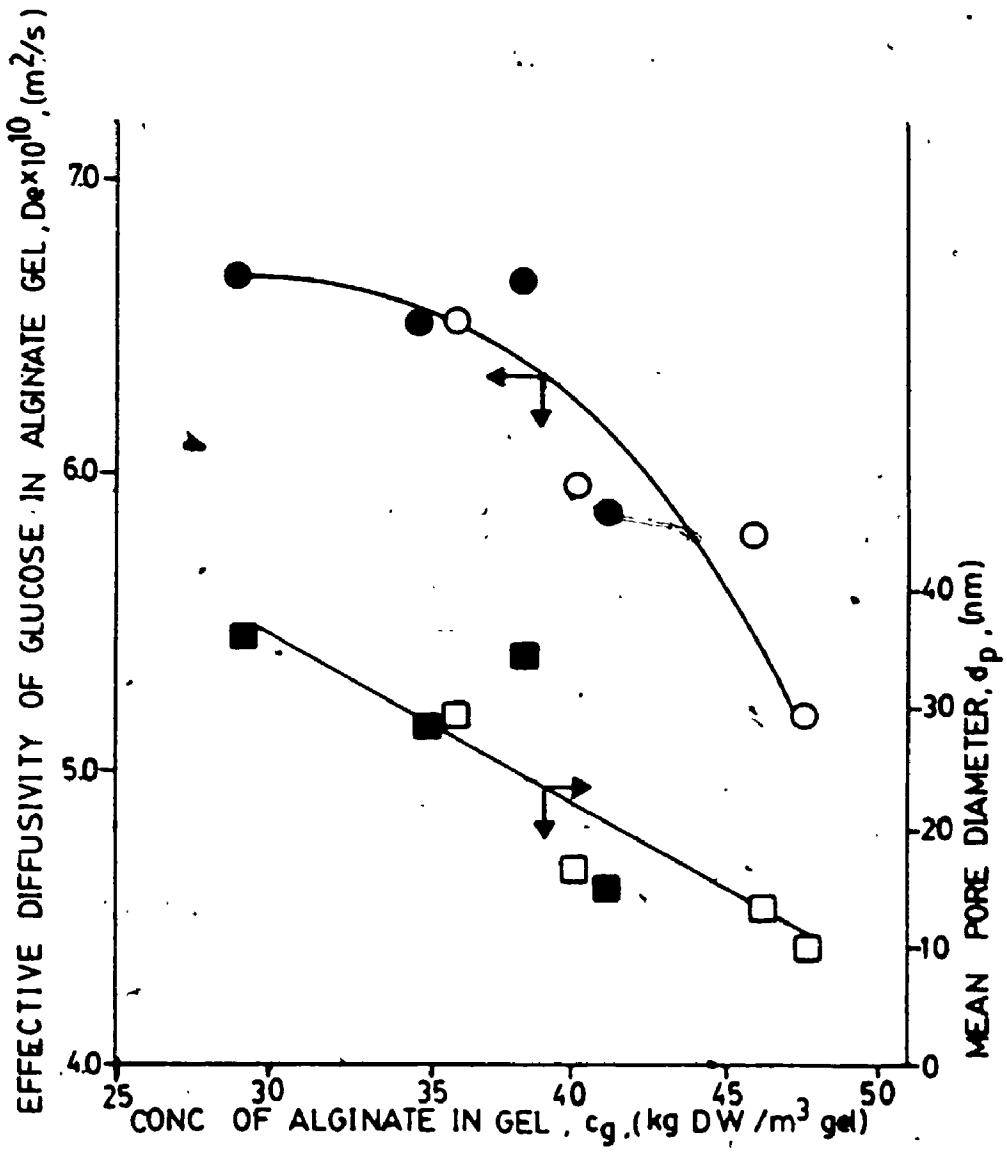
EFFECTIVE DIFFUSIVITY OF GLUCOSE IN ALGINATE GEL, De×10^10, (m²/s)
7.0
6.0
5.0
4.0
MEAN PORE DIAMETER, dp, (nm)
40
30
20
10
0
25
30
35
40
45
50
CONC OF ALGINATE IN GEL, cg, (kg DW/m³ gel)

mized. However, such gels are less likely to have good mechanical stability characteristics (Smidsrod, 1974) and higher rates of cell leakage may be anticipated (Cheetham et al., 1979).

5.3.5 Effect of Alginate Type and Concentration

From the total of 16 different commercial samples of Na-alginates listed in the Table 4.1, five were selected for further study based on their differences in guluronic acid content and degree of polymerization (DP) as shown in the table below:

Increase in Guluronic Acid Content →	Low guluronic acid content (G ≈ 40%)	High guluronic acid content (G ≈ 70%)	Increase in Degree of Polymerization ↓
Very low DP (DP ≈ 525)	Sample #1	not available	
Low DP (DP ≈ 1,200)	Sample #9	Sample #15	
High DP (DP ≈ 3,050)	Sample #13	Sample #4	

The following concentrations of Na-alginate solutions were prepared for gel formation depending on the type of alginate used:

Sample # 1 : 120, 160, and 200 $kg.m^{-3}$

Sample # 9 : 20, 40, and 60 $kg.m^{-3}$

Sample # 15 : 40, 60, and 80 $kg.m^{-3}$

Sample # 13 : 20 $kg.m^{-3}$

Sample # 4 : 20 and 40 $kg.m^{-3}$

Thus, a total of 12 different Na-alginate solutions were used for gel formation, differing in their guluronic acid content (G-content), degree of polymerization (DP) and concentration. Calcium chloride (40 kg. m^{-3}) was employed as the gelling agent for preparing large Ca-alginate beads using the various Na-alginate solutions listed above. All diffusivity measurements were carried out at 30°C with an initial 'cold' glucose concentration of 20 kg. m^{-3}.

In Figure 5.30, the effective diffusivity of glucose is plotted as a function of Na-alginate concentration (i.e. before gelation). When, DP exceeds 1200 (plot 1) the D_e values do not appear to differ in alginate gels containing different amounts of guluronic acid. Thus, with the exception of sample #1 (plot 2) the D_e values in all other Ca-alginate gels can be expressed by the following linear equation ($r > 0.96$)

$$D_e = (7.06 \times 10^{-10}) - (2.32 \times 10^{-12})\acute{c} \qquad 5.47$$

where, $\acute{c}$ is the concentration of Na-alginate in solution prior to gelation ($kg.m^{-3}$ of solution). The above equation

Figure 5.30: Effect of Na-alginate concentration in solution on the effective diffusivity of glucose (△, sample #1; ○, sample #9; □, sample #13; ●, sample #15; ■, sample #4). See text for explanation of different plots.

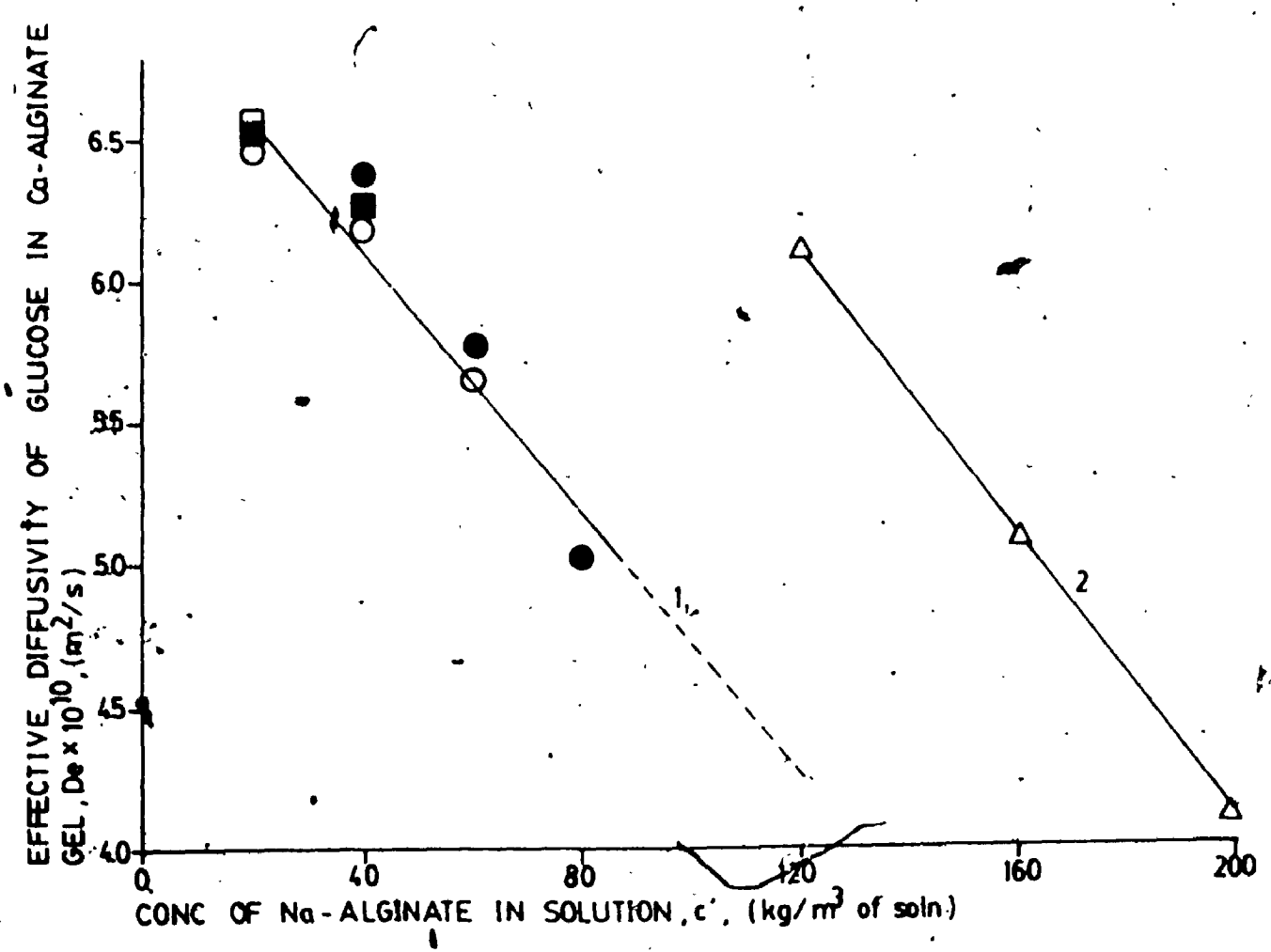
EFFECTIVE DIFFUSIVITY OF GLUCOSE IN Ca-ALGINATE GEL, De x 10^10, (m^2/s)
6.5
6.0
5.5
5.0
4.5
4.0
0
40
80
120
160
200
CONC OF Na-ALGINATE IN SOLUTION, c', (kg/m^3 of soln.)
1
2

4

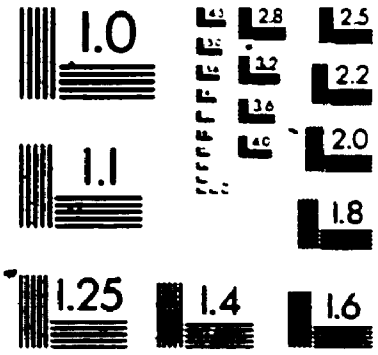

is valid only for Na-alginates with DP ranging from 1200 to 3000 and a guluronic acid content of 40 to 70 percent. Na-alginates possessing these characteristics are commonly used for cell immobilization (Klein et al., 1983) whereas Na-alginates of the type represented by sample #1 are used as thickeners in the food industry (McDowell, 1977). Thus, with sample #1, stable Ca-alginate beads could only be prepared when the concentration of Na-alginate solution exceeded 120 kg. m^{-3}. Figure 5.30 also shows that the D_e value of glucose in Ca-alginate gel prepared from a 120 kg. m^{-3} solution of sample #1 is substantially higher (> 42%) than the extrapolated D_e value (represented by the broken line) at 120 kg. m^{-3} in other Ca-alginate gels. High D_e value in alginate #1 may be attributed to the more open pore structure and fewer cross-links between adjacent alginate chains which is characteristic for Na-alginates with a very low DP and low G content (Smidsrod, 1974).

Since synerisis commonly occurs during gel formation (Section 2.4.2), the concentration of Na-alginate may not truly represent the actual concentration of Ca-alginate within the gel.

In Figure 5.31, the effective diffusivity of glucose was therefore plotted as a function of Ca-alginate concentration in the gel (c_g). As before, the D_e values decreased linearly with increase in Ca-alginate concentration in alginates with DP = 1200 to 3000, (represented by plots 1 and 2 in Figure 5.31) and lower D_e values were obtained when the

Figure 5.31: Effect of Ca-alginate concentration on the effective diffusivity of glucose (△, sample #1; ○, sample #9; □, sample #13; ●, sample #15; ■, sample #4). See text for explanation of different plots.

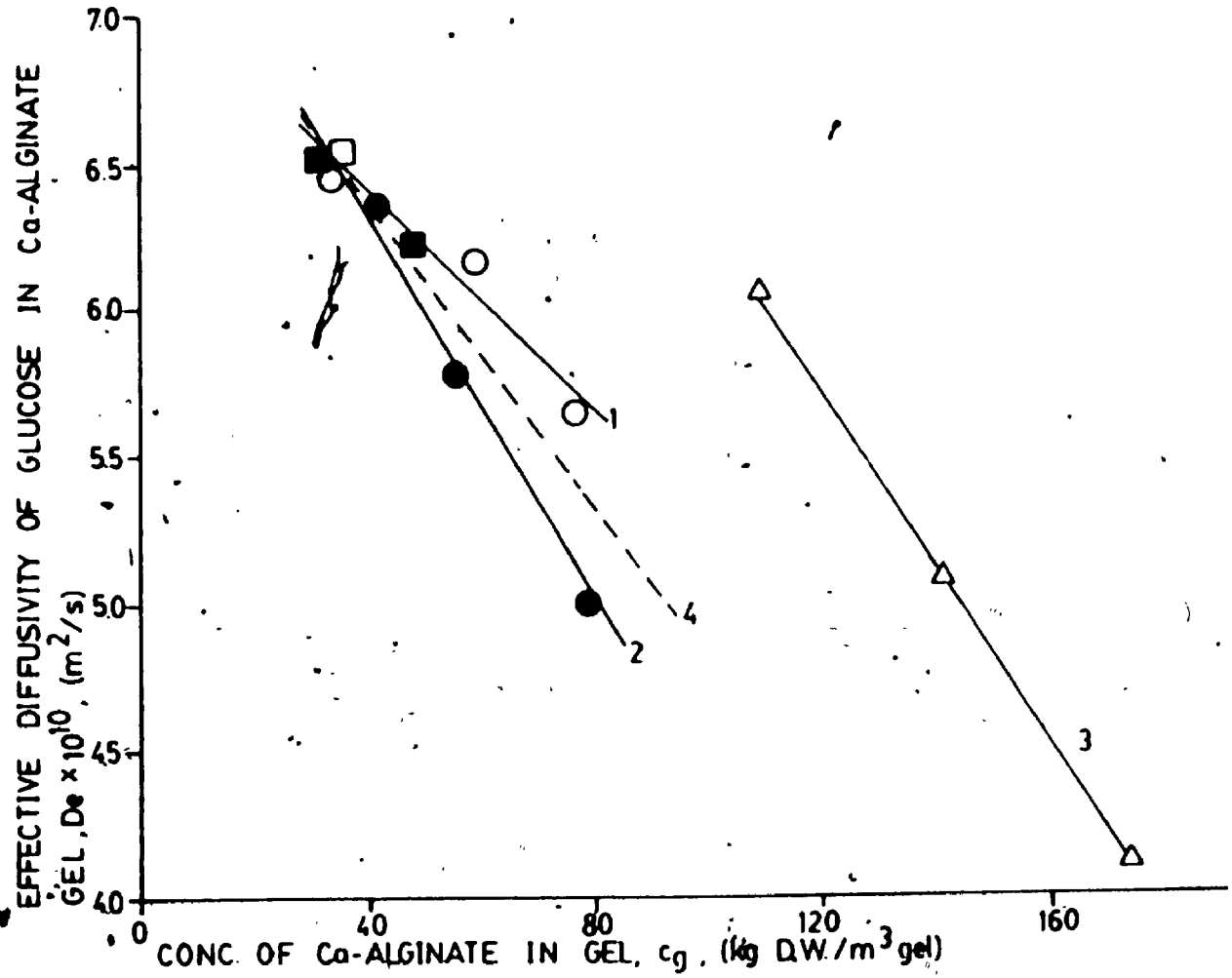
EFFECTIVE DIFFUSIVITY OF GLUCOSE IN Ca-ALGINATE GEL, De × 10^10, (m^2/s)
7.0
6.5
6.0
5.5
5.0
4.5
4.0
0
40
80
120
160
CONC. OF Ca-ALGINATE IN GEL, cg, (kg D.W./m^3 gel)
1
2
3
4

G-content was high (plot 2). This was evident at high concentrations of Ca-alginate, whereas at low concentrations (c_g < 50 $kg.m^{-3}$ of gel), differences in D_e values were not significant as shown by plots 1 and 2 in Figure 5.31.

Thus, for alginates with DP ranging from 1,200 to 3,000 (which are commonly used for cell immobilization) the effective diffusivity of glucose correlated well (r > 0.97) with the following linear equations. When G ≈ 70%,

$$D_e = (7.65 \times 10^{-10}) - (3.3 \times 10^{-12})c_g \qquad 5.48$$

and, when G ≈ 40%,

$$D_e = (7.17 \times 10^{-10}) - (1.9 \times 10^{-12})c_g \qquad 5.49$$

The best-fit linear equations are represented by plots 1 (Equation 5.49) and 2 (Equation 5.48) in Figure 5.31.

Alternatively, D_e values of glucose in Ca-alginate gels (1200 < D_e < 3000) could be estimated reasonably well using the following linear equation (plot 4, in Figure 5.31) when the guluronic acid content is between 40 to 70%. Thus,

$$D_e = (7.40 \times 10^{-10}) - (2.6 \times 10^{-12})c_g \qquad 5.50$$

in which the intercept (7.40×10^{-10} $m^2.s^{-1}$) is the effective diffusivity in the absence of the gel matrix (i.e. c_g = 0 kg. m^{-3}) and corresponds to the diffusivity of glucose in

water ($D = 7.30 \times 10^{-10}\ m^2.s^{-1}$). It must be noted that Equation 5.50 will over estimate the D_e values in high-G alginate gels and under estimate the corresponding values in low-G alginate gels. However, even at a Ca-alginate concentration of 80 $kg.m^{-3}$, the percentage error in either case was calculated to be less than 6%.

Tanaka et al. (1984) did not observe any difference in D_e values of glucose and other high molecular weight solutes (e.g. α - lactoalbumin, MW = 15,600) when the concentration of Na-alginate was increased from 20 to 40 $kg.\ m^{-3}$. However, Hannoun and Stephanopoulos (1986) reported a significant decrease in D_e values of glucose and ethanol when the concentration of Na-alginate was increased from 10 to 40 $kg.\ m^{-3}$. In other qualitative studies, slower diffusion rates of NAD, haemoglobin (Kierstan et al., 1982) and sucrose (Cheetham et al., 1979) have also been observed at higher concentrations of alginate in the gel.

As in the present study, lower D_e values with increase in gel concentration has also been reported by other workers. Thus, a linear decrease in D_e values of glucose, sucrose, oligosaccharides, and other low molecular weight solutes with increase in concentration of agar (Friedman, 1930b; Ackers and Steere, 1962; Belton and Wilson, 1982; Busk and Labuza, 1979), gelatin (Friedman and Krammer, 1930; Busk and Labuza, 1979), cellulose acetate (Klemm and Friedman, 1932), hydroxyethyl cellulose (Brown et al., 1976), carrageenan (Nguyen and Luong, 1986) and agarose (Belton and

Wilson, 1982) has also been observed. In highly cross-linked gels such as polyacrylamide and dextran, the D_e values of low molecular weight solutes decreased exponentially as a function of gel concentration (White and Dorion, 1961; Nakanishi et al., 1977; Brown and Johnsen, 1981b).

Increase in alginate concentration has also been reported to significantly alter the kinetic properties of entrapped viable and non-viable cells. For instance, Johansen and Flink (1986) observed lower rates of sucrose inversion by immobilized non-viable cells of Saccharomyces cerevisiae as the concentration of alginate was increased from 10 to 30 kg. m^{-3}. A three-fold increase (20 to 60 kg. m^{-3}) in alginate concentration also reduced the specific oxygen uptake rate by immobilized microbial cells (Gosman and Rehm, 1986). Similarly, the rate of glucose oxidation to gluconic acid by Ca-alginate entrapped cells of Gluconobacter oxydans decreased with increase in the concentration of the gel (Tramper et al., 1983).

Results presented in Figure 5.31 show that in alginate gels with DP = 1200 to 3000, the guluronic acid content, may, to a lesser extent, influence the rate of solute transport in gels with a high concentration of Ca-alginate. Thus, Kierstan et al. (1982) observed reduced effusion rates of haemoglobin from Ba-alginate gels as the guluronic acid content was increased. However, Johansen and Flink (1986) did not observe significant changes in the rates of sucrose inversion as the guluronic acid content was increased from

40 to 70%, when using dilute (20 kg. m^{-3}) Ca-alginate gels. Similarly, the release rates of NAD from Ba-alginate gels, containing different amounts of guluronic acid, did not vary appreciably (Kierstan et al., 1982).

Since Ca-alginate gels with high G-content do not significantly alter the D_e values of glucose and other low molecular weight solutes, such gels should be preferentially used for cell immobilization due to their superior mechanical stability characteristics (see Section 2.4.4).

Most correlations available in the literature, express the effective solute diffusivity as a function of the polymer volume fraction (λ) in the gel. The validity of these correlations (see Section 5.3.3) for estimating D_e values of glucose as a function of alginate volume fraction was therefore tested as shown in Figure 5.32.

The volume fraction of Ca-alginate in different types of gels was determined as described in Section 4.5 and the corresponding values are listed in Table C.3 (Appendix C). As shown in Figure 5.32, two distinct plots (#7 and #8), based on the experimental data, result when D_e is expressed in terms of the alginate volume fraction. Plot 7 refers to alginate gels with a high guluronic acid content whereas plot 8 represents alginates with a low G-content.

From Figure 5.32, it is apparent that the literature correlations (plotted as broken lines) given by plots #1 (Equation 5.34) #2 (Equation 5.36), #3 (Equation 5.37) and #4 (Equation 5.38) substantially over-estimate the D_e values of

Figure 5.32: Application of literature correlations for predicting D_e values as a function of alginate volume fraction in the gel [(——), experimental results; (---), literature correlations, symbols are the same as in Figure 5.31; see text for explanation of each plot].

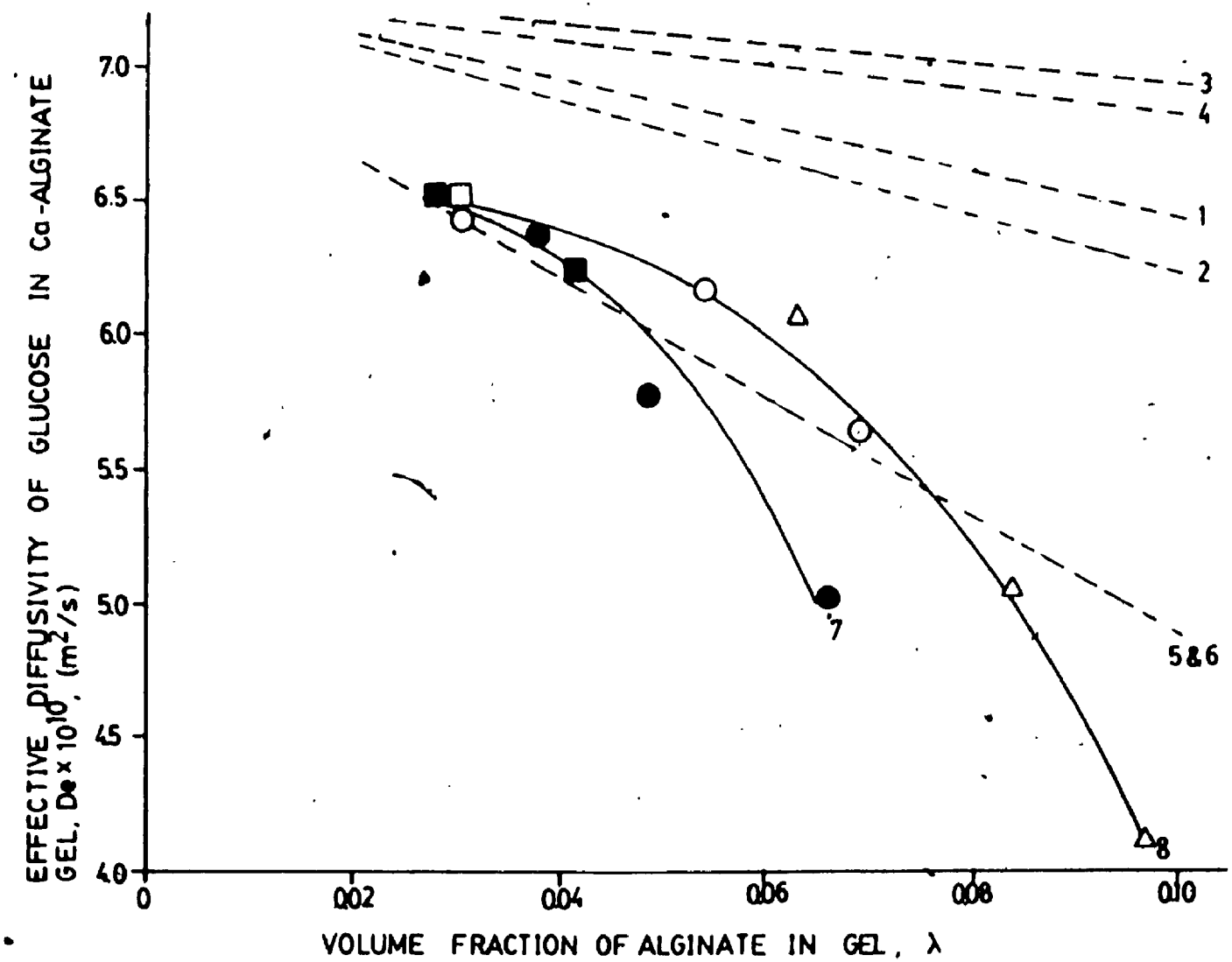
EFFECTIVE DIFFUSIVITY OF GLUCOSE IN Ca-ALGINATE GEL, De x 10^10, (m^2/s)
7.0
6.5
6.0
5.5
5.0
4.5
4.0
0
0.02
0.04
0.06
0.08
0.10
VOLUME FRACTION OF ALGINATE IN GEL, λ
1
2
3
4
5&6
7
8

glucose especially at high volume fractions of the alginate polymer. Plots 5 and 6, representing Equations 5.35 (Mackie and Meares, 1955) and 5.39 (Klein and Schara, 1981) appear to give better estimates of D_e. However, the experimental D_e values (plot 7 and 8) deviate substantially from all the predicted curves (at high λ) indicating that the obstruction effect (or tortuosity, on which all the above correlations are based) may not be the only factor responsible for reduced diffusional rates at high concentrations of the alginate polymer. Thus, at high alginate concentrations, the influence of hydrodynamic drag may be significant, due to reduced pore sizes.

Using Equation 5.45 (Renkin, 1954) and from known values of D_e/D (Table C.3) the mean pore diameter in different alginate gels was estimated and the values plotted as a function of alginate concentration in Figure 5.33 (plots 1, 2 and 3).

For alginates with 1200 < DP < 3000 and a G-content of 40 to 70%, the best-fit correlation (plot 4 in Figure 5.33) could be expressed by Equation 5.51 ($r > 0.95$)

$$d_p = 37.3 - 0.35\, c_g \qquad 5.51$$

Thus, for a Ca-alginate concentration range of 30 to 80 kg/m^3 of gel, the mean pore diameter decreases from 28 to 8 nm. Using size-exclusion chromatography Klein et al. (1983) estimated the mean pore diameter in various Ca-alginate gels

Figure 5.33: Estimated mean pore diameter plotted as a function of Ca-alginate concentration. (Symbols are the same as in Figure 5.31; see text for explanation of each plot).

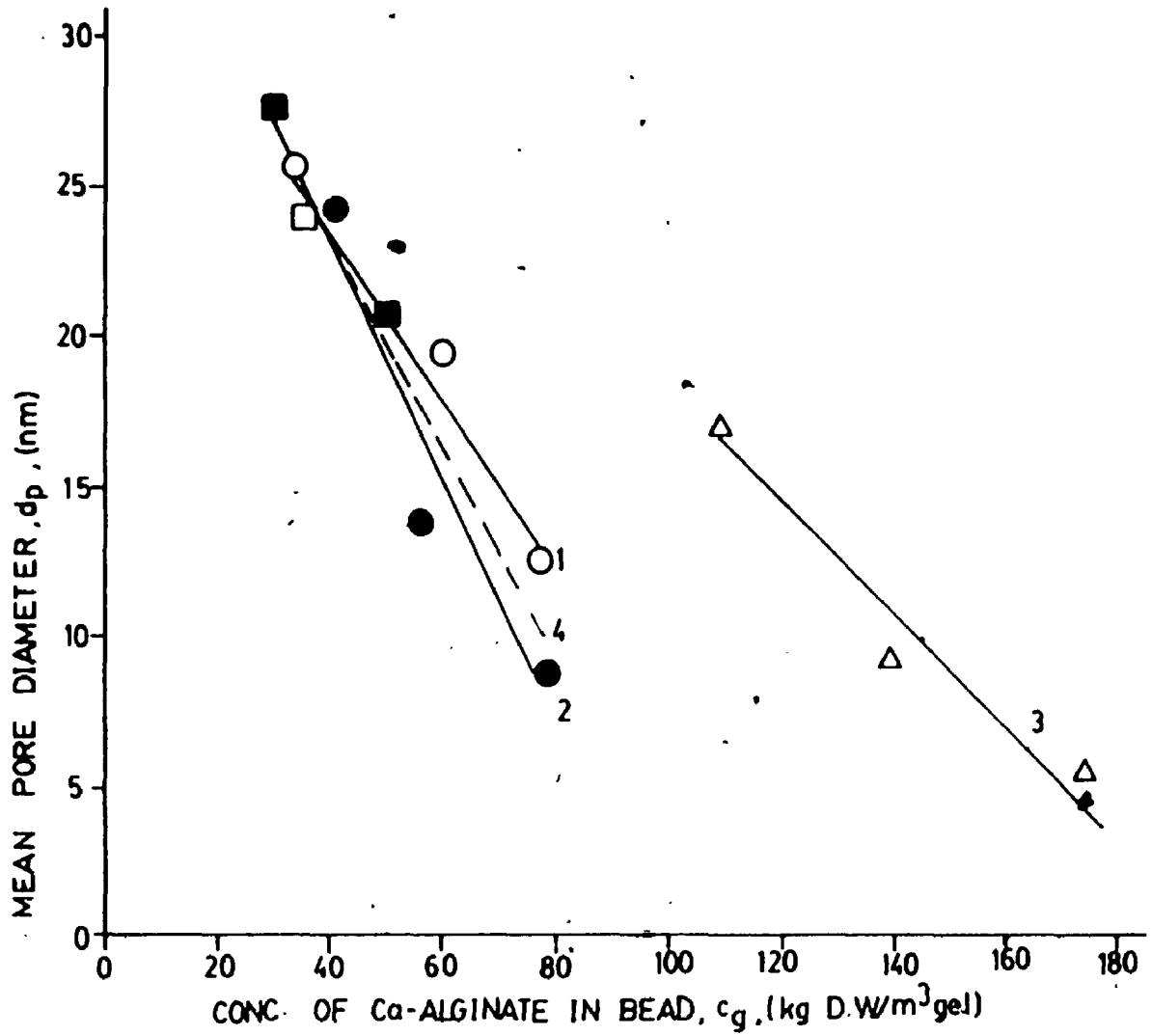
MEAN PORE DIAMETER, d_p, (nm)
30
25
20
15
10
5
0
0
20
40
60
80
100
120
140
160
180
CONC. OF Ca-ALGINATE IN BEAD, c_g, (kg D.W/m^{3}gel)
1
2
3
4

(prepared from different types and concentrations of Na-alginate solutions) to range from 7 to 17nm. The pore sizes estimated in this study using diffusivity data (i.e. D_e/D values of glucose) agree very well with the experimentally measured values of Klein et al. (1983). Thus, the correlation presented above (Equation 5.51) may be used to estimate pore sizes in Ca-alginate gels provided that the polymer concentration in the gel (c_g) is known.

Furthermore, if the size of the diffusing species is known, then by using the Renkin equation (Equation 5.45) or Figure 5.26, the corresponding D_e/D value may be determined enabling one to obtain a useful 1st estimate of the effective diffusivity of a given solute in Ca-alginate gel.

Studies reported in Sections 5.3.4 and 5.3.5 indicate that the diffusivity of glucose (and other solutes) in Ca-alginate gels vary appreciably with the type and concentration of both, the chelating agent and Na-alginate. In the rationale selection of the most suitable alginate entrapment matrix, consideration should also be given to other parameters (see Chapter 2) such as the mechanical stability of the gel, toxicity of the chelating agent used etc., in addition to the diffusivity characteristics of the substrate and product into and out of the immobilization matrix.

5.4 Effective Diffusivity of Glucose in Ca-alginate Beads Containing Entrapped Yeast Cells

As described in Sections 4.3.2 and 4.3.3, viable and non-viable yeast cells were entrapped in Ca-alginate beads using a 20 kg. m^{-3} solution of Na-alginate (sample #17, Fisher Chemicals) and a 40 kg. m^{-3} $CaCl_2$ solution as the gelling agent. Unless otherwise stated, all D_e values were determined at 30°C. The initial 'cold' glucose concentration was kept constant at 20 kg. m^{-3}.

5.4.1 Effect of Entrapped Yeast Cell Concentration

The partition coefficients and effective diffusivity of glucose (D_e) were determined in Ca-alginate beads containing five different concentrations of non-viable yeast cells. The results are summarized in Table C.4 (Appendix) and plotted in Figures 5.34 and 5.35. The actual concentration of yeast cells within the Ca-alginate matrix (c_x) was determined as described in Section 4.6 and expressed in terms of kg D.W cells/m^3 of gel.

Figure 5.34 shows that the partition coefficient of glucose decreased as a linear function of yeast cell concentration and correlated well ($r > 0.97$) with the following equation

$$K_p = 0.983 - (6.63 \times 10^{-4})\, c_x \qquad 5.51$$

Figure 5.34: Effect of entrapped yeast cell concentration on the partition coefficient of glucose

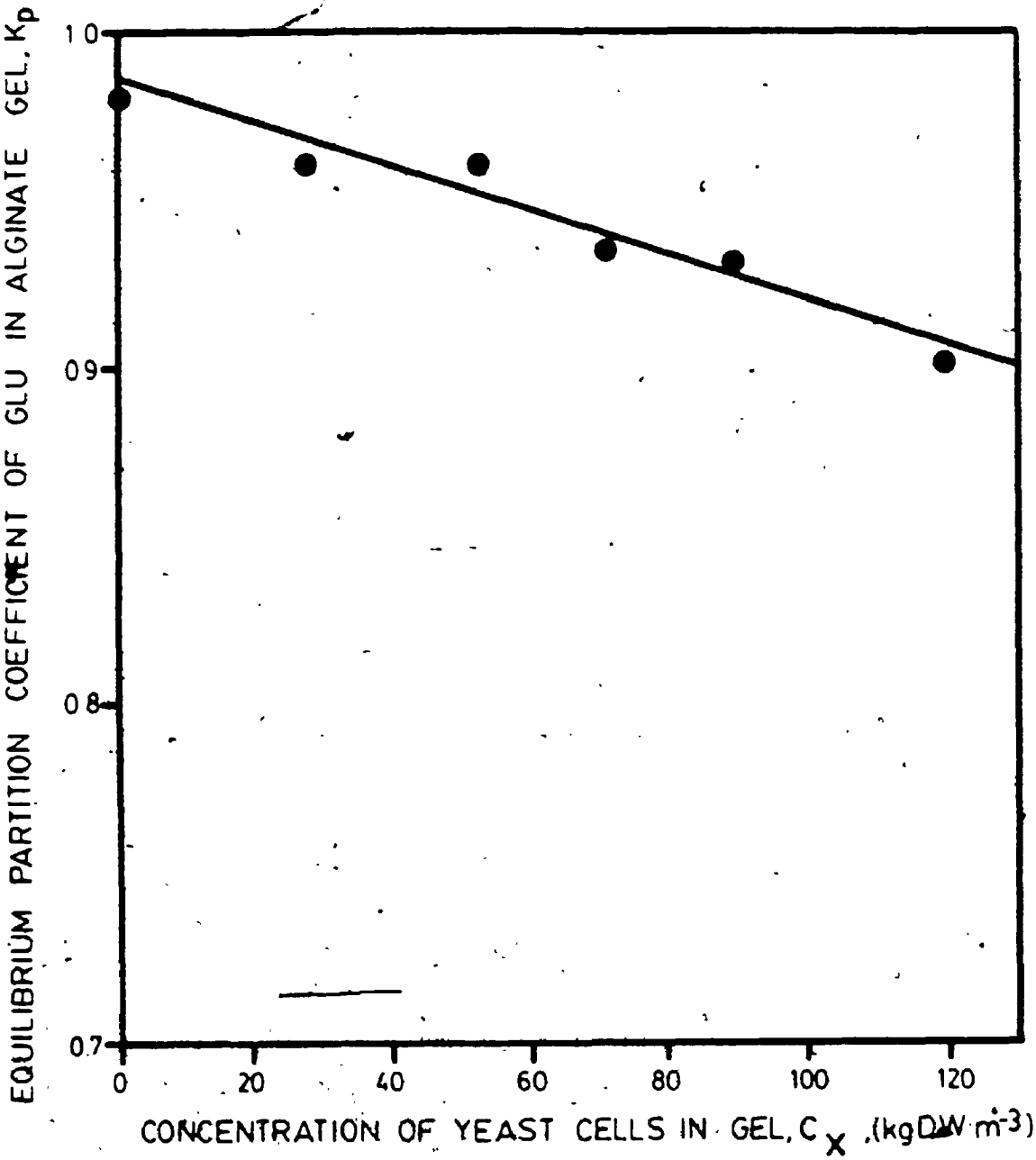
EQUILIBRIUM PARTITION COEFFICIENT OF GLU IN ALGINATE GEL, K_p
1.0
0.9
0.8
0.7
0
20
40
60
80
100
120
CONCENTRATION OF YEAST CELLS IN GEL, C_X ,(kgDW m^{-3})

Figure 5.35: Effect of entrapped yeast cell concentration on the effective diffusivity of glucose (●, experimental values, ——, best fit linear relationship given by Equation 5.52, ---, literature correlations as described in the text)

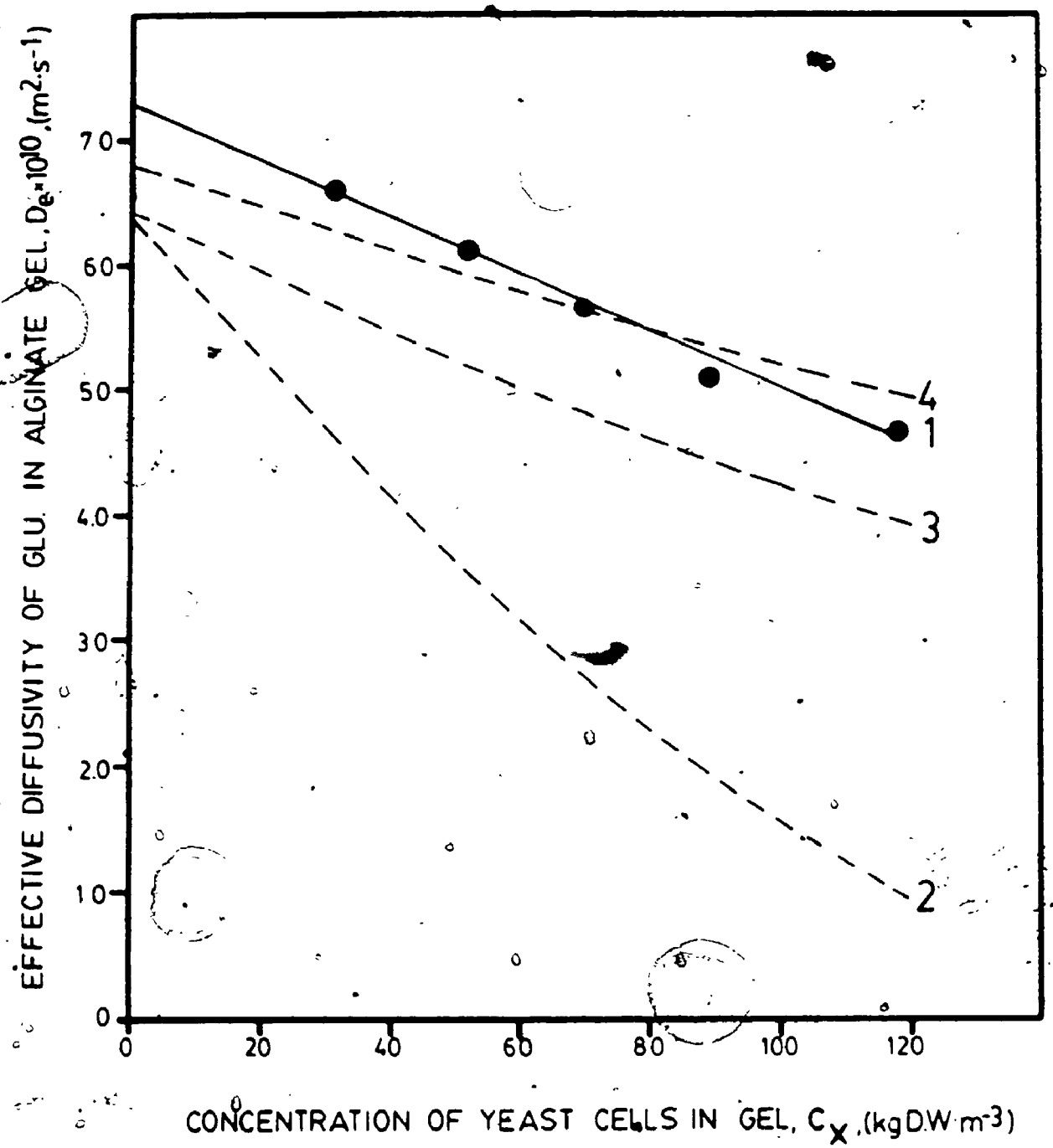
EFFECTIVE DIFFUSIVITY OF GLU. IN ALGINATE GEL, $D_e \cdot 10^{10}$, ($m^2 \cdot s^{-1}$)
0
1.0
2.0
3.0
4.0
5.0
6.0
7.0
0
20
40
60
80
100
120
CONCENTRATION OF YEAST CELLS IN GEL, C_X, (kg D.W. m^{-3})
1
2
3
4

Partition coefficients of less than unity indicate that the glucose molecule is not preferentially adsorbed by Ca-alginate beads containing entrapped yeast cells. Decrease in K_p values with increase in cell concentration may be attributed to a reduction in accessible gel-volume (i.e. decrease in the void fraction, ε).

As shown in Figure 5.35, with increase in cell concentration, the effective diffusivity of glucose decreases, and the relationship (shown as plot 1 in Figure 5.35) can be expressed by the following linear equation ($r > 0.98$)

$$D_e = (7.25 \times 10^{-10}) - (2.25 \times 10^{-12})\, c_x \qquad 5.52$$

In Equation 5.52, the intercept (7.25×10^{-10} $m^2.s^{-1}$) corresponds to the free-phase diffusivity of glucose (7.30×10^{-10} $m^2.s^{-1}$) at the same temperature (30°C) and glucose concentration (20 $kg.\ m^{-3}$).

Furui et al. (1985) also observed a linear decrease in D_e values of ammonium-fumarate diffusing in polyacrylamide and κ-carrageenan gels, as the concentration of entrapped E. coli cells was increased. In other studies the D_e values of glucose in polyacryamide gel containing non-viable cells of Streptomyces sp. (Taguchi et al., 1975), and that of L-tryptophan in chitosan gel with entrapped E. coli cells (Vorlop and Klein, 1983), also decreased with increase in entrapped cell concentration.

With the exception of the present study, no attempt has

as yet been made to correlate the D_e values of glucose or other solutes as a function of entrapped cell concentration in alginate gels. D_e values lower than the corresponding free phase diffusivities have however been reported for diffusion of sucrose and yohimbine in Ca-alginate beads containing entrapped plant cells (Pu and Yang, 1986). Cheetham et al. (1979) observed slower rates of sucrose transport in Ca-alginate beads when non-viable cells were entrapped within the gel matrix whereas Hiemstra et al., (1983) reported that the effective diffusivity of oxygen in Ba-alginate gels (containing Hansenula polymorpha cells) was only 25% of that in water.

In a recent study, Hannoun and Stephanopoulos (1986) did not observe any changes in the D_e values of glucose and ethanol when a low concentration of non-viable yeast cells was entrapped in Ca-alginate membranes. Due to problems associated with gel-rupture when using the conventional diffusion cell, Hannoun and Stephanopoulos (1986) could not study the diffusivity characteristics of glucose and ethanol in Ca-alginate gel at higher cell concentrations.

However, with highly cross-linked gels such as polyacrylamide, the conventional diffusion cell has been used with some success for measuring D_e values of phenol over a wide range of polymer volume fractions and cell loadings (Klein and Schara, 1981). Thus, Klein and co-workers, (Klein and Schara, 1981; Klein and Manecke, 1982) suggested the following correlations (Equations 5.53 and 5.54) for

estimating D_e values as a function of either entrapped cell concentration (X) or volume fraction of cells (β)

$$D_e = D.(1 - X)^2 \exp(-4\lambda) \qquad 5.53$$

and

$$D_e = D. \exp[-4(\lambda + \beta)] \qquad 5.54$$

where X is concentration of cells (in kg wet weight per litre) and β is the volume fraction of entrapped cells defined by Equation 4.12, and '4' is constant for low molecular weight solutes such as glucose.

The validity of these correlations for estimating D_e values of glucose in Ca-alginate gels was examined. In applying the above equations, the volume fraction of alginate (λ) was determined to be 0.033 (± 0.004) whereas the volume fraction of yeast cells (β) was calculated as described in Section 4.6. The concentration of entrapped yeast cells on a wet weight basis (i.e. X kg wet weight/litre of gel) was estimated by assuming a water content of 80% in the yeast cells (Bailey and Ollis, 1977). The values of X and β used in the above correlations are listed in Table C.4 (Appendix).

The D_e values of glucose calculated by using Equations 5.53 and 5.54 are respectively represented by plots 2 and 3 in Figure 5.35. Thus, Equation 5.53 does not appear to be

suitable at all for estimating D_e values of glucose in Ca-alginate entrapment matrix, whereas Equation 5.54 gives more reliable estimates of D_e.

The exponential constant "a = 4", has been selected by Klein and co-workers as a convenient factor, and is based on correlation studies using highly cross-linked gels such as chitosan (Klein and Manecke, 1982) and polyacrylamide (Klein and Schara, 1981). This constant may therefore not only depend on the solute molecular weight but also on the type of immobilization matrix used. For instance, if the exponential constant in Equation 5.54 is taken to be 2.5 instead of 4, then the estimated D_e values (plot #4 in Figure 5.35) agree very well with the experimental data for diffufusion of glucose in Ca-alginate gel.

Several studies conducted to determine the diffusivity characteristics of various solutes including, oxygen (Mueller et al., 1966; Yano et al., 1961; Ngian and Lin, 1976; Bungay et al., 1969; Williamson and McCarty, 1976), glucose (Matson and Characklis, 1976; Onuma et al., 1985), sucrose (Dibdin, 1981); and inulin (Takevossian, 1979) through microbial films and aggregates have also reported D_e/D values of less than unity. Furthermore, in several of the studies mentioned above, decrease in D_e values with increase in cell densities has been observed.

Based on the work reported in this section, and data provided by other workers, one might anticipate reduced specific reaction rates at sufficiently high concentrations

of entrapped cells. Thus, beyond a critical entrapped cell concentration, the intraparticle mass transfer resistance becomes the rate limiting-step in the overall reaction-rate process (Johansen and Flink, 1986; Gosmann and Rehm, 1986; Hiemstra et al., 1983).

In addition to cell concentration it is believed that the type of microbial cell and its structure may also influence the diffusivity characteristics of a given solute (Matson and Characklis, 1976). For instance, Pu and Yang (1986) recently reported that the effective diffusivity of sucrose depended on the size of plant cells entrapped in Ca-alginate beads.

Another parameter that may affect the diffusivity characteristics of a gel-entrapped cell system, is the production and excretion of extracellular polysaccharides which may further reduce the D_e values of a solute (Bailey and Ollis, 1977). Thus, Matson and Characklis (1976) reported that by varying the sluge age and carbon-nitrogen ratio in growth media, the diffusivity values of glucose in microbial aggregates changed from 30 to 50% of its value in water. Low D_e values were observed when a high C/N ratio (and high glucose concentration) was used in the growth media which is also known to enhance the biosynthesis of extracellular polysaccharides.

5.4.2 Effect of Temperature

The influence of temperature, on the effective diffusivity of glucose in Ca-alginate beads containing non-viable yeast cells, was studied at temperatures of 20, 30, 40, and 50°C with a constant entrapped cell concentration of 118 kg D.W/m^3 of gel.

As shown in Figure 5.36, the D_e values increase exponentially with temperature and can be represented by the Arrhenius relationship plotted in Figure 5.37. Using non-linear regression analysis and the least-squares method, the Arrhenius pre-exponential constant (A_g) and activation energy (E_{ag}) for diffusion of glucose in Ca-alginate beads containing entrapped yeast cells were respectively calculated to be 2.17×10^{-6} $m^2.s^{-1}$ and 21.10 kJ. mol^{-1}. Thus, the influence of temperature on D_e values can be estimated using the following Arrhenius equation.

$$D_e = 2.17 \times 10^{-6} \exp(-20.1/\bar{R}T) \qquad 5.55$$

The Arrhenius parameters (A_g and E_{ag}) for diffusion of glucose in Ca-alginate gel with entrapped yeast cells are comparable to the corresponding values in cell-free Ca-alginate gel (i.e. $A_g = 3.15 \times 10^{-6}$ $m^2.s^{-1}$ and $E_{ag} = 21.37$ kJ. mol^{-1}). Furthermore, as in the case of cell-free Ca-alginate gel (see Section 5.3.1.1), the activation energy for diffusion of glucose in Ca-alginate beads with entrapped

Figure 5.36: Effect of temperature on the effective diffusivity of glucose in Ca-alginate gel containing non-viable yeast cells at a concentration of 118 kg D.W./m^3 of gel.

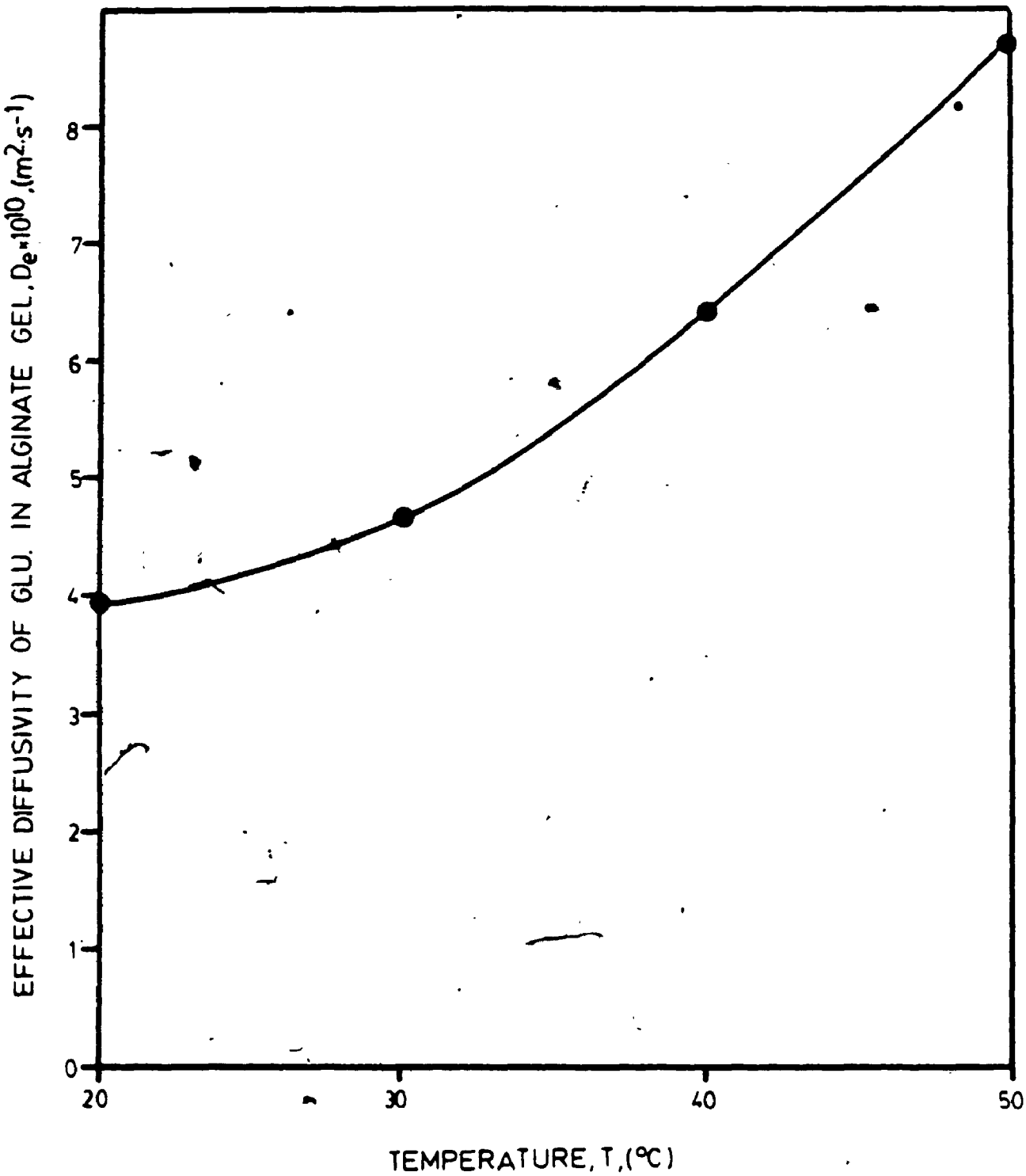
EFFECTIVE DIFFUSIVITY OF GLU. IN ALGINATE GEL, $D_e \times 10^{10}$, $(m^2 \cdot s^{-1})$
0
1
2
3
4
5
6
7
8
20
30
40
50
TEMPERATURE, T, (°C)

Figure 5.37: The Arrhenius plot used to determine the activation energy for diffusion of glucose in entrapped yeast cell Ca-alginate beads (c_g = 118 kg D.W./m^3 gel).

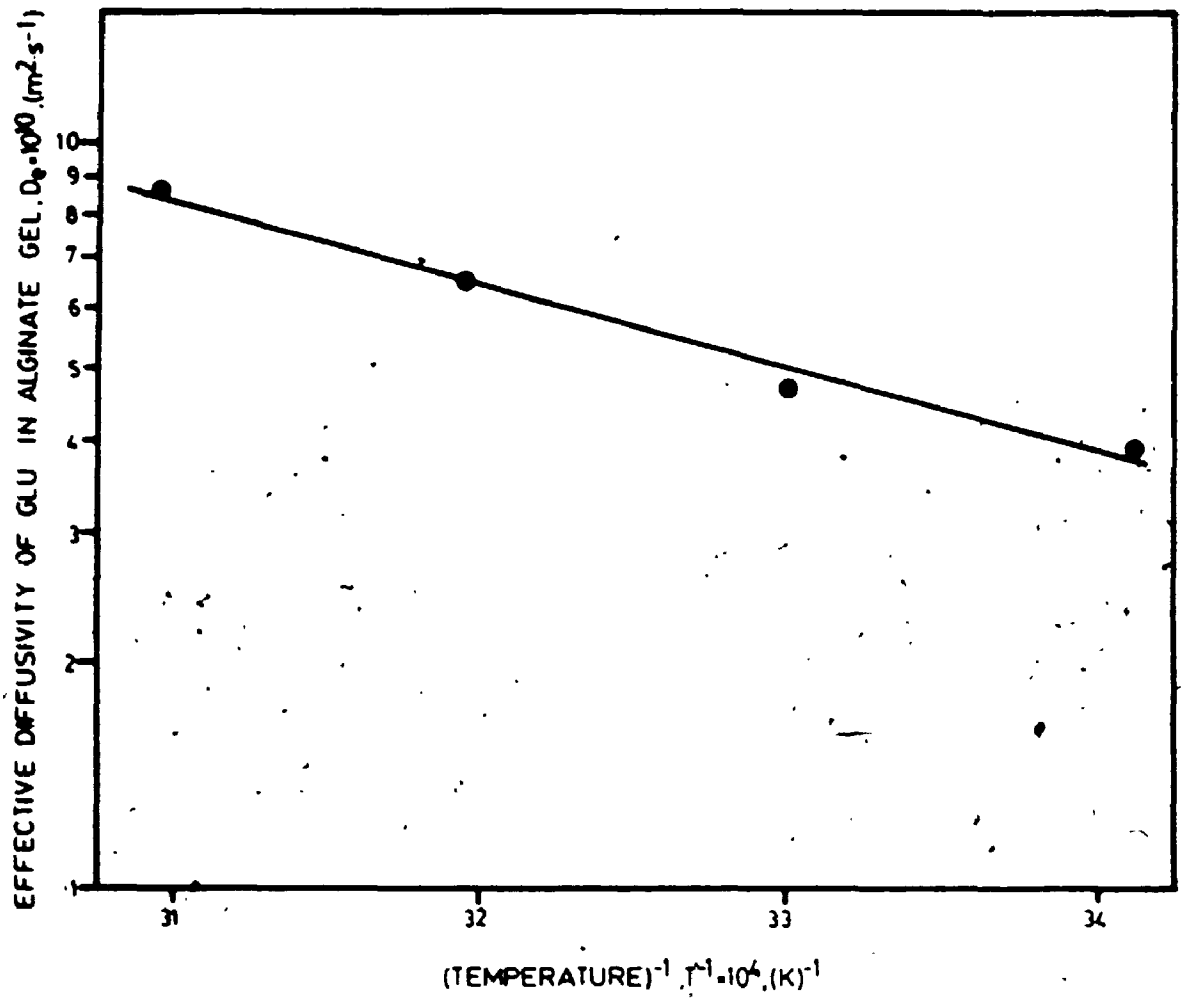
EFFECTIVE DIFFUSIVITY OF GLU IN ALGINATE GEL. $D_e \cdot 10^{10}$ ($m^2 \cdot s^{-1}$)
10
9
8
7
6
5
4
3
2
1
31
32
33
34
(TEMPERATURE)$^{-1}$, $T^{-1} \cdot 10^4$, $(K)^{-1}$

yeast cells does not differ substantially from the corresponding value in water (ΔE = 2.0 kJ. mol^{-1}).

Based on the diffusivity data presented by Taguchi et al. (1975) the Arrhenius parameters E_{ag} and A_g, for diffusion of glucose in polyacrylamide gel containing non-viable cells of Streptomyces sp. were calculated to be 26.7 kJ. mol^{-1} and 7.7 x 10^{-6} $m^2.s^{-1}$, respectively. These parameters are based on diffusivity values determined at temperatures of 50 to 70°C with a glucose concentration of 180 kg. m^{-3}. The corresponding values of E_a and A for diffusion of glucose in water when C_o = 180 kg. m^{-3}, were calculated (using Equations 5.13 and 5.15) to be 20.74 kJ. mol^{-1} and 2.13 x 10^{-6} $m^2.s^{-1}$, respectively. Thus, with a highly cross-linked gel such as polyacrylamide, the ΔE value is only 5.96 kJ. mol^{-1} even if non-viable cells of Streptomyces sp. are entrapped within the gel matrix.

An exponential increase in D_e values of glucose and oxygen, diffusing in microbial aggregates has also been reported by Onuma et al., 1985. Furui and Yamashita (1985) observed that the temperature dependent increase in diffusivity values of amino acids in κ-carrageenan and polyacrylamide containing non-viable bacterial cells could be expressed by the Arrhenius equation, however, no attempt was made to evaluate the relevant parameters.

5.4.3 Effective Diffusivity of 3-0-Methyl Glucose in Ca-Alginate Beads with Entrapped Viable Yeast Cells

The effective diffusivity of a non-metabolizable analogue of glucose, 3-0-methyl glucose, was determined as described in Section 5.1.4 except that viable yeast cells were entrapped within the Ca-alginate matrix. The entrapped cell concentration was 106.4 kg/m^3 of gel, and the K_p and D_e values were evaluated to be 0.93 and 4.60×10^{-10} $m^2.s^{-1}$, respectively.

In the case of non-viable yeast cells, the D_e value at a cell concentration of 106.4 kg/m^3 of gel, was calculated (using the best-fit linear relationship given by Equation 5.52) to be 4.86×10^{-10} $m^2.s^{-1}$, which is only slightly higher (by about 6%) than the corresponding value obtained with viable yeast cells. The correlations developed in this section (Equations 5.52 and 5.55) may therefore also be used to give reliable estimates of D_e values of glucose in Ca-alginate gel containing viable yeast cells.

Pu and Yang (1986) reported higher D_e values of yohimbine when apple cells were permeabilized with a 2% (v/v) solution of dimethyl sulfoxide (DMSO) prior to entrapment in Ca-alginate gel. However, with sucrose as the diffusing species, increases in D_e values were not as significant.

In general, the lower D_e values of glucose in Ca-alginate beads containing viable or non-viable yeast cells

when compared to that in a cell-free matrix, may be attributed to the blockage (Bailliez et al., 1985) of pores in the gel matrix by entrapped yeast cells, and thereby introducing steric contraints for solute transport.

CHAPTER 6

CONCLUSIONS AND RECOMMENDATIONS

The novel radiotracer diffusivity measurement technique developed in this study, allows conditions of near ideal mixing and negligible film mass transfer resistance to be achieved and at the same time retain the structural integrity of the alginate gel even at high cell-loadings. Additionally, both, partition coefficients, K_p and effective diffusivities, D_e, can be accurately ($\pm$ 2 to 3%) determined from the same experiment. Furthermore, the simple design of the novel diffusion apparatus requires only small volumes of the liquid phase to be used, which in turn facilitates the economical use of radiotracer analytical techniques. The latter allows ease and accuracy in rapidly measuring solute concentration changes in the liquid phase.

Although the exact solutions used to evaluate D_e are mathematically cumbersome and require suitable optimization computer programs, it was shown that Lee's approximate analytical solution (Lee, 1980b) gave extremely reliable estimates of D_e values.

Two correlations (Equation 5.17 and 5.24) were developed to accurately predict the free-phase diffusivities, D, of glucose in water. These correlations were capable of accurately predicting D values of glucose in water at temperatures of 20 to 50°C over a glucose concentration range of 0-500 kg. m^{-3}, which facilitated comparison of the

effective diffusivity values with the corresponding values in water. It is anticipated that these correlations will have wider applications for predicting the mass transfer characteristics of hexoses in fermentation media.

The effect of temperature on the D_e values of glucose in Ca-alginate beads, with or without entrapped yeast cells, showed an Arrhenius relationship. The activation energy for diffusion of glucose, in cell-free or entrapped-cell, Ca-alginate beads, was approximately 2.0 $kJ.mol^{-1}$ higher than that for diffusion of glucose in water.

It must be stressed that when measuring D_e values, the glucose concentration, and consequently, D_e, does not remain constant, as was assumed in applying the model equations. The D_e values determined were therefore designated as being only average values. From the results obtained in this study, the average D_e values in cell-free Ca-alginate gel increases exponentially as a function of glucose concentration.

Amongst the various literature correlations tested, those proposed by Ogston (1958), Klein and Schara (1981), and, Mackie and Meares (1955) gave reasonable estimates of D_e values in a variety of cell-free, dilute Ca-alginate beads, at temperatures of 20 to 50°C and glucose concentrations of 3 to 300 $kg.m^{-3}$. At higher concentrations of gel, these correlations were not valid, indicating that hydrodynamic drag effects on the glucose molecule become more significant as the gel concentration is increased. Thus,

using the pore-diffusion model, the diameter of the pores in Ca-alginate gels was estimated to vary from 8 to 35 nm, depending on the type and concentration of Ca-alginate. These values were comparable to the experimental values reported in the literature.

The D_e values were also found to depend on the type and concentration of the chelating agent used, whereas the effect of guluronic acid content on D_e values was not readily apparent at low alginate concentrations. In view of the latter observation, entrapment matrices should be prepared using alginates with a high guluronic acid content due to their superior mechanical stability characteristics. However, this cannot be generalized for higher molecular weight substrates.

An increase in entrapped cell concentration resulted in a linear decrease in D_e values as predicted by Equation 5.52. Unlike conventional diffusion-diaphragm cells, the Ca-alginate bead retained its spherical shape and structural integrity even at high yeast cell loadings at 118 kg. dry weight/m^{-3} of gel.

Thus in the rationale selection of a suitable method for cell immobilization in alginate gels, consideration should be given to the type and concentration of both, the chelating agent and alginate as well as the concentration of entrapped cells. In each of these cases, an increase in the concentration of one or more components will result in a decrease in D_e values. However, by increasing the alginate

and/or chelating agent concentration, the mechanical stability of the matrix will improve, whereas, when the entrapped cell concentration, is increased, the reverse is true. Furthermore, the specific rates of reaction decline with increase in concentration of each of these three components. Consequently, for any given alginate-entrapped cell bioreactor system, it is important to select the appropriate type and concentration of chelating agent and alginate, and entrapped cell concentration in order to achieve an optimum balance in terms of good mass transfer characteristics, minimal toxicity to cell components and long-term mechanical stability of the matrix.

The following recommendations are offered as possible areas for future research, which should enhance understanding of the intraparticle mass-transfer phenomenon in alginate and other entrapment matrices:

(i) Molecular weight dependence on the diffusivity characteristics of a homologous series of compounds should be studied in cell-free and entrapped-cell alginate gels.

(ii) The influence of hardening procedures such as glutaraldehyde treatment, and other stabilizing agents on the diffusivity characteristics of alginate gels should be examined.

(iii) With the use of radio-labelled probe solutes, the presence of other fermentation media components on the diffusivity characteristics of the labelled compound can be studied.

(iv) The diffusivity characteristics of alginate gels containing different types and concentrations of either bacterial, fungal, mammalian or plant cells needs extensive study due to the wide-scale applications of alginate gels in various biological processes.

(v) For a given type of immobilized cell system the influence of cell age, permeabilization of cell wall and composition of growth media (i.e. different C/N ratios) used to cultivate the cells prior to cell immobilization may also be examined.

APPENDIX A

Estimation Of The Average Molecular Weights Of Different Types Of Sodium Alginates Using Literature Data And Viscosity Measurements (see Section 4.2 for details)

Figure A.1: The relative viscosity (μ_r) at 20°C, of Na-alginate solutions of varying concentrations (c) in 0.1 M NaCl for samples with different values of intrinsic viscosity, [μ] (From, Haug and Smidsrod, 1962).

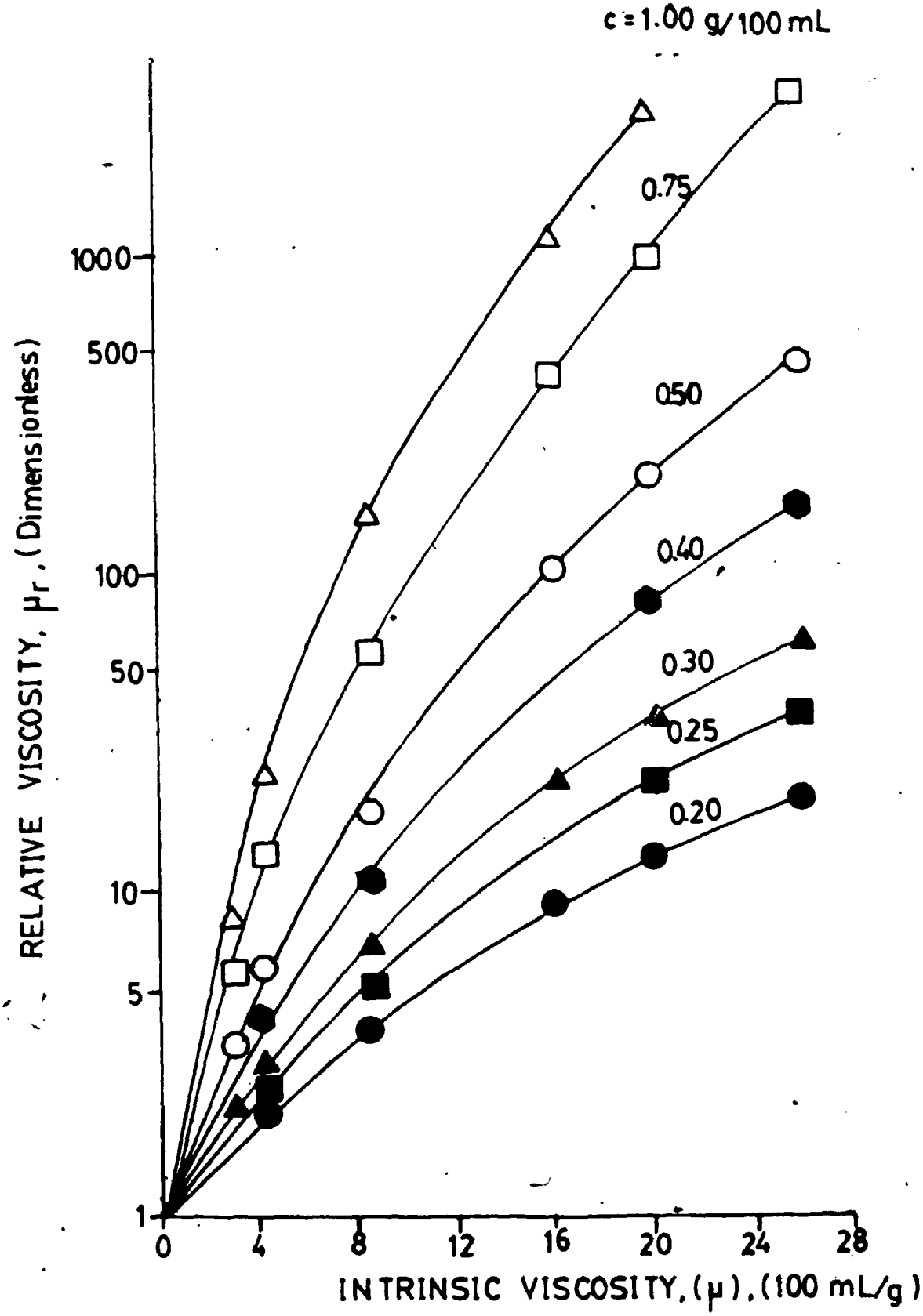
c = 1.00 g/100 mL
0.75
0.50
0.40
0.30
0.25
0.20
1000
500
100
50
10
5
1
0
4
8
12
16
20
24
28
RELATIVE VISCOSITY, μr, (Dimensionless)
INTRINSIC VISCOSITY, (μ), (100 mL/g)

Table A.1: Correlating the Influence of Polymer Concentration (c) and Intrinsic Viscosity ($[\mu]$) on the Specific Viscosity (μ_{sp}) of Dilute Na-Alginate Solutions (Based on the data of Haug and Smidsrod, 1962).

$[\mu]_{exp}$ (100mL/g)	Experimental values of μ_{sp}/c at different concentrations of Na-alginate, (100mL/g)							Non-Linear regression analysis,** $\mu_{sp}/c = [\mu]_{pred} \cdot e^{bc}$		
	Conc. of Na-alginate*, c, (g D.W./100mL)							$[\mu]_{pred}$ (100mL/g)	b (100mL/g)	Coefficient of determination r^2
	0.2	0.25	0.30	0.40	0.50	0.75	1.00			
4.2	5.5	6.0	6.7	7.5	9.6	16	23	3.8	1.84	0.9952
8.4	14	16	19	25	34	72	149	7.8	2.97	0.9999
16	40	-	70	-	198	532	-	16.7	4.70	0.9939
20	55	84	113	198	398	1265	-	20.1	5.66	0.9921
26	95	140	210	398	898	4265	-	25.4	6.92	0.9978

* Dilute Na-alginate solution prepared in aqueous 0.1 M NaCl

** The regression coefficients, $[\mu]_{pred}$ and b, were obtained by fitting the experimental data to the model equation using the least-squares method.

Figure A.2: The regression coefficient, b, (●) of Equation 4.5, plotted as a function of the intrinsic viscosity, [μ], to give a linear relationship (—) expressed by Equation 4.6.

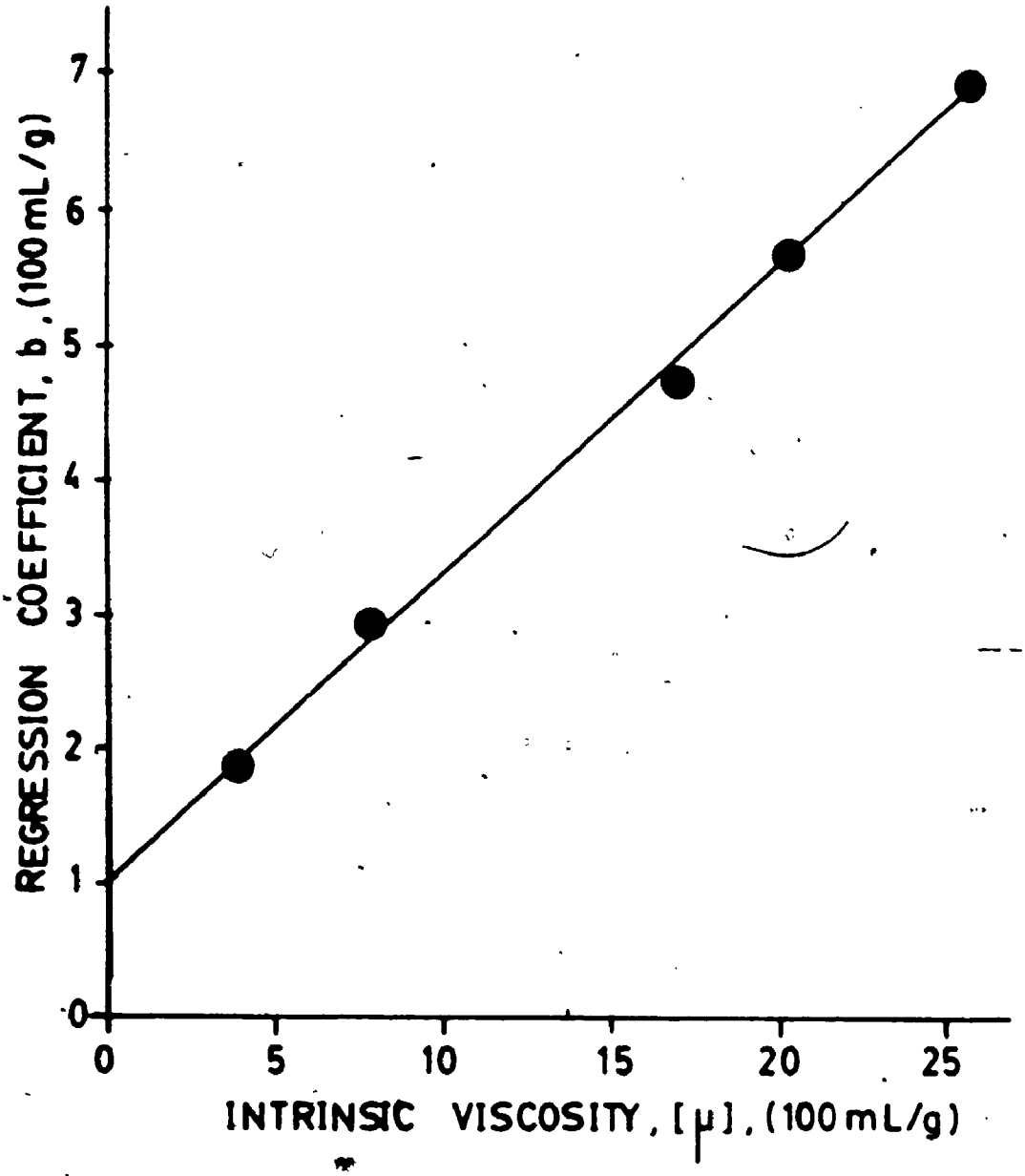
REGRESSION COEFFICIENT, b, (100 mL/g)
0
1
2
3
4
5
6
7
0
5
10
15
20
25
INTRINSIC VISCOSITY, [μ], (100 mL/g)

Figure A.3: Correlating the influence of concentration (c) and intrinsic viscosity (■, 4.2; ▲, 8.4; ●, 16; ●, 20; □, 26 [100mL/g]) on the specific viscosity of dilute Na-alginate solutions; (—) represents the best fit exponential relationship (Equation 4.7), and the symbols represent experimental data of Haug and Smidsrod, (1962).

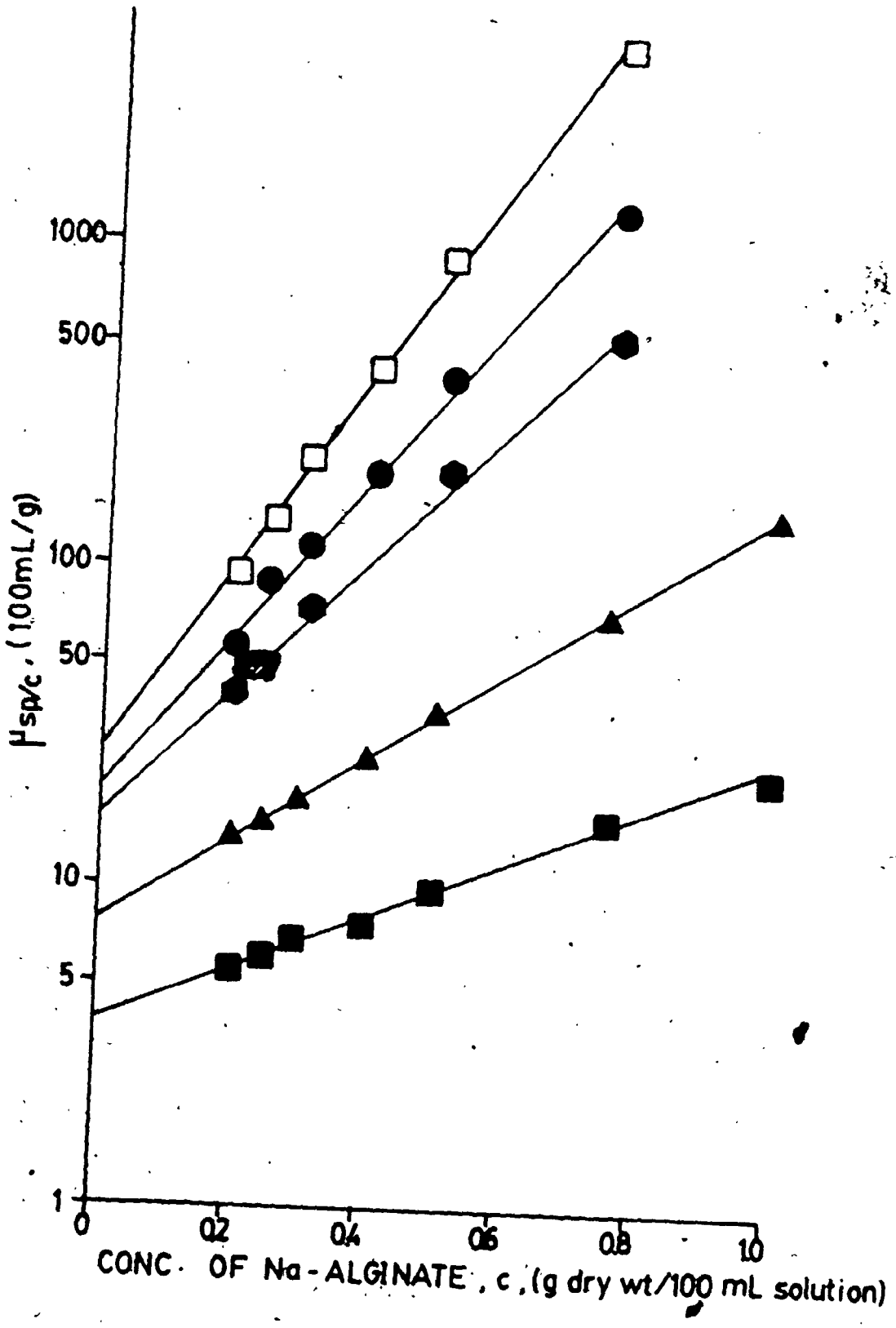
1000
500
100
50
10
5
1
μ_{sp}/c, (100mL/g)
0
0.2
0.4
0.6
0.8
1.0
CONC. OF Na-ALGINATE, c, (g dry wt/100 mL solution)

Figure A.4: Shear rate calibration of the Brookfield Synchro-Lectric Viscometer, (Model LVT) as a function of spindle rotational speed using different spindle sizes

■, spindle #1, R_c = 0.942 cm; L_c = 6.5 cm;

▲, spindle #2, R_c = 0.513 cm, L_c = 5.4 cm;

●, spindle #3, R_c = 0.295 cm, L_c = 4.3 cm .

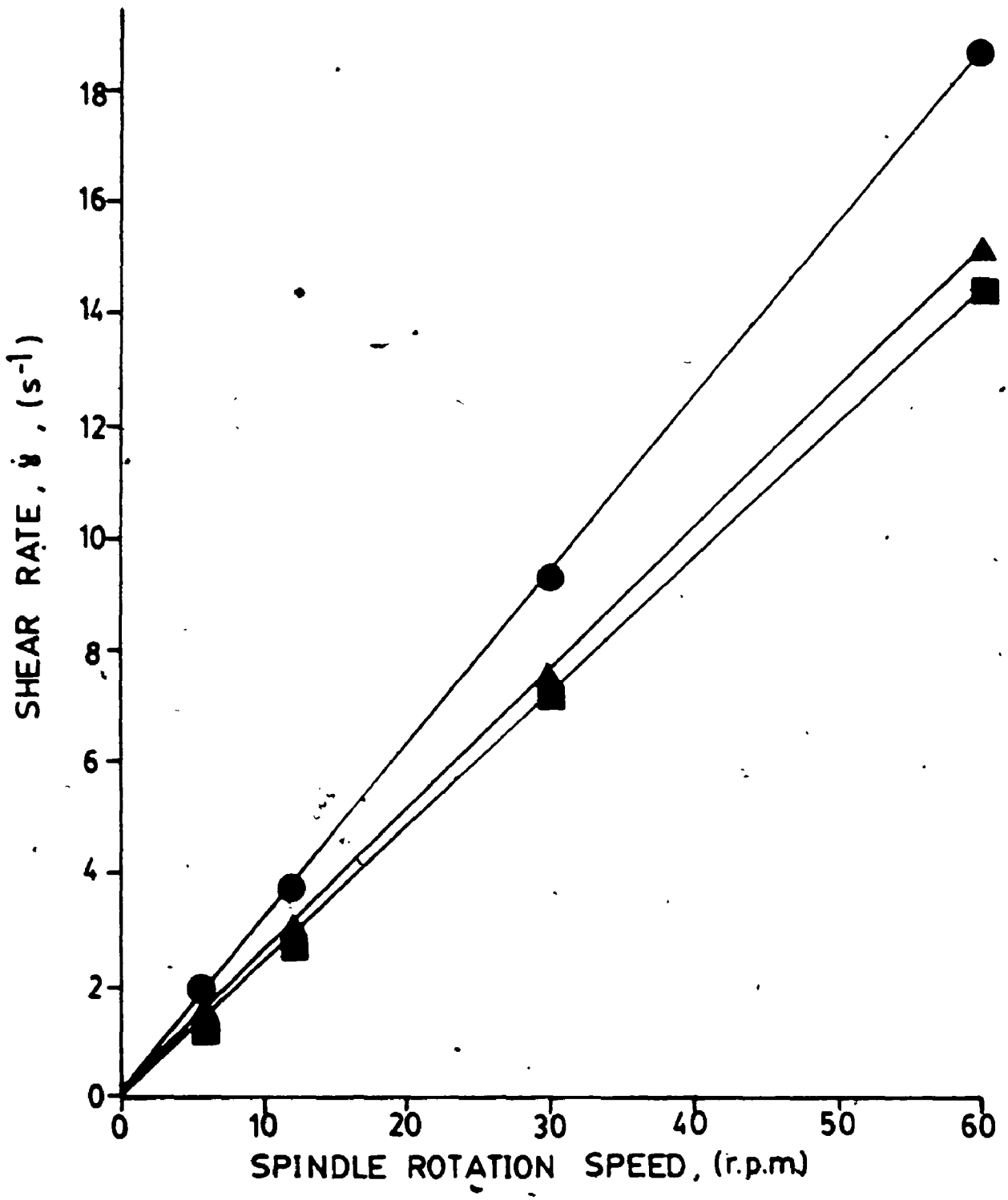
SHEAR RATE, $\dot{\gamma}$, (s^{-1})
0
2
4
6
8
10
12
14
16
18
0
10
20
30
40
50
60
SPINDLE ROTATION SPEED, (r.p.m)

Figure A.5: Viscosity (at 25°C) of dilute Na-alginate solutions at low shear rates. The numbers on the figure refer to the different types of Na-alginates listed in Table 4.1.

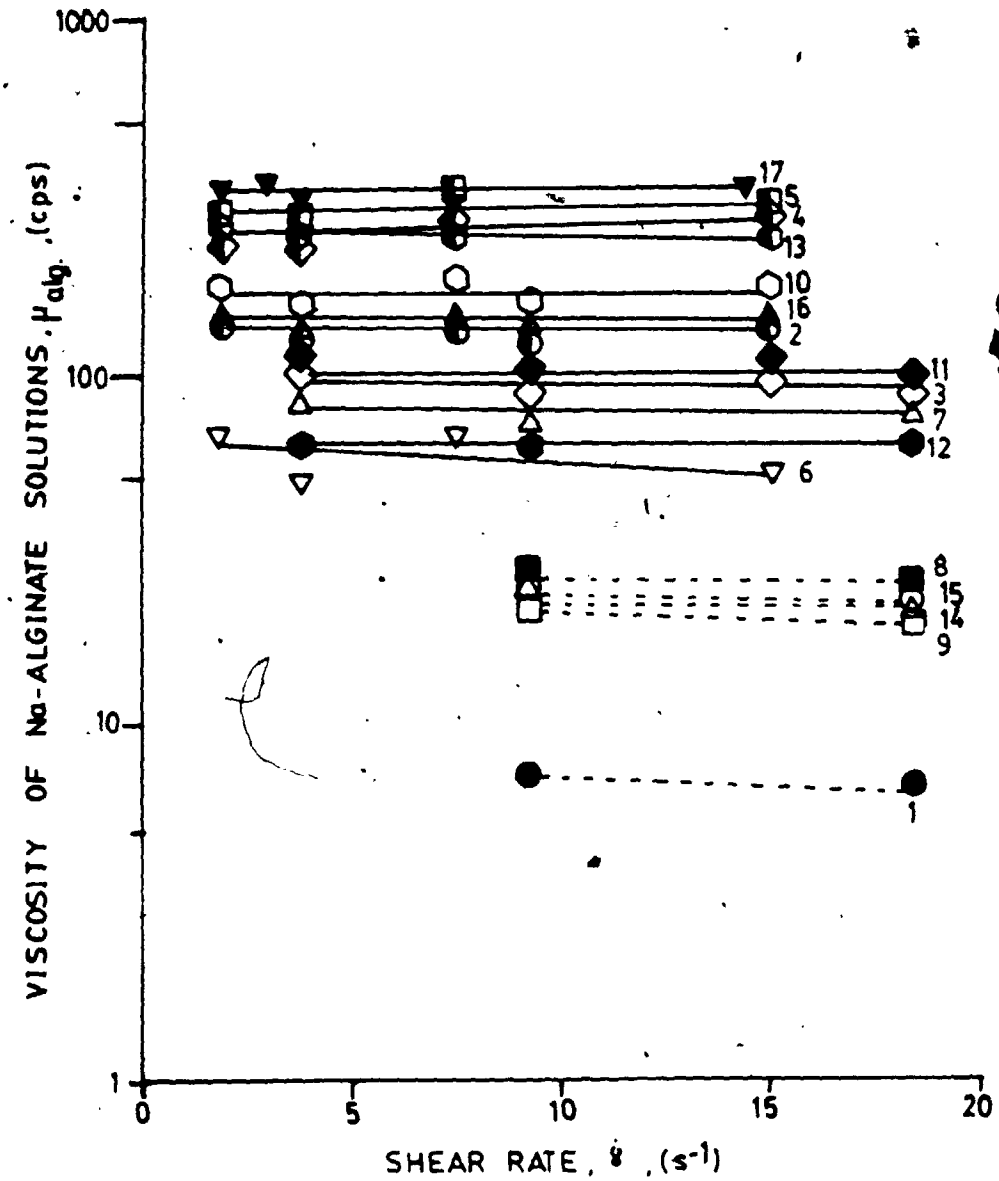
1000
100
10
1
0
5
10
15
20
VISCOSITY OF Na-ALGINATE SOLUTIONS, $\mu_{alg.}$ (cps)
SHEAR RATE, $\dot{\gamma}$, (s^{-1})
17
5
4
13
10
16
2
11
3
7
12
6
8
15
14
9
1

APPENDIX B

Examples Of Calculation Procedures And Data Analysis For Determination Of Effective Diffusivity And Concentration Profile Of Glucose In Ca-Alginate Spherical Bead Using The Computer Programs DIFPREP, DIFFIT And PROFILE

Appendix B1

Data Input and Calculation Steps Used in the Computer Program DIFPREP

A. Data Input

t = sampling time, minutes

m_L^t = radioactivity measured in 3 μL liquid sample when counted in scintillation spectrometer for either 5 minutes (diffusion experiment), or 20 minutes (effusion experiment), counts.

m_L^{BG} = background radioactivity in 3 μL 'cold' glucose solution (diffusion) or distilled water (effusion) when counted for 5 or 20 minutes, respectively, counts, (constant)

t_c = counting time, minutes, (constant)

v_s = sample size, μL, constant

V_L^o = intial volume of liquid phase in diffusion vessel, μL, (constant)

M_L^o = amount of labelled solute in liquid phase at time, t = 0 min., cpm, (constant); Diffusion only

M_S^o = amount of labelled solute in spherical alginate bead at time, t = 0 min., cpm (constant); Effusion only

V_B = bead volume, μL, (constant)

K_p = equilibrium partition coefficient, dimensionless, (constant)

$\bar{V}_L$ = average liquid phase volume, μL, (constant)

B. Calculation Steps

1. Amount of labelled solute in liquid sample at time, t, (m_L^t):

$$m_L^t = m_L^{t*} - m_L^{BG} \text{; counts}$$

2. Volume of liquid phase at time, t, (V_L^t):

$$V_L^t = V_L^o - \sum_{t=o}^{t} v_s \quad ; \quad \mu L$$

where, $\sum_{t=o}^{t} v_s$ is the cumulative amount of liquid phase withdrawn due to sampling (μ L)

3. Concentration of labelled solute in the liquid phase at time, t, (C_L^t):

$$C_L^t = \frac{m_L^t}{v_s \; t_c} \quad ; \quad cpm/\mu L$$

4. Amount of labelled solute in liquid phase at time, t, (M_L^t):

$$M_L^t = C_L^t \; V_L^t \quad ; \quad cpm$$

5. Cumulative amount of labelled solute withdrawn due to sampling at time, t, ($\sum M_s^t$):

$$\sum M_s^t \doteq \frac{1}{t_c} \sum_{n=1}^{N} m_L^1 + m_L^2 + \ldots . M_L^N \quad ; \quad cpm$$

where, N is the total number of samples

6. Amount of labelled solute in spherical alginate bead at time, t, (M_S^t):

(a) For diffusion,

$$M_S^t = M_L^o - M_L^t - \Sigma M_s^t \quad ; \text{ cpm}$$

(b) For effusion,

$$M_S^t = M_S^o - M_L^t - \Sigma M_s^t \quad ; \text{ cpm}$$

7. Concentration of labelled solute in bead at time, t, (C_S^t):

$$C_S^t = M_S^t / V_S \quad ; \text{ cpm}/\mu L$$

8. Solute concentration ratio at time, t, = C_S^t / C_L^t, (dimensionsless).

9. Alpha factor, α:

$$\alpha = \frac{\bar{V}_L}{V_S \; K_p} \quad ; \text{ dimensionless (constant)}$$

10. Amount of solute in the bead at equilibrium, (M_S^∞), for diffusion experiment only:

$$M_S^\infty = \frac{M_L^o}{1 + \alpha} \quad ; \text{ cpm (constant)}$$

11. Amount of solute in the liquid phase at equilibrium, (M_L^∞), for effusion experiment only:

$$M_L^\infty = \frac{M_S^o}{1 + 1/\alpha} \quad ; \text{ cpm (constant)}$$

12. Calculate the fractional uptake of the solute during diffusion (M_S^t / M_S^∞) or the fractional release of solute during effusion (M_L^t / M_L^∞) as a function of time, and store in the DIFFIT input file.

13. Calculate the percentage standard error (S.E.) in radioactivity counts which is given by,

$$[(M_L^t)^{1/2} / M_L^t] \times 100$$

APPENDIX B2

A Typical Output File Using the Computer Program

DIFPREP

INPUT AND CALCULATED DATA

SAMPLE NUMBER	TIME MINUTES	SAMPLE COUNTS	STANDARD ERROR %	LIQUID VOLUME MICRO-LITRES	CONCENTRATION COUNTS/MIN /MICRO-L	LIQUID COUNTS COUNTS/MIN	BEAD COUNTS COUNTS/MIN	BEAD CONCENTRATION COUNTS/MIN /MICRO-L	CONCENTRATION RATIO
1	0.000000E+00	0.000000E+00	0.000000E+00	4000.0	0.000000E+00	0.000000E+00	[illegible]	0.000000E+00	0.000000E+00
2	3.3300	1004.0	3.0234	3997.0	18.233	99473.	0.367[illegible]E+06	334.37	21.735
3	6.3300	1343.0	2.7037	3994.0	22.406	81043.	0.34963E+06	374.54	15.513
4	9.3300	1652.0	2.4267	3991.0	24.200	96592.	0.34604E+06	370.52	15.315
5	9.3300	1810.0	2.4922	3988.0	25.633	0.107016E+06	0.33353E+06	359.29	13.393
6	9.3300	2313.0	2.2166	3985.0	33.963	0.135422E+06	0.305025E+06	328.59	9.5533
7	10.300	1985.0	2.2445	3982.0	33.093	0.131745E+06	0.302605E+06	332.44	10.049
8	12.300	2260.0	2.0997	3979.0	34.167	0.151197E+06	0.298365E+06	310.64	6.1389
9	14.300	2254.0	2.1054	3976.0	37.600	0.149506E+06	0.290625E+06	313.06	8.3252
10	15.300	2487.0	2.0057	3973.0	41.450	0.164685E+06	0.275331E+06	296.57	7.1553
11	17.300	2797.0	1.8922	3970.0	45.550	0.184905E+06	0.255005E+06	274.75	5.9022
12	21.300	2821.0	1.8538	3967.0	47.093	0.187298E+06	0.246565E+06	237.01	5.5772
13	25.300	2914.0	1.8444	3964.0	45.435	0.186042E+06	0.253354E+06	273.12	5.3193
14	30.300	3233.0	1.7571	3961.0	53.563	0.213863E+06	0.225598E+06	243.01	4.5315
15	35.300	3254.0	1.7424	3958.0	54.571	0.217298E+06	0.221968E+06	239.13	4.3557
16	40.300	3444.0	1.6765	3955.0	59.300	0.236535E+06	0.204545E+06	220.36	3.7157
17	45.300	3457.0	1.6536	3952.0	60.950	0.240987E+06	0.199325E+06	215.31	3.4394
18	50.300	3591.0	1.6220	3949.0	61.350	0.250117E+06	0.195535E+06	235.39	3.2359
19	55.300	3984.0	1.5064	3946.0	64.733	0.255446E+06	0.183075E+06	197.21	3.0455
20	70.300	4192.0	1.5416	3943.0	66.367	0.269577E+06	0.169735E+06	181.77	2.5597
21	80.300	4375.0	1.5119	3940.0	72.517	0.287256E+06	0.153798E+06	162.44	2.2277
22	90.300	4593.0	1.4604	3937.0	76.15[illegible]	0.307[illegible]E+06	0.130175E+06	143.23	1.7963
23	100.00	4545.0	1.4633	3934.0	75.750	0.298095E+06	0.133625E+06	153.41	1.5355
24	110.00	4520.0	1.4277	3931.0	72.100	0.322345E+06	0.115037E+06	123.92	1.5112
25	120.00	4830.0	1.4359	3928.0	80.5[illegible]	0.314272E+06	0.123835E+06	153.27	1.5193
26	130.00	5097.0	1.4119	3925.0	89.617	0.329205E+06	0.133695E+06	117.38	1.4302
27	135.00	5053.0	1.4061	3922.0	86.300	0.330627E+06	0.109501E+06	116.13	1.3565
28	140.00	5291.0	1.3768	3919.0	89.363	0.345585E+06	90776.	97.797	1.1399
29	145.00	5363.0	1.3655	3916.0	89.363	0.350603E+06	86073.	92.721	1.0373
30	150.00	5205.0	1.3861	3913.0	86.757	0.339455E+06	96385.	103.83	1.1959
31	200.00	5500.0	1.3494	3910.0	91.667	0.359425E+06	77146.	83.105	0.93562
32	210.00	5354.0	1.3628	3907.0	89.233	0.350597E+06	94706.	101.248	1.0159
33	220.00	5304.0	1.3728	3904.0	88.473	0.345924E+06	99785.	105.720	1.0957
34	230.00	5334.0	1.3687	3901.0	88.967	0.347065E+06	97733.	104.677	1.0519
35	240.00	5357.0	1.3663	3898.0	89.283	0.348[illegible]E+06	96467.	103.145	1.0453
36	250.00	5331.0	1.3446	3895.0	87.183	0.359095E+06	75163.	93.969	0.97834
37	260.00	5403.0	1.3604	3892.0	90.050	0.350475E+06	83473.	99.929	0.99955
38	265.00	5430.0	1.3571	3889.0	90.500	0.351195E+06	81721.	98.033	0.97274
39	310.00	5430.0	1.3496	3886.0	91.500	0.355575E+06	77832.	93.864	0.91557
40	320.00	5399.0	1.3441	3883.0	92.250	0.358215E+06	74919.	93.704	0.97696
41	330.00	5434.0	1.3541	3880.0	93.673	0.351665E+06	83195.	97.465	0.96535

MORE IMPORTANT DATA

BACKGROUND RADIOACTIVITY	=	0.8100[illegible]E+00	COUNTS
INITIAL LIQUID VOLUME	=	4000.[illegible]	MICRO-L
SAMPLE VOLUME	=	3.0000	MICRO-L
VOLUME OF SOLID	=	928.30	MICRO-L
EVAPORATION RATE	=	0.00000[illegible]E+00	MICRO-L/MIN
SAMPLE COUNTING TIME	=	20.000	MINUTES
INITIAL SOLUTE IN BEAD	=	0.4408[illegible]E+06	COUNTS/MIN
BEAD VOLUME	=	928.30	MICRO-L
PARTITION COEFFICIENT	=	0.9300[illegible]	
AVERAGE LIQUID VOLUME	=	3940.[illegible]	MICRO-L
ALPHA	=	4.5633	
MAX M IN LIQUID AT T=INFINITY	=	0.36159[illegible]E+06	COUNTS/MIN

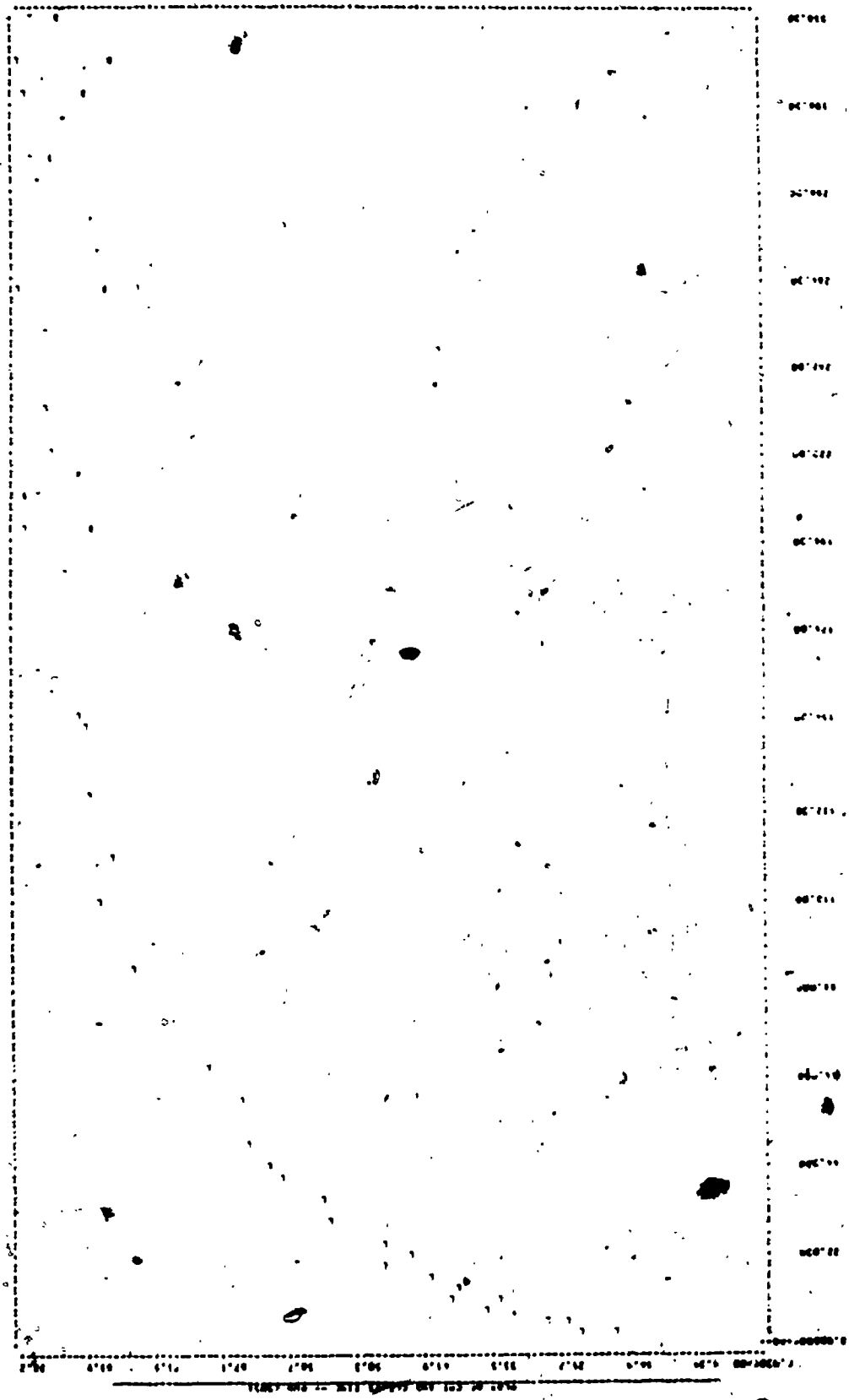

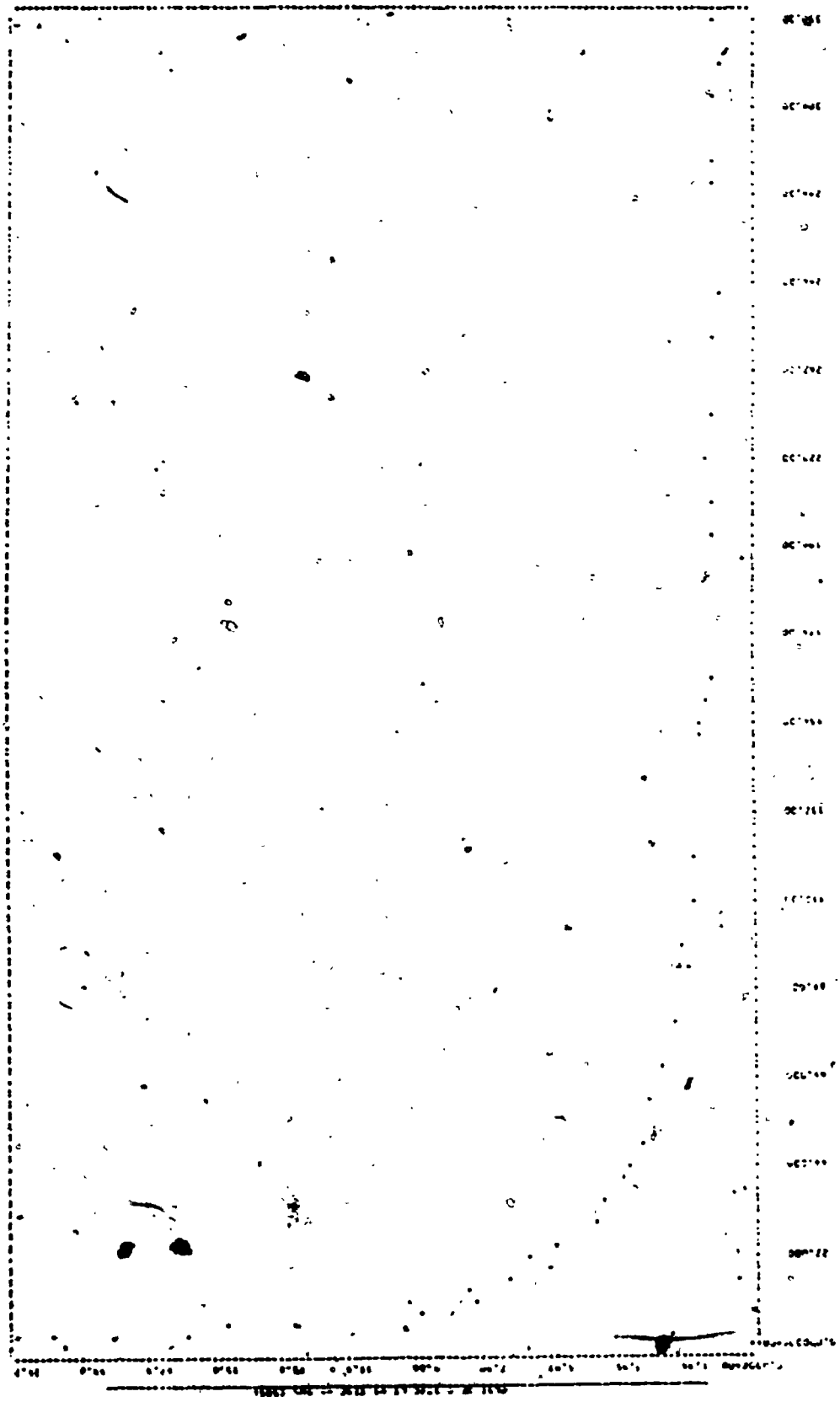

APPENDIX B3

A Typical Output File Using the Computer Program DIFFIT

```
FROM OPTIMIZATION SUBROUTINE

     N= 1     NCM= 1000        NODE=11

     I          X(I)          DX(I)          MIN(I)         MAX(I)
     1      0.100000E-03   0.100000E-05   0.000000E+00   1.000000

NC=  1  U=  2.47220      X(I)  0.100000E-05
NC=  2  U=  2.40312      X(I)  0.111200E-05
NC=  3  U=  2.54855      X(I)  0.102610E-05
NC=  4  U=  2.26460      X(I)  0.105236E-05
NC=  5  U=  2.17406      X(I)  0.104472E-05
NC=  6  U=  1.24070      X(I)  0.116326E-05
NC=  7  U=  1.96664      X(I)  0.127416E-05
NC=  8  U=  1.30540      X(I)  0.165[illegible]E-05
NC=  9  U=  0.79044      X(I)  0.174355E-05
NC= 10  U=  0.452[illegible]      X(I)  0.221774E-05
NC= 11  U=  0.123[illegible]      X(I)  0.297392E-05
NC= 12  U=  0.161452E-01  X(I)  0.420772E-05
NC= 13  U=  0.137025E-01  X(I)  0.413525E-05

NC  21  [illegible]


  SENSITIVITY ANALYSIS


REF.PT  U=  0.137025E-01  X(I)  0.413525E-05

BEST P  U=  0.136775E-01  X(I)  0.411478E-05

OB.MIN  U=  0.136775E-01  X(I)  0.411478E-05

GRADIENT VECTOR (1ST DERIV.)
        F=  24.4770      G(I)  24.4770

HESSIAN MATRIX (2ND DERIV.)
                    H( 1,1)  0.119562E+06


REVISED VALUES -     DX(I)  0.103300E-05
```

INPUT AND CALCULATED VALUES

OPTIMUM SENSITIVITY = 0.431485E-03 CHI-SQ/MIN = 1.65360E-13 MEAS/SEC

	T	CMST/MSEC(MEAS)	CMST/MSEC(MODEL)	RESIDUAL
1	[illegible]	[illegible]	0.290551E-01	0.250551E-31
2	3.00000	0.231550	0.220050	0.135003E-31
3	4.00000	0.251640	0.250777	-0.106293E-32
4	5.00000	0.267[illegible]	0.277353	0.1[illegible]5353E-31
5	6.00000	0.295950	0.300446	0.449771E-32
6	7.00000	0.316524	0.340545	-0.539765E-31
7	10.0000	0.354833	0.376562	0.102324E-31
8	12.0000	0.389990	0.406236	-0.157646E-31
9	14.0000	0.413453	0.430773	0.173226E-31
10	17.0000	0.455440	0.454713	-0.727177E-33
11	19.0000	0.511[illegible]	0.466351	-0.242588E-31
12	21.0000	0.479257	0.506235	0.268545E-31
13	25.0000	0.514527	0.541110	0.265[illegible]E-31
14	30.0000	0.533360	0.578959	-0.124035E-31
15	35.0000	0.600[illegible]	0.611916	0.109751E-31
16	40.0000	0.643615	0.641042	-0.755[illegible]E-32
17	45.0000	0.656150	0.667071	0.92[illegible]E-33
18	50.0000	0.691242	0.690593	-0.132655E-32
19	60.0000	0.726430	0.731266	0.246361E-31
20	70.0000	0.765510	0.765409	0.199781E-31
21	80.0000	0.796522	0.796052	0.131607E-31
22	90.0000	0.450000	0.826602	-0.242975E-31
23	100.000	0.824142	0.841510	0.173705E-31
24	110.000	0.891467	0.860470	-0.309950E-31
25	120.000	0.874487	0.877053	0.257299E-32
26	130.000	0.917657	0.915620	0.797046E-32
27	135.000	0.914563	0.920730	0.636971E-32
28	140.000	0.935750	0.925526	-0.302245E-31
29	145.000	0.950029	0.930023	-0.379513E-31
30	150.000	0.956762	0.946753	0.997257E-32
31	200.000	0.931227	0.954749	-0.364718E-31
32	210.000	0.959571	0.960042	-0.952828E-32
33	220.000	0.954730	0.964716	0.992428E-32
34	230.000	0.959-10	0.968360	0.902987E-32
35	250.000	0.952693	0.975079	0.132[illegible]E-31
36	260.000	0.932599	0.978546	-0.144501E-31
37	270.000	0.959269	0.985219	0.159591E-31
38	285.000	0.973353	0.990310	0.127597E-31
39	310.000	0.993559	0.998472	0.512231E-32
40	320.000	0.990643	0.999[illegible]	-0.920657E-33
41	330.000	0.972535	0.991709	0.184795E-31

PERCENT DEVIATION OF EXPERIMENTAL POINTS = 0.414716E-01

INTERNAL VALUES AND # OF TERMS USED

NUMBER OF ROOT CALCULATIONS = 26

NUMBER OF TERMS USED IN SUM = 25

TERM #	Z	BETA
1	3.326	[illegible]
2	5.7142	[illegible]
3	[illegible]	[illegible]
4	12.61[illegible]	[illegible]
5	15.75[illegible]	[illegible]
6	1[illegible]	[illegible]
7	2[illegible]	[illegible]
8	25.15[illegible]	[illegible]
9	2[illegible]	[illegible]
10	31.[illegible]	[illegible]
11	36.[illegible]	[illegible]
12	37.[illegible]	[illegible]
13	41.[illegible]	[illegible]
14	43.[illegible]	[illegible]
15	47.[illegible]	[illegible]
16	52.[illegible]	[illegible]
17	53.[illegible]	[illegible]
18	55.[illegible]	[illegible]
19	58.[illegible]	[illegible]
20	62.[illegible]	[illegible]
21	65.[illegible]	[illegible]
22	69.125	[illegible]
23	72.26[illegible]	[illegible]
24	75.[illegible]	[illegible]
25	78.[illegible]	[illegible]

VOLUME OF LIQUID (MC) = 5.9401

VOLUME OF SOLID (MC) = 0.92[illegible]

PARTICLE COEFFICIENT = 0.[illegible]

RADIUS OF PARTICLE (CM) = 0.60520

BLOWS FACTOR = 6.5634

[illegible] VALUES IN FIVE DIFFUSIVITIES

	TIME [illegible]	D=0.40 CM**2/MIN D=0.100E-05 M**2/SEC	D=0.40E-01 CM**2/MIN D=0.100E-06 M**2/SEC	D=0.33E-01 CM**2/MIN D=0.550E-07 M**2/SEC	D=0.60E-02 CM**2/MIN D=0.100E-07 M**2/SEC	D=1.30E-02 CM**2/MIN D=0.500E-08 M**2/SEC	D=0.60E-03 CM**2/MIN D=0.100E-08 M**2/SEC	D=0.60E-04 CM**2/MIN D=0.100E-09 M**2/SEC	D=0.60E-05 CM**2/MIN D=0.100E-10 M**2/SEC
1	[illegible]	0.29055E-01	0.29055E-01	0.29055E-01	0.29055E-01	0.29055E-01	0.29055E-01	0.29055E-01	0.29055E-01
2	1.000	1.0000	[illegible]	[illegible]	[illegible]	0.91425	[illegible]	0.33700E-01	0.37675E-01
3	4.000	1.0000	[illegible]	0.69552	0.77495	0.67500	0.24673	0.13179	0.60395E-01
4	5.000	1.0000	[illegible]	0.55415	0.77444	0.62074	0.32715	0.11327	0.62553E-01
5	6.000	1.0000	[illegible]	[illegible]	0.91779	[illegible]	0.35396	0.12357	0.65392E-01
6	8.000	1.0000	[illegible]	[illegible]	0.27174	0.77435	0.39950	0.14163	0.69793E-01
7	10.000	1.0000	[illegible]	[illegible]	[illegible]	0.77444	0.43757	0.15761	0.56223E-01
8	12.000	1.0000	[illegible]	[illegible]	[illegible]	[illegible]	0.47127	0.17165	0.55620E-01
9	14.000	1.0000	[illegible]	[illegible]	[illegible]	0.56565	0.50471	0.18424	0.52438E-01
10	16.000	1.0000	[illegible]	1.0000	[illegible]	[illegible]	0.52712	0.19431	0.55195E-01
11	18.000	1.0000	[illegible]	[illegible]	[illegible]	[illegible]	[illegible]	0.21217	0.71565E-01
12	21.000	1.0000	1.0000	1.0000	0.99792	[illegible]	0.53630	0.22212	0.76357E-01
13	25.000	1.0000	1.0000	1.0000	0.99615	0.96756	0.56274	0.24367	0.81364E-01
14	30.000	1.0000	1.0000	1.0000	0.99768	0.99615	0.58750	0.25139	0.89730E-01
15	35.000	1.0000	1.0000	1.0000	0.99504	[illegible]	[illegible]	0.27359	0.95580E-01
16	40.000	1.0000	1.0000	1.0000	0.99561	[illegible]	[illegible]	0.29675	0.10175
17	45.000	1.0000	1.0000	1.0000	0.99564	[illegible]	[illegible]	0.31245	0.10775
18	50.000	1.0000	1.0000	1.0000	0.99554	0.99615	[illegible]	0.32715	0.11327
19	60.000	1.0000	1.0000	1.0000	[illegible]	[illegible]	0.99373	0.35358	0.12357
20	70.000	1.0000	1.0000	1.0000	1.0000	0.99504	0.96505	0.37762	0.13299
21	80.000	1.0000	1.0000	1.0000	1.0000	0.99961	0.97174	0.39356	0.14155
22	90.000	1.0000	1.0000	1.0000	1.0000	[illegible]	0.98697	0.42523	0.15212
23	100.00	1.0000	1.0000	1.0000	1.0000	0.99994	0.99107	0.43797	0.15761
24	110.00	1.0000	1.0000	1.0000	1.0000	0.99997	0.99587	0.45517	0.16452
25	120.00	1.0000	1.0000	1.0000	1.0000	0.99997	0.99621	0.47127	0.17165
26	130.00	1.0000	1.0000	1.0000	1.0000	1.0000	0.99615	0.49425	0.18024
27	140.00	1.0000	1.0000	1.0000	1.0000	1.0000	0.99725	0.52077	0.19015
28	150.00	1.0000	1.0000	1.0000	1.0000	1.0000	0.97709	0.52712	0.19531
29	160.00	1.0000	1.0000	1.0000	1.0000	1.0000	0.97269	0.53552	0.19982
30	170.00	1.0000	1.0000	1.0000	1.0000	1.0000	0.99264	0.56224	0.21217
31	180.00	1.0000	1.0000	1.0000	1.0000	1.0000	0.99552	0.57300	0.21722
32	190.00	1.0000	1.0000	1.0000	1.0000	1.0000	0.99792	0.58930	0.22212
33	200.00	1.0000	1.0000	1.0000	1.0000	1.0000	0.99992	0.59319	0.22599
34	210.00	1.0000	1.0000	1.0000	1.0000	1.0000	0.99159	0.60271	0.23153
35	220.00	1.0000	1.0000	1.0000	1.0000	1.0000	0.99615	0.62074	0.24367
36	230.00	1.0000	1.0000	1.0000	1.0000	1.0000	0.99512	0.62329	0.24673
37	240.00	1.0000	1.0000	1.0000	1.0000	1.0000	0.99715	0.63529	0.25213
38	250.00	1.0000	1.0000	1.0000	1.0000	1.0000	0.99741	0.65707	0.25912
39	310.00	1.0000	1.0000	1.0000	1.0000	1.0000	0.99903	0.65937	0.26635
40	320.00	1.0000	1.0000	1.0000	1.0000	1.0000	0.99635	0.67513	0.26374
41	350.00	1.0000	1.0000	1.0000	1.0000	1.0000	0.99363	0.68199	0.27245

LEGEND FOR FIGURES 1 AND 2

E - EXPERIMENTAL POINTS

M - MODEL POINTS ESTIMATED USING A REGRESSION ANALYSIS

2 - MODEL POINTS USING D = 0.40 CM**2/MIN = 0.10[illegible] - 5 M**2/SEC

3 - MODEL POINTS USING D = 0.60E-01 CM**2/MIN = 0.1[illegible]E-06 M**2/SEC

4 - MODEL POINTS USING D = 0.3[illegible]E-01 CM**2/MIN = 0.5[illegible]E-07 M**2/SEC

A - MODEL POINTS USING D = 0.6[illegible]E-02 CM**2/MIN = 0.1[illegible]E-07 M**2/SEC

B - MODEL POINTS USING D = 0.30E-02 CM**2/MIN = 0.5[illegible]E-08 M**2/SEC

C - MODEL POINTS USING D = 0.6[illegible]E-03 CM**2/MIN = 0.1[illegible]E-08 M**2/SEC

D - MODEL POINTS USING D = 0.4[illegible]E-04 CM**2/MIN = 0.1[illegible]E-09 M**2/SEC

F - MODEL POINTS USING D = 0.4[illegible]E-05 CM**2/MIN = 0.1[illegible]E-10 M**2/SEC

LEGEND FOR FIGURE 3

M - MODEL POINTS ESTIMATED USING REGRESSION ANALYSIS
(K = 0.[illegible])

A - MODEL POINTS USING K = 0.7[illegible]

B - MODEL POINTS USING K = 0.9[illegible]

C - MODEL POINTS USING K = 0.9[illegible]

D - MODEL POINTS USING K = 1.0000

E - MODEL POINTS USING K = 1.1000

APPENDIX B4

A Typical Output File Using the Computer Program

INPUT DATA : PROFILE

BEAD VOLUME	824.30	MICRO-L
LIQUID VOLUME	3041.0	MICRO-L
PARTITION COEFFICIENT	0.95000	
PARTICLE RADIUS	0.00520	CM
DIFFUSIVITY	0.41147E-03	CM**2/MIN
ALPHA	4.5638	
CONCENTRATION - INF	389.52	

**** DIFFUSION EXPERIMENT ****

RADIAL POSITION	CB(T)
CONCENTRATION - 0	474.87
0.10000E-01	507.34
0.50000E-01	454.38
0.10000	467.91
0.15000	470.22
0.20000	472.70
0.25000	480.10
0.30000	479.56
0.35000	475.32
0.40000	477.25
0.45000	471.04
0.50000	477.40
0.55000	475.23
0.60000	471.82
0.65000	474.55
0.70000	473.17
0.75000	472.93
0.80000	479.93
0.85000	469.55
0.90000	475.16
0.95000	467.94
1.0000	371.36

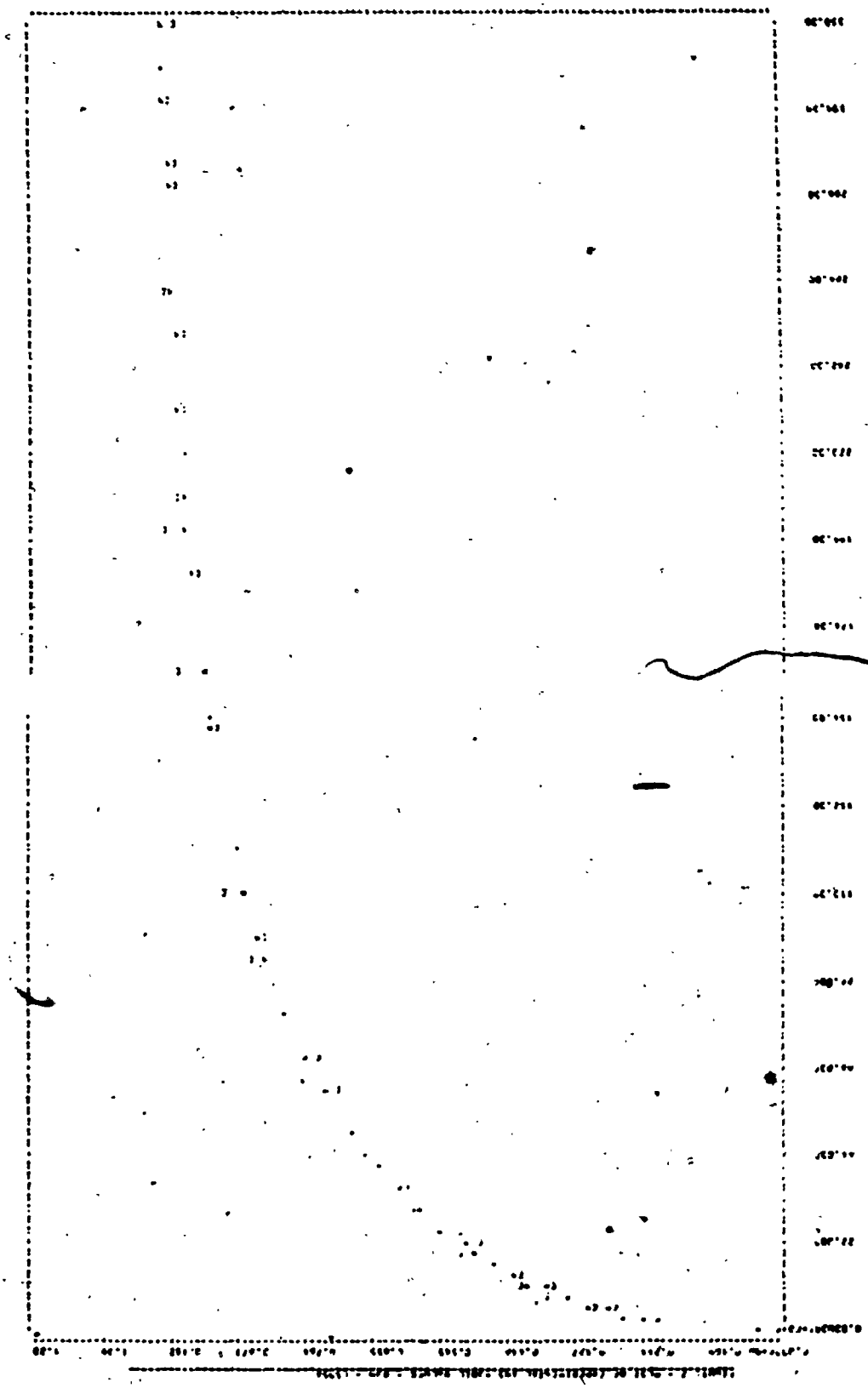

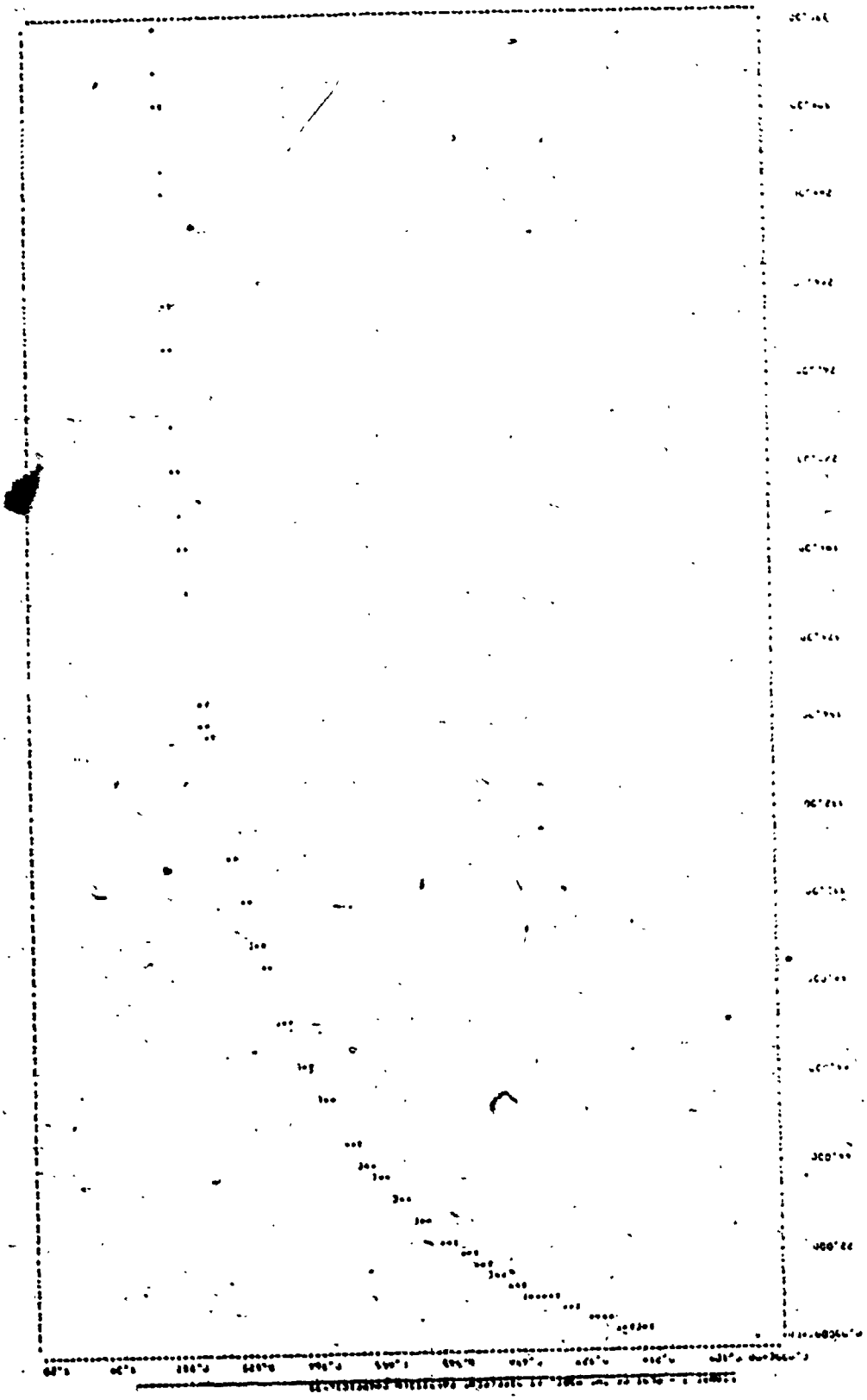

APPENDIX B4

A Typical Output File Using the Computer Program

INPUT DATA : PROFILE

BEAD VOLUME	824.30	MICRO-L
LIQUID VOLUME	5341.0	MICRO-L
PARTITION COEFFICIENT	0.93000	
PARTICLE RADIUS	0.00520	CM
DIFFUSIVITY	0.41147E-03	CM**2/MIN
ALPHA	4.5638	
CONCENTRATION - INF	305.52	

**** EFFUSION EXPERIMENT ****

RADIAL POSITION	CB(T)
CONCENTRATION - 0	474.87
0.10000E-01	467.34
0.50000E-01	454.38
0.10000	467.91
0.15000	470.22
0.20000	472.70
0.25000	480.10
0.30000	479.56
0.35000	475.32
0.40000	477.25
0.45000	471.06
0.50000	477.40
0.55000	475.25
0.60000	471.32
0.65000	474.55
0.70000	473.17
0.75000	477.93
0.80000	479.93
0.85000	469.55
0.90000	475.16
0.95000	467.94
1.0000	371.36

CONCENTRATION PROFILE FOR T = 0.0000E+00 MINUTES

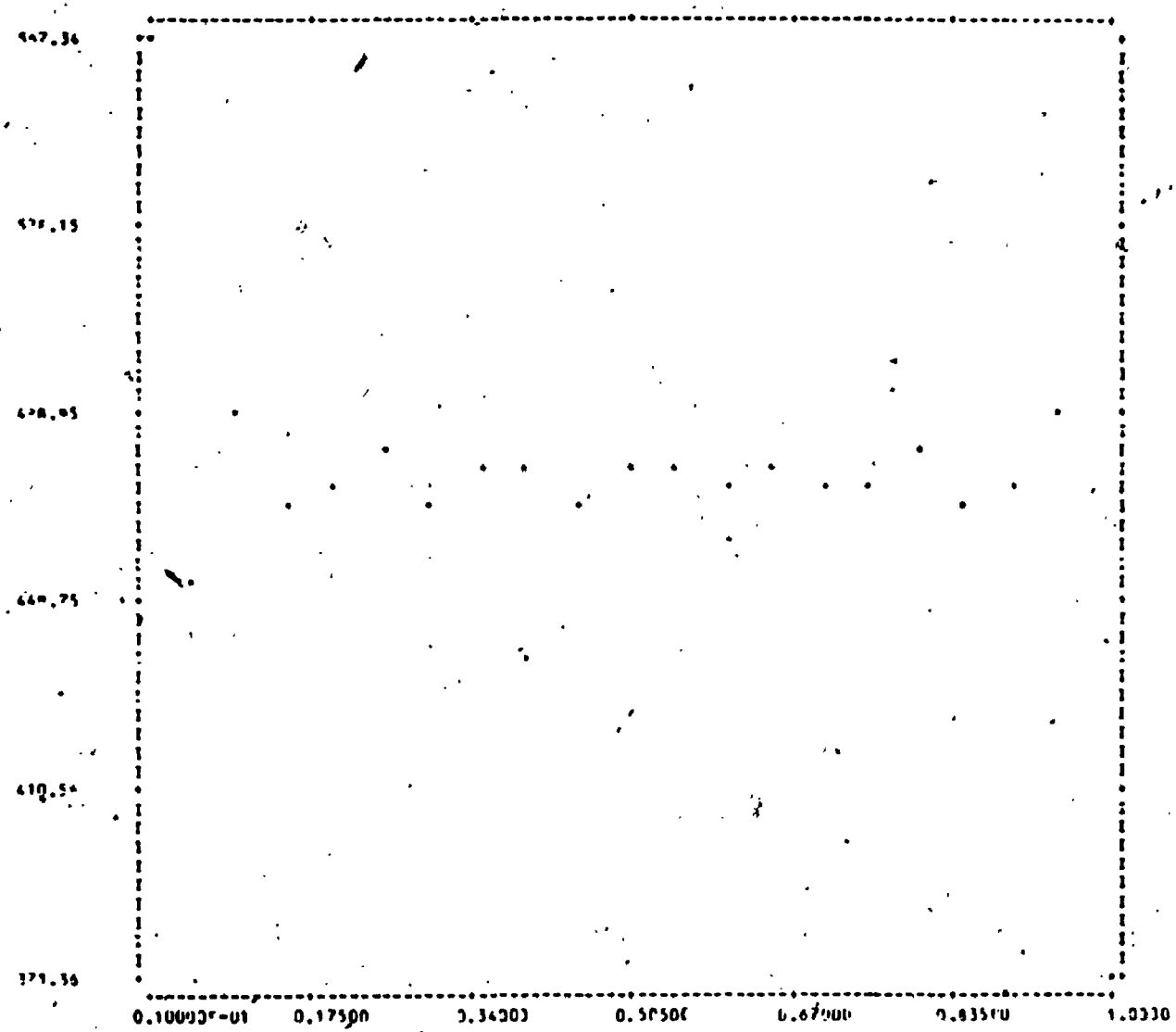

CONCENTRATION PROFILE FOR T = 5.0000 MINUTES

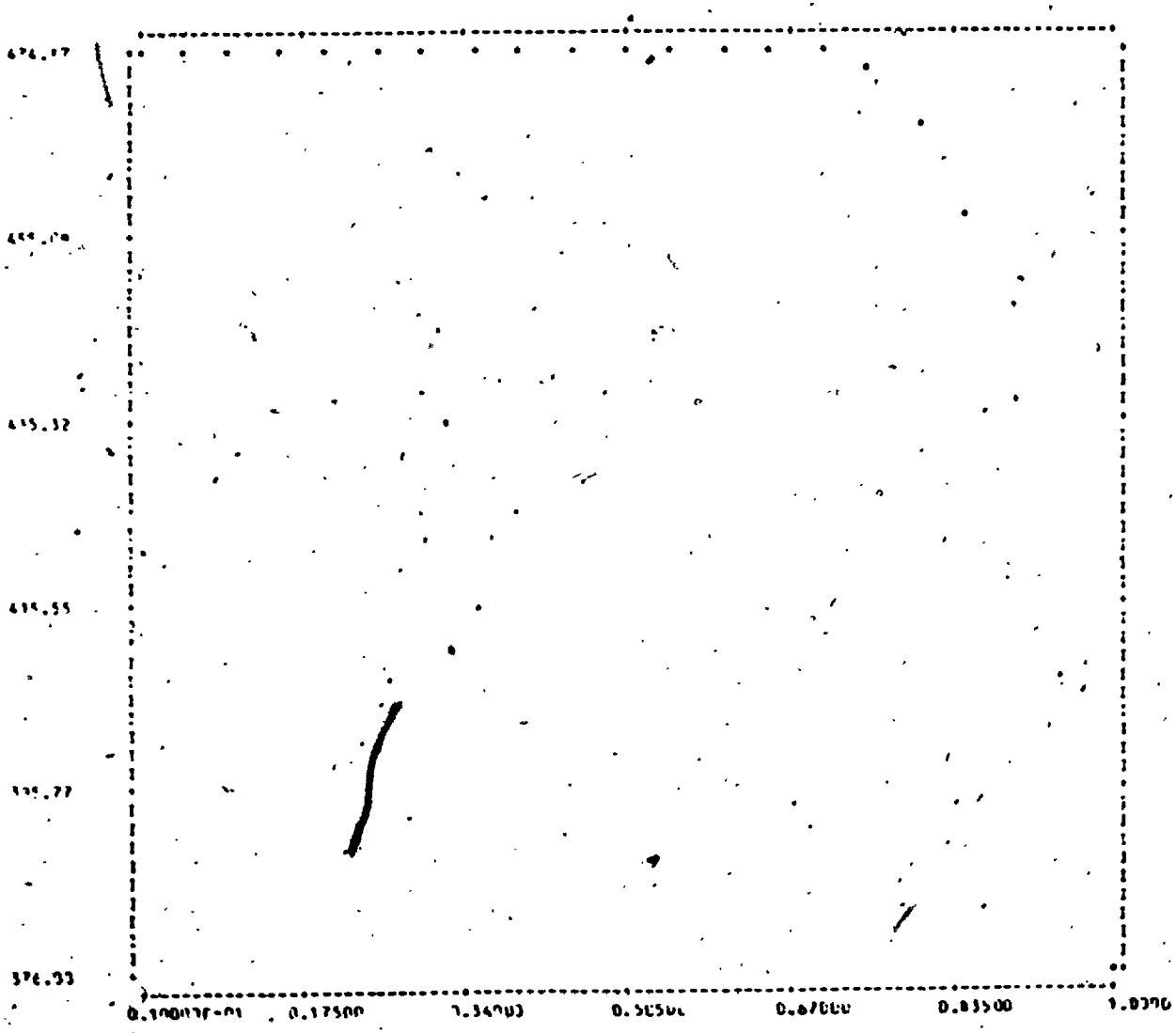

CONCENTRATION PROFILE FOR T = 10.000 MINUTES

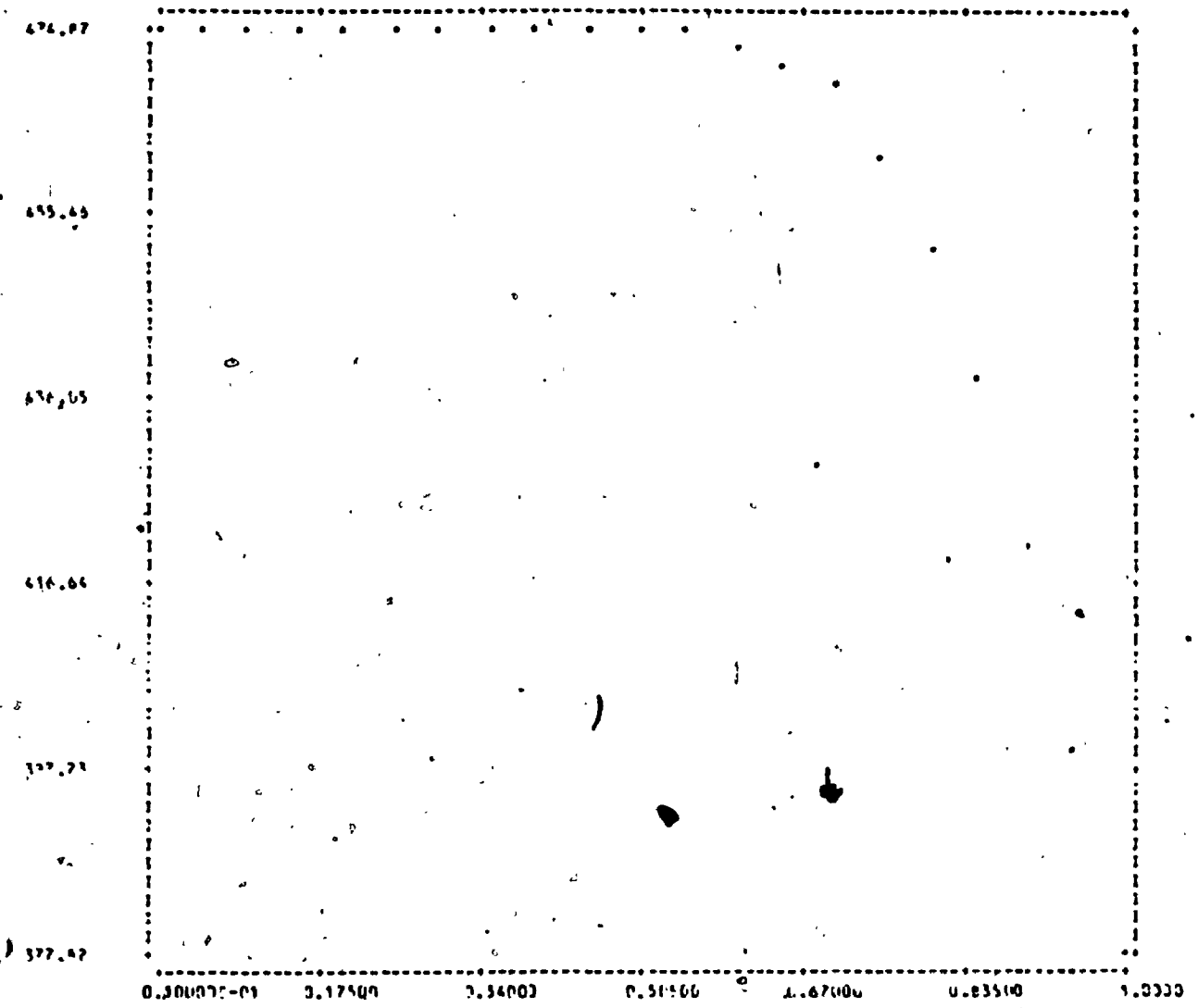

CONCENTRATION PROFILE FOR T = 25.000 MINUTES

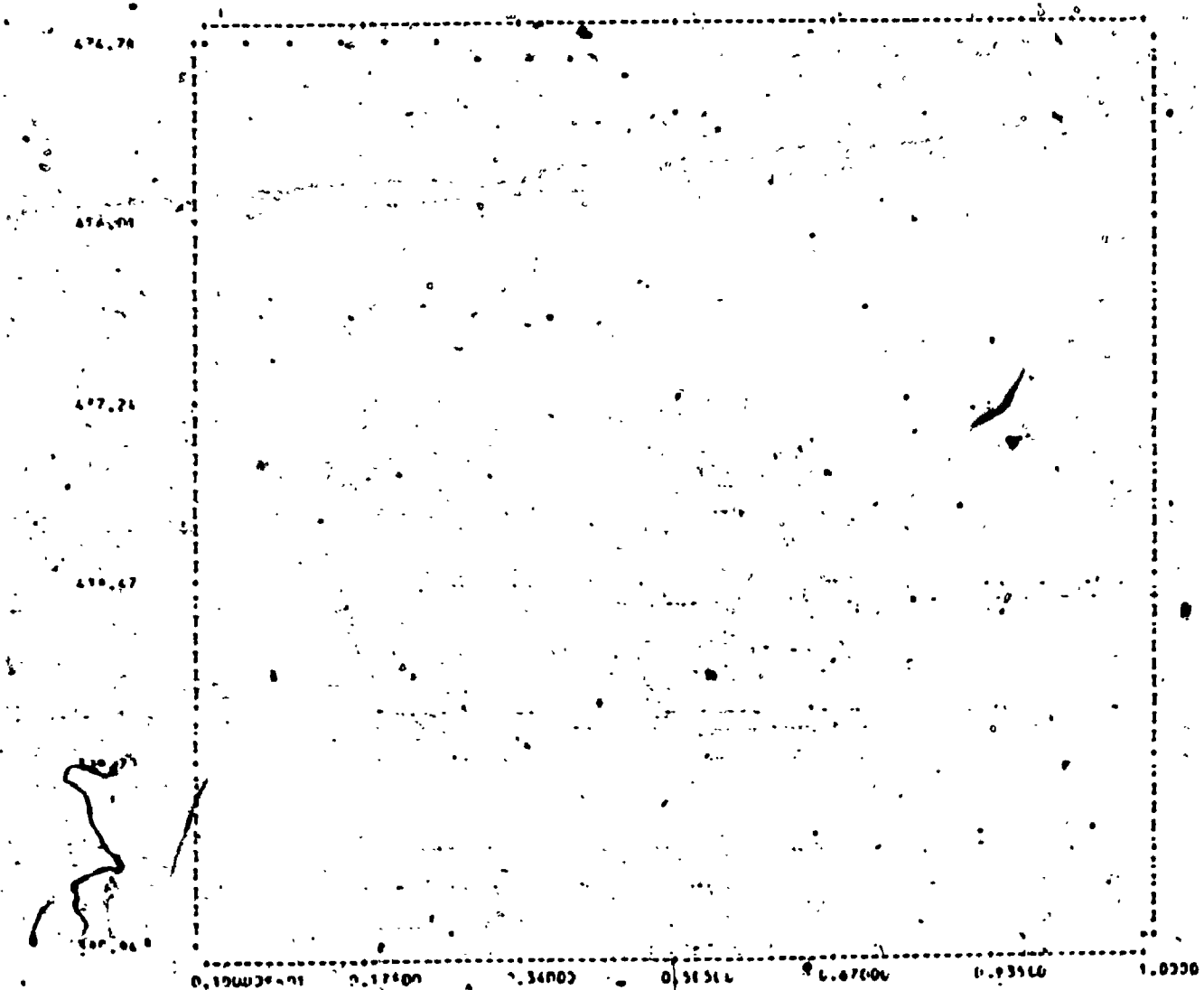

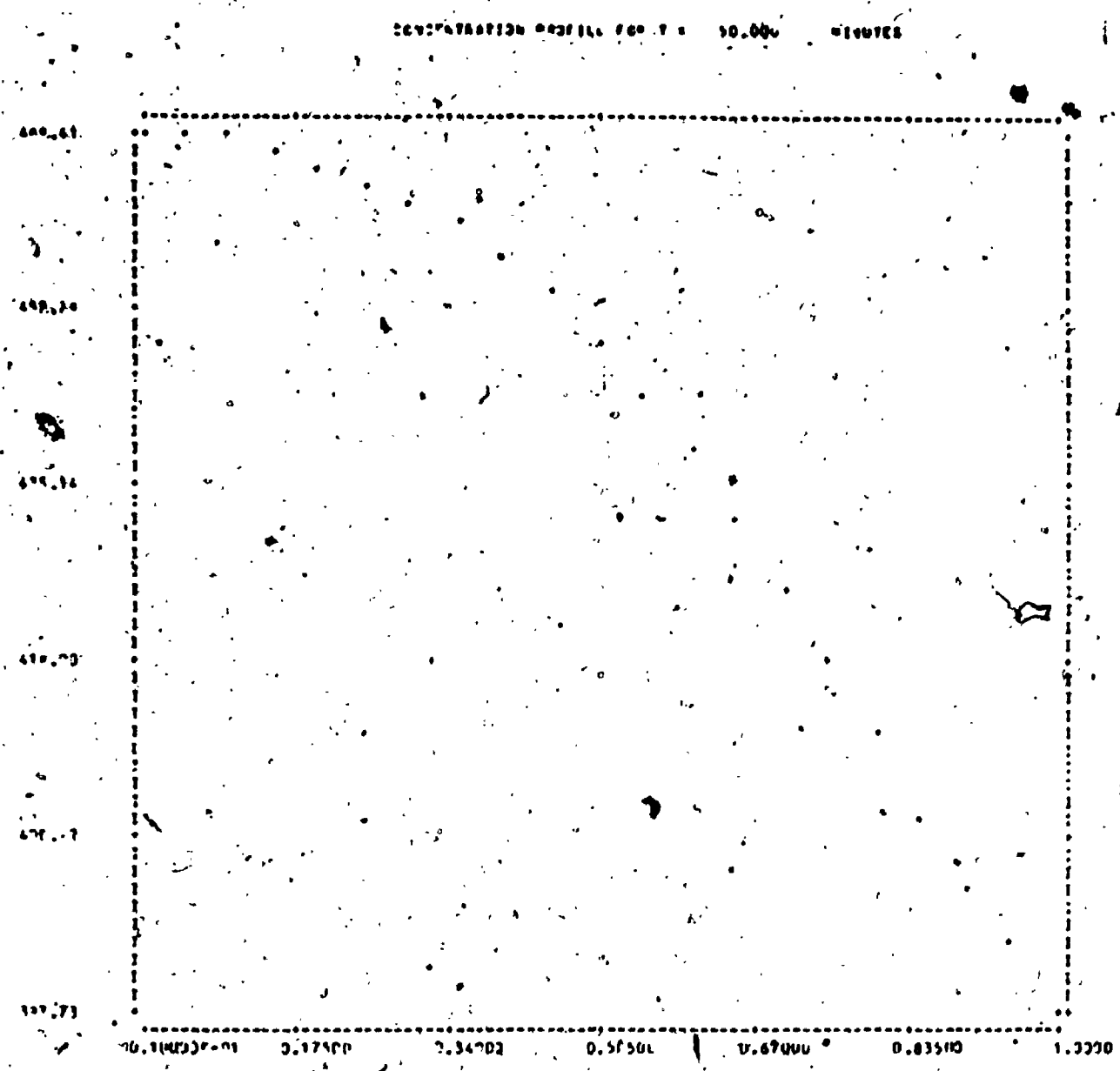
CONCENTRATION PROFILE FOR T = 50.000 MINUTES
0.17500
0.34002
0.50500
0.67000
0.83500
1.0000

CONCENTRATION PROFILE FOR T = 150.00 MINUTES

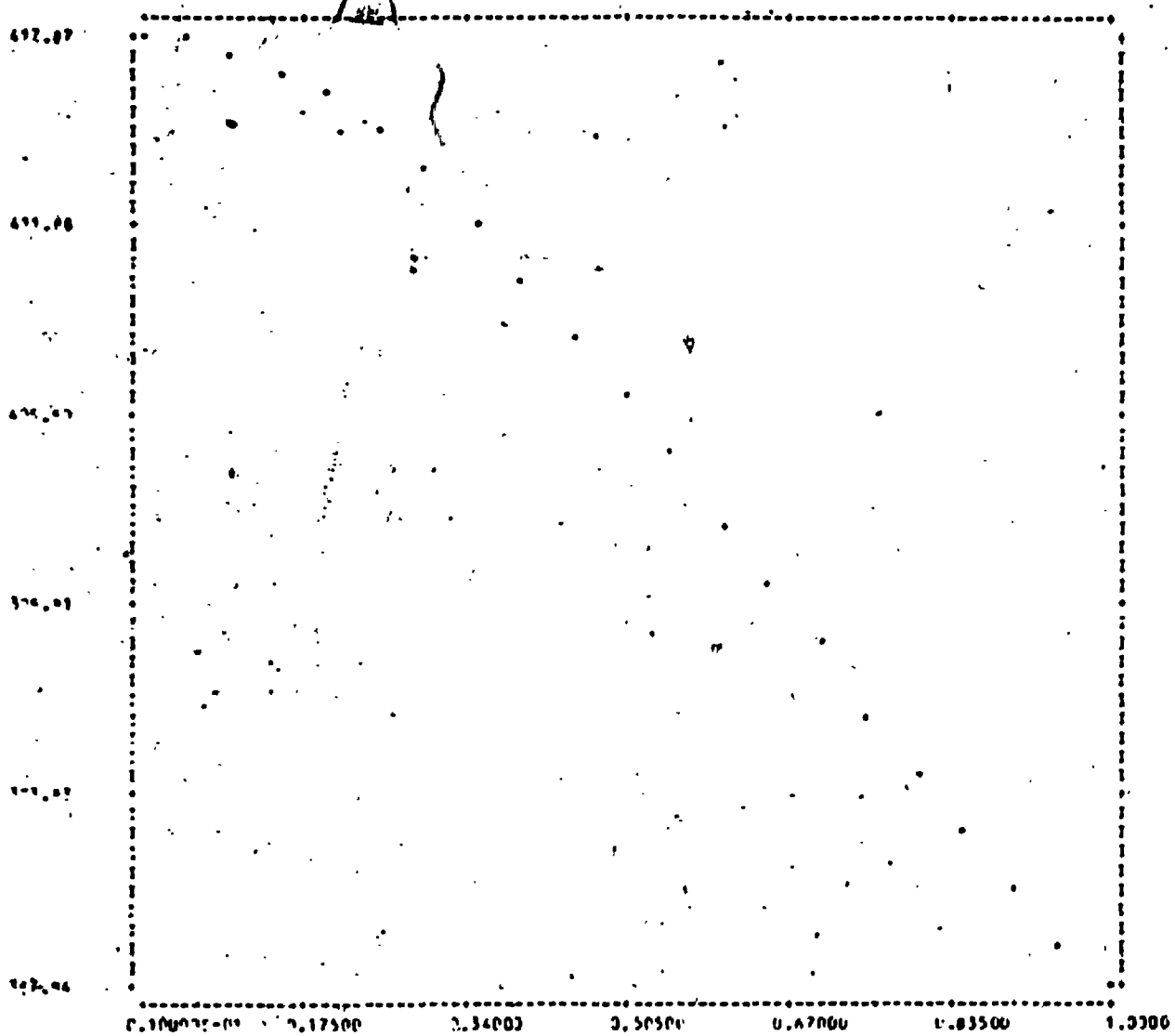

CONCENTRATION PROFILE FOR T = 200.00 MINUTES

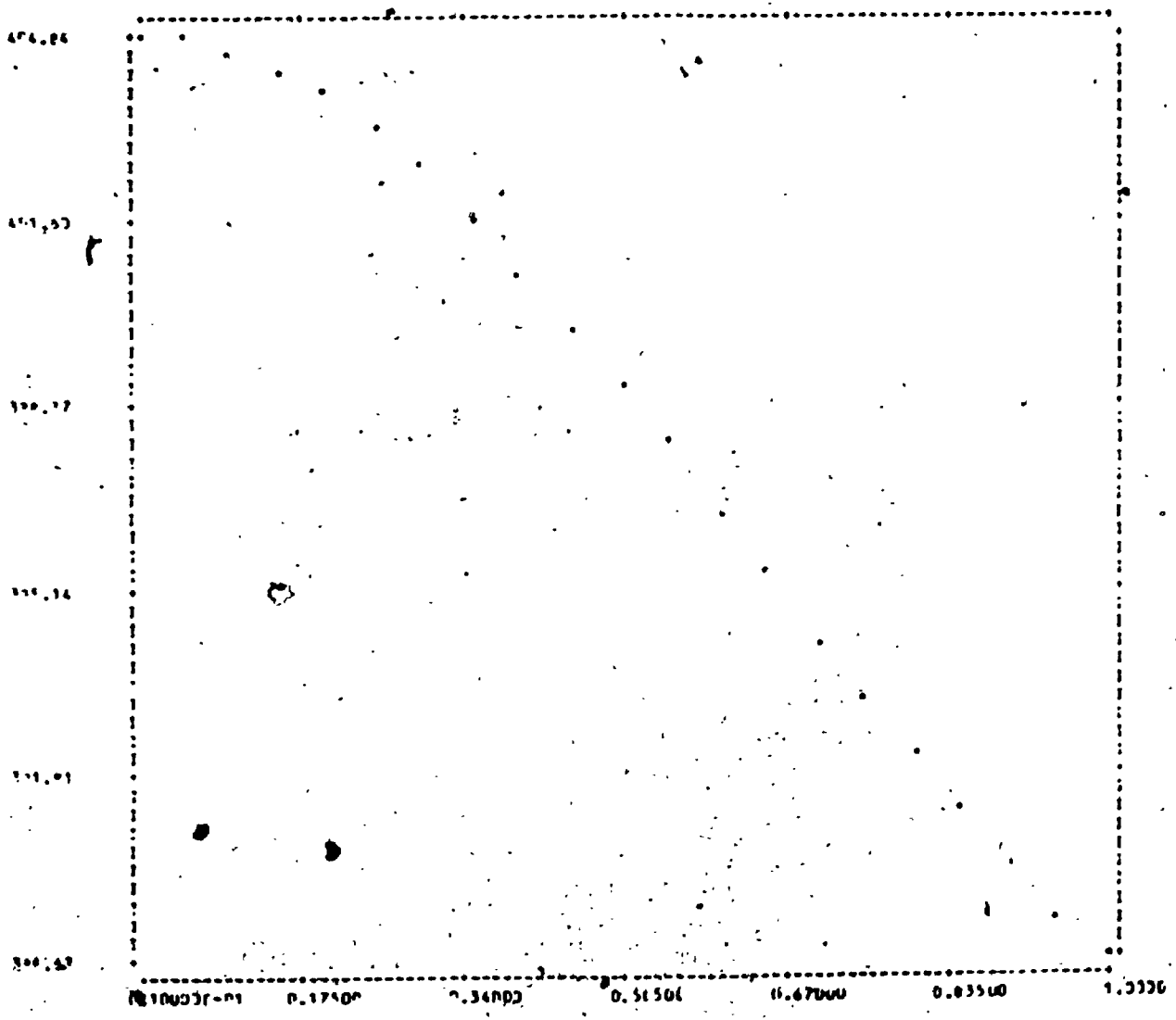

CONCENTRATION PROFILE FOR T = 250.00 MINUTES

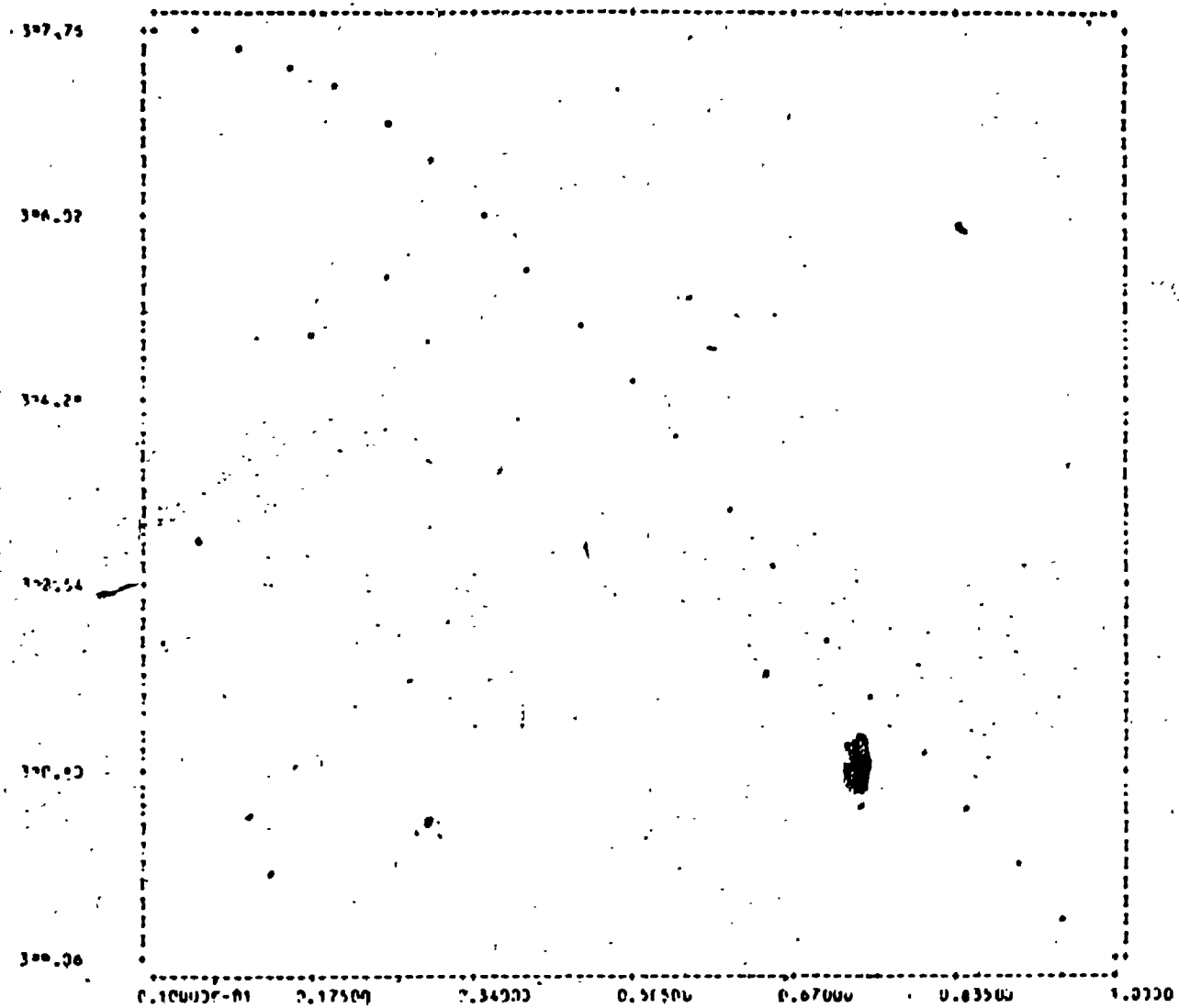

CONCENTRATION PROFILE FOR T = 330.00 MINUTES

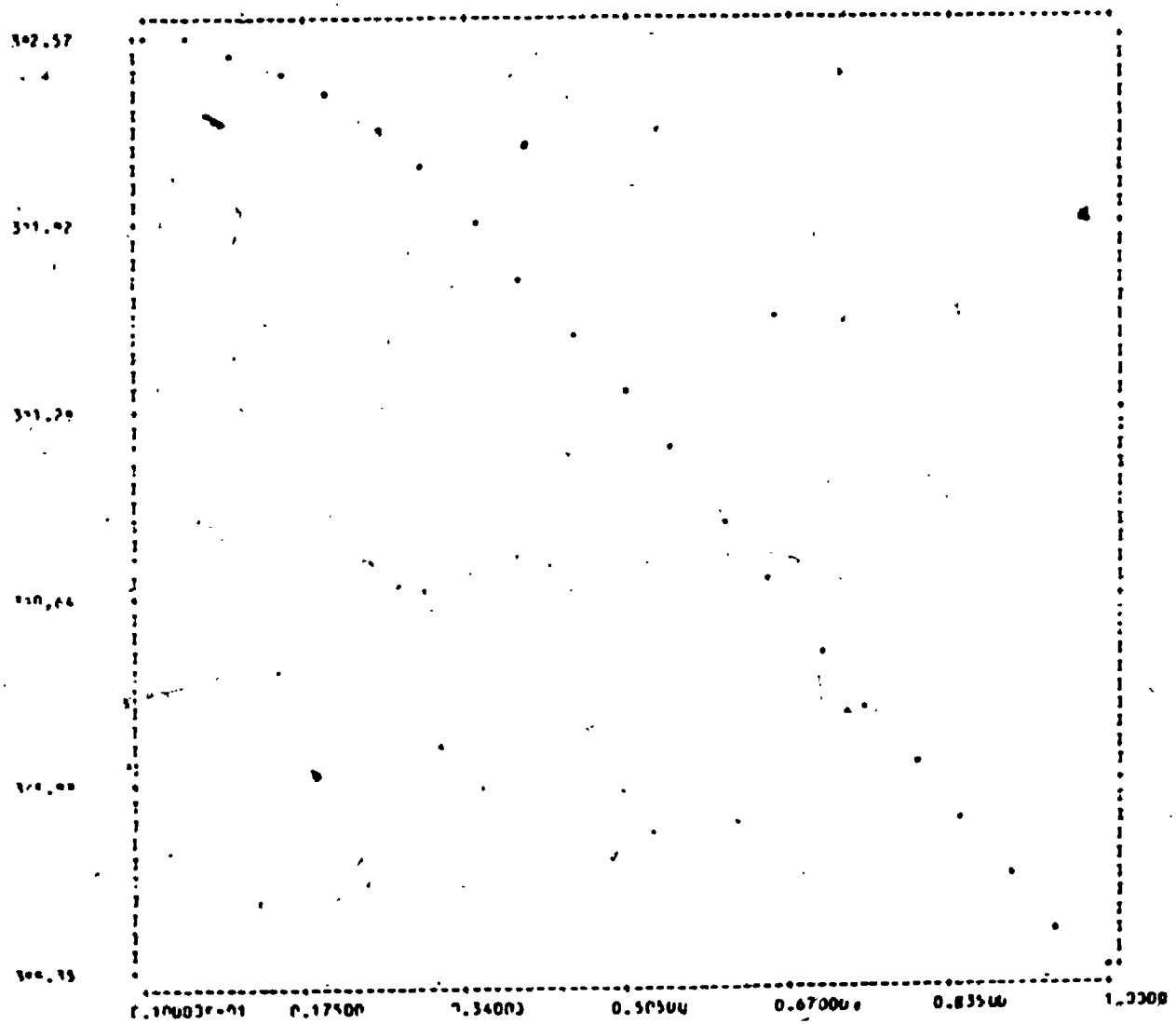

APPENDIX C

A SUMMARY OF SOME EXPERIMENTAL DATA

Table C.1: Equilibrium Data Used to Determine the Adsorption Isotherm of Glucose in Calcium Alginate Gel

Initial conc. of glucose in the liquid phase, C_L^o ($kg \cdot m^{-3}$)	Equilibrium conc. of glucose in the liquid phase, C_L^∞ ($kg.m^{-3}$)	Equilibrium conc. of glucose in calcium alginate gel		
		kg of glucose / m^3 of gel (C_S^∞)	kg of glucose / kg of wet gel(a) $[C_S^\infty]_{wet} \times 10^3$	kg of glucose / kg of dry gel (b) $[C_S^\infty]_{dry} \times 10^3$
3	2.447	2.442	2.435	63.63
5	3.933	3.921	3.909	102.2
10	8.010	7.850	7.827	204.5
20	16.39	16.39	16.34	427.1
40	32.48	31.47	31.38	820.0
50	39.62	37.80	37.69	984.9
60	49.05	48.36	48.22	1260
120	99.23	98.83	98.53	2575
200	164.0	164.0	163.5	4273
300	252.2	235.3	234.6	6131

Note: Initial concentration of glucose in calcium-alginate gel, $C_S^o = 0\ kg.m^{-3}$

(a) Density of wet Ca-alginate gel = 1,003 $kg \cdot m^{-3}$

(b) Concentration of Ca-alginate in gel on dry wt basis = 38.38 $kg.m^{-3}$

Table C.2: Effect of Calcium Chloride and Barium Chloride Concentration on the Effective Diffusivity of Glucose, Partition Coefficient and Mean Pore Size in Alginate Gels

Characteristics of Na-alginate solution	Type and concentration of chelating agent ($kg.m^{-3}$)	Concentration of alginate in gel, c_g, (kg D.W./m^3 of gel)	Density of spherical alginate bead, ρ, ($kg.m^{-3}$)	Effective diffusivity of glucose, ($D_e \times 10^{10}$, ($m^2.s^{-1}$)	Partition coefficient, K_p	$(D_e/D)^*$	Mean pore diameter,† d_p, (nm)
Na-alginate from Fisher chemicals, Sample #17	$CaCl_2$						
	5	29.1	1,000	6.66	0.983	0.912	36
	20	34.9	1,000	6.54	1.00	0.895	28
conc. of Na-alginate solution =	40	38.4	1,003	6.66	0.98	0.912	36
20 $kg.m^{-3}$	80	41.2	1,005	5.83	0.977	0.800	14
(or on a dry wt. basis = 17.3 kg	$BaCl_2$						
	5	36.1	1,000	6.51	0.98	0.892	29
D.W./m^3)	20	40.0	1,001	5.94	1.00	0.813	15
	40	46.0	1,005	5.83	1.00	0.800	14
	80	47.4	1,014	5.13	0.975	0.703	9.1

* Free phase diffusivity of glucose at 30°C and C_L^o = 20 $kg.m^{-3}$ was taken as 7.30×10^{-10} $m^2.s^{-1}$ (Calculated using Equation 5.17)

† Estimated using the Renkin equation (see also Figure 5.26)

Table D.1: The Effect of Glucose Concentration and Temperature on Diffusion Coefficients, D, of Glucose in Water (From Dadenkova et al., 1973)

Glucose Concentration, C_L ($kg.m^{-3}$)	Diffusion Coefficient, D, of Glucose in Water $D \times 10^{10}$, ($m^2\ s^{-1}$)					
	T=25°C	T=30°C	T=40°C	T=50°C	T=60°C	T=70°C
25.2	6.3	7.1	9.2	11.4	14.3	17.5
50.9	6.0	6.7	8.8	11.0	13.7	16.8
103.7	5.5	6.25	8.2	10.3	12.9	16.0
215.9	4.6	5.3	6.9	8.9	11.2	14.3
337.4	3.8	4.5	5.9	7.6	9.8	12.6
469.0	3.2	3.7	4.95	6.4	8.2	10.8
611.7	2.5	3.0	4.1	5.3	7.0	9.4
707.6	1.9	2.2	3.3	4.2	5.7	7.9
937.0	1.25	1.6	2.4	3.2	4.4	6.2

Table C.4: Effect of Entrapped Yeast Cell Concentration on Effective Diffusivity and Partition Coefficient of Glucose

Conc. of Yeast Cells		Volume Fraction of Cells, β	Density of Alginate Bead, ρ_b, ($kg.m^{-3}$)	Effective Diffusivity of Glucose, $D_e \times 10^{10}$, ($m^2.s^{-1}$)	Partition Coefficient, K_p	(D_e/D)**
c_g, (kg D.W./m^3 of gel)	X,* (kg wet wt./L of gel)					
27.14	0.136	0.027	1,003	6.61	0.960	0.906
51.72	0.259	0.051	1,000	6.19	0.960	0.848
71.04	0.355	0.070	1,005	5.67	0.933	0.777
88.74	0.444	0.088	1,000	5.09	0.930	0.697
118.3	0.592	0.119	1,002	4.67	0.898	0.640

* Calculated by assuming 80% water content in yeast cells (i.e., $X = 5\ c_g/1000$)

** Free phase diffusivity of glucose was taken as $7.30 \times 10^{-10}\ m^2.s^{-1}$ (at 30°C and $C_L^o = 20\ kg.m^{-1}$)

APPENDIX D

Analysis of Literature Data On Diffusivity of Glucose in Water

Table D.1: The Effect of Glucose Concentration and Temperature on Diffusion Coefficients, D, of Glucose in Water (From Dadenkova et al., 1973)

Glucose Concentration, C_L ($kg.m^{-3}$)	Diffusion Coefficient, D, of Glucose in Water $D \times 10^{10}$, ($m^2\ s^{-1}$)					
	T=25°C	T=30°C	T=40°C	T=50°C	T=60°C	T=70°C
25.2	6.3	7.1	9.2	11.4	14.3	17.5
50.9	6.0	6.7	8.8	11.0	13.7	16.8
103.7	5.5	6.25	8.2	10.3	12.9	16.0
215.9	4.6	5.3	6.9	8.9	11.2	14.3
337.4	3.8	4.5	5.9	7.6	9.8	12.6
469.0	3.2	3.7	4.95	6.4	8.2	10.8
611.7	2.5	3.0	4.1	5.3	7.0	9.4
707.6	1.9	2.2	3.3	4.2	5.7	7.9
937.0	1.25	1.6	2.4	3.2	4.4	6.2

Figure D.1: Arrhenius plots for determination of activation energies for diffusion of glucose at different concentrations (Based on the data from Dadenkova *et al.*, 1973).

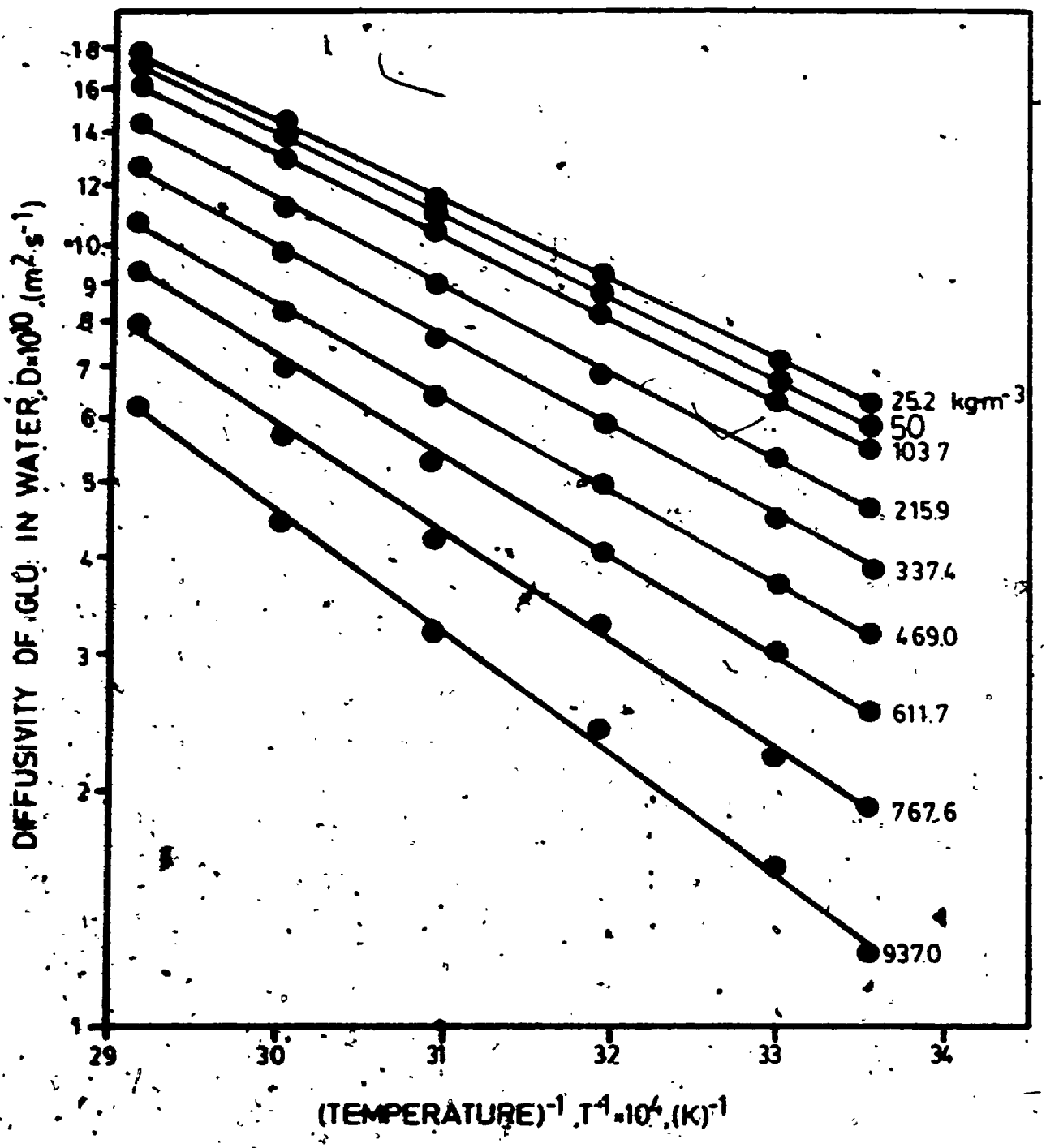
DIFFUSIVITY OF GLU. IN WATER, D=10^10 (m^2·s^-1)
18
16
14
12
10
9
8
7
6
5
4
3
2
1
29
30
31
32
33
34
(TEMPERATURE)^-1, T^-1·10^4, (K)^-1
25.2 kgm^-3
50
103.7
215.9
337.4
469.0
611.7
767.6
937.0

Table D.2: Activation Energy for Diffusion of Glucose in Water at Different Concentrations (Based on the Data of Dadenkova et al., 1973)

Glucose Concentration, C_L, ($kg.m^{-3}$)	Arrhenius Parameters: Pre-exponential Constant,* $A \times 10^6$, ($m^2.s^{-1}$)	Arrhenius Parameters: Activation Energy,* E_a, ($kJ.mol^{-1}$)	Coefficient of determination, (r^2)
25.2	1.551	19.36	0.9999
50.9	1.634	19.61	0.9998
103.7	1.895	20.18	0.9999
215.9	2.478	21.29	0.9999
337.4	3.156	22.34	0.9998
469.0	3.085	22.74	0.9996
611.7	5.009	24.52	0.9994
707.6	8.852	26.65	0.9985
937.4	18.86	29.46	0.9987

Non-Linear Regression Analysis: $A=A^o \exp(b_c C_L)$,	Linear Regression Analysis: $E_a = E_a^o + mC_L$
$A^o = 1.36 \times 10^{-6}\ m^2.s^{-1}$	$m = 0.01028\ kJ.mol^{-1}/kg.m^{-3}$
$b_c = 2.48 \times 10^{-3}\ m^3.kg^{-1}$	$E_a^o = 18.89\ kJ.mol^{-1}$
$r^2 = 0.9506$	$r = 0.9868$

* Calculated using the Arrhenius relationship, $D = A \exp(-E_a/\bar{R}T)$ by non-linear regression analysis with $\bar{R} = 8.3143\ kJ.mol^{-1}$.

Figure D.2: Effect of glucose concentration on the activation energy for diffusion of glucose in water.

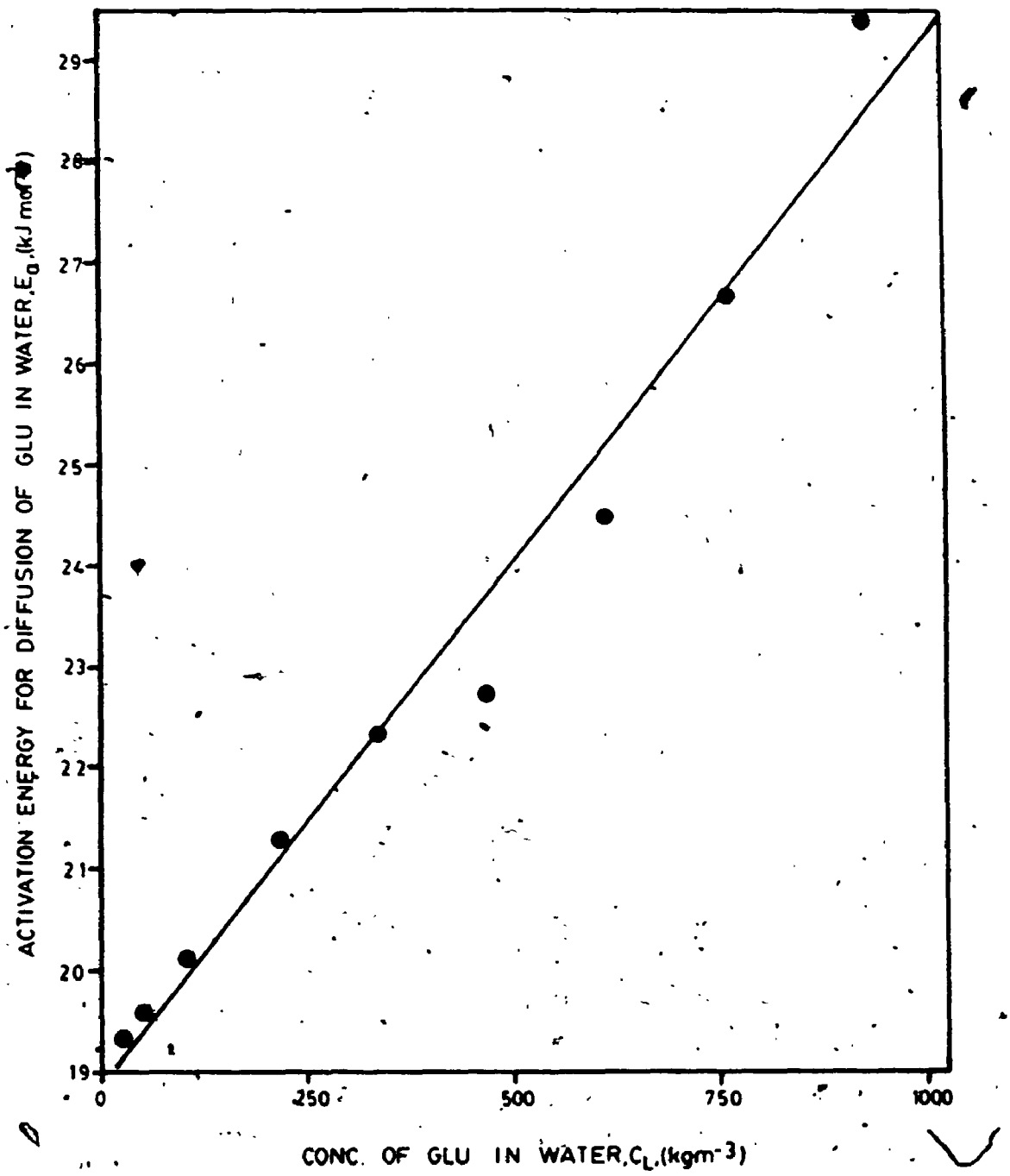
ACTIVATION ENERGY FOR DIFFUSION OF GLU IN WATER, E_a, (kJ mol^{-1})
29
28
27
26
25
24
23
22
21
20
19
0
250
500
750
1000
CONC. OF GLU IN WATER, C_L, (kgm^{-3})

Figure D.3: The Arrhenius pre-exponential constant, A, plotted as a function of glucose concentration.

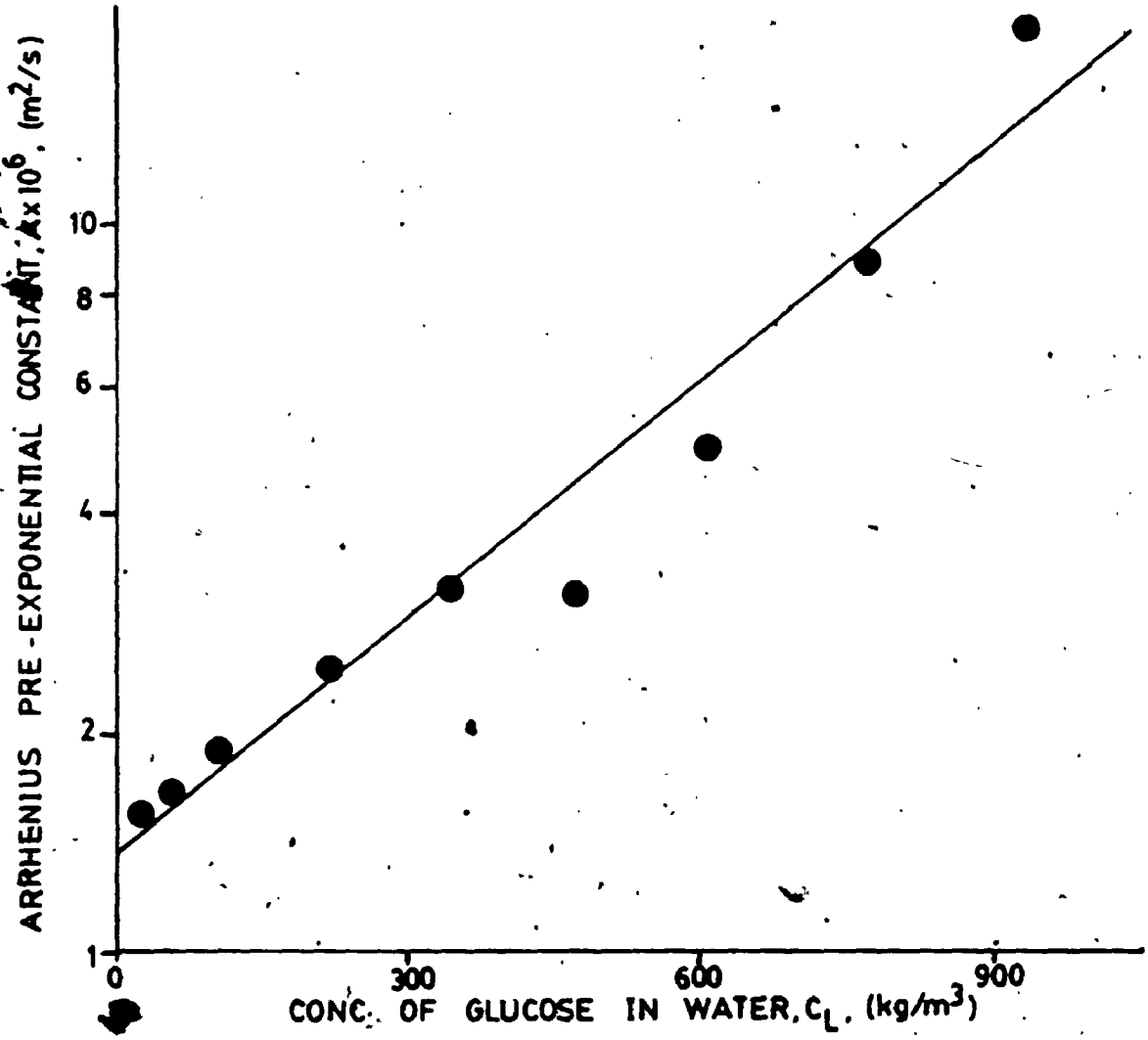
ARRHENIUS PRE-EXPONENTIAL CONSTANT, A x 10^6, (m^2/s)
10
8
6
4
2
1
0
300
600
900
CONC. OF GLUCOSE IN WATER, C_L, (kg/m^3)

Figure D.4: Diffusion coefficients of glucose in water plotted as a function of its concentration, with temperature as the variable parameter (Based on the data from Dadenkova et al., 1973).

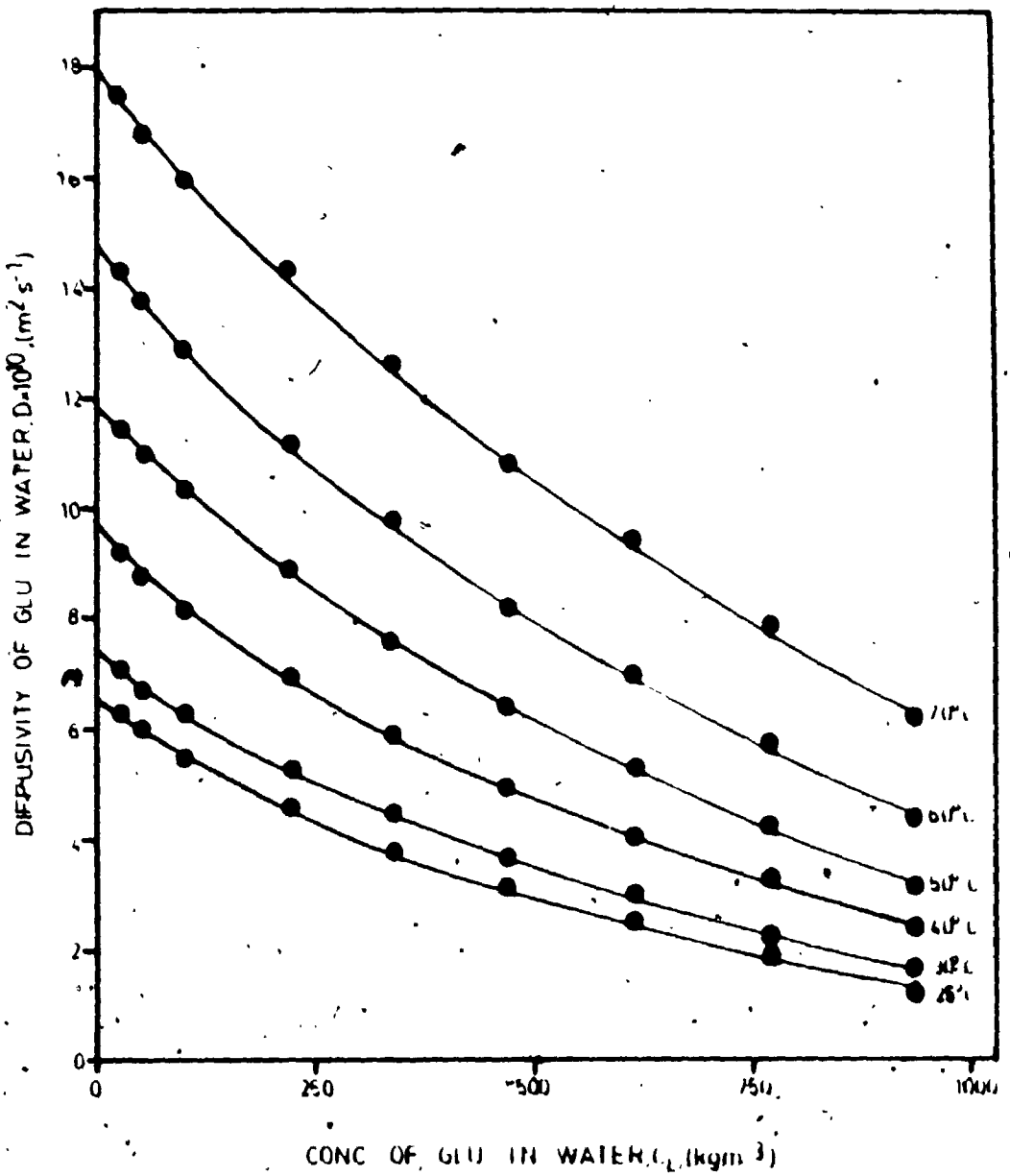
DIFFUSIVITY OF GLU IN WATER, D×10^10 (m² s⁻¹)
CONC OF GLU IN WATER, C_L (kgm⁻³)
0
2
4
6
8
10
12
14
16
18
0
250
500
750
1000

Table D.3: Non-Linear Regression Analysis of Diffusivity Values of Glucose in Water as a Function of Glucose Concentration at Different Temperatures to Determine D_o and b_T (Analysis Based on the Experimental Data of Dadenkova et al., 1973)

Temperature, (K).	298	303	313	323	333	343	Regression Analysis
y-intercept = diffusivity at infinite dilution, $D_o \times 10^{10}$, $(m^2.s^{-1})$	6.68	7.48	9.53	11.94	14.78	18.06	Non-Linear:- $D_o = A^o \exp(-E_a^o/RT)$ $A^o = 1.36\times10^{-6} m^2.s^{-1}$ $E_a^o = 18.89\ kJ.mol^{-1}$ $r^2 = 0.9990$
Temperature dependent exponential constant, $b_T \times 10^3$, $(m^3.kg^{-1})$	1.69	1.59	1.42	1.37	1.26	1.10	Linear:- $b_T = b_o - yT$ $y = 1.22\times10^{-5} m^3.kg^{-1}.K^{-1}$ $b_o = 5.29\times10^{-3} m^3.kg^{-1}$ $r = 0.9885$

Figure D.5: The Arrhenius plot for diffusion of glucose at infinite dilution.

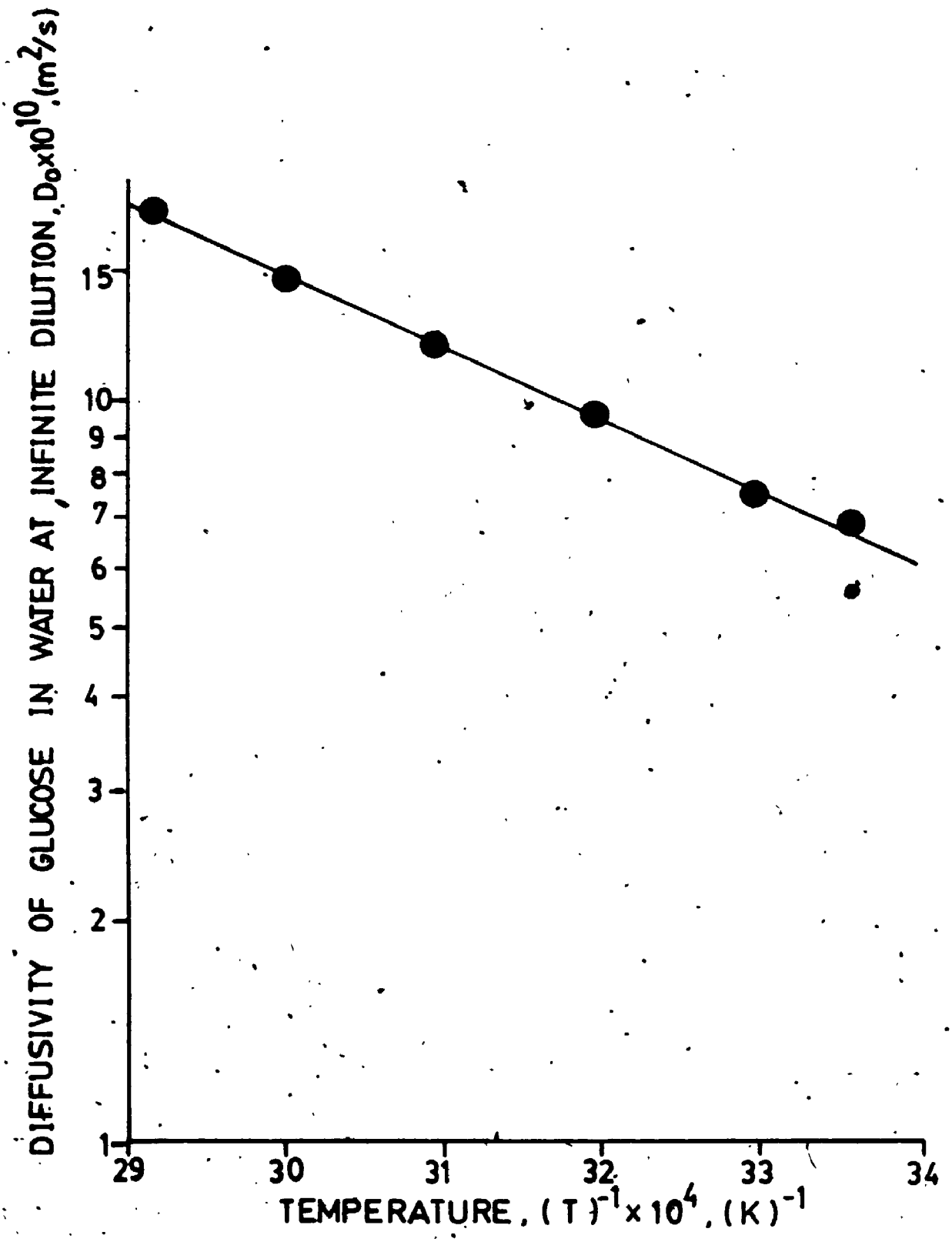
DIFFUSIVITY OF GLUCOSE IN WATER AT INFINITE DILUTION, $D_0 \times 10^{10}$, (m^2/s)
15
10
9
8
7
6
5
4
3
2
1
29
30
31
32
33
34
TEMPERATURE, $(T)^{-1} \times 10^4$, $(K)^{-1}$

Figure D.6: The exponential constant in Equation 5.18, b_T, plotted as a function of absolute temperature.

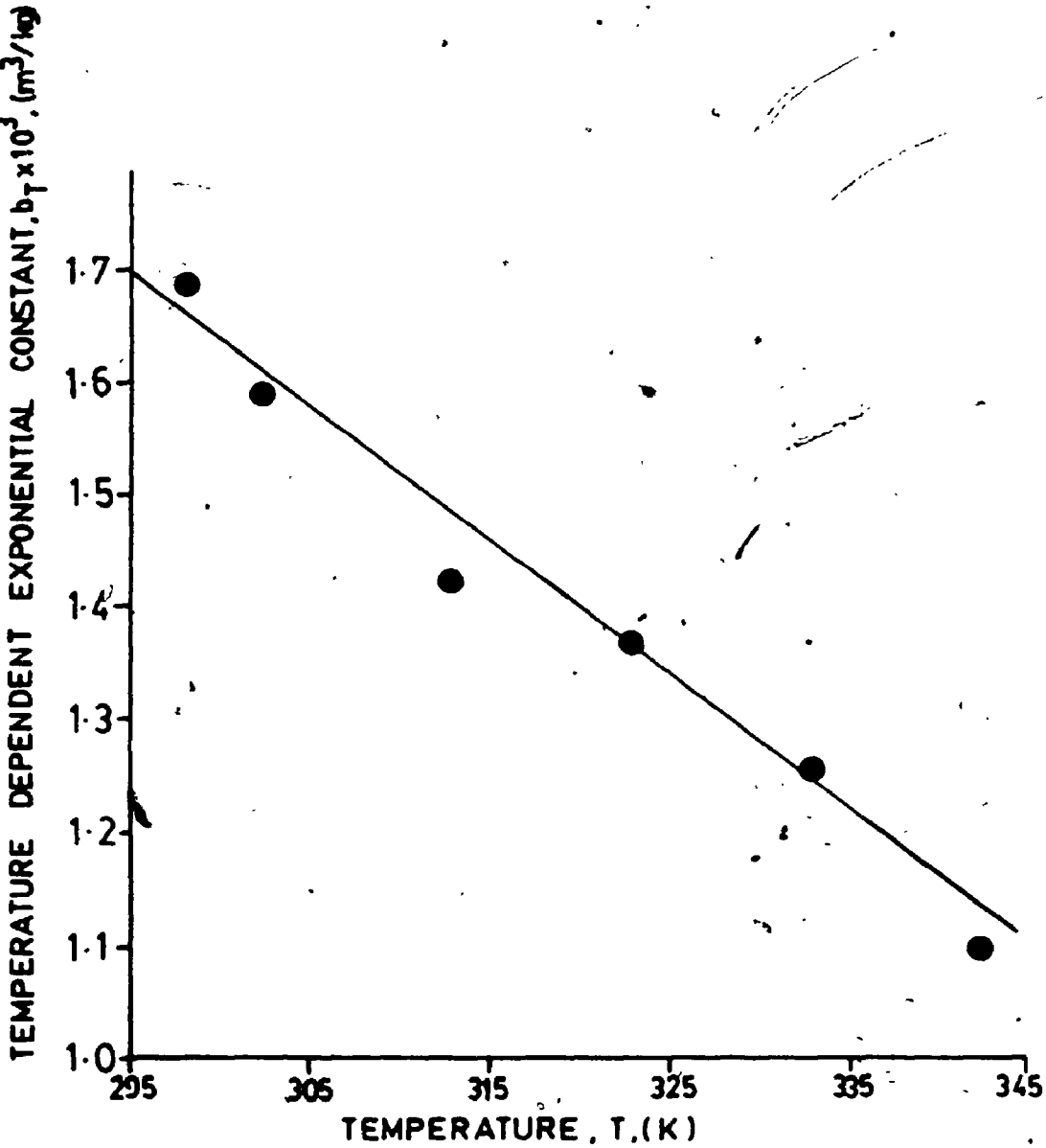
TEMPERATURE DEPENDENT EXPONENTIAL CONSTANT, $b_T \times 10^3$, (m^3/kg)
1·7
1·6
1·5
1·4
1·3
1·2
1·1
1·0
295
305
315
325
335
345
TEMPERATURE, T, (K)

REFERENCES

Abbott, B.J. 1977. Immobilized cells, In, Annual Reports on Fermentation Processes, vol. I, Perlman, D., (ed.), Academic Press, New York, 205.

Ackers, G.K., and Steere, R.L. 1962. Restricted diffusion of macromolecules through agar-gel membranes, Biochem. Biophys. Acta, 59, 137.

Aris, R. 1957. Shape factors for irregular particles. I. The steady-state problem. Diffusion and reaction, Chem. Eng. Sci., 6, 262.

Aris, R. 1965a. A normalization for the Thiele modulus, Ind. Eng. Chem. Fundamentals, 4, 227.

Aris, R. 1965b. A normalization for the Thiele modulus, Ind. Eng. Chem. Fundamentals, 4, 487.

Aris, R. 1975. The Mathematical Theory of Diffusion and Reaction in Permeable Catalysts, Clarendon Press, Oxford.

Atkins, E.D.T., Mackie, W., Parker, K.D., and Smolko, E.E. 1971. Crystalline structures of poly-D-mannuronic and poly-L-guluronic acids, J. Polymer Sci., Part B: Polymer Lett., 9, 311.

Atkinson, B. 1974. Biochemical Reactors, Pion Ltd., London.

Atkinson, B., Black, G.M., and Pinches, A. 1980. Process intensification using cell support systems, Process Biochem., May 1980, 24.

Bailey, J.E., and Cho, Y.K. 1983. Immobilization of glucoamylase and glucose oxidase in activated carbon: Effects of particle size and immobilization conditions on enzyme activity and effectiveness, Biotechnol. Bioeng., 25, 1923.

Bailey, J.E., and Ollis, D.F. 1977. Biochemical Engineering Fundamentals, 1st Edition, McGraw-Hill, New York.

5 of/de 5

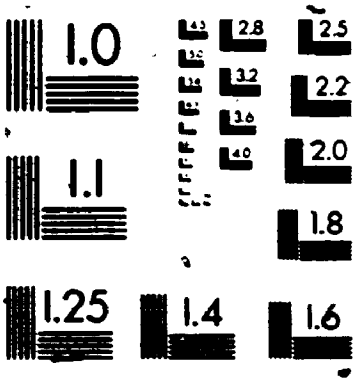

Bailey, J.E., and Ollis, D.F. 1986. Biochemical Engineering Fundamentals, 2nd Edition, McGraw-Hill, New York.

Bailliez, C., Largeau, C., and Casadevall, E. 1985. Growth and hydrocarbon production of Botryococcus braunii immobilized in calcium alginate gel, Appl. Microbiol. Biotechnol., 23, 99.

Bates, F., Phelps, F.P., and Syner, C.F. 1929. Saccharimetry, the properties of commercial sugars and their solutions, In, International Critical Tables, Washburn, E.W., (ed.), McGraw-Hill, New York.

Beck, R.E., and Schultz, J.S. 1972. Hindrance of solute diffusion within membranes as measured with microporous membranes of known pore geometry, Biochim. Biophys. Acta, 255, 273.

Belton, P.S., and Wilson, R.H. 1982. An experimentally simple method for measuring diffusion in food gels, J. Fd. Technol., 17, 531.

Birnbaum, S., Pendleton, R., Larsson, P.O., and Mosbach, K. 1981. Covalent stabilization of alginate gel for the entrapment of living whole cells, Biotechnol. Lett., 3, 393.

Bischoff, K.B. 1965. Effectiveness factors for general reaction rate forms, A.I.Ch.E.J., 11, 351.

Blanch, H.W. 1984. Engineering challenges of genetic engineering, Biotechnol. Bioeng. Symp. Ser., No. 13, 467.

Bordelius, P. 1984. Immobilized viable plant cells, Ann. N.Y. Acad. Sci., 419, 382.

Bordelius, P., Deus, B., Mosbach, K., and Zenk, M.H. 1979. Immobilized plant cells for the production and transformation of natural products, FEBS Lett., 103, 93.

Bressan, J.A., Carroud, P.A., Merson, R.L., and Dunkley, W.L. 1981. Modeling of isothermal diffusion of whey components from small curd cottage cheese during washing, J. Food. Sci., 47, 84.

Brink, L.E.S., and Tramper, J. 1986. Modelling the effects of mass transfer on kinetics of propene epoxidation of immobilized Mycobacterium cells: 1. Pseudo-one-substrate conditions and negligible product inhibition, Enzyme Microb. Technol., 8, 281.

Brown, W., and Chitumbo, K. 1975a. Solute diffusion in hydrated polymer networks, Part I. - Cellulose gels, J. Chem. Soc. Faraday Trans.I., 71, 1.

Brown, W., and Chitumbo, K. 1975b. Solute diffusion in hydrated polymer networks, Part II - Polyacrylamide, hydroxyethylcellulose and cellulose gels, J. Chem. Soc. Faraday Trans. I, 71, 12.

Brown, W., and Johnsen, R.M. 1981a. Diffusion in polyacrylamide gels, Polymer, 22, 185.

Brown, W., and Johnsen, R.M. 1981b. Transport from an aqueous phase through cellulosic gels and membranes, J. Polymer Sci., 26, 4135.

Brown, W., Kloow, G., Chitumbo, K., and Amu, T. 1976. Solute diffusion in polymer networks. Part 3. - Hydroxyethylcellulose gels; solvent effects and fluoresence depolarization measurements, J. Chem. Soc. Faraday Trans., I, 72, 485.

Bryce, T.A., McKinnon, A.A., Morris, E.R., Rees, D.A., and Thom, D. 1974. Chain conformation in the sol-gel transitions for polysaccharide systems and their characterization by spectroscopic methods, Faraday Discuss. Chem. Soc., 57, 221.

Buccholz, K. 1979. External mass transfer, In, Characterization of Immobilized Biocatalysts, DECHEMA Monograph No. 1724-1731, Verlag-Chimie, Weinheim, 84, 212.

Buccholz, K. 1982. Reaction engineering parameters for immobilized biocatalysts, Adv. Biochem. Eng., 24, 39.

Buchholz, K., and Godelmann, B. 1978. Pressure drop across compressible beds, In, Enzyme Engineering, vol. 4, Broun, G.B., Manecke, G., and Wingard, L.B. Jr., (eds.), Plenum Press, New York, 89.

Bungay, H.R., Whalen, W.J., Sanders, W.M. 1969. Microprobe techniques for determining diffusivities and respiration rates in microbial slime systems, Biotechnol. Bioeng., 11, 765.

Bunting, P.S., and Laidler, K.J. 1972. Kinetic studies on solid-supported β-galactosidase, Biochemistry, 11, 4477.

Burns, M.A., Kvesitadze, G., and Graves, D.J. 1985. Dried calcium alginate/magnetite spheres: A new support for chromatographic separations and enzyme immobilization, Biotechnol. Bioeng., 27, 137.

Busk, G.G., and Labuza, T.P. 1979. A dye diffusion technique to evaluate gel properties, J. Food Sci., 44, 1369.

Carberry, J.J. 1976. Chemical and Catalytic Reaction Engineering, McGraw-Hill, New York.

Carman, P.C., and Haul, R.A.W. 1954. Measurement of diffusion coefficients, Proc. Royal Soc., (London), A222, 109.

Cheetham, P.S.J. 1979. Physical studies on the mechanical stability of columns of calcium alginate gel pellets containing entrapped microbial cells, Enzyme Microb. Technol., 1, 183.

Cheetham, P.S.J., Blunt, K.W., and Bucke, C. 1979. Physical studies on cell immobilization using calcium alginate gels, Biotechnol. Bioeng., 21, 2155.

Chen, W.P., Chen, J.Y., Chang, S.C., and Su, C.L. 1985. Bacterial alginate produced by a mutant of Azotobacter vinelandii, Appl. Environ. Microbiol., 49, 543.

Cho, G.H., Choi, C.Y., Choi, Y.D., and Han, M.H. 1982. Ethanol production by immobilized yeast and its CO_2 gas effects in a packed bed reactor, J. Chem. Tech. Biotechnol., 32, 959.

Cranks, J. 1975. The Mathematics of Diffusion, Clarendon Press, Oxford.

Cussler, E.L. 1984. Diffusion - Mass Transfer in Fluid Systems, Cambridge University Press, Cambridge.

Dadenkova, M.N., Zhomyrya, L.P., Danileiko, V.M., Burdukova, R.S. 1973. Coefficient of mutual diffusion in glucose-water system, Izv. Vyssh. Ucheb. Zaved., Pishch.Tekhnol., 5, 124.

Dainty, A.L., Goulding, K.H., Robinson, P.K., Simpkins, I., and Trevan, M.D. 1986. Stability of alginate-immobilized algal cells, Biotechnol. Bioeng., 28 210.

Derbyshire, W., and Duff, I.D. 1974. NMR of agarose gels, Faraday Discuss. Chem. Soc., 57, 243.

Desai, M., and Schwartzberg, H. 1980. Mathematical modeling of leaching processes, In, Food Process Engineering, vol.1, Linko, P., and Larinkari, J., (eds.), Applied Science, London, 86.

Dibdin, G.H. 1981. Diffusion of sugars and carboxylic acids through human dental plaque in vitro, Arch. Oral Biol., 26, 515.

Dickinson, J.R. 1982. ESOP: Users Instructions, Engineering Systems Optimization Package, System Analysis, Control and Design Activity - Report No. SACDA 80-21, Faculty of Engineering, University of Western Ontario, London, Canada.

Donnan, F.G., and Rose, R.C. 1950. Osmotic pressure, molecular weight, and viscosity of sodium alginate, Can. J. Research, 28B, 105.

Engasser, J.M. 1978. A fast evaluation of diffusion on bound enzyme activity, Biochim. Biophys. Acta, 526, 301.

Engasser, J.M., and Horvath, C. 1973. Effect of internal diffusion in heterogeneous enzyme systems: Evaluation of true kinetic parameters and substrate diffusivity, J. Theor. Biol., 42, 137.

Engasser, J.M., and Horvath, C. 1976 . Diffusion and kinetics with immobilized enzymes, In, Applied Biochemistry and Bioengineering, Vol. 1, Wingard, L.B., Katchalski, E., and Goldstein, L., (eds.), Academic Press, New York, 127.

Ferrero, F., Campagna, P., and Piccinini, N. 1982. Kinetics of shrinking of Ca-alginate beads, Chem. Eng. Commun., 15, 197.

Ferry, J.D. 1936. Statistical evaluation of sieve constants in ultrafiltration, J. Gen. Physiol., 20, 95.

Fink, D.J., Na, T.Y., and Schultz, J.S. 1973. Effectiveness factor calculations for immobilized enzyme catalysts, Biotechnol. Bioeng., 15, 879.

Friedman, L. 1930a. Diffusion of non-electrolytes in gelatin gels, J. Am. Chem. Soc., 52, 1305.

Friedman, L. 1930b. Structure of agar gels from studies on diffusion, J. Am. Chem. Soc., 52, 1311.

Friedman, L., and Kramer, E.O. 1930. The structure of gelatin gels from studies of diffusion, J. Am. Chem. Soc., 52, 1295.

Friedman, L., and Carpehter, P.G. 1939. Diffusion velocity and molecular weight. I. The limits of validity of the Stokes-Einstein diffusion equation, J. Am. Chem. Soc., 61, 1745.

Fukushima, S., and Hanai, S. 1982. Pilot operation for continuous alcohol fermentation of molasses in an immobilized bioreactor, In, Enzyme Engineering, Vol. 6, Chibata, I., Fukushima, S., and Wingard, L.B., (eds.), Plenum Press, New York, 347.

Furui, M., and Yamashita, K. 1985. Diffusion coefficients of solutes in immobilized cell catalysts, J. Ferment. Technol., 63, 167.

Furui, M., and Yamashita, K. 1985. Horizontal baffle effects on compaction of immobilized cell catalyst beads, J. Ferment. Technol., 63, 73.

Furusaki, S., Okamura, Y., and Miyauchi, T. 1982. Influence of compaction in gel-immobilized enzyme packed bed reactors, In, Enzyme Engineering, vol. 6., Chibata, I., Fukui, S., and Wingard, L.B., (eds.), Plenum Press, New York, 315.

Furusaki, S., Seki, M., and Fukumura, K. 1983. Reaction characteristics of an immobilized yeast producing ethanol, Biotechnol. Bioeng., 25, 2921.

Furusawa, T., and Smith, J.M. 1973. Fluid-particle and intraparticle mass transport rates in slurries, Ind. Eng. Chem. Fundam., 12, 197.

Geankoplis, C.J. 1972. Mass Transport Phenomena, Holt, Rinehart and Winston, New York.

Geankoplis, C.J. 1983. Transport Processes and Unit Operations, Allyn and Bacon, Massachusetts.

Georgiou, G., Chalmers, J.J., Shuler, M.L., and Wilson, D.B. 1985. Continuous immobilized recombinant protein production from E. coli capable of selective protein excretion: A feasibility study, Biotechnol. Progress, 1, 75.

Ghose, T.K., and Bandyopadhyay, K.K. 1982. Studies on immobilized Saccharomyces cerevisiae. II. Effect of temperature distribution on continuous rapid ethanol formation in molasses fermentation, Biotechnol. Bioeng., 20, 1903.

Gladden, J.K., and Dole, M. 1953. Diffusion in supersaturated solutions. II. Glucose solutions, J. Am. Chem. Soc., 75, 3900.

Glasstone, S., Laidler, K.J., and Eyring, H. 1941. The Theory of Rate Processes, McGraw-Hill, N.Y.

Goldstein, L. 1976. Kinetic behaviour of immobilized enzyme systems, In, Methods in Enzymology, vol. 44, Mosbach, K., (ed.), Academic Press, New York, 397.

Goldstein, L., Levin, Y., and Katchalski, E. 1964. A water-insoluble polyanionic derivative of trypsin. II. Effect of the polyelectrolyte carrier on the kinetic behaviour of the bound trypsin, Biochemistry, 3, 1913.

Gondo, S., Isayama, S., and Kusunoki, K. 1975. Effects of internal diffusion on the Lineweaver-Burk plots for immobilized enzymes, Biotechnol. Bioeng., 17, 423.

Gosmann, B., and Rehm, H.J. 1986. Oxygen uptake of microorganisms entrapped in Ca-alginate, Appl. Microbiol. Biotechnol., 23, 163.

Grant, G.T., Morris, E.R., Rees, D.A., Smith, P.J.C., and Thom, D. 1973. Biological interactions between polysaccharides and divalent cations: The egg-box model, FEBS Lett., 32, 195 . .

Hackel, U., Klein, J., Megnet, R., and Wagner, F. 1975. Immobilization of microbial cells in polymeric matrices, Eur. J. Appl. Microbiol., 1, 291.

Hadler, N.M. 1980. Enchaned diffusivity of glucose in a matrix of hyaluronic acid, J. Biol. Chem., 255, 3532.

Hamilton, B.K., Gardner, C.R., and Colton, C.K. 1974. Effect of diffusional limitations on Lineweaver-Burk plots for immobilized enzymes, A.I.Ch.E.J., 20, 503.

Hannoun, B., and Stephanopoulos, G. 1986. Diffusion coefficients of glucose and ethanol in cell-free and cell occupied calcium alginate membranes, Biotechnol. Bioeng., 28, 829.

Hashimoto, K., Miura, K., and Nagata, S. 1975. Intraparticle diffusivities in liquid-phase adsorbtion with non-linear isotherms, J. Chem. Eng. Japan, 8, 367.

Haug, A., and Larsen, B. 1962. Quantitative determination of the uronic acid composition of alginates, Acta. Chem. Scand., 16, 1908.

Haug, A., and Smidsrod, O. 1962. Determination of instrinsic viscosity of alginates, Acta Chem. Scand., 16, 1569.

Haug, A., and Smidsrod, O. 1965. The effect of divalent metals on the properties of alginate solutions, II. Comparison of different metal's ions, Acta Chem. Scand., 19, 329.

Haug, A., Larsen, B., and Smidsrod, O. 1966. A study of the constitution of alginic acid by partial acid hydrolysis, Acta Chem. Scand., 20, 183.

Haug, A., Larsen, B., and Smidsrod, O. 1967a. Studies on the sequence of uronic acid residues in alginic acid, Acta Chem. Scand., 21, 691.

Haug, A., Mykiestad, S., Larsen, B., and Smidsrod, O. 1967b. Correlation between chemical structure and physical properties of alginates, Acta Chem. Scand., 21, 768.

Haug, A., Larsen, B., and Smidsrod, O. 1974. Uronic acid sequence in alginate from different sources, Carbohydrate Res., 32, 217.

Helfferich, F. 1962. Ion Exchange, McGraw-Hill, New York.

Heimstra, H., Dijkhuizen, L., and Harder, W. 1983. Diffusion of oxygen in alginate gels related to the kinetics of methanol oxidation by immobilized Hansenula polymorpha cells, Eur. J. Appl. Microbiol. Biotechnol., 18, 189.

Hirst, E.L., Percival, E., and Wold, J.K. 1964. The structure of alginic acid. Part 4. Partial hydrolysis of the reduced polysaccharide, J. Chem. Soc., 57, 1493.

Horowitz, S.B., and Fenichel, I.R. 1964. Solute diffusional specificity in hydrogen-bonding system, J. Phys. Chem., 68, 3378.

Horvath, C., and Engasser, J.M. 1974. External and internal diffusion in heterogenous enzyme systems, Biotechnol. Bioeng., 16, 909.

Hu, M.C., Haering, E.R., and Geankoplis, C.J. 1985. Diffusion and adsorption phenomena in an immobilized enzyme reactor using adsorbed polymer for attachment of the enzyme in porous alumina particles, Chem. Eng. Sci., 40, 2241.

Huang, T.C., and Li, K.Y. 1973. Ion-exchange kinetics for calcium radiotracer in a batch system, Ind. Eng. Chem. Fundam., 12, 50.

Hubble, J., and Newman, J.D. 1985. Alginate ultrafiltration membranes, Biotechnol. Lett., 7, 273.

Imeson, A.P., Mitchell, J.R., and Ledward, D. 1980. Rheological properties of spinning dopes and spun fibres produced from plasma-alginate mixtures, J. Food Technol., 15, 319.

Jain, D., and Ghose, T.K. 1984. Cellobiose hydrolysis using Pichia etechellsii cells immobilized in calcium alginate, Biotechnol. Bioeng., 26, 340.

Johansen, A., and Flink, J.M. 1986a. Immobilization of yeast cells by internal gelation of alginate, Enzyme Microb. Technol., 8, 145.

Johansen, A., and Flink, J.M. 1986b. Influence of alginate properties on sucrose inversion by immobilized whole cell invertase, Enzyme Microb. Technol., 8, 485.

Karabelos, A.J., Wegner, T.H., and Hauratty, T.J. 1971. Use of asymptotic relations to correlate mass transfer data in packed beds, Chem. Eng. Sci., 26, 1581.

Karel, S.F., Libicki, S.B., and Robertson, C.R. 1985. The immobilization of whole cells: Engineering principles, Chem. Eng. Sci., 40, 1321.

Kasche, V. 1983. Correlations of experimental and theoretical data for artificial and natural systems with immobilized biocatalysts, Enzyme Microb. Technol., 5, 2.

Kennedy, J.F., and Cabral, J.M.S. 1983. Immobilized living cells and their applications, In, Applied Biochemistry and Bioengineering, vol. 4, Chibata, I., and Wingard, L.B., (eds.), Academic Press, New York, 189.

Klein, J., Washausen, P., Kluge, M., and Eng. H. 1980. Physical characterization of biocatalyst particles obtained from polymer entrapment of whole cells, In, Enzyme Engineering, vol. 5, Weetall, H.H., and Royer, G.P., (eds.), Plenum Press, New York, 359.

Klein, J., Stock, J., and Vorlop, K.D. 1983. Pore size and properties of spherical calcium alginate biocatalysts, Eur. J. Appl. Microbiol. Biotechnol., 18, 86.

Klemm, K., and Friedman, L. 1932. The structure of cellulose acetate gels from studies of diffusion, J. Am. Chem. Soc., 54, 2637.

Komiyama, H., and Smith, J.M. 1974a. Intraparticle mass transport in liquid filled pores, A.I.Ch.E.J., 20, 728.

Komiyama, H., and Smith, J.M. 1974b. Surface diffusion in liquid filled pores, A.I.Ch.E.J., 20, 1110.

Krouwel, P.G., Harder, A., and Kossen, N.W.F. 1982. Tensile stress-strain measurements of materials used for cell immobilization, Biotechnol. Lett., 4, 103.

Kuu, W.Y. 1982. Fermentation Kinetics for the Production of Ethanol by Immobilized Yeast Cells, Ph.D. Thesis, Dept. of Chemical Engineering, Louisiana State University.

Lamberti, F.V., and Sefton, M.V. 1983. Microencapsulation of erythrocytes in Eudragit-RL-coated calcium alginate, Biochim. Biophys. Acta, 759, 81.

Lane, J.A. 1950. Dialysis, In, Chemical Engineers Handbook, 3rd ed., p. 753, McGraw-Hill, N.Y.

Lauffer, M.A. 1961. Theory of diffusion in gels, Biophys.J., 1, 205.

Laurent, T.C. 1967. Determination of the structure of agarose gels by gel chromatography, Biochim. Biophys. Acta, 136, 199.

Lee, G.K., Lesch, R.A., and Reilly, P.J. 1981. Estimation of intrinsic kinetic constants for pore-diffusion-limited immobilized enzyme reactions, Biotechnol. Bioeng., 23, 487.

Lee, P.I. 1980a. Determination of diffusion coefficients by sorption from a constant finite volume, In, Controlled Release of Bioactive Materials, Baker, R., (ed.), Academic Press, New York, 1985.

Lee, P.I. 1980b. Diffusional release of a solute from a polymeric matrix-approximate analytical solutions, J. Mem. Sci., 7, 255.

Lee, T.H., Ahn, J.C., and Ryu, D.D.Y. 1983. Performance of an immobilized yeast reactor system for ethanol production, Enzyme Microb. Technol., 5, 41.

Leung, Y.F., O'Shea, G.M., Goosen, M.F.A., and Sun, A.M. 1983. Microencapsulation of cystalline insulin or islets of Langerhans: An insulin diffusion study, Artificial Organs, 7, 208.

Leyva-Ramos, R., and Geankoplis, C.J. 1985. Model simulation and analysis of surface diffusion of liquids in porous solids, Chem. Eng. Sci., 40, 799.

Lim, F., and Sun, A.M. 1980. Microencapsulated islets as bioartificial endocrine pancreas, Science, 210, 908.

Linko, P., and Linko, Y.Y. 1984. Industrial applications of immobilized cells, CRC Crit. Rev. Biotechnol., 1, 289.

Linse, L., and Bordelius, P. 1984. Immobilization of plant protoplasts, Ann. N.Y. Acad. Sci., 419, 487.

Longsworth, L.G. 1952. Diffusion measurements, at, 1°, of aqueous solutions of amino acids, peptides and sugars, J. Am. Chem. Soc., 74, 4155.

Longsworth, L.G. 1953. Diffusion measurements, at, 25°C, of aqueous solutions of amino acids, peptides and sugars, J. Am. Chem. Soc., 75, 5705.

Longsworth, L.G. 1954. Temperature dependence of diffusion in aqueous solutions, J. Am. Chem. Soc., 76, 770.

Ma, Y.H., and Evans, L.B. 1968. Transient diffusion from a well-stirred reservoir to a body of arbitrary shape, A.I.Ch.E.J., 14, 956.

Mackie, J.S., and Meares, P. 1955. Sorption of electrolytes by a cation-exchange resin membrane, Proc. R. Soc. Lond. A., 232, 498.

Mackie, W., Sellen, D.B., and Sutcliffe, J. 1977. Spectral broadening of light scattered from alginate gels, J. Polymer Sci.: Polymer Symp., 61, 191.

Manson, J.A., and Chiu, E.H. 1973. Permeation of liquid water in a filled epoxy resin, J. Polym. Sci., C, 41, 95.

Margaritis, A., and Rowe, G.E. 1983. Ethanol production using Zymomonas mobilis immobilized in different carrageenan gels, Dev. Ind. Microbiol., 24, 329.

Margaritis, A., and Merchant, F.J.A. 1984. Advances in ethanol production using immobilized cell systems, CRC Crit. Rev. Biotechnol., 1, 339.

Margaritis, A., and Merchant, F.J.A. 1987. Technology of anaerobic yeast growth, In, Yeast Biotechnology, Berry, D.R., Stewart, G.G., and Russell, I., (eds.), George, Allen and Unwin Ltd., London, In Press.

Margaritis, A., and Pace, G.W. 1985. Microbial polysaccharides, In, Comprehensive Biotechnology, vol. 2, Moo-Young, M., (ed.), Pergamon Press, Oxford, 1005.

Margaritis, A., and Wallace, J.B. 1984. Novel bioreactor systems and their applications, Bio/Technology, 2, 447.

Margaritis, A., Bajpai, P.K., and Wallace, J.B. 1981. High ethanol productivities using small calcium alginate beads of immobilized cells of Zymononas mobilis, Biotechnol. Lett., 3, 613.

Margaritis, A., te Bokkel, D., and El-Khashab, M. 1983. Pilot plant production of ethanol using immobilized yeast cells in a novel fluidized bioreactor system, paper presented at the 186th ACS National Meeting, Washington, D.C. 28th August - 2nd September, 1983.

Marignan, R., and Crouzat-Reynes, G. 1956. Diffusion of electrolytes in solutions, sols, and gels, Trav. Soc. Pharm. Montpelier, 16, 171.

Mathews, A.P., and Weber, W.J.Jr. 1976. Effects of external mass transfer and intraparticle diffusion on adsorbtion rates in slurry reactors, A.I.Ch.E., Symp. Ser., 73, 91.

McCune, L.K., and Wilheim, R.H. 1949. Mass and momentum transfer in solid-liquid systems. Fixed and fluidized beds, Ind. Eng. Chem., 41, 1124.

Matson, J.V., and Characklis, W.G. 1976. Diffusion into microbial aggregates, Water Research, 10, 877.

McDowell, R.H. 1977. Properties of Alginates, 4th Edition, Alginate Industries Ltd., London, England.

Merchant, F.J.A. 1981. The Characteristics of Saccharomyces cerevisiae Immobilized in Calcium Alginate Gel Performing Ethanol Production, M.Sc. Thesis, Dept. of Chemical Engineering, University of Birmingham, England.

Metzner, A.B. 1965. Diffusive transport rates in structured media, Nature, 208, 267.

Michaels, A.S., Vieth, W.R., and Bixler, H.J. 1963. The Measurement of diffusion constants of gases in polymers by sorption techniques, Polymer Lett., 1, 19.

Miller, D.M., and Harun, S.H. 1978. The kinetics of the active and de-energized transport of 0-methyl glucose in Ustilago maydis, Biochim. Biophys. Acta, 514, 320.

Miller, G.L. 1959. Use of dinitrosalicylic acid reagent for determination of reducing sugar, Anal. Chem., 31, 426.

Mitchell, J.R. and Blanshard, J.W.V. 1976. Rheological properties of alginate gels, J. Texture Studies, 7, 219.

Moo-Young, M., and Blanch, H.W. 1981. Design of biochemical reactors. Mass transfer criteria for simple and complex systems, Adv. Biochem. Eng., 19, 1.

Moo-Young, M., and Blanch, H.W. 1983. Kinetics and transport phenomena in biological reactor design. In, Foundations of Biochemical Engineering: Kinetics and Thermodynamics in Biological Systems, Blanch, H.W., Papoutsakis, E.T., and Stephanopoulos, G. (eds.), ACS Symp. Ser., 207, 335-354, ACS, Washington, D.C.

Morris, E.R., Rees, D.A., and Thom, D. 1973. Characterization of polysaccharide structure and interactions of circular dichroism, Order-disorder transition in the calcium alginate system, J. Chem. Soc., Chem, Commun., No. 7, 245.

Mosbach, K. 1984. New immobilization technique and examples of their applications, Ann. N.Y. Acad. Sci., 419, 239.

Mosbach, K., and Birnbaum. S., Hardy, K., Davies, J., and Buelow, L. 1983. Formation of proinsulin by immobilized Bacillus subtilis, Nature, 302, 543.

Mueller, J.A., Boyle, W.C., and Lightfoot, E.N. 1966. Oxygen diffusion through a pure culture floc of Zoogloea ramigera, In, Proceedings 21st Annual Industrial Waste Conference, 964.

Muhr, A.H., and Blanshard, J.M.V. 1982. Diffusion in gels, Polymer, 23, 1012.

Nakanishi, K., Adachi, S., Yamamoto, S., Matsuno, R., Tanaka, A., and Kamikubo, T. 1977. Diffusion of saccharides and amino acids in cross-linked polymers, Agric. Biol. Chem., 41, 2455.

Neretnieks, I. 1976. Adsorbtion in finite batch and counter current flow with systems having a non-linear isotherm, Chem. Eng. Sci., 31, 107.

Ngian, K.F., and Lin, S.H. 1976. Diffusion coefficient of oxygen in microbial aggregates, Biotechnol. Bioeng., 18, 1023.

Nguyen, A.L., and Luong, J.H.T. 1986. Diffusion in κ-carageenan gel beads, Biotechnol. Bioeng., 28, 1261.

Nilsson, K., and Mosbach, K. 1980. Preparation of immobilized animal cells, FEBS Lett., 118, 145.

Nilsson, K., Scheirer, W., Merten, O.W., Östberg, L., Liehl, E., Katinger, H.W.D., and Mosbach, K. 1983. Entrapment of animal cells for production of monoclonal antibodies and other biomolecules, Nature, 302, 629.

Nixon, J.R., Georgakopoulos, P.P., and Carless, J.E. 1967. Diffusion from gelatin-glycerin-water gels, J. Pharm. Pharmac., 19, 246.

Noordsij, P., and Rotte, J.W. 1967. Mass transfer coefficients to a rotating and a vibrating sphere, Chem. Eng. Sci., 22, 1475.

Norton, J., Urban, J., Maroudas, A., Parker, K.H., and Winlove, C.P. 1982. A failure to observe enhanced diffusivity of glucose in a matrix of hyaluronic acid, J. Biol. Chem., 257, 14134.

Ogston, A.G. 1958. The spaces in a uniform random suspension of fibres, Trans. Faraday Soc., 53, 1754.

Onuma, M., Omura, T., Umita, T., and Aizawa, J. 1985. Diffusion coefficient and its dependency on some biochemical factors, Biotechnol. Bioeng., 27, 1533.

Paul, F., and Vignais, P.M. 1980. Photophosphorylation in bacterial chromatophores entrapped in alginate gel: Improvement of the physical and biochemical properties of gel beads with barium as the gel-inducing agent, Enzyme Microb. Technol., 2, 281.

Penman, A., and Sanderson, G.R. 1972. A method for the determination of uronic acid sequence in alginates, Carbohyd. Res., 25, 273.

Pitcher, W.H. Jr., 1978. Design and operation of immobilized enzyme reactors, Adv. Biochem. Eng., 10, 1.

Pu, H.T., and Yang, R.Y.K. 1986. Diffusion of sucrose and yohimbine in calcium alginate gel beads with or without entrapped plant cells, Paper presented at the 192nd ACS National Meeting. September 7-12, 1986, Anaheim, California.

Rabek, J.F., 1980. Experimental Methods in Polymer Chemistry, John Wiley and Sons, Chichester.

Radovich, J.M. 1985. Mass transfer effects in fermentations using immobilized whole cells, Enzyme Microb. Technol., 7, 2.

Rees, D.A. 1969. Structure, conformation and mechanism in the formation of polysaccharide gels and networks. In, Advances in Carbohydrate Chemistry and Biochemistry, Vol. 24, Wolfrom, M.L., and Tipson, R.S., (eds.), Academic Press, New York, 267.

Rees, D.A. 1972a. Polysaccharide gels - A molecular view, Chemistry and Industry, 19 August 1972, 630.

Rees, D.A. 1972b. Shapely polysaccharides, Biochem. J., 126, 257.

Renkin, E.M. 1954. Filtration, diffusion, and molecular sieving through porous cellulose membranes, J. Gen. Physiol., 38, 225.

Rochefort, W.E., Rehg, T., and Chan, P.C. 1986. Trivalent cation stabilization of alginate gel for cell immobilization, Biotechnol. Lett., 8, 115.

Rovito, B.J., and Kittrell, J.R. 1973. Film and pore diffusion studies with immobilized glucose oxidase, Biotechnol. Bioeng., 15, 143.

Ryu, D.D.Y., Kim, H.S., and Taguchi, H. 1984. Intrinsic fermentation kinetic parameters of immobilized yeast cells, J. Ferment. Technol., 62, 255.

Samejima, H., Nagashima, M., Azuma, M., Noguchi, S., and Inuzuka, K. 1984. Semicommercial production of ethanol using immobilized microbial cells, Ann. N.Y. Acad. Sci., 419, 394.

Satterfield, C.N. 1970. Mass Transfer in Heterogenous Catalysis, M.I.T. Press, Cambridge, Mass.

Satterfield, C.N., Cotton, C.K., and Pitcher, W.H. Jr., 1973. Restricted diffusion in liquid within fine pores, A.I.Ch.E.J., 19, 628.

Schantz, E.J., and Lauffer, M.A. 1962. Diffusion measurements in agar gel, Biochem., 1, 658.

Schwartzberg, H.G., and Chao, R.J. 1982. Solute diffusivities in leaching processes, Food Technol., Feb., 73.

Segeren, A.J.M., Boskamp, J.V., and Van den Tempel, M. 1974. Rheological and swelling behaviour of alginate gels, Faraday Discuss. Chem. Soc., 57, 255.

Selegny, E., Broun, G., and Thomas, D. 1971. Enzymatically active model membranes: experimental illustrations and calculations on the basis of diffusion-reaction kinetics of their functioning, of regulatory effects, of facilitated, retarded, and active transports, Physiol. Veg., 9, 25.

Sellen, D.B. 1980. The diffusion of compact molecules through biological gels, In, The Application of Laser Light Scattering to the Study of Biological Motion, vol. 59, Steer, M.W., and Earnshaw, J.C., (eds.), NATO ASI series, Series A: Life Sciences, 209.

Shaw, M., and Schy, A. 1981. Diffusion coefficient measurement by the 'stop-flow' method in a 5% collagen gel, Biophys. J., 34, 375.

Sherwood, T.K., Pigford, R.L., and Wilke C.R. 1975. Mass Transfer, McGraw-Hill, U.S.A.

Sirotti, D.A., and Emery A. 1983. Mass transfer parameters in an immobilized glucoamylase column by pulse response analysis, Biotechnol. Bioeng., 25, 1773.

Skelland, A.H.P. 1984. Diffusional Mass Transfer, Wiley Interscience, New York.

Smidsrod, O. 1974. Molecular basis for some physical properties of alginates in gel state, Faraday Discuss. Chem. Soc., 57, 263.

Smidsrod, O., and Haug, A. 1965. The effect of divalent metals in the properties of alginate solutions, I. Calcium ions, Acta Chem. Scand., 19, 329.

Smidsrod, O. and Haug, A. 1986a. A light scattering complete study of alginate, Acta Chem. Scand., 22, 797.

Smidsrod, O., and Haug, A. 1968b. Dependence upon uronic acid composition of some ion-exchange properties of alginates, Acta Chem. Scand., 22, 1979.

Smidsrod, O., and Haug, A. 1972a. Dependence upon the gel-sol state on ion-exchange properties of alginates, Acta Chem. Scand., 26, 2063.

Smidsrod, O., and Haug, 1972b. Properties of poly (1,4-hexauronates) in the gel state. II. Comparison of gels of different chemical composition, Acta Chem. Scand., 26, 79.

Smidsrod, O., Haug, A., and Lian, B. 1972. Properties of poly (1,4-hexauronates) in the gel state. I. Evaluation of a method for the determination of stiffness, Acta Chem. Scand., 26, 71.

Soldano, B.A. 1953. Kinetics of ion-exchange processes, Ann. N.Y. Acad. Sci., 57, 116.

Somogyi, E. 1952. Notes on sugar determination, J. Biol. Chem., 195, 19.

Sonomoto, K., Tanaka, A., Omata, T., Yamane, T., and Fukui, S. 1979. Application of photo-crosslinkable resin, pre-polymers to entrap microbial cells. Effects of increased cell-entrapping gel hydrophobicity on the hydrocortisone Δ^1-dehydrogenation, Eur. J. Appl. Microbiol. Biotechnol., 6, 325.

Spalding, G.E. 1969. A sensitive method for measuring diffusion coefficients in agarose gels of electrolyte solutions, J. Phys. Chem., 73, 3380.

Spriggs, D.H., and Gainer, J.L. 1973. Predicting binary diffusivities in homogeneous swollen films, Ind. Eng. Chem. Fundam., 12, 291.

Stiles, W. 1923. Indicator method for the determination of coefficients of diffusion in gels, with special reference to the diffusion of chlorides, Proc. R. Soc., 103A, 260.

Stockton, B., Evans, L.V., Morris, E.R., Powell, D.A., and Rees, D.A. 1980. Alginate block structure in Laminaria digitata: Implication for holdfast attachment, Botanica Marina, 23, 563.

Suhaila, M., and Salleh, A.B. 1982. Physical properties of polyethleneimine-alginate gels, Biotechnol. Lett., 4, 611.

Suzuki, M., and Kawazoe, K. 1975. Effective surface diffusion coefficients of volatile organics on activated carbon during adsorbtion from aqueous solution, J. Chem. Engng. Japan, 8, 379.

Taguchi, H., Suga, K., Yoshida, T., and Sadayuki, Y. 1975. Effect of mixing and mass transfer on the glucose isomerization by entrapped cells in a vertical plate type reactor, In, Immobilized Enzyme Technology, Weetal, H.H., and Suzuki, S., (eds.), Plenum Press, New York, 151.

Tanaka, H., Matsumura, M., and Veliky, I.A. 1984. Diffusion characteristics of substrates in calcium alginate gel beads, Biotechnol. Bioeng., 26, 53.

Takevossian, A. 1979. Diffusion of radiotracers in human dental plague, Caries Res., 13, 154.

te Bokkel, D.W. 1983. Study of Terminal Velocities of Air Bubbles in Non-Newtonian Polysaccharide Solutions Using Laser Techniques, M.E.Sc., Faculty of Engineering Science, University of Western Ontario, London, Canada.

Thiele, E.W. 1939. Relation between catalytic activity and size of particle, Ind. Eng. Chem., 31, 916.

Thiele, H. 1954. Ordered coagulation and gel formation, Faraday Discuss. Chem. Soc., 18, 294.

Thiele, H., and Hallick, K. 1957. Capillary structure in ionotropic gels, Kolloid - Z, 151, 1.

Thomas, D.G. 1965. Transport characteristics of suspension. VIII. A note on the viscosity of Newtonian suspensions of uniform particles, J. Colloid Sci., 20, 267.

Tramper, J., Luyben, K.Ch.A.M., and van den Tweel, W.J.J. 1983. Kinetic aspects of glucose oxidation by Gluconobacter oxydans cells immobilized in calcium alginate, Eur. J. Appl. Microbiol. Biotechnol., 17, 13.

Updike, S.J., Harris, D.R., and Shrago, E. 1969. Microorganisms alive and imprisoned in a polymer cage, Nature, 24, 1122.

van Grinkel, G.G., Tramper, J., Luyben, K.Ch.A.M., and Klapwijk, A. 1983. Characterization of Nitrosomonas europea immobilized in calcium alginate, Enzyme Microb. Technol., 5, 297.

van Wazer, J.R., Lyons, J.W., Kim, K.Y., and Colwell, R.E. 1963. Viscosity and flow measurement, A Laboratory handbook of rheology, Interscience Publishers, London.

Vaija, J., Linko, Y.Y., and Linko, P. 1982. Citric acid production with alginate bead entrapped Aspergillus niger, ATCC 9142, Appl. Biochem. Bibtechnol., 7, 51.

Velicky, I.A., and Williams, R.E. 1981. The production of ethanol by Saccharomyces cerevisiae, immobilized in polycation-stabilized calcium alginate gels, Biotechnol. Lett., 3, 275.

Venkatsubramanian, K., Karkare, S.B., and Vieth, W.R. 1983. Chemical engineering analysis of immobilized-cell systems, In, Applied Biochemistry and Bioengineering, vol. 4, Chibata I., and Wingard, L.B., (eds.), Academic Press, New York, 312.

Vieth, W.R., Venkatsubramanian. K., Constantinides, A., and Davidson, B. 1976. Design and analysis of immobilized-enzyme flow reactors, In, Applied Biochemistry and Bioengineering, Vol. 1, Wingard, L.B., Katchalski, E., and Goldstein, L., (eds.), Academic Press, New York, 221.

Vorlop, K.D., and Klein, J. 1981. Formation of spherical chitosan biocatalysts by ionotropic gelation, Biotechnol. Lett., 3, 9.

Vorlop, K.D., and Klein, J. 1983. New developments in the field of cell immobilization - Formation of biocatalysts by ionotropic gelation, In, Enzyme Technology, Lafferty, R.M., and Maier, E., (eds.), Springer-Verlag, Berlin, 219.

Wada, M., Kato, K., and Chibata, I. 1981. Continuous production of ethanol in high concentration using immobilized growing yeast cells, Eur. J. Appl. Microbiol. Biotechnol., 11, 67.

Weetal, H.H., and Pitcher, W.H.Jr. 1986. Scaling up an immobilized enzyme system, Science, 232, 1396.

Weisz, P.B. 1973. Diffusion and Chemical transformation, Science, 179, 433.

White, M.L. 1960. The permeability of an acrylamide polymer gel, J. Phys. Chem., 64, 1563.

White, M.L., and Dorian, G.H. 1961. Diffusion in a cross-linked acrylamide polymer gel. J. Polymer Sci., 55, 731.

Wilke, C.R., and Chang, P.C. 1955. Correlation of diffusion coefficients in dilute solutions, A.I.Ch.E.J., 1, 264.

Williamson, J.E., Pazaire, K.E., and Katchalski, E. 1963. Liquid-phase mass transfer at low Reynolds' numbers, Ind. Eng. Chem. Fundam., 2, 126.

Williamson, K., and McCarty, P.L. 1976. Verification studies of the biofilm model for bacterial substrate utilization, J. Water Pollut. Control Fed., 48, 281.

Yamane, T. 1981. On approximate expressions of effectiveness factors for immobilized biocatalysts, J. Ferment. Technol., 59, 375.

Yamane, T., Araki, S., and Sada, E. 1981. Overall effectiveness factor incorporating partition coefficient for gel-immobilized enzyme pellet, J. Ferment. Technol., 59, 367.

Yano, T., Kodama, T., and Yamada, K. 1961. Fundamental studies on the aerobic fermentation. Part VIII. Oxygen transfer within a mold pellet, Agr. Biol. Chem., 25, 580.

Yasuda, H., Lamaze, C.E., and Ikenberry, L.D. 1968. Permeability of solutes through hydrated polymer membranes. I. Diffusion of sodium chloride, Makromol. Chem., 118, 1935.